Dermatopharmocokinetics: An approach to evaluate topical drug bioavailability

Russell, Lisa

Award date:
2008

Awarding institution:
University of Bath

Dermato-pharmacokinetics: an approach to evaluate topical drug bioavailability

Lisa Maria Russell

A thesis submitted for the degree of Doctor of Philosophy

Department of Pharmacy and Pharmacology
University of Bath

December 2008

DECLARATION OF MATERIAL FROM A PREVIOUSLY SUBMITTED THESIS AND OF WORK DONE IN CONJUNCTION WITH OTHERS

Chapter 1: This chapter has been accepted for publication by the *Expert Opinion on Drug Delivery*, and Prof. R.H. Guy is listed as a co-author.

Chapter 2: This chapter includes data from 31 tape stripping sites. The raw data from 9 of these sites was provided by Dr. S. Wiedersberg. All development, testing and analysis of goodness-of-fit of the mathematical models were performed by the author of this thesis. The information in this chapter has been published: Russell, L.M., S. Wiedersberg, and M.B. Delgado-Charro, *The determination of stratum corneum thickness - An alternative approach.* Eur J Pharm Biopharm, 2008. 69(3): p. 861-870.

Appendix A – preliminary future work (Deducing the stratum corneum – vehicle partition coefficient from dermato-pharmacokinetic studies): The ideas behind this chapter were first discussed in the PhD viva of Dr. S. Wiedersberg, who was also involved in further discussions concerning this work.

Contents

Acknowledgements

My three years in Bath have been very enjoyable, and it is a pleasure to thank the many people who have been involved with my PhD.

First and foremost, I thank my PhD supervisor, **Prof. Richard Guy** for his approachable and friendly nature; for sharing his insight and rounded vision of skin research with me during many stimulating discussions, leading to several 'great ideas'; for his encouragement and enthusiasm to explore new avenues; for the many development and networking opportunities he presented to me; and for persevering with my abbreviations.

Dr. Begoña Delgado-Charro for her collaboration on my first academic paper; for her guidance on the research ethics approval process; for sharing her wisdom on statistics; and for introducing me to many useful textbooks, especially the work of Jerrold Zar.

Prof. Jonathan Hadgraft and **Prof. Rex Tyrrell** for accepting to evaluate this work.

Leo Pharma A/S for funding this work.

All my **volunteers**, who donated their time and their forearms.

The University of Bath's photographer, **Nic Delves-Broughton**, for introducing me to the basics of analytical photography, such that I was able to develop the imaging method presented in this thesis.

Dr. Dan Weiner for scientific input during the development and assessment of the non-linear models and **Pharsight Corporation Inc.** for a Pharsight Academic Licence for WinNonlin®.

Other staff members of the Department of Pharmacy and Pharmacology, especially **Dr. Jenny Scott** for guidance on *in vivo* research ethics, and the technical staff for their friendly, helpful attitude.

My colleagues, past and present, of the Skin, Nail and Eye group for contributing to a pleasant working environment. I would like to thank especially: **Tomek** for being a voice of reason on 'Pharmacy Mondays', for our mathematical derivation sessions and for always being happy to discuss our very different research projects; **Sandra** for sharing her love and experience of tape stripping with me in the early days, for collaborating on certain studies, and for numerous thought-provoking discussions; **Sevgi** for sharing her experience of designing experiments; and **Sarah** for always taking an interest in my work, and her excellent technical help.

My prospective parents-in-law, **Robin** and **Liz**, for their support, interest in my work and for making our garden in Bath more colourful and productive with every visit!

My parents, **Albert** and **Teresa**, and my brothers, **Ronan** and **Enda**, for their encouragement and support throughout these years of studying and great relaxing times.

And finally, my fiancé, **Nick**, for moving to Bath to accompany me through this PhD; for learning a bit about skin and tape stripping; for endless patience during long evenings in the lab (labelling vials…) and while waiting for holidays; for suggestions and motivation; for making my posters and thesis beautiful; and for making life outside the lab so much fun.

Thesis Abstract

Tape stripping

Skin, more specifically the outermost skin layer, the stratum corneum (SC), forms an extremely effective barrier, preventing both the loss of heat and water, and the ingress of micro-organisms and chemicals. Assessing the rate and extent of drug permeation into or through the skin is important both to evaluate the usefulness of a drug for topical or transdermal delivery, and to compare different formulations to assess their bioequivalence.

Prediction of drug permeation is logistically, ethically and economically preferable to *in vivo* measurements. The recent progress that has been made with empirical and mechanistic mathematical models, along with *in vitro* diffusion cell techniques has been reviewed**.** However, currently, *in vivo* measurements, in man, are still required. For new chemical entities, the need for clinical trials is clear. In the case of generic products, however, there is considerable effort currently being expended to replace expensive, subjective clinical trials with objective, validated measurements of drug permeation, *in vivo*, in particular to assess bioequivalence.

The tape stripping technique has emerged as a promising technique to objectively measure drug permeation through skin, and is the focus of this thesis. After formulation application and removal, layers of SC are sequentially removed by adhesive tapes. As the SC performs the main barrier function of the skin, measuring the rate and extent of drug permeation through this layer is assumed to be related to overall topical bioavailability.

The work in this thesis concentrates on performing tape stripping studies such that all tapes are analysed individually, and drug concentration as a function of SC depth is measured. The concentration depth profiles across the SC may be fitted to an appropriate solution of Fick's second law of diffusion to obtain estimates of the vehicle-SC partition coefficient and the drug's diffusivity in the membrane. These dermato-pharmacokinetic parameters may be compared for different formulations.

Models to estimate SC thickness

SC thickness varies between volunteers, and within volunteers according to season, skin condition and skin treatment. Therefore, it is important to measure each volunteer's SC thickness at an untreated site to normalize drug permeation profiles in dermato-pharmacokinetic studies at adjacent sites.

Traditionally, a linear transformation of Fick's first law has been used to correlate the progressively thinner barrier with the corresponding increase in transepidermal water loss and to estimate the thickness by linear regression. However, the data from an important subset of subjects are poorly fitted to this linear model. This is typically due to the removal of loose outer layers of SC, which do not contribute significantly to barrier function.

This work proposes two alternative non-linear models. All three approaches were used to fit data from in vivo tape-striping experiments and their outcomes and goodness-of-fit compared. The results suggest that the linear model may overestimate the SC thickness and is open to subjectivity regarding the selection of data points to be fitted. The non-linear models satisfactorily fitted all the data, including all data points. No significant differences were found between the thicknesses derived from the two non-linear models. However, the analysis of the goodness-of-fit of the models to the data suggests a

preference for the baseline-corrected non-linear model described.

Quantifying the amount of SC per tape strip

Each tape strip removes a variable amount of SC. In order (i) to express the mass of drug extracted from each tape as a concentration; (ii) to measure the depth reached within the SC with each successive tape strip; and indeed (iii) to measure the total SC thickness as above, the amount of SC per tape must be known. The amount of SC per tape is thus crucial to produce robust, reproducible drug penetration profiles.

In this work, four methods to quantify the amount of SC per tape are studied. First, the traditional method of weighing tapes before and after stripping. The weighing method was found to be laborious and slow; to have poor precision and reproducibility; and to be fundamentally flawed due to the mass of SC being 200-2000 times smaller than the mass of a tape strip. Alternative methods must therefore be urgently investigated.

Second, keratin was extracted from the tape strips and analysed by protein analysis. It was shown that the concentrated NaOH solution, suggested in the literature as an extraction solution, degrades keratin and fails to extract keratin from SC. A urea/thiol mixture was tested and preserves and extracts keratins satisfactorily. However, the protein assay method used is insufficiently sensitive to accurately distinguish between the low amounts of keratin on tape strips.

Third, the UV pseudoabsorption of corneocytes at 430nm, as reported in the literature, was examined. This method was shown to be rapid, precise and reproducible. However, the signal of the SC layer was only 1 to 10 times larger than the noise of a blank tape; light scattering may affect the results from inhomogeneous layers; and a maximum of 44% of the SC strip may be analysed.

A novel imaging method to measure the amount of SC per tape strip

Fourth, a novel imaging method was developed during this work. For this method, a high resolution image is taken of each tape under controlled conditions. Each pixel of the resultant image has a greyscale value (on a 16 bit scale) which may be measured in the range 0 to 64608, where 0 and 64608 designate black and white respectively. The mean greyscale value across all pixels can be calculated, and corrected by subtracting from that of a blank tape. When an appropriate scale is applied to the image, the area of the strip may also be measured, which is multiplied by the mean corrected greyscale value to obtain the integrated pixel density for the tape. Both the mean greyscale value and the integrated pixel density are used as relative measures of SC amount. An example image, with relevant measurements is shown below:

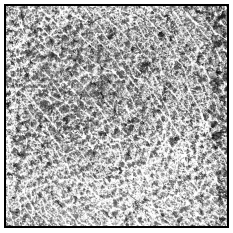

Number of pixels = 4875239
Mean greyscale value of tape = 46451
Mean greyscale of blank tape = 64355
Mean corrected greyscale value of tape = 17904
Scale (for analysis) = 159.07 pixels/mm
Area of strip = 195.1 mm^2
Integrated pixel density = 3493270 mm^2

The imaging method was shown to be the most rapid and simple of the four methods; has high precision and reproducibility; has SC signals 20 to 100 times larger than the noise of a blank tape; and can fully analyse any strip size up to 2.3 cm x 3.5 cm. Furthermore, permanent records of the amount of SC per tape are obtained which may be further analysed in terms of inhomogeneity, strip area, and 3-dimensional stacks.

Application of the novel imaging method in tape dermato-pharmacokinetic studies

The imaging method thus provides a sensitive relative measure of the amount of SC per tape. To verify the usefulness of the mean greyscale value as a measure of SC thickness in our existing dermato-pharmacokinetic models, sites were stripped and the SC on tapes assayed by the traditional weighing and novel imaging methods.

Firstly, sites were examined to assess total SC thickness. Cumulative integrated pixel densities (derived from imaging method) were substituted into the non-linear model previously developed (in place of cumulative thickness values derived from mass measurements) to derive a 'greyscale' estimate of the SC thickness, G. The traditional SC thickness, H, with SC mass measured per tape, was also estimated. H and G correlated well but intra-subject variability was favourably lower for the imaging measurements. The plots of TEWL as a function of depth within the SC were normalised using the H and G estimates, respectively, such that the normalised plots and parameter estimates from both the weighing and imaging methods could be directly compared. Improved sensitivity was found for the imaging method.

Secondly, a full dermato-pharmacokinetic study was performed to compare two acyclovir creams. Again, the amount of SC per tape was assayed using the weighing and imaging methods to construct two types of drug permeation profiles. The normalised profiles from both SC quantification methods are comparable, as are the resultant dermato-pharmacokinetic parameters, the SC-vehicle partition coefficient and the diffusivity. The partition coefficient of acyclovir was found to be numerically close to 1, similar to other drugs such as ibuprofen and betamethasone valerate, despite differences in their physicochemical properties. This could be due to residual formulation on the skin after cleaning, or the result of excipient 'carrying' the drug into deeper layers of the SC.

In conclusion, a new method to estimate the total SC thickness is demonstrated. It has been shown that the mean greyscale value of a tape may be used as a sensitive, reproducible and precise relative measurement of the amount of SC per tape. This greyscale value may be used directly in the appropriate mathematical models (i) to estimate total SC thickness, and (ii) to estimate dermato-pharmacokinetic parameters.

Chapter summaries

Assessing the rate and extent of drug permeation into or through the skin is important both to evaluate the usefulness of a drug for topical or transdermal delivery, and to compare different formulations to assess their bioequivalence.

Prediction of drug permeation is logistically, ethically and economically preferable to *in vivo* measurements. The recent progress that has been made with empirical and mechanistic mathematical models, along with *in vitro* diffusion cell techniques has been reviewed in **Chapter 1.** However, currently, *in vivo* measurements, in man, are still required. For new chemical entities, the need for clinical trials is clear. In the case of generic products, however, while testing of efficacy remains a requirement, there is considerable effort currently being expended to replace expensive, subjective clinical trials with objective, validated measurements of drug permeation, in particular to assess bioequivalence. In **Chapter 1**, three prominent methods are discussed: microdialysis, pharmacodynamic approaches, and tape stripping.

The tape stripping technique is the focus of this thesis, where, after formulation application and removal, layers of SC are sequentially removed by adhesive tapes. As the SC performs the main barrier function of the skin, measuring the rate and extent of drug permeation through this layer is assumed to be related to overall topical bioavailability.

The work in this thesis concentrates on performing tape stripping studies such that all tapes are analysed individually, and drug concentration as a function of SC depth is measured. The concentration depth profiles across the SC may be fitted to an appropriate solution of Fick's second law of diffusion to obtain estimates of the vehicle-SC partition coefficient and the drug's diffusivity in the membrane. These dermato-pharmacokinetic parameters may be compared for different formulations.

SC thickness varies between volunteers, and within volunteers according to season, skin condition and skin treatment. Therefore, it is important to measure each volunteer's SC thickness in order to express the depth reached with each successive tape strip relative to this total. SC relative depth therefore has a value of 0 at the skin surface and 1 at the SC-stratum granulosum interface. This eases comparison between the drug penetration profiles from different volunteers and on different occasions. SC thickness, H, is measured at an adjacent, untreated site, by fitting the increase in transepidermal water loss (TEWL) as progressive layers of SC are removed with each tape, to an appropriate model. A linear model was previously described [1, Section 5.2.4], but can overestimate SC thickness due to the influence of the stratum corneum disjunctum. In **Chapter 2**, a baseline-corrected non-linear model is described to objectively estimate SC thickness irrespective of the SC disjunctum, and full analysis of the non-linear goodness-of-fit is performed.

Each tape strip removes a variable amount of SC. In order to (i) express the mass of drug extracted from each tape as a concentration; (ii) measure the depth reached within the SC with each successive tape strip; and indeed (iii) measure the total SC thickness as above, the amount of SC per tape must be measured. The amount of SC per tape is thus crucial to produce robust, reproducible drug penetration profiles.

Traditionally, weighing tapes before and after stripping has been often used to derive a mass of SC per tape, but this is a time-consuming and laborious process.

Protein forms ~80% of the total SC mass, and as such, extraction of protein from tapes as a SC quantification method has been explored. In **Chapter 3**, two extraction solutions are tested for their potential to degrade and extract SC keratins. Furthermore, the protein

concentrations extracted from more than 300 tape strips were correlated with two other measures of SC thickness: the gravimetric method and a novel imaging method.

The novel imaging method, as a method to quantify the amount of SC per tape, features heavily in the remainder of the thesis. For this method, a high resolution image is taken of each tape under controlled conditions. Each pixel of the resultant image has a greyscale value (on a 16 bit scale) which may be measured in the range 0 to 64608, where 0 and 64608 designate black and white respectively. The mean greyscale value across all pixels can be calculated, and corrected by subtracting from that of a blank tape. When an appropriate scale is applied to the image, the area of the strip may also be measured, which is multiplied by the mean corrected greyscale value to obtain the integrated pixel density for the tape. Both the mean greyscale value and the integrated pixel density are used as relative measures of SC amount. An example image, with relevant measurements is shown below:

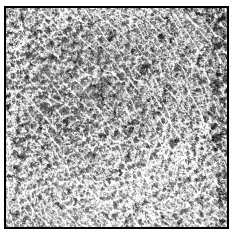

Number of pixels = 4875239
Mean greyscale value of tape = 46451
Mean greyscale of blank tape = 64355
Mean corrected greyscale value of tape = 17904
Scale (for analysis) = 159.07 pixels/mm
Area of strip = 195.1 mm^2
Integrated pixel density = 3493270 mm^2

In **Chapter 4**, three methods to quantify the amount of SC per tape, namely weighing, UV pseudo-absorption and the imaging method, were assessed in terms of practical features: (i) reproducibility and precision, (ii) signal:noise ratio, (iii) proportion of the total strip sample, (iv) time cost. Next, more than 600 tape strips were analysed by each method, and correlations compared.

In **Chapter 5**, cumulative integrated pixel densities were substituted into the non-linear model developed in Chapter 2 (in place of cumulative thickness values derived from mass measurements) to derive a 'greyscale' estimate of the SC thickness, G. The true SC thickness, H, with SC mass measured per tape, was also estimated, and H and G were correlated. The plots of TEWL as a function of depth within the SC were normalised using the H and G estimates, respectively, such that the normalised plots and parameter estimates from both the weighing and imaging methods may be directly compared.

In **Chapter 6**, two different acyclovir creams were compared using dermatophamacokinetic profiles. Two types of drug penetration profiles are fitted where (i) the mass of SC per tape, and (ii) the integrated pixel density per tape, are used as measures of SC amount. The normalised profiles from both SC quantification methods are compared. Furthermore, use of the imaging method to assess SC inhomogeneity is examined.

Abbreviations

AIC	Akaike Information Criterion
ACV	Acyclovir
ANG_i	Absolute normalised greyscale of SC on tape *i*
ANN	Artificial Neural Network
ANOVA	Analysis of Variance
ANT_i	Absolute normalised thickness of SC on tape *i*
ASCII	American Standard Code for Information Interchange
AUC	Area Under the Curve
B	Baseline correction factor for non-linear model using cumulative thickness
BC-NL	Baseline-corrected Non-Linear Model
B_g	Baseline correction factor for non-linear model using cumulative greyscale
bit	Binary digit, taking a value of either 0 or 1.
C_g	Concentration of drug at position, g, within the SC, as measured by cumulative integrated pixel densities
C_{max}	Maximum drug concentration achieved in SC
Corr.	Corrected
Cum.	Cumulative
CV	Coefficient of variation
C_v	Concentration of drug in the vehicle
C_x	Concentration of drug at position, *x*, within the SC, as measured by thickness measurements
D	water's diffusivity in the SC
D/H^2	Drug's diffusivity in the SC
DPK	Dermato-pharmacokinetics
EDETOX	Evaluations and Predictions of Dermal Absorption of Toxic Chemicals
FDA	U.S. Food and Drug Administration
Fluo.	Fluorescence
G	Total SC thickness, estimated by greyscale non-linear model
g	Cumulative integrated pixel density of SC removed by tape stripping
g/G	Relative depth reached within the SC, measured by integrated pixel density of SC per tape
h	Cumulative thickness of SC removed by tape stripping
H	Total SC thickness, estimated by thickness non-linear model
h/H	Relative depth reached within the SC, measured by weighing SC per tape
HPLC	High Performance Liquid Chromatography
IAM	Immobilised Artificial Membrane
K	SC-viable epidermal partition coefficient of water

KB	Kilobyte. 1024 bytes where a byte is an ordered collection of 8 bits.
K_g	SC-vehicle partition coefficient of drug, as measured from drug concentration as a function of cumulative integrated pixel density profiles
K_m	SC-vehicle partition coefficient of drug, as measured from drug concentration as a function of cumulative thickness profiles.
$K_{o/w}$	Oil-water partition coefficient
k_p	Permeability coefficient of drug through SC
LM	Linear Model
MW	Molecular Weight
NSAID	Non-Steroidal Anti-Inflammatory Drug
Pred.	Predicted
Q	Total quantity of drug in SC after a given time
QRPR	Quantitative Retention Permeability Relationship
QSPR	Quantities Structure Permeability Relationship
r	Molecular radius
R_g	Average concentration of drug in SC, with SC amount quantified by mean greyscale value
R_m	Average concentration of drug in SC, with SC amount quantified by mass
r_s	Spearman's correlation coefficient (non-parametric correlation)
SC	Stratum Corneum
SER	Standard Error of Regression
SES	Stable Extraction Solution; namely 8M urea, 50mM Tris, 0.1M β-mercaptoethanol, pH 8.4
TEWL	Transepidermal Water Loss
$TEWL_0$	Initial transepidermal water loss measured before tape stripping
T_{max}	Application time after which maximum concentration measured
UV	Ultra-violet
VE	Viable epidermis
WRSS	Weighted Residual Sum of Squares
Zov.	Zovirax
ΔC	Concentration gradient of water across the SC

Chapter 1

Measurement and prediction of the rate and extent of drug delivery into and through the skin

1 Measurement and prediction of the rate and extent of drug delivery into and through the skin

1.1 Abstract

Empirical mathematical models retrospectively analyse data to predict skin permeation from drug physico-chemical properties. Quantitative Structure Permeability Relationships are discussed along with alternatives to linear modelling. Mechanistic mathematical models, derived from first principles are also considered. Further, in vitro experiments allow predictions to be made using suitable membranes (cultured cell lines or excised skins). In vivo methods to assess (trans)dermal drug delivery aim to minimise clinical studies, especially to determine bioequivalence. Microdialysis is discussed, together with the FDA-approved skin blanching (pharmacodynamic) assay for corticosteroids. Progress made with the tape-stripping methodology is reviewed. Two distinct strategies have emerged: (i) in which the total amount of drug in the stratum corneum (SC) at one uptake and one clearance time are compared; and (ii) another which generates drug permeation profiles across the SC, and allows dermato-pharmacokinetic parameters to be derived.

1.2 Introduction

The skin is the largest organ of the human body. Skin forms an extremely effective barrier, preventing both the loss of heat and water, and the ingress of microorganisms and chemicals. Drugs may be applied topically to skin for the local treatment of inflammation, infections (bacterial, viral or fungal) or to anaesthetise an area. The target site may be the outermost layer of the skin, the stratum corneum (SC), or deeper layers. Potent drugs may also be administered transdermally, travelling through the skin to the dermal blood vessels and into the systemic circulation.

Assessing drug permeation into or penetration through the skin is important both to evaluate the usefulness of a drug for topical or transdermal delivery, and to compare different formulations to assess their bioequivalence.

Prediction of drug movement through skin layers is logistically, ethically and economically preferable to *in vivo* measurements. With respect to permeation prediction, mathematical models, based on empirical measurements or mechanistic deductions, have been explored. The most important predictors of permeation are lipophilicity and molecular weight (MW). *In vitro* measurements of skin penetration using diffusion cells, separated by an appropriate membrane, either synthetic or *ex vivo,* provide important empirical measurements to use in the development of mathematical models. Bioengineered skin is being developed but currently, excised pig skin offers the most frequently chosen match to human skin.

Predictions help to reduce the number of *in vivo* measurements required, by focusing experimental strategy, but the latter are currently still required. The *in vivo* strategies developed are intended to provide objective measurements of drug permeation, and minimise the need for expensive, subjective clinical trials. Three prominent methods are discussed: microdialysis, phamacodynamic approaches, and tape stripping. Within tape stripping, two improved metrics for evaluating the data are presented alongside the approach originally proposed by the (U.S.) Food and Drug Administration.

1.3 The prediction of topical and transdermal drug delivery

The main benefits of predictions over measurement of drug delivery are clear: it is usually cheaper and quicker. Furthermore, there are no problems with ethical issues, recruiting volunteers, or housing animals.

Ideally, predictions should provide a reliable indication of the extent to which drugs are going to permeate the skin, either to the target skin layers (for topical products) or to the systemic circulation (for transdermal products). Predictions are also useful to select and design the best drug molecules for these purposes.

Mathematical models, developed using existing experimental results, provide self-evidently the most convenient predictive tools. *In vitro* experiments can assess drug permeability through various membranes, which bear increasing relevance to human skin.

1.3.1 Mathematical models

Two main approaches have emerged for the prediction of drug permeation: empirical models and mechanistic models. The former are derived from a retrospective analysis of experimental results, and correlate skin permeation data with drug properties. Mechanistic models are derived from first principles. Permeation is predicted and modelled based on skin compartments and diffusion pathways. Within these broad categories, several other classes of models may be differentiated and are reviewed here.

1.3.1.1 Empirical models

The most intensively researched area involves quantitative structure permeability relationships (QSPRs) which correlate experimental permeation data with (i) physico-chemical properties, or (ii) molecular structural properties of the permeant.

1.3.1.1.1 Quantitative structure permeability relationships (QSPRs)

Before any empirical modelling based on permeability can begin, the permeability of the chemical through the skin must be measured. The permeability coefficient, k_p (units: distance/time) is defined as:

$$k_p = \frac{K_m \cdot D}{H} \qquad \text{Eq. 1-1}$$

Where K_m is the drug's SC-vehicle partition coefficient; D is the diffusivity of the drug in the SC; and H is the SC thickness.

In vitro experiments are performed to generate data as shown in Figure 1-1. Using the appropriate solution of Fick's second law (Figure 1-1, legend, [2]) for non-steady state diffusion, the data in Figure 1-1 may be modelled and K_m and D/H^2 derived [3, 4].

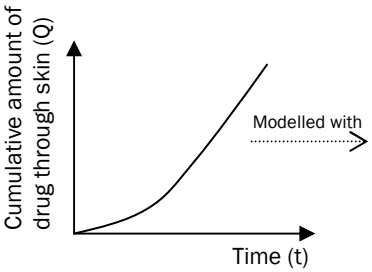

$$Q = (K_m H) C_v \left[\frac{D}{H^2} t - \frac{1}{6} - \frac{2}{\pi^2} \sum_{n=1}^{\infty} \frac{(-1)^n}{n^2} \exp\left(\frac{-Dn^2 \pi^2 t}{H^2} \right) \right]$$

Figure 1-1: The cumulative amount of drug permeating the skin, Q, under non-steady state conditions, after application of an infinite dose, as a function of time, t, may be modelled using the appropriate solution of Fick's second law (equation as shown above); where K_m is the drug's SC-vehicle partition coefficient; H is the SC thickness; C_v is the drug concentration in the vehicle; and D is the diffusivity of the drug in the SC.

1.3.1.1.1.1 Databases of k_p values

Databases of k_p values have been created retrospectively. The most extensively used of these is the so-called *Flynn database* [5]. It comprises 97 k_p values, for 94 compounds, covering a broad range of molecular weights (18-765), and octanol-water partition coefficients (-3 to +6). The values are mostly from human skin *in vitro*, with the drug usually delivered from an aqueous solution. Its principal shortcomings are: the proportionally small number of both hydrophilic compounds (9/94 with log $K_{o/w} \leq 0$) and highly lipophilic compounds; and the lack of consideration of the chemical's ionisation state and of the temperature at which measurements were made [6].

Several other compilations of log k_p values have been assembled, often using some values from the original Flynn database. The value of these other databases have been described succinctly by Vecchia and Bunge [6].

Recently, a European Union funded study, "Evaluations and Predictions of Dermal Absorption of Toxic Chemicals" (EDETOX), produced a database containing permeation data for 300 compounds (http://edetox.ncl.ac.uk). The work also generated new data for the *in vitro* transport of 60 chemicals across human skin [7]. The experiments were well-designed and allowed comparison of: rat vs. human skin; static vs. flow-through diffusion cells; finite vs. infinite dose; skin thickness; vehicle composition; and physico-chemical properties (MW, log $K_{o/w}$ solubility) [7]. The results have been modelled using QSPRs and a novel mechanistic model, the Kruse model [8], developed.

1.3.1.1.1.2 QSPR models

The most cited QSPR proposed is that reported by Potts and Guy [9]. Their equation was derived from linear regression of the k_p, MW and log $K_{o/w}$ values in the Flynn database (93 compounds). The best fit equation was:

$$\log k_p (cm.h^{-1}) = -2.72 + 0.71(\log K_{o/w}) - 0.0061(MW) \qquad \text{Eq. 1-2}$$

which had an overall correlation coefficient (r^2) of 0.67. The model indicates that the permeability coefficient will be highest for smaller molecules, with higher log $K_{o/w}$. Given the typical level of variability in skin permeability measurements, the Potts and Guy equation performs remarkably well and certainly provides reasonable predictions. However, the approach focuses on the stratum corneum as the exclusive rate-limiting barrier and therefore significantly over-estimates k_p for highly lipophilic compounds. This issue was successfully addressed by Bunge, Vecchia and Cleek [6, 10] whereby a corrected k_p value of lipophilic compounds ($k_{p\,(lip)}$) may be calculated using Eq. 1-3:

$$k_{p\,(lip)} = \frac{k_p}{1 + \left(\frac{k_p + \sqrt{MW}}{2.6} \right)}$$ Eq. 1-3

where k_p is that derived from the Potts and Guy equation (Eq. 1-2). The rationale behind this correction equation is discussed further below (section 1.3.1.2.1).

Many other models have been proposed and compared [6]. Inconsistencies in the Flynn database relating to ionisation state (which affects $K_{o/w}$), inter-dependence of MW and $K_{o/w}$ in some homologous series, and temperature (which affects diffusivity) have been identified. These factors have been explored, suitable adjustments to the permeability prediction equations have been proposed [6, 11-13] and slight improvements recorded. For example, using the logarithm of the chemical's diffusion coefficient, log D, instead of log $K_{o/w}$ allows the effects of pH on ionisation to be incorporated [14], although sufficient data do not yet exist for ionisable compounds. The comprehensive review of these factors is presented elsewhere [13]. If reliable data regarding log $K_{o/w}$ are not readily available, estimates can be derived from the molecular structure, incorporating the contributions which various groups make to the overall lipophilicity [15]. Diffusion has also been shown to be related to partial charge interactions (such as H bonding), which may be predicted [16-19].

1.3.1.1.2 Quantitative retention permeability relationships (QRPRs)

Quantitative *retention* permeability relationships relate chromatographic parameters (rather than molecular parameters as in QSPRs) to permeability coefficients derived experimentally. Biopartitioning micellar chromatography uses modified high performance liquid chromatography (HPLC) columns as surrogates for biological barriers [20-24]. Solute capacity factors, directly calculated from retention times on the column, are used to derive QRPR models.

The first modified HPLC column used cell membrane-mimicking phospholipids on a silica surface, the so-called Immobilised Artificial Membrane (IAM) columns. The resultant retention times correlated well with (human derived) log k_p values for steroids, and slightly better in fact than the corresponding log $K_{o/w}$ values [21]. Phenolic and ionic compounds showed a poorer correlation [21].

A second column, with keratin immobilised on a silica support, was produced to mimic solute interaction with keratin in skin [20]. When a series of solutes were run on both this column and an IAM column, the resulting capacity factors were incorporated into one QRPR model which showed a good correlation ($r^2 = 0.87$) with experimental log k_p values for 17 compounds [20].

Theoretically, by manipulating the HPLC method, the effects of pH, temperature, ionisation and presence of excipients on permeability may also be measured [23, 24]. This would be a potentially significant advantage when attempting to optimise formulations.

1.3.1.1.3 Artificial Neural Networks (ANNs)

In QSPRs, multiple linear regression is used to determine correlations between physico-chemical properties (such as log $K_{o/w}$ and MW) and permeability. Both linear and non-linear correlations may be investigated using artificial neural networks (ANNs). ANN modelling uses computer algorithms to learn from data in a manner similar to the brain's

use of webs of interconnected neurons [25].

ANNs have been successfully used [25] to predict skin permeation of 40 compounds (MW range ~30-390 and log $K_{o/w}$ = -0.77 – 2.94). Further work, using different input parameters [26, 27], has again shown an improvement over multiple linear regression models.

1.3.1.1.4 Fuzzy modelling

Fuzzy models cluster data for different compounds into appropriate subsets based on their properties. For example, a subset may contain compounds with a log $K_{o/w}$ around +2. Each compound will have a degree of membership of this set, between 0 and 1; that is, a compound with a log $K_{o/w}$ exactly equal to 2 would be assigned a membership degree of 1.0; if log $K_{o/w}$ = +1.8, then the membership degree may be ~0.9; for compounds with log $K_{o/w} \leq +1$ or $\geq +3$, the membership degree is zero. Of course, compounds may be members of several subsets as these may not be mutually exclusive.

The Fuzzy model algorithms consider all the compounds in the data set and, after a learning period, cluster the data points into appropriate subsets and determine the degrees of membership of each compound to each subset. Fuzzy modelling can simplify complex models by revealing patterns in the data. The algorithms are numerous and complex but they essentially find links between inputs and outputs via Fuzzy clustering techniques [28].

Fuzzy modelling has been used [28] to analyse the molecular parameters (including MW, log $K_{o/w}$, H-bond donor activity, H-bond acceptor activity, and polarizability) from three sources [5, 29, 30]. The correlation between the (Fuzzy) predicted and experimental log k_p was very good, with r^2 of 0.83, 0.97 and 0.96 for three distinct data sets (with 94, 37 and 54 compounds per dataset, respectively). In addition, fewer molecular parameters were required for the Fuzzy model compared with the original multiple linear regressions.

1.3.1.2 Mechanistic models

Mechanistic models predict permeation based on knowledge of skin compartments and diffusion pathways.

1.3.1.2.1 Stratum corneum and viable epidermal contributions to barrier function

To evaluate the normalised cumulative mass of drug absorbed into the SC, a series of three mechanistic models were derived [10], all related to exposure time, and such that unsteady state exposure may also be estimated.

The three models (Figure 1-2) consider (1) the SC alone as a single finite membrane; (2) the SC alone where it is assumed that the membrane is sufficiently thick, and the exposure time short enough, such that it behaves as a semi-infinite membrane; and (3) both the SC and viable epidermis (VE) as a finite two-membrane composite, incorporating the partition, diffusivity and pathlength variables for both skin layers.

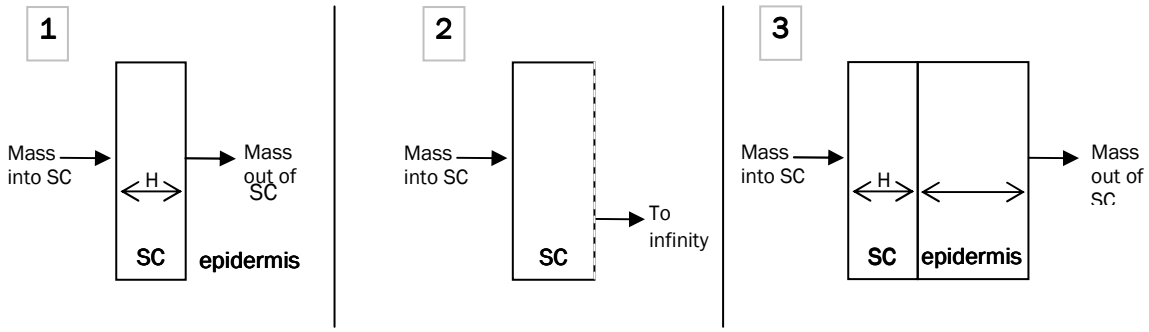

Figure 1-2: 3 mechanistic models proposed by Cleek and Bunge. Models based on: 1. Single finite membrane; 2. Semi-Infinite membrane; 3. Finite two-membrane composite. H: SC thickness. Redrawn from [10].

For unsteady state (short) exposure times, the drug will not have reached the VE to any significant extent and models 1 and 2 are applicable.

Model 3 is important for longer exposure times, when steady state may be reached, and the overall drug flux may be affected by the hydrophilic VE. This is indeed the case for highly lipophilic chemicals which will partition slowly from the SC and eventually become rate-limited by the VE. The extent to which the VE contributes to the total resistance to transport may be captured in a modified expression to calculate the normalised cumulative mass of drug absorbed into the SC, incorporating a SC-VE permeability ratio, B [10]. For lipophilic compounds, for which B ≥100, it is apparent that the VE affects the skin permeation process [31].

Experimentally, however, B is difficult to measure and various approximations have been introduced to enable its use in Model 3 [31]. For example, the $K_{o/w}$ is used to estimate the chemical's SC/VE partition coefficient, and molecular weight is used to correct diffusivities. Both parameters are extracted from the Potts and Guy equation [29].

The correction introduced in this way places a limit on the calculated values of the cumulative mass of drug absorbed into the SC. The impact is greatest for lipophilic compounds to which the skin is exposed for long application times (and longer than the conventional lag time for diffusion across the skin) [32].

1.3.1.2.2 Scaled particle theory

Scaled particle theory calculates the work required for solutes to be incorporated into lipid bilayers [33]. This theory has been applied to transdermal permeation, and used to calculate diffusion and partition coefficients of solutes [33]. These parameters will depend on lipid density and lipid disorder (assumed constant) [33].

The model first assumed a tortuous pathway for diffusion across the SC [34]. Empirical data was used to derive the relationship $K_m = (K_{o/w})^{0.7}$ which was then used to estimate K_m in the model [33]. The solute's diffusivity through the SC was estimated from the molecular radius (r, (Å)) which, in turn, was calculated empirically from the MW [33, 35], using data from Mitragotri et al [Table 1 of reference 35] to derive:

$$r = \sqrt[3]{0.22 \times MW} \qquad \text{Eq. 1-4}$$

The final expression for the permeability coefficient was:

$$k_p(cm.hr^{-1}) = (K_{o/w})^{0.7} * 0.02\exp(-0.46r^2) \qquad \text{Eq. 1-5}$$

Or, in logarithmic form:

$$\log k_p(cm.hr^{-1}) = 0.7K_{o/w} - 1.70 + 0.20r^2 \quad \text{Eq. 1-6}$$

This model and the Potts and Guy equation give very similar results [12]. Although they are derived in very different ways, by re-substituting MW in place of the radius (using Eq. 1-4), Eq. 1-6 can be rewritten as:

$$\log K_p(cm.hr^{-1}) = 0.7\log K_{o/w} - 1.70 + 0.072MW^{2/3} \quad \text{Eq. 1-7}$$

which bears remarkable similarity to the Potts and Guy equation (Eq. 1-2) [12].

The model was tested using a compilation of experimental values [34], and a slightly lower mean absolute error was found for the mechanistic model (5%) as compared with Potts and Guy (6.3%) [33]. Notable deviations from Eq. 1-6 are molecules with MW > 400 Da.

Subsequently, the model in its original form (which focussed on solute permeation through the intercellular lipid domains of the SC) was expanded to include alternative, parallel pathways, including transport via putative aqueous 'pores' and through various shunts, such as hair follicles and sweat glands [36]. This more complex approach was not only able to match the predictions of the Potts and Guy equation, but could also fit the results for larger hydrophilic compounds, the permeability of which is usually underestimated by earlier models. On the other hand, it should be pointed out that the 'price' for this improvement is a more complex model containing an increased number of adjustable parameters.

In summary, the most straightforward and widely used mathematical model is the empirical Potts and Guy equation (Eq. 1-2). It provides an adequate prediction based on two easily obtainable physicochemical properties, MW and $\log K_{o/w}$. Modifications and refinements have been proposed, and the adaptation for lipophilic compounds [10, 31, 32] is a sensible and necessary development. Introduction of additional parameters or incorporation of other parallel pathways can improve the overall correlation between predicted and experimental results but there is a cost in terms of simplicity and practicality.

1.3.2 In vitro experiments

In vitro experiments use vertical or side-by-side diffusion cells, with the receptor fluid separated from the solution/formulation by an appropriate membrane. Measurements of drug flux through the membrane are obtained from the cumulative amount transported as a function of time (Figure 1-1). Solutions of Fick's first and second laws can then be used to derive the permeability coefficient, or other representative transport metrics in steady or unsteady state situations, respectively [3]. *In vitro* experiments provide a quantitative measure of drug penetration, and are cheaper and are less complicated to perform than *in vivo* studies.

1.3.2.1 Choice of membranes

The best membrane for *in vitro* studies is human skin, which may be obtained from surgical procedures. However, a regular supply is not always available; the use of cadaver skin is not generally possible and frequently leads to highly variable data. As a result, alternatives have been investigated.

1.3.2.1.1 Cultured cell lines

Cultured cell lines represent a development from the field of tissue engineering (i) to provide biomimetic, non-immunogenic skin layers to protect, and aid the healing of, acute and chronic wounds, burns and ulcers; and (ii) as a model for permeation and toxicological assessment of cosmetic and medicinal products. Research has accelerated because, from 2009, European Union directives will prohibit the use of animals in toxicity studies for cosmetic products [37]. In addition, the use of donated human tissue for purposes of financial gain is prohibited [38].

There are two principal categories of cultured skin tissues: living skin equivalents comprising a dermis, epidermis and partially differentiated SC, but without skin appendages; and human reconstructed epidermis which consists simply of keratinocytes grown on a substrate. Examples of the latter are more common (EpiSkin® (L'Oréal, Clichy-Cedex, France), SkinEthic® (SkinEthic Laboratories, Nice, France), EpiDerm® (MatTek Corporation, Ashland, MA, USA)) than the former (Apligraf®, Graftskin® (Organogenesis, Canton, MA, USA)).

The morphology and biochemistry of human reconstructed epidermis has been compared with *ex vivo* human tissues [39-41]. Both have a differentiated epithelium, with stratum corneum, stratum granulosum, stratum spinosum and stratum basale but several histological and biochemical differences are apparent [39]. The SC is typically thicker and more variable that human skin, and is not always fully keratinised [39]. The morphology, lipid composition, and biochemistry of Epiderm®, SkinEthic® and EpiSkin® have been reviewed, together with their applications in phototoxicity, irritancy and absorption testing [41].

Generally speaking, chemical penetration across human reconstructed epidermis is quite reproducible, but significantly higher than through human, pig or rat skin [40-44]. They have thus been proposed as useful tools with which to compare and optimise formulations [45], but care must be exercised if excipients are present which may alter barrier function (and result in artefactually amplified penetration results).

Living skin equivalents, despite their greater similarity with human skin [41], have shown to similarly overestimate chemical penetration [43, 44, 46].

Overall, therefore, while valuable, for example, for skin irritation assessment, skin cell culture models are not yet able to provide quantitative predictions of percutaneous penetration.

1.3.2.1.2 Excised skins

Many animal models have been suggested for evaluating percutaneous penetration, including primates, ungulates (pigs, including miniature pigs), rodents (mice, rats and guinea pigs) and reptiles (snakes).

Rodent skin is widely available and is often used. Hairless species are preferred since potentially damaging shaving or depilation is avoided, and the follicular density resembles human skin more closely. Results show that penetration rates are higher for rodent skin than human skin, with rat skin up to ten times more permeable [47, 48]

Pig skin has been repeatedly shown to be a relevant and convenient animal model for *in vitro* penetration studies [43, 44]. When compared to human skin, pig skin is similar in terms of histology and dimensions but the diameter of porcine hair follicles is larger [49].

Flux profiles of diverse compounds across pig skin are similar to those through the human barrier [44, 50] and it appears unlikely that the use of the porcine model will over-estimate the results in man. Equally, when using the tape-stripping methodology

discussed below, the concentration profiles of drugs (such as ibuprofen) across pig SC closely resemble those observed *in vivo* in humans [51].

1.4 Measurement of (trans)dermal drug delivery in vivo

Clearly, for transdermal products, whose target site is the systemic circulation, well-established *in vivo* pharmacokinetic studies, taking blood and/or urine samples at particular times post application and removal of the product, provides the most reliable measurement of transdermal drug penetration. These pharmacokinetic studies, similar to those of controlled release formulations, are accepted from a regulatory perspective for transdermal products [52, 53].

Despite the advances made in predictive models and *in vitro* testing, and their inherent advantages, the ultimate evaluation of topical drug delivery into and though the skin has to be performed *in vivo,* in man. For new chemical entities, the necessity of clinical trials is clear. In the case of generic products, while testing of efficacy remains a requirement, there is considerable effort currently directed at the assessment and validation of alternative approaches, with which to assess bioequivalence.

1.4.1 Microdialysis

Microdialysis is an *in vivo* technique for sampling free drug concentrations in the extracellular fluid within tissues or organs. A thin dialysis membrane tube is inserted into the site of interest and perfused with a site-compatible physiological solution (Figure 1-3). Molecules of interest (usually small and water soluble) diffuse across the membrane, are collected and measured.

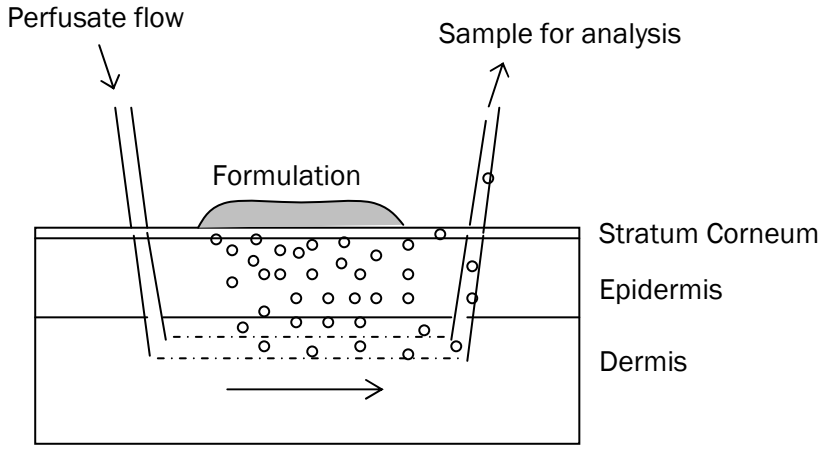

Figure 1-3: Schematic of microdialysis membrane used for dermato-pharmacokinetics.

With respect to (trans)dermal drug delivery, the microdialysis probe is inserted subcutaneously or intradermally. The technique boasts many advantages: (i) continuous measurements of drug concentration with time are possible, allowing pharmacokinetics to be followed; (ii) large molecules are size-excluded by the dialysis membrane, limiting analytical interference and enzymatic degradation [54, 55]; (iii) no tissue or bodily fluids are removed permitting an unlimited number of samples to be taken; and (iv) endogenous compounds, such as lactate, glucose, neurotransmitters, etc may also be measured.

Limited experiments have assessed drug concentrations in subcutaneous tissue and

underlying muscle after topical and oral administration of ibuprofen [56]. Dermal concentration profiles of lidocaine [57], salicylic acid [58] and 8-methoxypsoralen [59] have been measured, including comparisons with plasma levels for 8-methoxypsoralen.

The drawbacks of the technique include tissue reactions as the probe is inserted [60]; the choice of flow rate and sampling times requires fine tuning [61]; analytical techniques require high sensitivity due to dilution with perfusate [62]; and selection of perfusate and dialysis membrane depends on the drug of interest, with lipophilic, large drugs posing particular problems [63]. The mathematical extrapolation of extracellular fluid concentrations from the dialysate concentration is also challenging, often requiring the co-administration of a reference molecule (reviewed, [64]). Inter- and intra- individual variability is relatively large, with coefficients of variation between 50-100% [60].

1.4.2 Pharmacodynamic assessment of topical corticosteroids.

Corticosteroids typically exert a quantifiable blanching effect on the skin caused by vasoconstriction of dermal microvasculature after the drug has permeated through the epidermis. The FDA has adopted this pharmacodynamic effect as an acceptable method for assessing the bioavailability and bioequivalence of topical corticosteroids [65]. Originally the colour change of the skin was assessed by a trained operator, but the development of the chromameter has allowed objective, sensitive and quantifiable measurements to be made. This apparatus assesses (skin) colour based on the L-scale (light-dark), the a-scale (red-green) and the b-scale (yellow-blue). The FDA guidance document specifies only the use of the a-scale [65]; however, the L-score [66, 67] and all three [68] have also been used successfully.

The main advantage of the skin blanching assay is its non-invasive nature and that, as a result, many measurements may be made over an extended time period on the same site. Corrections for changes in skin colour unrelated to the formulation are made at an adjacent site. Further advantages, compared with clinical trials, are that formulations may be quickly and objectively assessed in a relatively small number of healthy participants, avoiding the problems associated with patient selection.

The FDA protocol involves two stages [65]. First, a pilot study determines the effect of dose duration (0.25 – 6.0 hours) on the blanching response for all the formulations of interest. Second, the "pivotal *in vivo* bioequivalence study" evaluates the pharmacodyanmic changes that occur (over 24-28 hours) after the formulation has been removed and the skin cleaned.

The degree of skin blanching has been correlated with drug potency [67] and with the permeation of the corticosteroid through the skin [66, 69-71]. Bioavailability has also been assessed using the technique [69] and formulations have been compared [66, 70, 72, 73]. Attempts to correlate skin blanching results with clinical results [69, 74] have been reported too.

However, the method has its limitations. The precision of chromameter readings has been unfavourably compared with the visual assessment of blanching [68, 75]. Skin colour may be affected by the pressure with which the chromameter is applied, by inhomogeneity in the initial skin colour and by circadian variation [75]. There is evidence that the blanching response can be saturated preventing differences between formulations from being observed [76, 77].

Clearly, the vasoconstrictor assay is only applicable to drugs eliciting the appropriate pharmacological response, and it is approved by the FDA uniquely for topical corticosteroids. No other drug has a 'surrogate' measure of this type although there have

been efforts to determine whether other types of compound may be amenable to a pharmacological assay.

For example, while non-steroidal anti-inflammatory drugs (NSAIDs) do not produce a comparable visual response *per se*, their ability to diminish the action of a subsequently applied vasodilator (such as an ester of nicotinic acid) may be assessed objectively using a chromameter [67, 78] or a laser Doppler velocimeter [79].

Equally, topical retinoids typically induce an increase in transepidermal water loss (TEWL) [80-83] a response which can again be quantified with existing biophysical tools. The same drugs also cause visible irritation [83], which can be assessed instrumentally as described above, and this action has been reported to be better quantifiable than the change in TEWL [83]. These two measurements should be correlated as well, although this has not been shown unequivocally.

1.4.3 Tape stripping

The removal of sequential layers of the stratum corneum using adhesive tapes can be performed with minimum discomfort and relative ease *in vivo,* usually on the volar forearm of healthy volunteers.

When a formulation has been applied to the skin prior to tape stripping, drug may be extracted from the tapes to quantify the amount of drug which has permeated into the SC. Since the SC is the principal barrier to drug absorption, it may be assumed that the (dermatopharmaco)-kinetics (DPK) of drug passage through this layer are related to topical bioavailability [84]. Formulations may be applied for various application times, or stripping delayed after formulation removal to measure SC clearance, and DPK parameters derived. The latter can be used to compare topical formulations and to assess bioequivalence. In the original application of tape-stripping to assess chemical uptake across the skin, good correlations were observed between those amounts recovered on the strips and that which penetrated through to the systemic circulation [85].

Three approaches, summarised schematically in Figure 1-4, have been proposed for the analysis of tape stripping data.

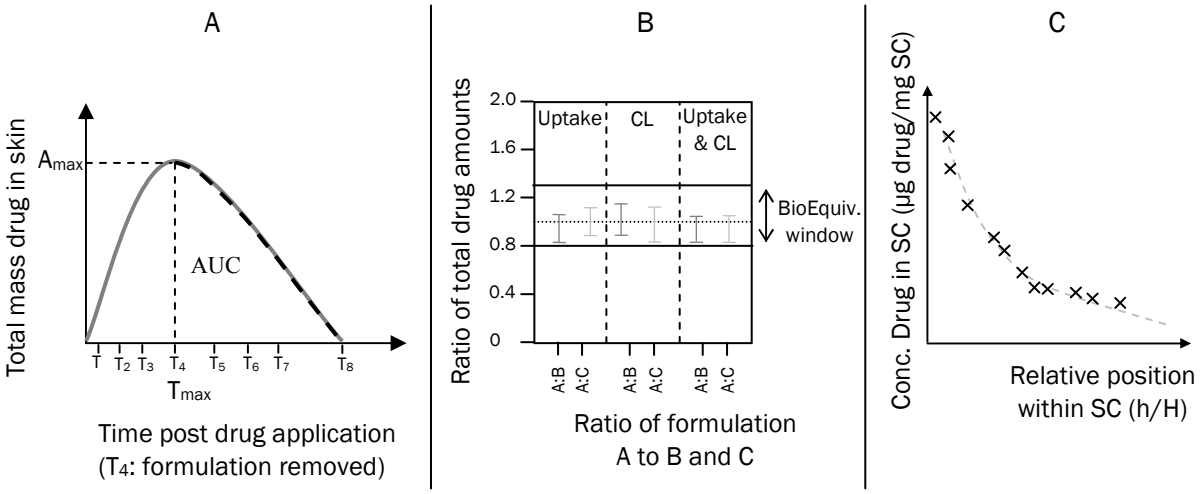

Figure 1-4: Three approaches for the analysis of dermato-pharmacokinetic (DPK) data. A. Original FDA metric. The total amount of drug in the SC after 4 application times (–) and 4 clearance times (- - -) are determined and plotted as a function of time. The maximum amount of drug in the SC (A_{max}), the time at which A_{max} was achieved (t_{max}), and the area under the curve (AUC) are found and used to evaluate and compare formulations. B. 'Two-time' method. Ratio of drug amounts (± 95% confidence interval) for an innovator drug A, compared with two generic formulations, B and C. Two application times (one uptake, and one clearance (CL)) and uptake + CL data combined are considered. To be bioequivalent, the ratio should lie in the 0.8-1.25 bioequivalence window. C. 'Drug in SC profile' method. For each tape, the concentration of drug in SC is plotted against the corresponding relative position within the SC (h/H). The curve is fitted to Eq. 1-9 to generate a best fit profile (- - -) and to extract partitioning and diffusivity parameters.

1.4.3.1 Original FDA dermato-pharmacokinetic (DPK) metric

In 1998, the FDA issued draft guidance for the DPK method to assess the bioequivalence of topical products for application to the skin, except those causing severe SC disruption [86]. The draft guidance required quantification of the total amount of drug in the SC as a function of time, akin to the typical concentration-time profiles of traditional pharmacokinetic studies using blood sampling. Four application times, and four elimination times were required per formulation. From these profiles, area under curve (AUC), C_{max} and T_{max} were evaluated per unit area of skin (Figure 1-4A). For the test products to be bioequivalent, the 90% confidence interval for the ratio of population geometric log means of test to reference should be 80-125% for AUC and 70-143% for C_{max}.

The draft guidance was withdrawn in 2002 [87] following the results of two studies which compared tretinoin gel formulations, specifically Retin-A, the innovator, and Avita, an approved generic product. Avita is qualitatively and quantitatively different, and has been found to be therapeutically inequivalent to Retin-A [88-90]. Both investigations concluded that the formulations were bio*in*equivalent but, worryingly, one measured higher retinoid levels from Retin-A than Avita [89, 90] while the other found the opposite [88]. Naturally, these opposing results prompted concern about reproducibility; furthermore, the adequacy of the method to assess drugs whose target site is beyond the SC was questioned.

Parenthetically, it should be noted that the divergent tretinoin findings were probably due to differences in the areas of SC stripped by the two laboratories. One group stripped an area exactly equal to the application area, while the other stripped an area larger than the treated site. Because one of the formulations was subsequently shown to spread radially on the skin surface during the application period, the drug amounts removed were

different, did not match and the two laboratories revealed opposite conclusions.

With this observation in mind, a subsequent large-scale study was performed comparing the innovator tretinoin gel with therapeutically inequivalent and equivalent formulations [89]. Following the FDA guidance, eight time points were examined per formulation in 49 volunteers, resulting in a total of 1176 sites. The results confirmed the clinical findings for the different gels. In contrast, another DPK study did not confirm the clinical findings for two miconazole nitrate vaginal creams [91], when compared using the FDA's DPK protocol; however, it could be expected that a pharmacokinetic study conducted on volar forearms would be difficult to compare with a clinical study where formulations were applied to vaginal epithelium, due to the inherent differences between these membranes.

In addition to ensuring that the area of SC stripped is less than, or equal to, the area of application, a further modification of the FDA guidance encourages analysing drug content from all tapes. The FDA proposal to discard the first two tape-strips was never validated and typically results in significant amount of compound being ignored. This is important because the first tape-strips invariably take off the largest amounts of SC [92]. Including all tapes, on the other hand, requires that the cleaning of the skin surface at the end of the application period is efficient to ensure that unabsorbed drug (i.e., that not taken up into the SC) is completely removed. This is particularly important for real formulations which may lodge in the 'furrows' of the skin [93]. It appears that an alcohol wipe, similar to that used to sterilise the skin before an injection, may offer a useful solution to this challenge [94].

A further stipulation of the 1998 FDA draft guidance was that, having discarded the first two strips, drug should be quantified in the subsequent ten tape-strips. Two obvious weaknesses of this approach are clear: (i) ten strips do not remove the same amount, nor the same fraction of the SC, in each volunteer, and (ii) ten strips will not remove (in most instances) the entire barrier layer and will not necessarily 'capture', therefore, all the drug taken up into the SC at the sampling time. A simple approach to overcome this problem is to continue stripping until most, if not all, of the SC is removed. Transepidermal water loss (TEWL) measurements provide a convenient means with which to ensure that this is the case [1, 93], as shown in Figure 1-5.

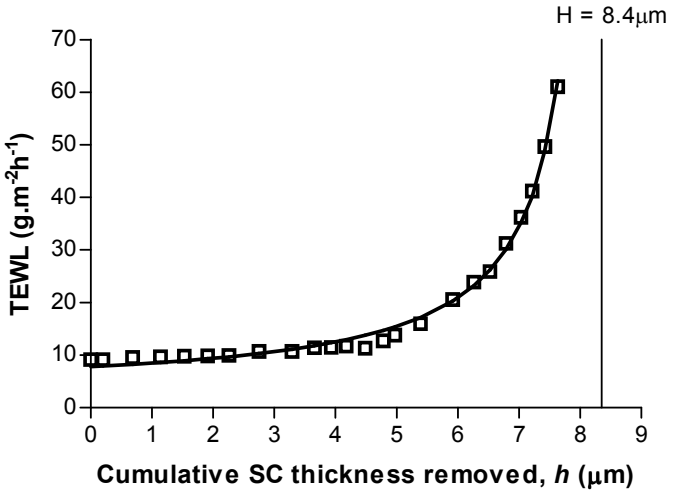

Figure 1-5: Example of experimental data (□) of TEWL against cumulative SC thickness removed, h. A non-linear fit to Eq. 1-8 produces the best fit (▬) and an estimate of the total SC thickness, H.

Other criticisms of the original FDA guidelines are apparent. For example, the requirement for eight time points (four for uptake, four for clearance) is very burdensome in terms of

study time and analytical work. Unlike the situation with oral drug administration, for which the pharmacokinetic parameters are determined by a complex function of absorption, distribution, metabolism and excretion, the uptake phase in a DPK experiment depends only upon drug partitioning and diffusion in the SC, while clearance is only dependent upon diffusion. Likewise, and specific to DPK, the clearance phase only begins after formulation removal at the longest application time [93]. It is a reasonable question, therefore, to ask whether the comparison between formulations requires such a large number of time points. The concomitant difficulty with a requirement for such a large number of test sites is that, for drugs which do not penetrate the SC well, it may be necessary to increase the surface area of application (and hence the area stripped) to have enough drug in the tape strips for reliable quantification. At some point, as a result, there may be insufficient skin surface to perform the experiment according to the FDA guidance. Furthermore, as no replicates are performed, the number of volunteers required to achieve statistical power is large.

Research into alternatives has focused on two areas: (i) comparing the total amounts of drug in the SC at one uptake and one clearance time; and (ii) modelling drug in SC permeation profiles showing drug concentration at progressive depths within the SC.

1.4.3.2 The 'two-time' metric

This method examines only one uptake and one elimination time per formulation. This allows replicate sites to be studied, and higher statistical power to be achieved with fewer volunteers [95]. No tapes are discarded, but tapes are combined and extracted in groups to achieve high concentrations for analysis. The total amount of drug in the SC is measured for each site. The ratio of total drug amounts in the SC from formulation A to B or A to C is determined (Figure 1-4B). The two-time method correctly predicts bioequivalence or bioinequivalence of retinoids [93, 95, 96] and econazole [93, 95].

The retinoid data produced to satisfy the full DPK metric [89, 97] have been reanalysed using four alternative metrics: (a) the sum of total drug amount from all four uptake time sites; (b) the sum of total drug amount from all four clearance time sites; (c) the sum of total drug amount from all uptake and clearance sites; and (d) the total drug amount from each uptake and clearance time separately [93, 96]. Ratios of each of these total amounts of drug in the SC were calculated and used to assess bioequivalence of formulations B (therapeutically inequivalent) and C (therapeutically equivalent) to the innovator (Retin-A). All four metrics confirmed the clinical results. Most interestingly, the fourth metric showed that the ratios were similar for each of the time periods examined individually, suggesting that information regarding bioequivalence may be gleaned from just one uptake and one clearance time. Considering the bioinequivalent gel, the reanalysis highlighted a greater difference from the innovator in the clearance phase than during the uptake phase.

The simplified approach was further tested using econazole nitrate creams, for which the drug's site of action is the SC. The innovator product (Spectazole®, Ortho-McNeil Pharmaceutical Inc., Rariton, NJ, USA) was studied alongside two therapeutically bioequivalent generics (made by Taro Pharmaceuticals USA Inc., Hawthorne, NY, USA and Clay-Park Laboratories Inc., Bronx, NY, USA). The general (controlled strip area; no tapes discarded; site cleaned with alcohol swab; number of tapes determined by TEWL) and specific (one uptake and one clearance time measured; duplicate measurements; tapes combined for analysis) modifications discussed above were all incorporated.

In a preliminary study [93], all creams were studied on three occasions (separated by at least four weeks) in a single volunteer to check the proposed methodology for the subsequent 'pivotal' study, and to assess the intra-subject variability when measurements were made at different times. It was found that using TEWL, to determine

when to terminate stripping, reduced variability in the amounts of SC and drug collected. The variability between sites studied on different occasions was also low compared with the retinoid data discussed above. In the preliminary study only, the tapes were weighed before and after stripping, and the SC thickness was determined at a separate skin site. However, as the SC was almost completely removed (as determined by TEWL), it was not considered necessary to quantify the SC on the tapes in the pivotal study.

The subsequent, larger, 'pivotal' study, involved just 14 volunteers, and confirmed the promising results obtained in the tretinoin reanalysis [93, 98]. When uptake and clearance were considered separately, the 90% confidence interval of the ratio of total drug amount in the SC (generic to innovator), conclusively lay within the 80-125% bioequivalence window, consistent with the clinical studies. The subject-to-subject variability was higher than the intra-subject variability, which may support the comparison of products within each subject [93].

1.4.3.3 Drug permeation profiles across SC

In this approach, the drug concentration profile across the SC is determined by quantification, on each tape, of (a) the amount of drug, and (b) the amount of SC removed, and hence the depth within the barrier at which each drug amount is determined. Analysis of the concentration profile permits parameters describing the partitioning and diffusivity of the drug (reflecting the rate and extent of permeation, respectively) to be estimated and used to compare different formulations.

Quantification of the SC removed on each tape is assessed by weighing the tape pre- and post-stripping. From the mass of SC, and its published density (1g/cm^3) [99], the volume of tissue removed is found. Then, given that the area stripped is known and controlled, the average SC thickness (*h*) removed on each tape (and hence the cumulative depth sampled) can be calculated. If measurements of TEWL are made during the sequential tape-stripping process, the total thickness of the SC (H) can be found by fitting the results to a recently published non-linear model which describes how TEWL increases as the SC barrier is removed [100]:

$$TEWL = B + \frac{D \cdot K \cdot \Delta C}{H - h} \qquad \text{Eq. 1-8}$$

where B is a constant, D is the diffusivity of water in the SC, K is the SC-viable tissue partition coefficient of water, and ΔC is the water concentration gradient across the SC. A typical fitted profile is shown in Figure 1-5.

This analysis represent a refinement of the originally reported approach [101]. For an important subset of volunteers, the TEWL value remains constant as the SC is initially stripped. This could be due to the stratum corneum disjunctum providing a lower contribution to SC barrier function; or structural variability across the SC affecting inter-cellular tortuosity, such that the diffusivity of water across the barrier is not constant. The refined model contains a constant, B, which allows a more precise estimate of H to be determined for sites where an initial plateau is apparent. Furthermore, by analysing the original values rather than reciprocal values, the errors associated with each point are not correspondingly distorted. Both the new approach and the method used earlier have the important benefit of allowing H to be found without having to completely remove the SC. Once TEWL has increased 4- or 5-fold (which corresponds to ~75% removal of the SC), sufficient information has been obtained to reliably find H.

This procedure to evaluate H is typically performed at a site adjacent to the treatment site, to avoid any potential artefacts affecting TEWL, for example evaporation of residual excipients from the formulation. Knowledge of H for each volunteer permits all SC

concentration profiles to then be expressed as a function of *h/H*, or relative depth reached within the SC. This value varies, therefore, between 0 at the skin surface, to 1 at the SC-stratum granulosum interface.

However, the drawbacks of the gravimetric (weighing) approach for the determination of the SC thickness are significant: the procedure is laborious and tedious; reproducibility and precision can be low as the mass of SC is small relative to the mass of the tape; and measurements can be influenced by environmental conditions (e.g., humidity) and static electricity.

Other methods have been investigated. The UV pseudo-absorption of corneocytes has been extensively researched [102], but the correlation between this measurement and the mass of SC is unsatisfactory unless those tapes with an inhomogeneous layer of SC are ignored. Hence, this strategy is inappropriate to accurately measure the position reached within the SC, where the contribution from every tape is required.

The extraction and quantification of proteins from tapes can also measure the amount of SC removed by tape-stripping [103-108]. However, this is a destructive test, often incompatible with drug extraction and quantification. While such an approach may be not useful for dermato-pharmacokinetic studies, a sensitive protein assay would be valuable to validate other techniques. Unfortunately such a sensitive technique does not currently exist.

Attempts have also been made to correlate spectroscopic absorbance (using infra-red light at 850nm) with masses of protein determined from SC extraction and assay [103] Correlation coefficients were high (r^2=0.85) with all 238 tapes included, but issues regarding sensitivity remain, as expressed above.

Most recently, a novel imaging method to quantify SC on tapes has been investigated and the results presented in this thesis. High-resolution images are taken of each tape under carefully controlled optical conditions. Photographs fully illustrating this method are shown in General Appendix I. An image is composed of ~64000 pixels, each of which has a greyscale value associated with it when examined using image analysis software. Statistical analysis on the distribution of these pixels provides a mean greyscale value that offers a relative measure of SC content of the tapes. The approach has been shown to be more rapid, simple, sensitive and precise than either the weighing or UV pseudoabsorption methods (Chapter 4). Further, the greyscale values have been shown to be a useful relative measure of SC amount per tape for the determination of SC total thickness in drug permeation experiments (Chapter 5), and for full dermato-pharmacokinetic studies of acyclovir creams (Chapter 6).

The concentration profiles of a drug as a function of the relative position in the SC (h/H) (Figure 1-4C) have typically been fitted to a solution of Fick's second law of diffusion assuming the following boundary conditions: (i) that an infinite dose is applied; (ii) that the SC is initially drug-free; (iii) that the SC is homogeneous in its barrier properties; and (iv) that the viable epidermis provides a perfect sink for permeating drug. Under these circumstances, the concentration (C_x) of drug, as a function of time (t) and of position (h) in the SC of total thickness (H) is given by:

$$C_x = K_m C_v \left[(1 - \frac{h}{H}) - \frac{2}{\pi} \sum_{n=1}^{\infty} \frac{1}{n} \sin(n\pi \cdot \frac{h}{H}) \exp(-\frac{D}{H^2} n^2 \pi^2 t) \right] \qquad \text{Eq. 1-9}$$

where C_v is the drug concentration in the vehicle. By fitting the concentration profile to this equation, estimates of the drug's SC-vehicle partition coefficient (K_m) and its characteristic diffusion parameter (D/H^2, which has units of $[time]^{-1}$ like a first order rate constant) can be obtained. If H has been separately evaluated, as described above, then

the drug's permeability coefficient (k_p) across the SC, when delivered from the vehicle under consideration, can be calculated from the three measured parameters:

$$k_p = \frac{K_m D}{H} = K_m(\frac{D}{H^2})H \qquad \text{Eq. 1-10}$$

Integration of Eq. 1-9 permits the entire amount of drug in the SC (Q) at time, *t*, to be found:

$$Q = \int_0^1 C_x d\left(\frac{h}{H}\right) = K_m C_v \left[\frac{1}{2} - \frac{4}{\pi^2}\sum_{n=0}^{\infty}\frac{1}{(2n+1)^2}\exp\left(-\frac{(2n+1)^2\pi^2 Dt}{H^2}\right)\right] \qquad \text{Eq. 1-11}$$

This estimation can be compared with the total drug recovered experimentally to check that the SC was indeed mostly removed during the tape stripping process. It can also be appreciated that K_m, D/H^2 and Q provide useful pharmacokinetic parameters with which to characterise and compare formulations. The value of K_m will impact significantly on the extent of uptake (Q), and D/H^2 offers a metric with which to characterise the rate of drug absorption across the SC. It will also be appreciated, once K_m and D/H^2 have been found from the concentration profile at a specific time, t, that these values can be substituted into Eq. 1-11 to predict the evolution of Q as a function of time (offering thereby a means with which to simplify a DPK study considerably).

Experiments, from which drug concentration profiles across the SC have been obtained, are robust and reproducible even with relatively small numbers (n = 4-6 per experiment) of subjects and sites [51, 109-112]. By judiciously using the data derived from individual tapes, information on the rate and extent of drug permeation has been derived both *in vivo* in man and *ex vivo* using porcine skin.

These experiments have allowed both the practical comparison of formulations (such as ibuprofen gels [110]) and the deduction of mechanistic information. For example, the addition of oleic acid to a formulation containing terbinafine, enhanced drug uptake into the SC by increasing the value of D/H^2 but had no effect on K_m [92]. On the other hand, the role of a co-solvent (propylene glycol) on ibuprofen formulations clearly had a major impact on K_m, while D/H^2 was unaltered [51, 111]. In this instance, it was possible to deduce that the excipients had increased the solubility of the drug in the SC, thereby significantly modifying their uptake into the skin [111, 113]. The effect of formulating betamethasone-17-valerate in novel microemulsions (with significant concentrations of different surfactants) showed that Q was dependent on both concentration in the vehicle, and the degree of saturation of the drug in the formulation [112].

Furthermore, as mentioned above, it has also been possible to use values of K_m and D/H^2, derived from SC concentration profiles observed following relatively short periods of exposure, to predict the uptake kinetics over time up to the attainment of steady state conditions using Eq. 1-11 [84, 94, 109] The value of this approach, of course, is the potential to significantly simplify a DPK protocol for the comparison of formulations. As fewer sites are required than for the original FDA guidance, replicates can also increase statistical power.

An important caveat to this strategy, however, is that it is sensitive to the application time chosen for the determination of K_m and D/H^2. This period must be long enough that a measurable profile of drug across the SC is achieved, but should not be too close to steady state because the information about D/H^2 will be lost. The use of too short an application period not only brings with it a potential analytical chemistry problem, it also risks the introduction of an artefact if the exposure time is similar to the time required to effectively strip the skin [114]. Selection of the optimal time at which to conduct the experiment needs to be confirmed by the drug's diffusion lag time across the SC, a

parameter largely determined by its molecular volume (or molecular weight) [93].

1.5 Conclusion

The empirical mathematical model proposed by Potts and Guy provides an adequate prediction of drug permeation based on two easily obtainable physicochemical properties, MW and $\log K_{o/w}$. Drug flux is the product of the permeability coefficient and drug solubility. There are numerous software programs which provide estimates of $\log K_{o/w}$ and solubility although experimental values are most certainly preferred. Mathematical models consider solely the drug molecule of interest, and cannot predict the significant effects of formulation on permeation.

For *in vitro* penetration studies, the use of porcine skin is favoured and provides a useful indication of *in vivo* penetration. The influence of formulation is measurable, and can thus be used for development work.

From a regulatory perspective, *in vivo* measurements are required, and there is certainly enthusiasm to replace subjective clinical trials with a sensitive objective method such as tape stripping. *In vivo* measurements offer scope for objectively comparing formulations. The pharmacodynamic assessment of corticosteroids is approved and improvements made to the tape stripping methodology have shown promise for comparing many drugs, and may offer explanations why formulations perform differently.

1.6 Notes

This chapter has been submitted for publication to the *Expert Opinion on Drug Delivery* with Prof. R.H. Guy as co-author.

Chapter 2

The determination of stratum corneum thickness – an alternative approach

2 The determination of stratum corneum thickness – an alternative approach

2.1 Abstract

The individual thickness of the stratum corneum (SC) is required to normalize drug permeation profiles in dermato-pharmacokinetic studies. The thickness is often estimated using tape-striping combined with transepidermal water loss measurements. A linear transformation of Fick's first law is used to relate the progressively thinner barrier with the corresponding increase in transepidermal water loss and to estimate the thickness by linear regression. However, the data from an important subset of subjects are poorly fitted to this linear model. This is typically due to the removal of loose outer layers of SC, which do not contribute significantly to barrier function. This work proposes two alternative non-linear models. All three models were used to fit data from 31 in vivo tape-striping experiments and their outcomes and goodness-of-fit compared. The results suggest that the linear model may overestimate the SC thickness and is open to subjectivity regarding the selection of data points to be fitted. The non-linear models satisfactorily fitted all the data, including all data points. No significant differences were found between the thicknesses derived from the two non-linear models. However, the analysis of the goodness-of-fit of the models to the data suggests a preference for a baseline-corrected approach.

2.2 Introduction

The individual thickness of the stratum corneum (SC) is required in order to normalise drug penetration profiles from different volunteers during dermato-pharmacokinetic studies. Bioavailability describes the rate and extent to which a drug, in an active form, reaches its target site. In the case of topical formulations seeking a local effect, the target site is the skin. By measuring the 'rate' and 'extent' of drug penetration into the skin, so-called dermato-pharmacokinetic parameters may be derived. These parameters and the drug penetration profiles provide information with which to assess bioavailability and demonstrate bioequivalence between different formulations. It has been suggested that since the SC is the principal barrier to drug absorption, that kinetic data of drug passage through this layer can be related to bioavailability in the target tissue [84, 86, 115].

The tape stripping technique has attracted considerable interest from regulatory bodies, such as the U.S. Food and Drug Administration, as a means to determine dermato-pharmacokinetic parameters, and ultimately test bioequivalence between formulations [86, 115]. Tape stripping involves the sequential removal of layers of the SC using adhesive tapes. It can be performed with minimum discomfort and relative ease *in vivo*. Typically, formulations are applied to the accessible volar forearm, which has a SC thickness shown to be consistently between 10-20 µm for most volunteers [116]. Restoration of the 80-90% of SC's barrier function is complete within 3 days [117] and transepidermal water loss (TEWL) values return to normal after eight [118] to eleven [119] days.

In 1998, the FDA issued guidance on the tape stripping technique for evaluating drug penetration through the SC [86]. It was later withdrawn when the comparison of three products by two laboratories resulted in contradictory outcomes. Since then, some problems with the original guidance have been identified: (i) discarding two tape strips has lost favour, as drug in these outer layers would probably become available for

absorption eventually [84, 120] (ii) in an attempt to relate the drug concentration to a particular depth within the SC, and in order to normalise the data derived from different volunteers [51, 84, 92, 109, 120, 121], the total thickness of the SC is now measured [101, 122].

An exact measurement of the SC thickness (H) is impossible in a completely non-invasive way. However, a solution of Fick's first law allows the easily measurable TEWL value from an intact SC, to be related to several SC parameters [1, 4]:

$$TEWL_0 = \frac{D \cdot K \cdot \Delta C}{H} \qquad \text{Eq. 2-1}$$

Where $TEWL_0$ is the baseline TEWL, D is the diffusion coefficient of water in the SC; K is the SC-viable tissue partition coefficient of water; ΔC is the water concentration gradient, and H is the thickness of the SC. This equation assumes that the SC is the main barrier to water loss, and that it provides a homogeneous barrier to water diffusion, justified by Kalia et al. [1].

Therefore, once a certain cumulative thickness of the SC, *h*, is removed by tape stripping, the TEWL will increase as follows:

$$TEWL = \frac{D \cdot K \cdot \Delta C}{H - h} \qquad \text{Eq. 2-2}$$

h is calculated from the area of strip; mass of SC on tape; and the density of the SC (~1g/cm^3 [99]). A reciprocal transformation of equation Eq. 2-2 provides a linear expression which relates 1/TEWL to h:

$$\frac{1}{TEWL} = \frac{H}{D \cdot K \cdot \Delta C} - \left(\frac{1}{D \cdot K \cdot \Delta C}\right) h \qquad \text{Eq. 2-3}$$

Experimental data expressed according to Eq. 2-3 should yield a single straight line that can be analyzed by simple linear regression. Extrapolation of this linear regression to 1/TEWL = 0 yields h = H, allowing H to be found.

However, data from a significant subset of subjects are not satisfactorily fitted by this Linear Model (LM). In these cases, representation of the data according to Eq. 2-3 yields an initial plateau followed by a declining straight line. This suggests that the barrier function to water loss across the SC is not homogeneous. It could be hypothesized that this initial plateau corresponds to the removal of the stratum corneum disjunctum; the looser outer SC layer [123-126] which does not provide a significant barrier to water loss. It follows that its removal would contribute a significant mass change without a corresponding increase in TEWL. Alternatively, variation in corneocyte size or arrangement at different SC depths may also account for variability in water diffusivity across the barrier. Thus, the Linear Model (Eq. 2-3) which assumes that the SC barrier properties are homogeneous, cannot reflect experimental findings accurately.

Another disadvantage of the LM results from the mathematical procedure: upon inversion of the TEWL values into 1/TEWL, there is also an inversion of the errors associated with each data point, which can skew the goodness-of-fit of the linear regression [127, Section 5.2.4].

The aim of this work was to develop an improved model which avoids the problems mentioned above. We propose first the Baseline-corrected Non-Linear (BC-NL) model (Eq. 2-4) which (a) fits directly TEWL versus cumulative thickness data, thus avoiding the errors associated with the reciprocal transformation [127, Section 5.2.4], and (b) incorporates a baseline parameter, B, to reflect the initial plateau during which TEWL remains constant despite removal of some layers of SC, observed for some

volunteers/sites.

$$TEWL = B + \frac{D \cdot K \cdot \Delta C}{H - h} \qquad \text{Eq. 2-4}$$

The second model proposed is the "Simple Non-Linear" (S-NL) model (Eq. 2-2) which also fits the data directly to Fick's first law equation (Eq. 2-2) but does not incorporate a baseline factor.

To decide on the best approach for estimating the SC thickness we examined data sets collected from different volunteers on different occasions. We evaluated the performance of the three models and compared their outcomes. Each set of data (TEWL versus cumulative thickness removed) has been analyzed separately using each of the three models: LM, S-NL and BC-NL. The SC thickness (H) estimated for each volunteer by each model is compared, along with a discussion of the goodness–of–fit, and the relative merits and weaknesses of each method.

2.3 Materials and Methods

2.3.1 Subjects

18 healthy volunteers (3 male, 15 female, age range 22-43 years), with no history of dermatological disease, participated in the study. Ethical approval was granted by Salisbury Local Research Ethics Committee, the Declaration of Helsinki protocols were followed, and written informed consent was obtained from all volunteers. A total of 31 sites were examined over a period of 2 years. Participants refrained from using any topical products on the test area on the day of the experiments.

As TEWL measurements may be affected by sweating or the changes to the relative humidity or temperature of the laboratory, the volunteers rested in the room for at least 15 minutes prior to taking first TEWL measurement; the experiment was completed in less than 1 hour; and repeated initial TEWL measurements were taken until they stabilised. Temperature and relative humidity in the study room was measured before each experiment, and the mean (±SD) were 21.9±1.5°C and 37.8±9.7% respectively.

Subjects were given code numbers (1 to 18) and nine subjects participated only once in the study. Six subjects participated twice; Subjects 9 and 14 participated thrice, and subject 8 participated four times. Repeated participation was coded with a letter, for example subject 1a and 1b for the first and second participation of subject 1. Repeat participation using the same arm was delayed by at least 1 month, which is sufficient for barrier regeneration [117-119].

2.3.2 Tape stripping procedure

Two tapes, with pressure applied using a roller, were taken and discarded. These pre-tapes are also taken before all dermato-pharmacokinetic experiments in our laboratories, to remove and exogenous substances and prepare the skin surface in a systematic way. A plastic template was applied, to delimit a constant area to be stripped. An initial TEWL measurement was taken with a closed-chamber evaporimeter (Biox Aquaflux AF102, Biox Systems Ltd, London, UK; measurement range 0-100 $g.m^2h^{-1}$; resolution ±0.05 $g.m^2h^{-1}$; the probe was applied for a minimum 60 s, the TEWL was obtained once the mean of 10 successive measurements had a CV<1%).

A pre-weighed (Sartorius Microbalance SE-2F, precision 0.1µg; Sartorius AG, Goettingen, Germany) piece of Scotch Book tape 845 (3M, St Paul, MN) was placed over the template and adhesion to the skin was assured systematically with a set number of rolls with a roller. The tape was removed swiftly and another TEWL measurement taken. The sequence was repeated until the TEWL value was 3-4 times its initial value (usually 60-80g.m^{-2}h^{-1}). All tapes were reweighed following completion of the stripping procedure, with prior removal of any hairs as necessary. To correct for any variations in environmental conditions, and the change in mass that may occur with time, 3-5 blank correction tapes were weighed at the same times as the tapes used for stripping. The change in mass of these blank tapes was used to correct the calculated mass of SC on each tape.

2.3.3 Models to estimate SC thickness, H

2.3.3.1 Linear model (LM)

Linear regressions were performed on each data set of 1/TEWL versus cumulative SC thickness removed, using GraphPad Prism® (version 4.00 for Windows, GraphPad Software, San Diego, CA). All the data points were fitted into the regression unless stated otherwise. All the slopes were significantly non zero ($p<0.0001$) which confirmed a statistically significant relationship between 1/TEWL and cumulative SC thickness removed.

2.3.3.2 *Non-linear (S-NL and BC-NL) models*

All data sets were evaluated separately using WinNonLin® software (Version 5.1, Pharsight Corporation, Mountain View, CA) using an ASCII user-defined model written for models S-NL and BC-NL. In all cases, no data points were excluded; uniform weighting was applied; no bounds were used; and the initial parameter estimates were: H = last *h* value + 1; (D.K.ΔC) = 30; B = initial TEWL value before stripping (for BC-NL model only). Iterations were continued until the relative change in weighted sum of squares was <0.0001. The model derived parameter estimates were used as the new 'initial' values in the model, and the model rerun until there was no change in the parameter output. All parameter estimates are those from the final iteration of the model, with the smallest resultant residual sum-of-squares; however, usually, no change was seen after the first run, suggesting the modelling was stable. All statistical tests for comparisons between parameter outputs for different data sets were done using GraphPad Prism®.

2.3.4 Evaluation of goodness-of- fit of each model

The statistical evaluation of 'goodness-of-fit' of a model is not a trivial matter, especially in the case of non-linear models [127, 128]. Obviously, a first step involves a visual graphical assessment of how well the model fits the experimental values. Models are usually evaluated for their *accuracy*; but this was not possible as there are no independent methods to obtain SC thickness that can be considered the "gold standard". Thus, in an effort to evaluate objectively all three models, a series of statistical tools were considered concurrently.

First of all, the *precision* of the parameter estimates is evaluated using the coefficient of variation (CV, %), which relates the parameter's standard error of the regression (SER) to its estimate (p):

$$CV(\%) = \frac{SER}{p} \cdot 100 \qquad \text{Eq. 2-5}$$

The SER is an absolute measure whereas CV is a relative error that can be used to compare the three models. Normally, the model resulting in the smaller CV should be preferred.

Next, the two non linear models were compared; it would be expected that the BC-LN would fit the data better than the S-NL model, simply because it has one extra parameter. Thus, two statistical tools, the Akaike Information Criterion and an F-test, that take into account the difference in the number of parameters, were used to compare objectively the two non-linear models.

The Akaike Information Criterion (AIC) for the S-NL and BC-NL models was calculated for each of the 31 data sets separately as follows [127]:

$$AIC = N_{obs} \cdot \ln(WRSS) + 2 \cdot N_{par} \qquad \text{Eq. 2-6}$$

where N_{obs} is the number of data points of each data set; WRSS is weighted residual sum of squares (provided by WinNonlin®); N_{par} is the number of parameters which were 2 ("DKΔC" and "H") and 3 ("DKΔC", "B" and "H") for the S-NL and the BC-NL models respectively. The absolute value of the AIC for a single model on its own is meaningless; hence the AIC is always used to compare several models. Briefly; the model with the lowest AIC is more likely to be correct. Furthermore, the probability that the BC-NL model is correct, rather than the S-NL model, for a given data set can calculated via the difference in the AIC scores, $\Delta AIC = AIC_{BC\text{-}NL} - AIC_{S\text{-}NL}$, as follows [128]:

$$\text{Probability} = \frac{e^{-0.5 \cdot \Delta AIC}}{1 + e^{-0.5 \cdot \Delta AIC}} \qquad \text{Eq. 2-7}$$

The S-NL and BC-NL models can be considered as nested models; that is, the BC-NL model can be considered an extension of the other. Crucially, both models would be identical if a single parameter, B, is set to zero. Under these conditions, an F test [127, 129] can examine the effect of the additional parameter on the WRSS. The *F** value was calculated separately for each data set:

$$F^* = \frac{df_2 \cdot \left| WRSS_1 - WRSS_2 \right|}{\left| df_1 - df_2 \right| \cdot WRSS_2} \qquad \text{Eq. 2-8}$$

where: df_1 and df_2 are the degrees of freedom for the S-NL and BC-NL models respectively, and $WRSS_1$ and $WRSS_2$ the corresponding weighted residual sum of squares (both provided by WinNonlin®). The *F** was then compared to critical values (F_{table}) taken from F tables [130] for a two-tailed test, with a p value of 0.05, column value = $|df_1\text{-}df_2|$; and row value = df_2. If *F** is greater than F_{table}, it can be concluded that the full model is better than the reduced model.

The AIC and the F test consider which model, S-NL or BC-NL, may be more appropriate for each data set individually. However, an overall preferred model may be suggested based on the preferred model selected for all 31 cases.

2.4 Results and Discussion

TEWL was measured before and after each tape strip in 31 experiments. The average baseline (before stripping) and final (after stripping) TEWL values, along with their standard deviations, were 10.12 ± 2.65 $g.m^{-2}h^{-1}$ and 61.48 ± 18.78 $g.m^{-2}h^{-1}$ respectively. This increase in TEWL is due to the barrier disruption and is in agreement with previous work [1, 101, 122, 131].

2.4.1 Evaluation of the linear model (LM)

The first method considered was the linear model, LM, which has been widely used [51, 84, 92, 101, 109, 110, 121] since its introduction [1, 122]. The linear transformation of Fick's first law (Eq. 2-3) predicts a straight line when the 1/TEWL values are plotted versus the cumulative thickness of the SC removed (h). Figure 2-1.a shows example plots for two volunteers: a single straight is observed for both subjects; the linear regression fits the experimental data well (R^2=0.99) and the thickness of the SC is easily extrapolated from the regression line.

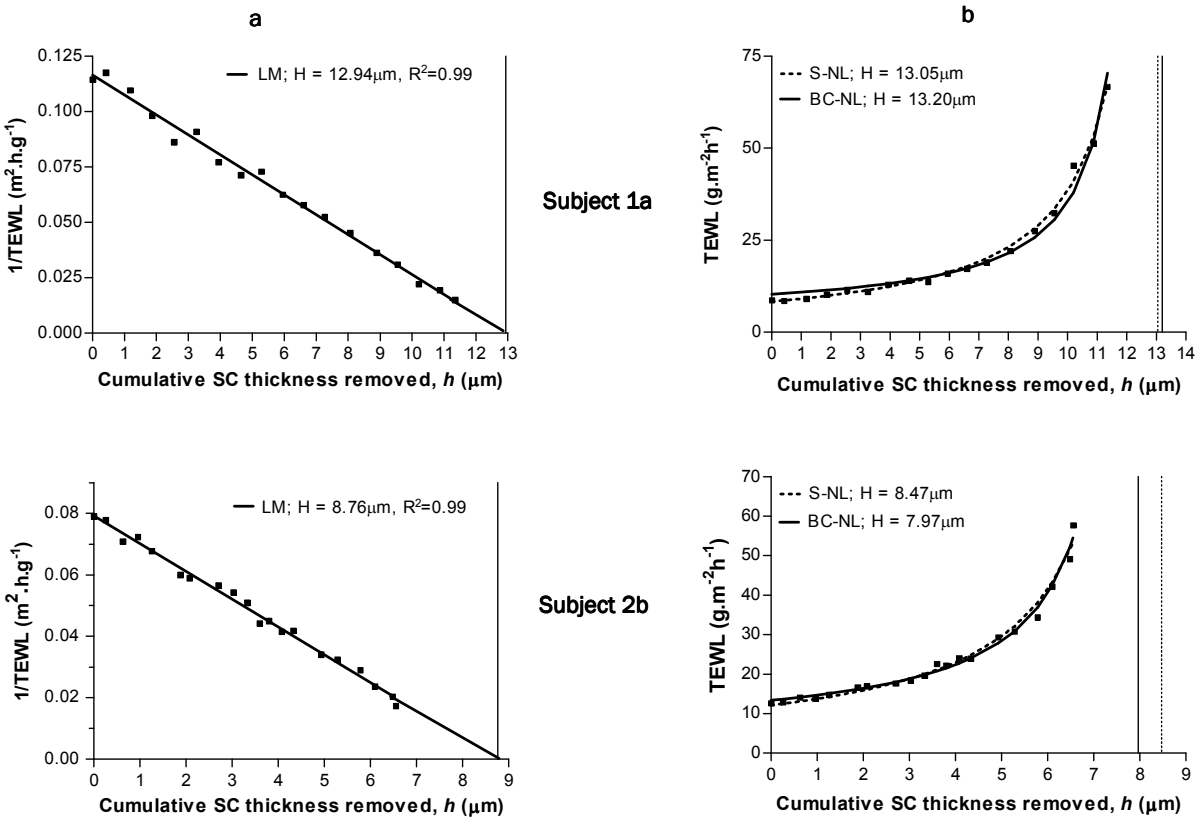

Figure 2-1: Estimation of SC thickness (H) by the linear model (panel a) and by the simple (S-NL) and baseline corrected (BC-NL) non-linear models (panel b) for subjects 1a and 2b. [■] Experimental data points. Panel a: [–] prediction by LM. Panel b: [–] prediction by BC-NL; […] prediction by S-NL model. The vertical lines mark the value of H estimated by the LM (panel a, solid line), the S-NL (panel b, dotted line), and the BC-NL (panel b, solid line).

However, there were several sets of data which were not satisfactorily described by the linear model. Figure 2-2.a illustrates five of these examples which show an initial plateau before a clear linear descent is observed. Clearly, the LM fails to fit all the experimental data to the regression line. Worryingly, there is a clear potential for overestimation of H as the slope of the regression line is shifted upwards to include the initial plateau as Figure 2-2 illustrates. The dilemma is how to deal with this type of data which was apparent in approximately half of the 31 experiments performed.

a

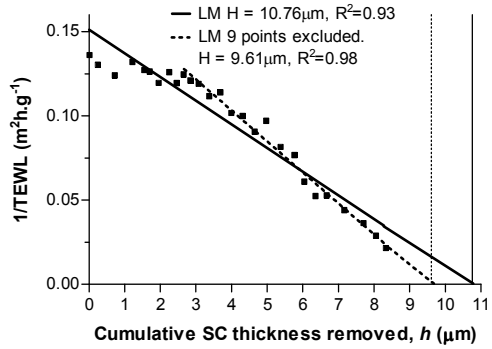

b

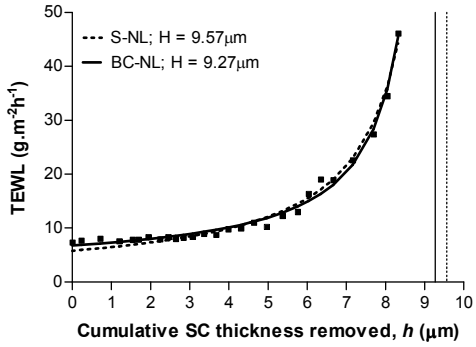

Subject 3a

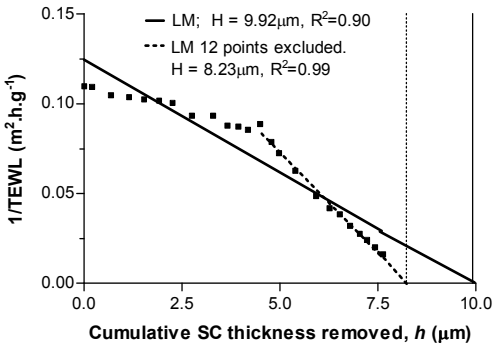

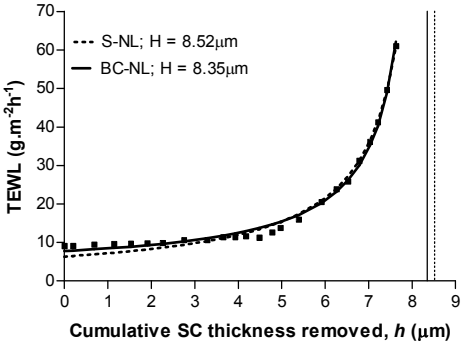

Subject 5a

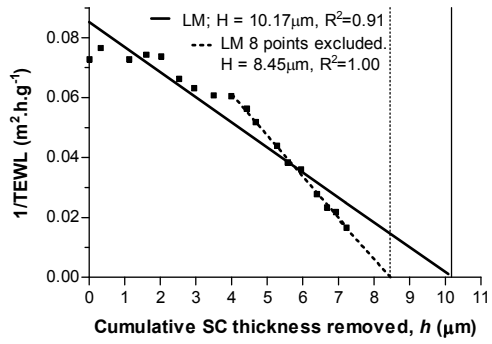

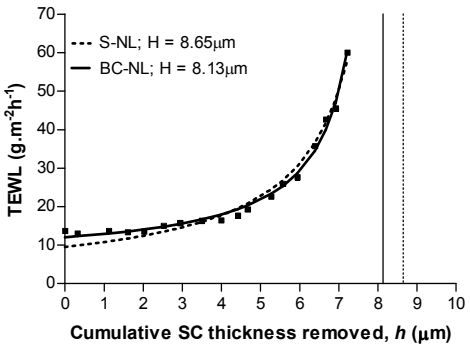

Subject 3b

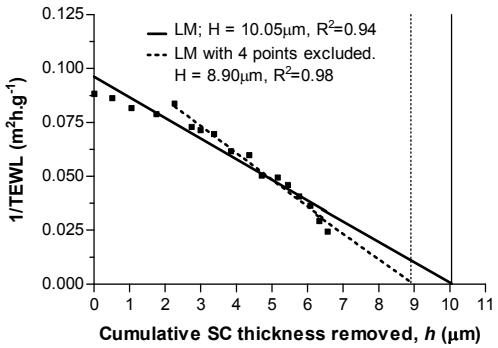

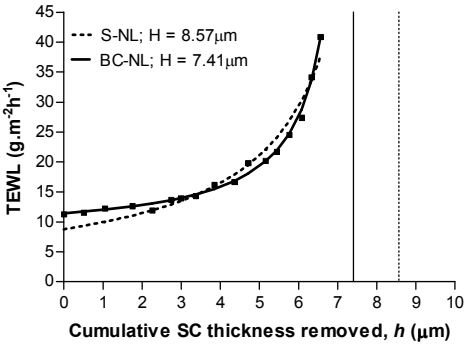

Subject 6

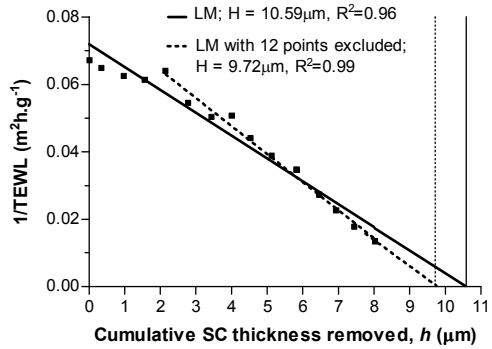

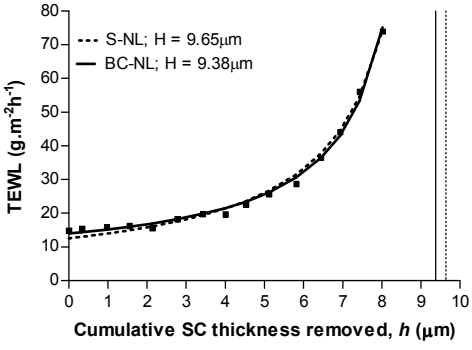

Subject 7a

Figure 2-2: Estimation of SC thickness (H) by the linear model (panel a) and by the simple (S-NL) and baseline corrected (BC-NL) non-linear models (panel b) for five subjects. [■] Experimental data points. Panel a: [–] prediction by LM including all experimental data; […] prediction by LM excluding a number of data points. Panel b: [–] prediction by BC-NL; […] prediction by S-NL model. The vertical lines mark the value of H estimated by: LM – all data points (panel a, solid line), LM – excluding data points (panel a, dotted line), the S-NL (panel b, dotted line) and the BC-NL (panel b, solid line).

Obviously, the key question is the reason for this initial plateau. We could not find any trend (age, gender…) that would assign this plateau to any "skin type". In any case, we hypothesised that the initial plateau is due to loose outer portions of SC, which are soon to be lost through natural shedding. These loose portions seem to constitute a minor barrier to water loss, but do represent a considerable mass when removed. This agrees with the heterogeneous nature of the SC structure [123, 124, 126, 132]; where the SC compactum evolves into the SC disjunctum as the corneocytes migrate towards the surface, and progressively loose their corneodesmosome links. The cells of the SC disjunctum do not contribute significantly to the water barrier function of the SC. Therefore, when the SC disjunctum layers are removed, a large mass change, and hence cumulative SC thickness removed, *h*, is registered, without a corresponding increase in TEWL, resulting in the plateau. Since these layers represent a poor barrier to water loss, it can be argued that they would also constitute a reduced barrier with regards drug ingress, and hence should be considered separately from the main SC barrier during the estimation of H. Alternatively, potential variation in corneocyte size or shape with SC depth could affect inter-cellular tortuosity, and lead to variability in water diffusivity across the barrier.

A potential solution is to subjectively exclude these initial plateau values and fit the rest with LM. An example of such procedure is illustrated in Figure 2-2.a. The exclusion of the initial plateau values provides higher R^2 values, and an 8.2 – 17% change (0.87-1.72 μm) in H. Because the regression line fits only the declining straight line, its gradient shifts downward, resulting in lower values of H as shown in Figure 2-2.a. It should be noted that these fits are produced through the exclusion of a considerable proportion of data points: 9 out of (27) total data points; 12 (24); 8 (18); 4 (17); and 4 (15) for the subjects sequentially shown in Figure 2-2.a. Unfortunately, is impossible to define an algorithm to exclude these points objectively, thus, a researcher would be forced to subjectively exclude points by eye in order to improve the linear fit if this approach was adopted. This potential subjectivity in deciding upon the portion to be fitted by the regression constitutes an important disadvantage of the LM. Clearly, any step of a future dermato-pharmacokinetic "modus operandi" aiming to compare topical formulations in an objective way, should allow minimal room for inter-laboratories or inter-researcher variability. Therefore, the crucial step of H determination, in order to normalise data from different volunteers, should clearly be standardised.

2.4.2 Evaluation of the non-linear models: S-NL and BC-NL

To attempt to remedy the problems associated with the LM, namely the poor fit and the potential subjectivity of removing data points, two alternative non-linear models have been proposed: the Simple Non-Linear (S-NL) (Eq. 2-2) and the Baseline-Corrected Non-Linear (BC-NL) models (Eq. 2-4) which were applied to all data sets with no data points excluded. The first step to evaluate their performance is a visual assessment of the model's predicted fit as compared to the raw data points. Figure 2-1 and Figure 2-2, panel b, show 7 examples of data fitted with the S-NL and BC-NL models. The predicted line fit the experimental data closely in all cases, independent of the existence of an initial plateau (Figure 2-2). A comparison of the two non linear models, suggests that the

BC-LN model fits the earlier TEWL values slightly better, which was the rationale behind the introduction of the baseline parameter, B, into this model. The baseline parameter allows some vertical translocation of the resultant fit, and thus improves the fitting in some cases (subjects 3a, 5b and 6).

Figure 2-1 shows two sets of data 1a and 2b which were well fitted by all three models. The estimated total SC thickness for subject 1a was 12.9±0.19μm (LM), 13.1±0.07μm (S-LN) and 13.2±0.16μm (BC-NL). The estimated H for subject 2b was 8.8±0.12μm, 8.5±0.10μm and 8.0±0.17μm according to the LM, the S-NL and the BC-NL models respectively. Thus, when there is no initial plateau, namely for subjects having little SC disjunctum, the three models fit well the data and the values of H obtained are very similar. Other sets of data that showed this behaviour are highlighted on Table 2-1.

Next, we should consider the data shown in Figure 2-2, or cases showing an apparent initial plateau. Contrary to the LM, both non-linear models fit the data very well. Both non-linear models resulted in very close values of H which were approximately 1μm smaller than those estimated by the linear model. Interestingly enough, when values are excluded from the linear fitting the differences become smaller. For example, the estimated values of H for subject 5a were 8.5±0.04μm (S-NL) and 8.4 ± 0.05μm (BC-NL); clearly lower that that estimated by linear regression 9.9 ± 0.45 μm. However, when 12 points were excluded from the linear regression, the value of H decreased to 8.26 ± 0.07μm, very similar to the non-linear estimates. A similar trend is observed for all the cases shown in Figure 2-2 and for a total of 16 of the 31 cases analyzed. This suggests that the three models would agree on a common value for H if the linear regression is applied only to the latter linear portion of the data. However, as discussed before, excluding the initial plateau values, and deciding on linearity is a process subjected to researchers' subjectivity. On the contrary, the two non-linear models fit all the experimental data letting the model to correct for the baseline in an objective way.

The values of H estimated by the S-NL and BC-NL models were very similar in cases 3a, 5a, 5b and 7 (Figure 2-2). Some differences between the S-NL and the BC-NL models are illustrated by Subject 6: the S-NL prediction misses six experimental points, while the BC-NL misses only two; the latter model is probably aided by the vertical translocation permitted by the baseline parameter. This results in a slightly larger (1.16μm) difference in the values of H estimated by the two non linear models in this case.

2.4.3 Variation in H estimated by each model

Before discussing the goodness of fit of the three models by statistical tools we should discuss whether H, the parameter of interest for dermato-pharmacokinetic studies, is significantly different when estimated by different models. A compilation of the H estimates together with the standard error of the regression (SER) and the coefficient of variation (CV(%)) for the 31 data sets are presented in Table 2-1. The H and corresponding SER may be compared graphically in Figure 2-3. A matched-observations Friedman test (equivalent to a non-parametric 1-way matched ANOVA) followed by the corresponding Dunn's post-test was used to compare the values of H estimated by the LM (with no data excluded), the S-NL and the BC-NL models. The test concluded that the value of H estimated by the linear model was statistically significantly greater than that derived from the S-NL ($p<0.01$) and the BC-NL ($p<0.001$) models. In other words, the linear model tends to overestimate the thickness of the SC. On the other hand, although the S-NL model tends to estimate a higher value of H than the BC-NL model, the differences between the non-linear models did not reach the level of statistical significance ($p <0.05$).

Table 2-1 also shows the coefficient of variation (CV%) associated with each value of H

and model. It is interesting to note that in 28 of the 31 cases considered, the highest relative error was associated with the linear method. The performance of the linear model can be improved but only via the exclusion of some data points. Overall, these results suggest that the two non-linear models proposed here offer a better-quality fit than the linear model; allowing a better estimation of the parameter H (lower CV%), in an objective way.

Subject[1]	LM			S-NL			BC-NL			ΔAIC[2]	Probability (%) BC-NL is preferred	F* / F_{table}
	H (µm)	SER	CV (%)	H (µm)	SER	CV (%)	H (µm)	SER	CV (%)			
1 a	12.9	0.19	1.5	13.1	0.07	0.6	13.2	0.16	1.2	0.39	45	1.4 / 6.2
1 b*	20.1	0.53	2.7	17.2	0.33	1.9	15.4	0.09	0.6	-37.74	100	101.5 / 56.0
2 a	11.5	0.25	2.2	11.4	0.15	1.3	11.5	0.34	3.0	1.84	29	0.1 / 5.8
2 b	8.8	0.12	1.4	8.5	0.10	1.2	8.0	0.17	2.2	-3.90	88	5.8 / 6.0
3 a*	10.8	0.41	3.8	9.6	0.06	0.6	9.3	0.08	0.8	-10.93	100	14.7 / 5.7
3 b	6.4	0.19	2.9	5.8	0.03	0.5	5.7	0.05	0.8	-2.43	77	4.2 / 6.0
4	10.5	0.25	2.4	10.1	0.06	0.6	9.9	0.13	1.3	-0.88	61	2.6 / 6.0
5 a*	9.9	0.45	4.5	8.5	0.04	0.5	8.4	0.05	0.6	-11.50	100	15.85/ 5.8
5 b*	10.2	0.51	5.0	8.6	0.10	1.2	8.1	0.08	1.0	-18.97	100	33.1 / 6.2
6*	10.0	0.44	4.4	8.6	0.20	2.3	7.4	0.07	1.0	-32.39	100	91.8 / 6.3
7*	10.6	0.41	3.8	9.6	0.08	0.8	9.4	0.11	1.2	-4.31	90	6.3 / 6.6
8 a*	7.4	0.29	3.8	6.8	0.07	1.0	6.5	0.05	0.7	-18.50	100	36.6 / 6.8
8 b	13.0	0.37	2.8	11.8	0.14	1.2	11.3	0.16	1.4	-7.19	97	9.9 / 6.1
8 c	10.0	0.20	2.0	9.5	0.04	0.5	9.5	0.08	0.8	1.36	34	0.5 / 9.9
8 d*	7.5	0.28	3.8	6.5	0.17	2.7	5.7	0.05	1.0	-26.04	100	70.5 / 6.7
9 a *	13.0	0.88	6.8	10.4	0.14	1.4	10.0	0.12	1.2	-9.29	99	13.2 / 6.3
9 b	8.8	0.14	1.5	8.7	0.05	0.6	8.8	0.09	1.1	-0.02	50	1.8 / 6.3
9 c	12.4	0.27	2.2	11.7	0.11	0.9	11.2	0.11	1.0	-10.86	100	15.0 / 5.9
10 a	6.4	0.17	2.6	5.9	0.04	0.7	5.7	0.05	0.9	-7.40	98	10.4 / 6.4
10 b*	8.6	0.33	3.9	7.2	0.06	0.9	7.0	0.05	0.7	-12.85	100	19.0 / 6.1
11	6.2	0.16	2.6	6.0	0.04	0.8	6.0	0.09	1.5	0.21	47	1.5 / 6.4
12 a*	13.1	0.38	2.9	11.3	0.10	0.9	10.8	0.07	0.7	-24.33	100	38.5 / 5.7
12 b	14.5	0.24	1.7	15.2	0.06	0.4	15.4	0.10	0.7	-9.18	99	12.6 / 5.9
13	8.1	0.25	3.1	7.6	0.05	0.6	7.6	0.09	1.2	1.76	29	0.2 / 6.2
14 a*	16.2	0.52	3.2	13.9	0.32	2.3	12.0	0.07	0.6	-53.67	100	192.6 / 5.8
14 b*	18.1	0.68	3.8	17.8	0.12	0.7	17.2	0.08	0.5	-25.40	100	56.2 / 6.3
14 c*	9.4	0.27	2.9	9.6	0.16	1.7	10.6	0.66	6.2	-3.41	85	5.3 / 6.0
15*	12.7	0.27	2.2	12.0	0.11	0.9	11.4	0.13	1.2	-10.28	99	14.2 / 5.9
16	9.1	0.20	2.2	8.5	0.06	0.7	8.4	0.09	1.1	-2.77	80	4.5 / 6.5
17*	8.8	0.34	3.9	7.5	0.09	1.2	7.1	0.05	0.7	-23.63	100	51.5 / 6.4
18	5.6	0.22	4.0	5.0	0.12	2.4	4.4	0.13	2.8	-7.81	98	11.1 / 6.6
Average	10.7	0.30	3.1	9.8	0.10	1.1	9.5	0.10	1.3		84	
H±SD[3]	10.7 ± 3.4			9.8 ± 3.2			9.5 ± 3.1					

Table 2-1: Estimation of SC thickness (H) by the linear model (LM) and by the simple (S-NL) and baseline corrected (BC-NL) non-linear models for 18 subjects (31 experiments).

[1] Cases were a plateau was apparent to the authors are indicated with *.

[2] ΔAIC=AICBC-NL – AICS-NL

[3] Average H (µm) with standard deviation (SD) for 31 volunteers measured according to the three models.

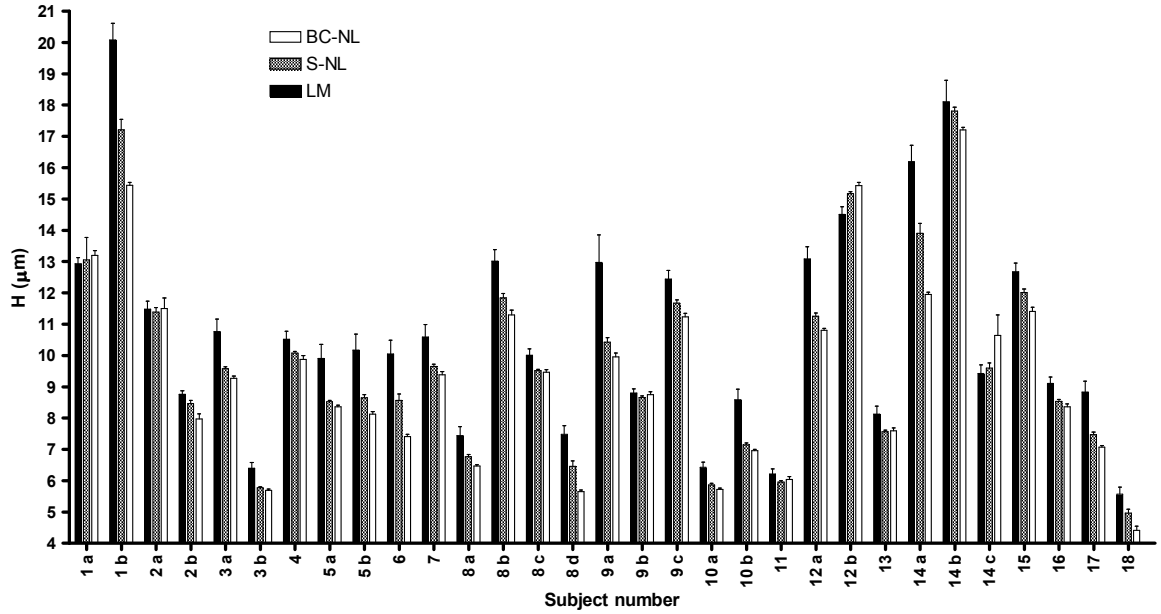

Figure 2-3: Stratum corneum thickness, H (µm) as determined by the LM, S-NL, and the BC-NL models, for 18 different volunteers at 31 different sites. The error bars show the standard error of the regression (SER) associated with each estimate.

2.4.4 Comparison of goodness-of-fit of the non-linear models, S-NL and BC-NL

Finally, we should discuss the relative performance of the two non-linear models. The S-NL model fits directly experimental values (TEWL and cumulative thickness removed) to Fick's first law. This basic difference already provides a certain advantage over linearly fitting the transformed values of water loss (1/TEWL) [Reference 127, Section 5.2.4]. The baseline parameter was built into the BC-NL model to describe the removal of the outer SC layers that do not significantly contribute to the barrier to water loss. However, the BC-NL model would be expected to fit the data better, and have smaller residual sum-of squares than the S-NL model simply because it has one extra parameter. Therefore, to decide which model was superior, the use of some statistical tools that take into consideration the number of parameters used by each model was required, as outlined in Materials and Methods. Two statistical tools: the AIC and an F Test (Table 2-1) (described in Materials and Methods) were used to compare the non linear models. The F test performed here is only applicable for nested models (i.e., where one model (S-NL) can be considered a simplified version of a more complex one (BC-NL). The value of F* calculated is compared to a critical F value obtained from published F tables [130]. If the value of F* is bigger than the critical value, the null hypothesis can be rejected and we can accept that the more complex model fits better the data. Table 2-1 shows that in 19 of the 31 cases, the BC-NL model is preferred ($p<0.05$).

The AIC offers complementary information as it tells us the probability of the preferred model being the correct one. The value $\Delta AIC = AIC_{BC\text{-}NL} - AIC_{S\text{-}NL}$ was calculated as described in materials and methods and the values are shown in Table 2-1. The model with the lowest AIC is considered superior, therefore negative values of ΔAIC indicate that the BC-NL is preferred. The magnitude of this difference can be used to determine the probability of this assumption being correct via Eq. 2-7. For simplicity, Table 2-1 always shows the probability of the BC-NL model being the correct one. For example, for subject 1b, the negative value of ΔAIC (-37.74) indicates that the BC-LN model fits better the data than the S-NL model, and that there is a 100% chance that the BC-NL model is the

correct one. On the contrary, in the case of subject 2a, the positive value of ΔAIC (1.84) indicates that the S-NL model is superior in this case, and that there is a 71% chance of the S-NL model being correct (29 % chance for the BC-NL model shown in the column). On the whole, the ΔAIC of 25 of the 31 data sets were negative, indicating a preference for the BC-NL model (probability of BC-NL being correct >61%). In fact, in 20 of the 31 cases there was a probability ≥90% of the model BC-NL being correct.

The use of these two parameters can be illustrated by considering subject 6. The SC thickness for subject 6 is 8.6±0.2μm (CV=2.3%) according to the S-NL model and 7.4±0.07 (CV=1%) according to the BC-NL model. The difference in the ΔAIC for this subject was -32.39, resulting in a probability of 100% the BC-NL model being correct; the F test also shows that the BC-NL model fits better the than the S-NL. This is in good agreement with the graphic representation: the S-NL prediction misses 6 experimental points, while the BC-NL misses only two. As discussed before, approximately 25 of the 31 cases were better modelled by the BC-NL model, indicating the usefulness of the inclusion of the baseline parameter to fit the full breadth of the experimental data. In summary, the results in Table 2-1 suggest that the BC-NL has a better overall performance than the S-NL model.

2.4.5 Intra-subject variation in H on different occasions

In addition, Table 2-1 and Figure 2-3 show the data for some volunteers who participated on different occasions. It is worth noting that the H estimated on different occasions may differ markedly for the same volunteer, independent of the model used to fit the data. See for example, subjects 1-3, 5, 8, 9, 10, 12 and 14 (Figure 2-3). These differences imply that the SC thickness changes with time, potentially due to environmental conditions and the use of drugs, cosmetics or exfoliating agents. It follows that a determination of the SC thickness is necessary every time a dermato-pharmacokinetic study is performed in a subject, so the correct thickness is used to normalise the drug-penetration profiles.

In summary, we believe that non-linear models perform better than the standard linear model typically used to estimate the SC thickness via tape-stripping experiments combined with TEWL measurements. When the LM performs well, that is in the absence of an initial plateau, the three models estimate comparable values of H. However, when an initial plateau appears, probably corresponding to the removal of the SC disjunctum, the SL model tends to overestimate the thickness of the SC unless some subjective exclusion of data is made. On the contrary, the non-linear models offer a robust procedure, incorporating all data points, reflecting better experimental observations, and estimating the thickness with a smaller coefficient of variation.

The incorporation, rather than the exclusion, of the initial plateau by the non-linear approach should be preferred as it follows more closely the SC physiology and its division into the SC compactum and disjunctum. The statistical comparison of the two non-linear models showed a higher probability for the baseline corrected model being the preferred one. However, there were no statistical differences between the values of H estimated from either of these models.

A full set of raw data and calculations (for Subject 7) is presented in Appendix 2-A as an example.

2.5 Notes

This chapter has been published: Russell, L.M., S. Wiedersberg, and M.B. Delgado-Charro, *The determination of stratum corneum thickness - An alternative approach.* Eur J Pharm Biopharm, 2008. 69(3): p. 861-870.

2.6 Acknowledgements

We thank Pharsight Corporation Inc. for a Pharsight Academic Licence for WinNonlin® and Dr. Dan Weiner for scientific input during the development and assessment of the non-linear models.

Chapter 3

Quantification of stratum corneum by protein assay: evaluation of extraction solutions, and comparison with gravimetric and imaging methods.

3 Quantification of stratum corneum by protein assay: *evaluation of extraction solutions, and* comparison with gravimetric and imaging methods.

3.1 Abstract

Tape stripping removes layers of the stratum corneum (SC), into which applied drug has permeated, to assess the topical bioavailability and measure dermato-pharmacokinetic parameters. To compare formulations of the drug and to determine their bioequivalence (or not), it is important to quantify the amount of SC removed on the tape strips. One approach involves extraction and quantification of protein and this study aims to examine the usefulness of such a strategy.

First, the stability of a commercially available solution of human epidermal keratins, when diluted with either a solution based on the commercial base (a urea/thiol mixture, referred to here as Stable Extraction Solution, SES) or concentrated sodium hydroxide, was measured. Second, protein was extracted directly from SC (obtained from heel scrapings), using either SES or concentrated sodium hydroxide, and was then quantified with a sensitive, fluorescence-based assay. Extraction with NaOH was inefficient and significantly lower than that achieved with SES, which resulted in an amount of protein equivalent to ~80% of that expected from the measured mass of SC used for extraction. Third, SC removed by a typical tape-stripping procedure was extracted from the individual tapes using SES, analysed for protein as before, and these values were then correlated with both the measured mass of SC removed and by a novel imaging technique (which also allows SC on tapes to be quantified). The correlation was significant but weak with both methods, which suggests that the protein assay is insufficiently sensitive to distinguish between tapes expressing small differences between tapes.

3.2 Introduction

There is currently a need for an objective method to assess the rate and extent of drug permeation through the skin from topical formulations. This method would be useful to assess whether different formulations of the same drug are bioequivalent, and would encourage the development of generic topical products. Such a method is desired by pharmaceutical companies and regulatory bodies such as the FDA [86].

Topically applied drugs have their target site within the skin, and as such, systemic absorption is very low. Thus, to assess the bioavailability of these formulations, drug levels within the skin must be sampled.

Since the stratum corneum (SC) is the principal barrier to drug absorption, it may be assumed that the (dermatopharmaco)-kinetics (DPK) of drug passage through this layer are related to topical bioavailability [84]. An intensely studied technique to sample the SC is 'tape stripping' where, after formulation application and removal, adhesive tapes are used to remove sequential layers of the SC.

The tape strips provide a wealth of information, which allows drug penetration profiles across the SC to be constructed. Firstly, using a suitable extraction and analytical technique, the mass of drug per tape may be measured. Secondly, as tape strips remove a variable amount of SC, the amount of SC per tape may be quantified. The amount of SC

per tape is used for three purposes:

- to express the mass of drug extracted as a concentration, in terms of the 'volume' of SC per tape
- to measure the depth reached within the SC by each successive tape strip
- to estimate a volunteer's total SC thickness, using tape stripping data from an untreated adjacent site coupled with transepidermal water loss measurements [1, 100]. As SC total thickness varies with volunteer, season and skin exposure, the total thickness may be used to express depth reached within the SC relative to total thickness.

Robust, reproducible normalised profiles of drug concentration against relative depth reached within the SC are thus produced, allowing profiles from different sites and volunteers to be compared [51, 84, 92, 94, 109-112, 120]. Analysis of these profiles using an appropriate solution of Fick's second diffusion law permits parameters describing the partitioning and diffusivity of the drug (reflecting the rate and extent of penetration, respectively) to be estimated and used to compare different formulations.

Unfortunately, there is no absolute way to measure the amount of SC per tape. Traditionally, weighing tapes before and after stripping has been used as the 'gold standard' to derive a mass of SC per tape, but it is time-consuming and laborious, and, as we shall see in Chapter 4, somewhat insensitive, irreproducible and unstable. A novel imaging technique has been investigated to quantify SC on tape strips. This involves taking high resolution images under highly controlled conditions. Each image comprises many pixels and the greyscale value of each one can be found. The mean greyscale value across all pixels is being evaluated as a relative measure of SC per tape.

Since the 75-80% of the SC mass is protein, notably keratin [133], a protein assay is logically a potentially useful approach to quantify SC on tape strips. Since protein extraction and quantification is unlikely to be compatible with drug extraction and analysis, the method would be most useful for validating other methods to quantify SC, rather than for use in tape stripping studies *per se*.

This work aimed to evaluate and optimise (i) a solution suitable for extracting protein from SC; (ii) to measure the amount of protein extracted from tape strips using a suitable protein assay, and (iii) correlate the amount of protein extracted and measured with two other measures of SC amount on the tape, namely the mass of SC and the mean greyscale value.

1M NaOH solution has been previously used to extract protein from SC-impregnated tape strips [103-108]. As 1M NaOH is incompatible with most protein assays, the solutions were neutralised with 1M HCl after extraction. Considering the work of other fields, keratin has been extracted from heel SC, nails and hair using a basic (pH 9) solution of Tris HCl, urea, phenylmethanesulfonyl fluoride and 2-mercaptoethanol [134, 135].

The Bio-Rad DC [104], Bio-Rad [106-108] and Micro BCA™ [103] protein assays have been used with NaOH extractions, which have increasing protein sensitivities of 200µg/ml [136], 100 µg/ml [137, 138] and 2 µg/ml [139] respectively. Recently, an enzyme linked assay, SkinMAP, has been used to simultaneously measure multiple skin biomarkers using Luminex® bead-based detectors [140]. This method has very high sensitivity (30pg/ml for keratin-6, and 570 pg/ml for keratins 1 and 10 combined) but the mild extraction solutions used to simultaneously extract many skin proteins resulted in very low levels of keratin from the tape strips.

The standards used to calibrate the protein assays have included bovine gamma globulin [103, 108]; and bovine serum albumin [107], although neither of these produced sufficiently accurate results when compared to pure SC separated from the epidermis of cadaver skin [104]. A commercial keratin solution extracted from human epidermis has also been used [106].

As a starting point, we noted that a dispersion of human epidermal keratins, from feet calluses, and with a protein molecular weight range of 45 – 60 kDa, is commercially available from Sigma-Aldrich (Sigma-Aldrich Company Ltd, Gillingham, UK). The protein concentration of this solution is assayed by Sigma, and provided upon purchase. This standard dispersion, in 8 M urea, 50 mM Tris, 0.1 M β-mercaptoethanol and 0.1% sodium azide (pH 8.4), is stable for 1 year at 2 – 8°C. This solution is remarkably similar to that used for SC extraction by Kitahara and Ogowa [134, 135]. We thus tested the solution of this commercial epidermal dispersion as an alternative for SC extraction (abbreviated Stable Extraction Solution, SES). Extraction with SES was compared with 1M NaOH.

To quantify the small amount of SC extracted with each solution, we need a sensitive compatible assay. Both the 1M NaOH and SES are incompatible with the majority of protein assays. Several protein assays, with their sensitivities and incompatibilities are summarised in Appendix 3-B. In addition, the conditions used for the studies reported above, along with the corresponding protein assay used, are summarised in Appendix 3-C.

We chose the EZQ method from Invitrogen, with a limit of quantification of 20 µg/ml, and universal compatibility due to its washing stages. Three studies were conducted. Firstly, the commercial epidermal solution from Sigma (of known concentration) was diluted in either 1M NaOH or the SES and the protein levels assayed to assess protein stability in each solution. Secondly, known masses of SC obtained from the heel of a volunteer were extracted in either 1M NaOH or the SES to establish extraction efficiency. Thirdly, a series of tape strips were taken from healthy volunteers and extracted using SES. The protein masses extracted were compared to the mass of SC measured on the tapes, and the mean greyscale values from a novel imaging method.

3.3 Materials and Methods

3.3.1 Materials

A standard keratin solution (K0253, Sigma-Aldrich Company Ltd) was used to prepare all standards. It consists of keratin extracted from human foot epidermis, at a concentration of 8500 µg/ml in a solution of 8 M urea, 50 mM Tris, 0.1 M β-mercaptoethanol and 0.1% sodium azide, pH 8.4. Methanol (HPLC grade) and acetic acid (Fisher Scientific, Loughborough, UK) were also used in this work.

3.3.2 Protein assay

The EZQ® protein quantification kit (R33200, Molecular Probes™ Inc., Invitrogen, OR, USA) was used for all protein quantification. The kit instructions were followed using the 96-well cassette, with 2 corner cells reserved for labelling and correct alignment. When necessary, the sample paper was dried with a hairdryer. The fluorescence was read on a microplate reader (Fluostar Optima, BMG Labtech, Offenburg, Germany; software version 1.32 R2) with excitation/emission settings of ~485/590 nm and a gain of 2213. All samples were spotted onto the plate three times and each spot was read in triplicate by the microplate reader. Mean values are reported. Three blank tapes were extracted and assayed in the same way, and the mean blank fluorescence used to correct all sample

values (denoted 'mean corrected fluorescence').

3.3.3 Keratin stability in 1M NaOH and SES

The standard keratin solution was diluted to produce standards in the approximate range of 20-1900 µg/ml range in either 1M NaOH (Fluka ion chromatography grade, Sigma-Aldrich) or a freshly-prepared admixed solution of 8 M urea (Sigma-Aldrich), 50 mM Tris (Acros Organics, Geel, Belgium), 0.1 M β-mercaptoethanol (Sigma-Aldrich), hereafter denoted 'Stable Extraction Solution' (SES). Each dilution was assayed for protein concentration after 1, 2 or 3 days vigorous shaking.

3.3.4 Extraction efficiency of 1M NaOH and SES

Foot SC was harvested from the clean heel of one female volunteer, dried in an oven at 25°C for 24 hours, and subsequently stored in a desiccator, until use.

Known masses of dried foot SC were extracted in 1ml of either 1M NaOH or SES for 48 hours before protein assay.

3.3.5 Extraction and quantification of protein from tape strips using SES

3.3.5.1 Subjects

A total of 21 sites were examined from 8 different healthy volunteers (3 male, 5 female, 24-38 years) with no history of dermatological disease. The number of volunteers who provided (number of sites) is as follows: 1 (5 sites); 1 (4 sites); 6 (2 sites). Ethical approval was granted by Salisbury Local Research Ethics Committee, the Declaration of Helsinki protocols were followed, and written informed consent was obtained from all volunteers. Participants refrained from using any topical products on the test area on the day of the experiments.

3.3.5.2 Tape stripping

A series of 2cm x 3cm tapes were cut from Scotch Book tape 845 (3M, St. Paul, MN) and stored in covered trays. Tapes were manipulated using a small corner of each tape folded back on itself.

Two tapes were applied, with pressure using a roller, to the study site, then removed and discarded. These pre-tapes remove exogenous substances, prepare the skin surface in a systematic way and are taken before all *in vivo* experiments. A plastic template was used to delimit a constant area (1.5cm x 1.5cm) within the study site. This template had an outline marked on its underside of 2cm x 3cm. An initial transepidermal water loss (TEWL) measurement was taken (Biox Aquaflux AF102, Biox Systems Ltd., London, UK; measurement range 0–100 g m^2 h^{-1}; resolution ±0.05 g m^2 h^{-1}; probe applied for a minimum 60 s, TEWL was obtained as mean of 10 successive measurements having a CV < 1%).

Pre-weighed tapes (2cm x 3cm) were positioned over the template, using the marked outline to ensure that the tape was always placed in the same position. Firm adhesion was achieved by using a weighted roller. The tape was then removed swiftly. The sequence was repeated, with intermittent TEWL measurements, until the TEWL value was 3–4 times its initial value (usually 60–80 g m^{-2} h^{-1}).

The amount of SC on the tapes was assessed by weighing the tapes before and after

stripping; with a novel imaging technique; and by protein extraction in SES, as described below.

3.3.5.3 Quantification of SC amount per tape

3.3.5.3.1 Mass measurement

Tapes to be used for stripping were cut and stored covered in ambient conditions for 12 hours before weighing. Static electricity was discharged from the tapes prior to weighing (R50 discharging bar and ES50 power supply from Eltex Elektrostatik GmbH, Weil am Rhein, Germany). The tapes were weighed, before and after stripping, using a microbalance with precision 0.1 µg (Sartorius SE-2F from Sartorius AG, Goettingen, Germany). Any hairs removed by the tape stripping procedure were carefully removed using fine tweezers before the second weighing. No tapes were discarded.

Five blank tapes were weighed at the same time as the tapes used for the tape-stripping experiments, both before and after stripping, to correct the calculated mass of SC for any variations in weight due to environmental or other conditions.

3.3.5.3.2 Imaging

After their second weighing, the tapes were mounted on standard slide holders (5 cm x 5 cm, with an internal window 2.3cm x 3.5cm) such that the 1.5cm x 1.5 cm square of SC was centrally aligned with its edges parallel to those of the slide.

The slide holding the tape + SC was photographed (14 bit) using a Coolscan V ED slide scanner (Nikon UK Limited, Kingston upon Thames, UK) at a resolution of 4000 pixels per inch (157.5 pixels/mm). A crop of 2213 x 2203 pixels (approximately 1.4cm x 1.4cm) was centred over the image. Photographs fully illustrating this method are shown in General Appendix I.

Cropped images (9822 KB each) were saved and analysed with ImageJ (Rasband, W.S., U. S. National Institutes of Health, Bethesda, Maryland, USA; freeware from http://rsb.info.nih.gov/ij/). A scale of 159.07 pixels/mm was applied. Full settings are described in General Appendix II. During image analysis, the greyscale value of each of the 4875239 pixels of the image is measured (16 bit) in the range 0 - 64608, where 0 and 64608 designate black and white respectively. The mean greyscale over all pixels was calculated and then subtracted from that obtained from blank tapes (see General Appendix III) to yield mean greyscale values which increase with image darkness (and hence with the amount of SC on the tape).

This novel imaging technique to assess SC the quantity of SC from a series of tape strips is described and evaluated in detail in Chapter 4.

3.3.5.3.3 Protein assay

After images were taken, each tape was cut from the slide holder and extracted for 48hrs in 1ml of SES with vigorous shaking. Three blank tapes were also extracted.

3.3.5.4 Statistics

All statistical tests, as detailed in the results section, were performed with Prism® version 4 (GraphPad Software, CA, USA).

For comparison of the linear regression outputs from the plots of mass of foot SC vs.

protein concentration, slopes were compared using the methods outlined by Zar [141, following example 17.1], and using the appropriate tables for the *t* distribution. This method is reproduced in Appendix 3-A.

3.4 Results and Discussion

3.4.1 Keratin stability in the extraction solutions

There was a linear relationship between the measured fluorescence and the concentration of keratin in the standards prepared in SES (Table 3-1). The absolute (corrected) fluorescence values changed slightly on different days, depending on the degree of fluorescent labelling, but the linear calibration curve was maintained, with r^2 values ≥0.97 on three different occasions.

Likewise, there was a correlation ($r^2 \geq 0.96$) between the measured fluorescence values and the protein concentration of the standards prepared in 1M NaOH (Table 3-1). This confirms that dilutions were performed correctly and that NaOH does not interfere with the protein assay.

However, it is clear that the absolute values of fluorescence determined in SES were significantly greater ($p<0.0001$ paired 2-tail t-test for each day) than those in NaOH, suggesting that the latter caused degradation, and ultimately complete destruction of the protein within 1 to 3 days.

The study was then repeated over a smaller concentration range, ~80 - 215 µg/ml, with similar results (Table 3-2). Linearity ($r^2 > 0.99$) was again achieved but the overall keratin degradation in 1M NaOH was 51-91% over the 48 hour period, confirming that this is not a suitable solution in which to dilute keratin solutions before analysis.

3.4.2 Evaluation of keratin extraction using protein extraction solutions

In previous studies [103-108], 1M NaOH was used to extract protein from the SC on tape strips. In this work, we evaluated the potential of SES, in which keratin is stable, to extract a quantifiable amount of protein from SC scrapings obtained from the heel of a foot. 1M NaOH was also used to extract protein from the foot SC, and the results compared. As it was possible to weigh accurately the foot SC used for each extraction, and 1ml of each solution was used, the extraction efficiency may be compared.

The experiments were performed on two separate occasions, and the results presented in Figure 3-1 A and B respectively.

For the first experiment (Figure 3-1 A), the samples were assayed after 24, 48 and 72 hours. It is clear that SES extracts a higher concentration of protein than the NaOH solution. The concentration of protein from SES is similar on the three successive days, although the concentration of protein in the NaOH samples decreases with increased extraction time.

		Day 1				Day 2				Day 3			
		SES	NaOH			SES	NaOH			SES	NaOH		
	Conc. (ug/ml)	Mean Fluor.	Mean Fluo.	Conc. (µg/ml)	% degradation	Mean Fluo.	Mean Fluo.	Conc. (µg/ml)	% degradation	Mean Fluo.	Mean Fluo.	Conc. (µg/ml)	% degradation
Std 1	1888.9	35358	6479	283.25	85.00	46688	5251	169.13	91.05	47545	1954	26.27	98.61
Std 2	1062.5	22067	3838	146.00	92.27	32297	3103	85.51	95.47	36330	2045	29.66	98.43
Std 3	850.0	19976	2961	100.40	94.68	22151	2005	42.78	97.74	24254	976	ND	100.00
Std 4	664.1	14332	2143	57.88	96.94	18988	2271	53.14	97.19	18876	1011	ND	100.00
Std 5	483.0	12163	1494	24.15	98.72	15210	1077	6.64	99.65	15801			
Std 6	265.6	5915	1036	ND	100.00	7372	297	ND	100.00	7840	246	ND	100.00
Std 7	106.3	1927	608	ND	100.00	3040	-72	ND	100.00	2994	39	ND	100.00
Std 8	53.1	978	143	ND	100.00	772	-212	ND	100.00	1102	-131	ND	100.00
Std 9	21.3	349	96	ND	100.00	223	-313	ND	100.00	512	11	ND	100.00
Correlation coefficient		0.983	0.996			0.983	0.982			0.967	0.961		
Slope		19.2				25.7				26.7			
Average (Stds 1-7)		1029.2			95.4	906.1			97.3	1253.2			99.5

Table 3-1: Standards were made in either SES or 1M NaOH, and shaken for a total of 72 hours, with samples taken every 24 hours. The mean corrected fluorescence (fluo.) of the standards in either solution is shown, along with the calculated concentration (conc.) of keratin in the NaOH solutions, and the percentage degradation. ND: Not detectable

		Day 1 Standards Set A				Day 2 Standards Set A				Day 3 Standards Set B			
		SES	NaOH			SES	NaOH			SES	NaOH		
	Conc. (ug/ml)	Mean Fluo.	Mean Fluo.	Conc. (µg/ml)	% degradation	Mean Fluo.	Mean Fluo.	Conc. (µg/ml)	% degradation	Mean Fluo.	Mean Fluo.	Conc. (µg/ml)	% degradation
Std 1	212.5	7255	2407	118	45	7068	1010	97	54	10255	1010	82	62
Std 2	159.4	4721	592	82	48	4254	918	95	40	6386	319	ND	100
Std 3	106.3	1658	441	80	25	1013	ND	ND	100	2523	ND	ND	100
Std 4	79.7	520	ND	ND	100	470	ND	ND	100	1083	ND	ND	100
Correlation coefficient		0.998				0.987				0.996			
Slope		51.7				51.8				69.9			
Average (Stds 1-4)		-3669.3			54.5	-4026.8			73.6	-4692.7			90.4

Table 3-2: Standards were made in either SES or 1M NaOH, and shaken for a total of 48 hours, with samples taken every 24 hours. The mean corrected fluorescence (fluo.) of the standards in either solution is shown, along with the calculated concentration (conc.) of keratin in the NaOH solutions, and the percentage degradation. ND: not detectable.

In the second experiment (Figure 3-1 B), the NaOH samples again have a lower concentration of protein than SES samples. On the second day, the concentration of protein in SES had increased; whereas the concentration in the NaOH samples had decreased.

The six samples, containing different initial masses of foot SC, are related with the results of the linear regression in the accompanying table (Figure 3-1). It can be noted that the correlation coefficient improves for SES after a longer extraction time. This suggests that the extraction is time-dependent and that up to 72 hours may be required to extract the keratin from SC. On the other hand, the correlation coefficient gets worse for the NaOH samples, consistent with our previous observation that the protein may be degraded with time by the NaOH solution. In addition, the concentration of protein in the NaOH samples decreases with extraction time.

For each set of samples on each day, a linear regression was performed. The slopes of these regressions were compared in pairs (e.g. Experiment 1, SES Day 1 slope compared with Experiment 1, NaOH Day 1 slope) as described in Appendix 3-A. A total of six pairs of slopes were compared. The slopes of each of the six pairs were found to be statistically significantly different. Since the slopes are different, the linear regression outputs are statistically different for the two extraction solutions.

The mass of SC used for each of the six extractions, for each solution, was known and is shown on the *x* axis of Figure 3-1 A and B. The concentration of protein quantified (*y* axis of Figure 3-1 A and B) relates to a mass of protein (as each extracted in 1ml) and may be compared to the mass of SC used. The proportion of SC mass extracted as protein, with each extraction solution may thus be calculated and the mean ± SD for each of the six samples are shown in Figure 3-2.

Firstly we can note that the percentage of SC mass extracted as protein is higher for the SES than the NaOH samples. The percentage of protein extracted relative to the SC mass is relatively stable for SES. SES extracts a mean percentage of 83.5 ±1.1 % with the first experiment (over three days) and 48.4 ± 5.5 % for the second experiment (over two days). These values suggest that SES is very efficient at extracting protein from SC, as it is known that approximately 75-80% of SC is protein [133].

The percentage of SC mass quantified as protein for the NaOH samples decreases with time. This suggests that the protein is not stable in the NaOH solution. NaOH also extracts a lower percentage of the SC mass as protein: 6.08 ± 6.75% for the first experiment (over three days) and 10.51 ± 9.1% for the second experiment. This implies that the NaOH solution is not suitable for extracting protein from SC, as these values are well below the 75-80% protein per mass of SC which would be predicted from the literature [133].

In summary, SES should be preferred over 1M NaOH for the extraction of protein from SC. Firstly, keratin is stable in SES and the fluorescence values are high enough to be quantified. Secondly, it is possible to extract protein from SC using SES, to levels consistent with those presented in the literature [133]. On the other hand, a standard solution of keratin showed degradation in 1M NaOH, and considerably lower masses of protein were extracted from SC and quantified.

	Day	Symbol	Slope	Intercept	R^2
SES	1	×	0.71	61.18	0.93
	2	●	0.66	80.80	0.98
	3	■	0.67	82.45	1.00
NaOH	1	×	0.22	-30.73	0.98
	2	●	0.11	-20.56	0.98
	3	■	0.03	-10.99	0.70

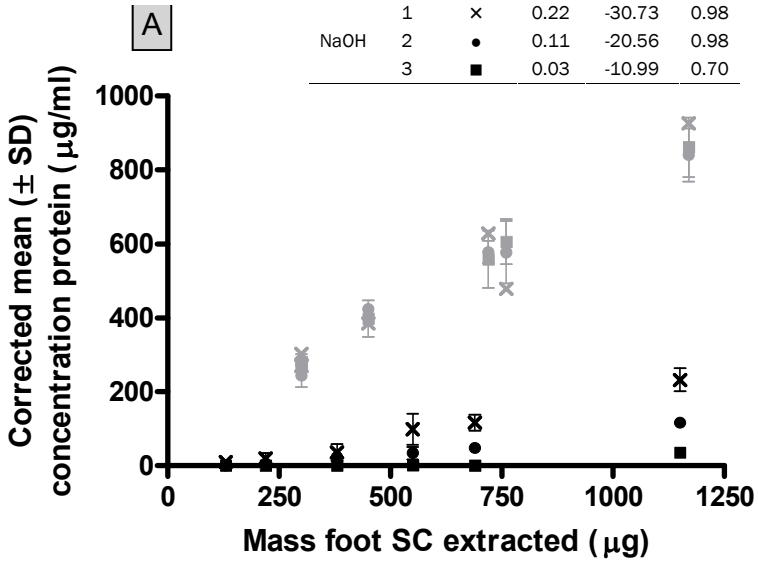

	Day	Symbol	Slope	Intercept	R^2
SES	1 A	×	0.12	299.40	0.81
	2 A	●	0.35	185.80	0.92
	2 B	■	0.25	205.00	0.97
NaOH	1 A	×	0.08	96.41	0.94
	2 A	●	0.04	89.42	0.95
	2 B	■	0.04	73.21	0.92

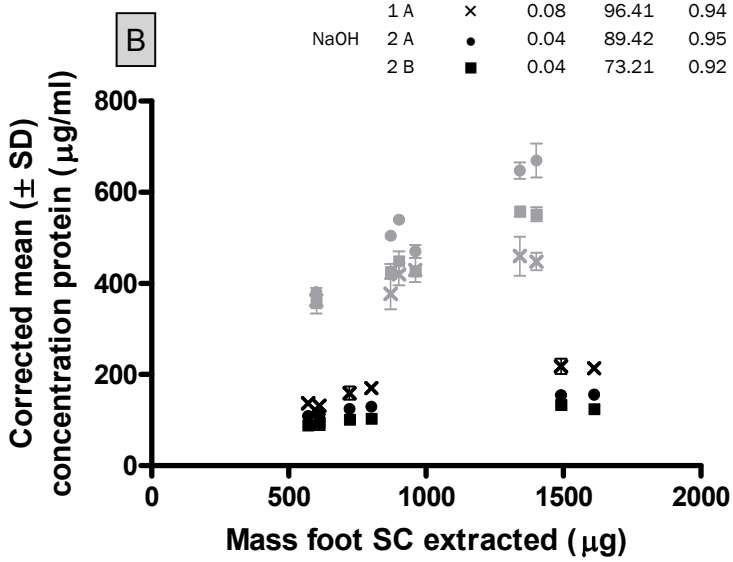

Figure 3-1: Comparison of the mean (± SD) protein concentration (n = 3) measured using EZQ assay when foot SC samples were extracted in SES (■) or 1M NaOH (■). Two sets of 6 samples were assayed on separate occasions (A and B). Pair-wise comparisons of slopes reveal statistically significant differences between the SES and NaOH samples for all pairs (population regression coefficients compared using a version of Student's t test (2 tailed t-test, $\alpha = 0.05$, $p<0.001$), as detailed in Appendix 3A.

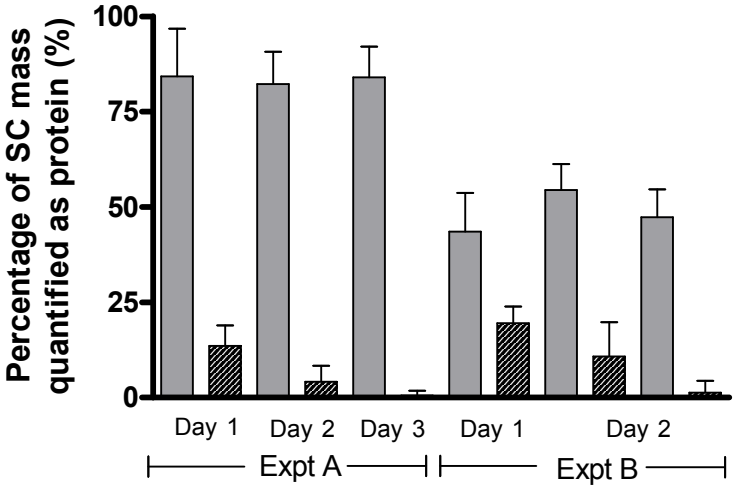

Figure 3-2: Mean (± SD) (n = 6) percentage of the total mass of SC detected as protein after 1-3 days extraction with either SES (■) 1M NaOH (◪). Two sets of 6 samples were assayed on separate occasions (Expt. A and Expt. B).

3.4.3 Quantification of protein extracted from tape strips, and comparison to mass of SC on tape strips

Quantification of the amount of protein extracted from tape strip samples was next examined, and correlations with the mass of SC determined gravimetrically, and with the greyscale values derived from the imaging method, were assessed.

A total of 349 tapes were each extracted in 1ml of SES. The protein concentration of each sample was assayed in triplicate, and the mean and standard deviation values are plotted against the corresponding SC masses and greyscale readings in Figure 3-3 and Figure 3-4, respectively.

The correlations however are not particularly impressive. Although there was a significant positive correlation between the protein measurement and the mass of SC ($\alpha = 0.05$, 2-tail $p<0.0001$), the Spearman correlation coefficient was only 0.37. Similarly, with the greyscale values, the positive correlation was significant ($\alpha = 0.05$, 2-tail $p<0.0001$) but again the Spearman correlation coefficient was only 0.44.

The relatively poor correlations are due, at least in part to (i) the high variability of the protein measurements (the average relative standard deviation (RSD) calculated from the data for 349 tapes was 18.9 (± 19.3%), and (ii) the low precision of the protein concentration measurements, most of which were in the range of 20-70 µg/ml and close to the limit of quantification. These factors contribute importantly, therefore, to the protein assay being unable to distinguish between tapes which have low and similar amounts of SC upon them. It seems unlikely, therefore, in the absence of a more sensitive test, that protein quantification can be used to quantify reliably SC on tape strips.

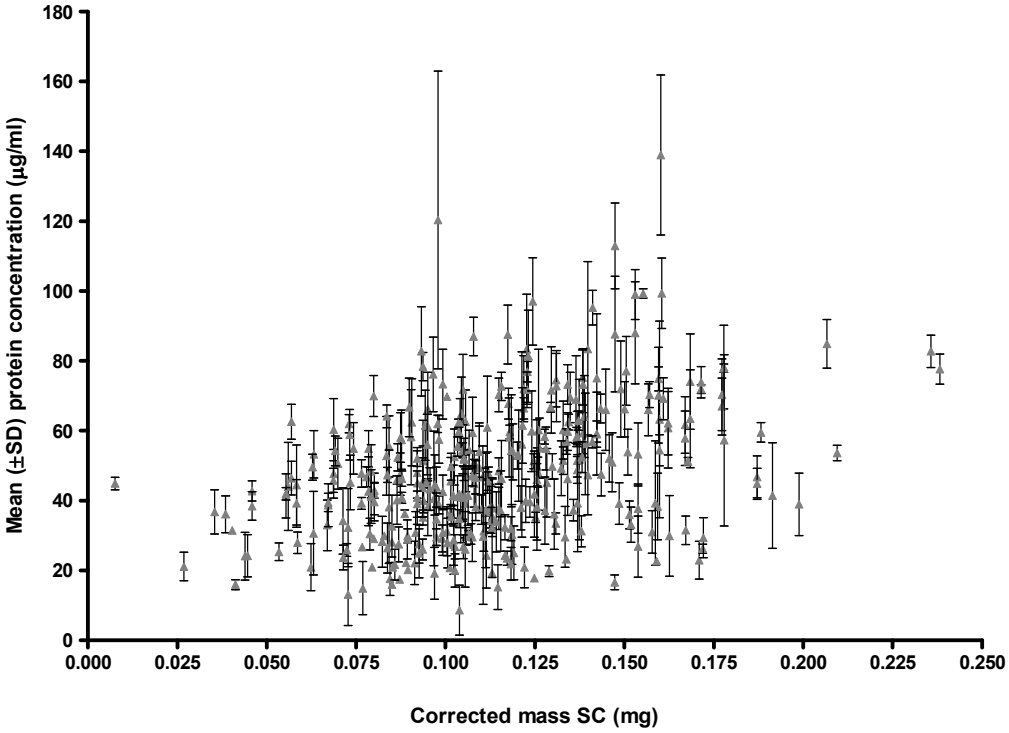

Figure 3-3: Correlation between the mass of SC on tape, with the protein concentration measured.

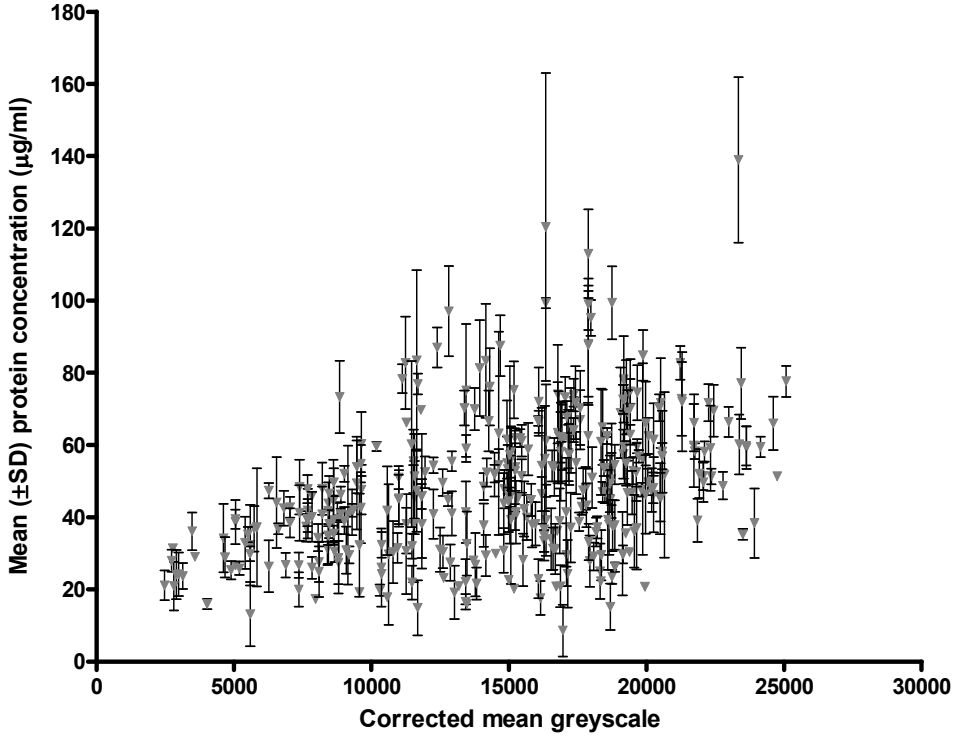

Figure 3-4: Correlation between mean greyscale value of tapes, with the protein concentration measured.

Full raw data and calculations for the tape set from one site, with SC measured by the three methods (weighing, imaging, and protein assay) is shown in Appendix 3-D, as an example.

3.5 Conclusions

It is important to be able to quantify the amount of SC per tape in order to express the mass of drug per tape relative to the 'volume' of SC and to plot relative depth reached within the SC with each successive tape strip for dermato-pharmacokinetic profiles. The weighing method is accepted but is tedious and somewhat unreliable. The greyscale technique used, while promising, requires further validation. A sensitive, accurate protein extraction and assay technique could provide this validation.

Keratin extraction with concentrated NaOH has been used previously, but is clearly not to be further recommended as it degrades a standard keratin solution, and fails to extract sufficient protein from an SC sample. SES appears, from these results, to be better.

Protein quantification, for assessment of the amount of SC per tape, even the more sensitive method described here, is still not sensitive enough to distinguish between the typically small amounts of SC removed on tape strips. With the present technique, better precision may be achieved either by stripping a larger area, or by combining tape strips appropriately.

3.6 Acknowledgements

We thank Dr. A MacKenzie for allowing access to the microplate fluorescence detector, and Miss C. Hobbs, Miss S. Moore and Dr. J. Hewinson from her research group for technical assistance.

Chapter 4

Methods to quantify the amount of stratum corneum on tape strips: experimental features

4 Methods to quantify the amount of stratum corneum on tape strips: experimental features

4.1 Abstract

An objective method to assess the rate and extent of drug permeation through the skin from topical formulations is required for bioequivalence purposes. Tape stripping the stratum corneum (SC) with adhesive tapes has emerged as a promising technique. When tapes are analysed individually, drug penetration profiles through the SC are constructed. For the profiles from different sites and different volunteers to be easily compared, they are normalised using the volunteer's total SC thickness, such that drug concentrations as a function of relative depth reached within the SC are obtained. To create such normalised profiles, the amount of SC per tape must be measured.

In this chapter, three methods to quantify SC amount per tape are compared in terms of practical usability: weighing, UV pseudo-absorption and a novel imaging technique. The imaging technique involved taking high resolution images under controlled conditions, and measuring the mean greyscale value across all pixels.

6 tapes were measured 15 times with each method. The weighing method exhibits low precision, extremely low signal:noise ratio (up to 1 : 2000), and a long, variable time needed to obtain measurements. The UV pseudo-absorption method has high precision, is quick to perform and has an acceptable signal:noise ratio. However, a fixed 1cm^2 of SC is analysed, and inhomogeneous tapes are affected by light scattering. The imaging method seems quite promising: not only is it very precise, but the signal for the SC layer is high relative to the blank tape. In addition, the method is quick, is able to measure any sample area up to 2.2 cm x 3.5 cm, and is unaffected by inhomogeneity.

Subsequently, more than 600 tapes were measured by each technique. No simple correlation was found between the weighing and either the UV pseudo-absorption or the imaging method. A strong (correlation coefficient 0.98) positive correlation was found between the UV pseudo-absorption and the greyscale values.

4.2 Introduction

There is currently a need for an objective method to assess the rate and extent of drug permeation through the skin from topical formulations for bioequivalence purposes. Topical formulations deliver very low levels of drug to the systemic circulation; therefore, drug levels should be sampled within the skin.

Since the stratum corneum (SC) is the principal barrier to drug absorption, it may be assumed that the (dermatopharmaco)-kinetics (DPK) of drug passage through this layer are related to topical bioavailability [84]. Tape stripping, where layers of SC are removed sequentially with adhesive tapes (after formulation application and removal), is being investigated as a potentially useful method.

When tapes are analysed individually, drug penetration profiles across the SC may be derived. The mass of drug per tape is found after drug extraction and analysis. However, since each tape removes a variable amount of SC, it is logical to measure the amount of SC per tape in order to:

- express the mass of drug extracted as a concentration, in terms of the 'volume' of SC per tape.
- measure the depth reached within the SC by each successive tape strip, rather than plotting tape strip number.
- estimate a volunteer's total SC thickness. SC thickness is estimated by tape stripping an untreated adjacent site with concomitant transepidermal water loss measurements [1, 100]. The depth reached within the SC is thus expressed relative to the volunteer's total SC thickness.

By measuring and using the amount of SC per tape, robust, reproducible normalised profiles of drug concentration against relative depth reached within the SC are thus produced, allowing profiles from different sites and volunteers to be compared [51, 76, 84, 92, 94, 109-111, 120]. Analysis of these profiles, using an appropriate solution of Fick's second law of diffusion, permits parameters describing the partitioning and diffusivity of the drug (reflecting the rate and extent of permeation, respectively) to be estimated and used to compare different formulations.

Traditionally, weighing tapes before and after stripping has usually been used to estimate a mass of SC per tape, but it is time-consuming and laborious. The pseudo-absorption of corneocytes at 430nm has also been used as a relative measure of SC, but inhomogeneous regions of SC cause light scattering.

Recently, a novel imaging method has been developed, whereby high resolution images are taken under highly controlled conditions. The pixels of the image each have an associated greyscale value which may be measured and analysed. The mean greyscale value across all pixels of the image offers a relative measure of SC per tape.

In this work, we compare the practical properties of the weighing, UV pseudo-absorption and the imaging methods. Firstly, six tapes were assayed 15 times by each method to measure reproducibility and precision. Secondly, the signal:noise ratio of each method is calculated. Thirdly, the proportion of the total tape strip which may be measured is compared. The time required to typically perform each measurement is also discussed.

A series of more than 600 tape strips were then assayed for SC amount by each of the three methods and the correlations between each pair of methods examined.

4.3 Methods

4.3.1 Materials

2cm x 3cm tapes were cut from Scotch Book tape 845 (3M, St. Paul, MN) and stored overnight in covered trays. Tapes were manipulated using a small corner of each tape folded back on itself.

4.3.2 Subjects

Ethical approval was granted by the Salisbury Local Research Ethics Committee, the Declaration of Helsinki protocols were followed, and written informed consent was obtained from all volunteers. No volunteers had any history of dermatological disease, nor recent topical formulation use.

For the reproducibility assessment, one volunteer (female, 30 years old) provided 6 tape strips from a single site on the volar forearm.

For the correlation study, a total of 39 sites, from the volar forearm, were stripped from 10 different volunteers (4 males, 6 females; age range 23-37 years), producing over 600 tape strips.

4.3.3 Tape stripping

Two pre-tapes (larger than 2cm x 3cm) were applied, with pressure from a roller, to each study site, stripped and discarded. These pre-tapes remove exogenous substances and prepare the skin surface in a systematic way. A plastic template was applied to delimit a constant area (1.5cm x 1.5cm) within the study site. This template had an outline marked on its underside of 2cm x 3cm to ensure the tape was always placed in the same position.

An initial TEWL measurement was taken with a closed-chamber evaporimeter (Biox Aquaflux AF102, Biox Systems Ltd., London, UK; measurement range 0–100 g m^2 h^{-1}; resolution ±0.05 g m^2 h^{-1}; probe applied for a minimum 60 s, TEWL was obtained as mean of 10 successive measurements having a CV < 1%). A pre-weighed (see 4.3.4.1) tape (2cm x 3cm) was positioned over the template. Adhesion was ensured with six rolls with a roller before swift removal. Tape stripping continued with fresh (pre-weighed) tapes, with intermittent TEWL measurements, until the TEWL increased to 4-5 times its original value.

4.3.4 Techniques to quantify amount of stratum corneum on tapes

For the reproducibility assessment, the amount of SC on each of six tape strips was measured 15 times by each of the three SC quantification methods in turn, as quickly as each method would allow.

For the tape strip correlation study, the amount of SC per tape was measured by each method once.

4.3.4.1 Weighing method

Tapes were stored for at least 12 hours before their first weighing. Static electricity was discharged from the tapes prior to weighing (R50 discharging bar and ES50 power supply from Eltex Elektrostatik GmbH, Weil am Rhein, Germany). The tapes were weighed, before and after stripping, using a microbalance with precision 0.1µg (Sartorius SE-2F from Sartorius AG, Goettingen, Germany). The mass difference equals the mass of SC.

Five blank tapes were weighed at the same time as the tapes used for the tape-stripping experiments, both before and after stripping, to correct the calculated mass of SC for any variations in weight due to environmental or other conditions.

4.3.4.2 UV pseudo-absorption method

After their second weighing, the tapes were mounted on slides (total size 5cm x 5cm, internal window 2.3cm x 3.5cm) such that the 1.5cm x 1.5cm square of SC was centrally aligned with its edges parallel to those of the slide. The mark showing the tape orientation after stripping was always positioned at the same edge of the slide.

The slide was inserted into a specially adapted UV-vis spectrophotometer (Lambda 35, Perkin Elmer, Massachusetts, USA). The incident light travelled perpendicular to the tape

and was delimited by a 1cm x 1cm square screen. The light passed through the tape from the sticky, SC-loaded side. Pseudo-absorption was measured first at 430nm then at 278nm. A total of four measurements at each wavelength were taken, with the slide rotated through 90° between each one. A blank tape was used to calibrate the instrument before the first tape and after every five tapes. The mean pseudo-absorption was taken as a measure of SC amount.

4.3.4.3 Imaging method

The slide holding the tape + SC was photographed (14 bit) using a Coolscan V ED slide scanner (Nikon UK Limited, Kingston upon Thames, UK) at a resolution of 4000 pixels per inch (157.5 pixels/mm). Photographs fully illustrating this method are shown in General Appendix I. Lighting conditions and photographic settings were kept constant, using the settings detailed in General Appendix II. A crop of 2213 x 2203 pixels (approximately 1.4cm x 1.4cm) was centred over the image, using the preview scan, before the full scan was taken.

Cropped images (9822 KB each) were saved and analysed with ImageJ (Rasband, W.S., U. S. National Institutes of Health, Bethesda, Maryland, USA; freeware from http://rsb.info.nih.gov/ij/). A scale of 159.07 pixels/mm was applied to the full image width. During image analysis, the greyscale value of all 4875239 pixels in the image is measured (16 bit) in the range 0- 64608, where 0 and 64608 designate black and white, respectively. The mean greyscale across all pixels was calculated and then subtracted from that obtained from blank tapes to yield mean corrected greyscale values which increase with image darkness (and hence with the amount of SC on the tape). The results used for the blank tape correction are detailed in General Appendix III.

The mean (corrected) greyscale value is used as a measure of SC amount, such that higher greyscale values correspond to darker images and more SC.

4.3.5 Statistics

All statistical tests, as detailed with the corresponding results, were performed using Prism® version 4 (GraphPad Software, CA, USA).

4.4 Results and Discussion

The 15 replicate measurements by each method were compared in terms of precision, signal-to-noise ratio, proportion of sample analysed and time costs.

4.4.1 Method practical features

4.4.1.1 Precision

It is important to bear in mind, when comparing the weighing, pseudo-absorption and imaging methods, that the quantification of the SC by the weighing approach is not direct; it requires two weighings of the tape, before and after stripping, and the SC mass is then deduced from the difference. Thus, errors inherent with the weighing method can affect either weighing, and so the total inherent error is double. This is different to both the UV pseudo-absorption method and the imaging method, which offer direct quantification.

The three methods for quantifying SC were assessed for their inherent precision. Six tapes of standard size (2cm x 3cm), with a SC strip of 1.5 cm x 1.5 cm, were assessed by

each method fifteen times, as quickly as each method would allow. Table 4-1 presents the results obtained.

Considering the weighing measurements, the standard deviation of the mass of the tape is very low, with relative standard deviations between 0.009% (tape 06) and 0.050% (tape 04). This represents the error of the balance and is indeed encouraging. However, we are not that interested in the mass of the tape!

For each tape, from the 15 repeated measurements, there is always a maximum and minimum mass measured for *blank tape* and *tape with SC* (presented in Table 4-1). It is thus possible to consider, that when tapes are typically weighed just once for a tape stripping experiment, that extreme weights may be measured by chance. If the minimum mass of the *tape with SC* has the maximum mass of the *blank tape* subtracted from it, the resultant *SC mass* will be low; and *vice versa*. These extremes of calculated *SC mass* are presented in Table 4-1 for each tape. The differences between the maximum and minimum *SC mass* calculated from these extreme masses of the tapes vary from 0.0326 mg (tape 02) and 0.1404mg (tape 04). When this is related to the average mass of SC on a tape, 0.1634mg, the large error calculating SC mass is now more apparent.

The difference between the maximum and minimum calculated *SC mass* can be related to the average *SC mass* using the 'extreme variability' (Eq. 4-1, results labelled (2) in Table 4-1). This value varies between 21.7% (tape 01) and 87.0% (tape 04). Looking at all 6 tapes, the overall 'extreme variability' is ~36% for 15 repeated measures.

$$\text{Extreme variability}\,(\%) = \frac{\text{Max. SC mass - Min. SC mass}}{\text{Ave. SC mass}} \times 100 \qquad \text{Eq. 4-1}$$

It is not possible to calculate a relative standard deviation (RSD) of SC mass. However, the average, rather than extreme, variability can be estimated from Eq. 4-2 for each tape.

$$\text{Weighing average variability}\,(\%) = \frac{1/2\,(\text{SD}_{\text{blank tape}} - \text{SD}_{\text{tape with SC}})}{\text{Average SC mass}} \qquad \text{Eq. 4-2}$$

This average variability (labelled (1) in Table 4-1) is between 3.1% (tape 01) and 10.7% (tape 04). The overall variability, for the six tapes, looking at average values is 5.6%.

The pseudo-absorption results are presented similarly in Table 4-1. It is clear that the precision of the measurement is very good. Although the absolute values are different between the measurements at 430nm and 278nm, there are no significant differences between either the extreme variability (Eq. 4-1) or the average measure (RSD) using a paired non-parametric 2-tailed Wilcoxon signed rank test and, thus, only the results at 430nm are discussed further.

The extreme variability over the 15 measurements varies between 0.2 – 0.9%, with an average extreme variability of 0.34%. This equates to ~100 times lower than that of the weighing method (namely 32.5%). The average error, denoted by the RSD, is 0.34% over all 6 tapes, which is ~43 times smaller than that of weighing (5.6%).

The imaging method similarly produces very precise values, with little overall variation in either the VA (0.8%) or the RSD (0.3%) over all replicates of the six tapes (Table 4-1). These are approximately 39 (=32.54/0.84) and 21 (=5.56/0.27) times lower than the corresponding VA and RSD values for the weighing method; and approximately double the variability seen for the pseudo-absorption method.

Comparing the precision of the three methods, it is clear that the weighing method is less precise than either the UV pseudo-absorption or the imaging methods. If we consider the most extreme 'amounts' of SC that could be derived, the VA for the weighing method is two orders of magnitude higher than that derived from the pseudo-absorption or the imaging method. Taking instead the error derived from the average 'amount' of SC, the average RSD is fairly similar for the pseudo-absorption and imaging methods, but one order of magnitude higher for the weighing method.

Although it may seem pedantic to consider these 'worst case' scenarios for the quantification of SC by the weighing approach, the mass can only be measured once during tape stripping experiments due to time constraints. Hence, we do not have the luxury of averaging an outlier value away and these values may occasionally arise.

Obviously, when trying to determine very slight differences in mass between different tapes, which is our aim for measuring the quantity of SC during tape stripping, an average error greater than 5% for each tape is not ideal.

		Weighing method			UV pseudo-abs.		Imaging
		Mass blank tape (mg)	Mass tape with SC (mg)	Calculated mass SC (mg)	Mean at 430nm	Mean at 278nm	Mean corrected greyscale
Tape 01	Average **value**	51.8474	52.0286	**0.1812**	**0.4961**	**0.5481**	**21389**
	SD	0.0056	0.0055		0.0005	0.0005	48
	RSD (%)	0.011	0.011	3.07 (1)	0.107	0.092	0.226
	Min value	51.8391	52.0195	0.1616 (2)	0.4955	0.5475	2[139]0
	Max value	51.8579	52.0401	0.2010 (2)	0.4969	0.5489	21455
	Max value - Min value	0.0188	0.0206	0.0394	0.0014	0.0014	155
	Extreme variability (%) (3)			21.7	0.3	0.3	0.7
Tape 02	Average **value**	51.0087	51.1456	**0.1369**	**0.4491**	**0.4939**	**20711**
	SD	0.0053	0.0042		0.0003	0.0003	41
	RSD (%)	0.010	0.008	3.44 (1)	0.058	0.054	0.196
	Min value	50.9996	51.1384	0.1208 (2)	0.4487	0.4935	20638
	Max value	51.0176	51.1528	0.1532 (2)	0.4495	0.4944	20780
	Max value - Min value	0.0180	0.0144	0.0324	0.0008	0.0009	143
	Extreme variability (%) (3)			23.7	0.2	0.2	0.7
Tape 03	Average **value**	48.8321	48.9746	**0.1425**	**0.4584**	**0.5104**	**21466**
	SD	0.0066	0.0065		0.0009	0.0010	59
	RSD (%)	0.013	0.013	4.58 (1)	0.191	0.204	0.277
	Min value	48.8178	48.9664	0.1199 (2)	0.4571	0.5090	21316
	Max value	48.8465	48.9892	0.1714 (2)	0.4597	0.5119	21576
	Max value - Min value	0.0287	0.0228	0.0515	0.0026	0.0029	260
	Extreme variability (%) (3)			36.1	0.6	0.6	1.2
Tape 04	Average **value**	48.7230	48.8843	**0.1613**	**0.4619**	**0.5142**	**21049**
	SD	0.0245	0.0101		0.0003	0.0003	61
	RSD (%)	0.050	0.021	10.74 (1)	0.064	0.064	0.290
	Min value	48.7010	48.8740	0.0715 (2)	0.4614	0.5137	20987
	Max value	48.8025	48.9129	0.2119 (2)	0.4623	0.5146	21191
	Max value - Min value	0.1015	0.0389	0.1404	0.0009	0.0009	205
	Extreme variability (%) (3)			87.0	0.2	0.2	1.0
Tape 05	Average **value**	50.8578	51.0270	**0.1691**	**0.4483**	**0.5150**	**20889**
	SD	0.0091	0.0134		0.0014	0.0020	40
	RSD (%)	0.018	0.026	6.66 (1)	0.321	0.379	0.189
	Min value	50.8459	51.0030	0.1295 (2)	0.4468	0.5130	20809
	Max value	50.8735	51.0564	0.2105 (2)	0.4509	0.5188	20934
	Max value - Min value	0.0276	0.0534	0.0810	0.0041	0.0058	124
	Extreme variability (%) (3)			47.9	0.9	1.1	0.6
Tape 06	Average **value**	50.0620	50.2510	**0.1891**	**0.4809**	**0.5558**	**21831**
	SD	0.0047	0.0137		0.0003	0.0002	90
	RSD (%)	0.009	0.027	4.86 (1)	0.053	0.043	0.412
	Min value	50.0517	50.2316	0.1630 (2)	0.4805	0.5553	21636
	Max value	50.0686	50.2817	0.2300 (2)	0.4814	0.5562	22002
	Max value - Min value	0.0169	0.0501	0.0670	0.0009	0.0009	366
	Extreme variability (%) (3)			35.4	0.2	0.2	1.7
Over all tapes	Ave RSD			5.56	0.13	0.14	0.27
	Average 'extreme variability' (%)			35.99	0.34	0.35	0.84
	Average **value**			0.1634	0.4658	0.5229	21222
	SD **value**			0.021	0.019	0.024	415
	RSD of **value** (%)			12.85	4.08	4.59	1.97

Table 4-1: Three quantification methods were compared for their variability over 15 repeated measurements, for 6 tapes. RSD: Relative standard deviation.

(1) It is not possible to calculate a true RSD for the calculated SC mass as this value is calculated from the measured masses of tape and tape with stripped SC. The value presented is a measure of the variability of the two masses measured, relative to the average SC mass calculated from Eq. 4-2.
(2) Minimum SC mass per tape is calculated from the *maximum mass* of blank tape, subtracted from the *minimum mass* of tape-with-SC; and *vice versa* for the maximum mass SC.
(3) The 'extreme variability' (%), of the calculated *SC mass,* is calculated from Eq. 4-1

4.4.1.2 Signal to noise ratio

Later in this chapter, more than 600 tapes with a 1.5 cm x 1.5 cm square layer of SC were analysed by each of the three methods. The range of values obtained for each method is used to calculate a range of signal:noise ratios.

The 3cm x 2cm tapes weigh approximately 50mg. The range of *SC masses* was between 0.025 – 0.25mg, but more typically in the range 0.05-0.15mg (Section 4.4.2). Therefore the signal:noise ratio lies somewhere in the 1: 200 to 1:2000 range (Table 4-2). The fact that the 'noise' of the blank tape is up to 2000 times higher than the signal of the SC undoubtedly contributes to the low precision of this method.

	Mean Value for *Blank tape* ("noise")	SC value ("signal") (1)	Signal:noise	Size of signal relative to noise
Mass (mg)	51.2	0.025	1 : 2048.0	
		0.25	1 : 204.8	
pseudo-abs. 430nm	0.047	0.053	1 : 0.887	~1
		0.453	1 : 0.104	~10
Mean greyscale value (2)	253	24600	1 : 0.010	~100
		4600	1 : 0.055	~20

Table 4-2: Calculation of the signal:noise ratio of each method using values for the blank tape and the range of tape *with* SC measurements.
(1) Ranges of values taken from section 4.4.2, where > 600 tapes with SC were measured with each method.
(2) The greyscale value of a pure white pixel is 64608, not 0. All measured values, including mean greyscale of blank tape, were thus subtracted from this value before calculating the signal to noise ratio.

The pseudo-absorption method provides a signal of 0.1 – 0.5 absorbance units for most samples (Section 4.4.2) at 430nm. 5 blank tapes assayed in the same way had a pseudo-absorption of 0.0474 ± 0.0012. This results in a signal to noise ratio of between 1 : 0.9 to 1 : 0.1 (Table 4-2). The signal is thus 1 to 10 times bigger than the noise value, which may mean that for some tapes, the signal may be difficult to distinguish from the noise.

6 blank tapes cropped to an area of 2213 x 2203 pixels, had a mean greyscale value of 64355 ± 29 over a total of 6×4875239 pixels (see General Appendix III). Approximately 98.5% of all pixels had a greyscale value of 64424 ± 7, which is very close to the absolute minimum of 64608. In order to calculate a signal:noise ratio comparable to the weighing and UV pseudo-absorption methods, all greyscale values, for both the *blank tape* and the *tapes with SC,* were subtracted from the greyscale value of a pure white pixel (64608).

Thus, tapes with small amounts of SC are closer in value to the blank tape than tapes with a large amount of SC.

The signal:noise ratio of the greyscale method is between 1 : 0.01 and 1 : 0.05 (Table 4-2). This is better than UV pseudo-absorption method. In addition, the signal is 20-100 times larger than the noise value, which means the signal will not be confused with the background noise.

4.4.1.3 Proportion of sample analysed

The weighing method measures all SC on the tape.

The pseudo-absorption is restricted to a 1cm^2 area. The slide holder positions the slides vertically. As such, it is awkward to see if the tape is correctly aligned with the incident beam. To avoid this problem, the SC strip should be at least 1.5cm x 1.5cm. The total area measured is 100mm^2, which is at most 44% of the total SC area sampled (225mm^2). Previous publications [102, 142] used very large tape strips (19mm x 57mm = 1083 mm^2) and presumably measured a lower proportion of the total SC. If there is any inhomogeneity, the results from this method will be affected by light scattering [143]; and if inhomogeneous tapes must be discarded (as in [102, 142]), the method cannot be generally suitable for assessing the amount of SC.

The imaging method is the most flexible in this respect as the crop can be adjusted to fit any size of strip, up to 2.3 cm x 3.5 cm (internal measurements of the slide). In these experiments, a crop of 1.4 cm x 1.4cm was applied over the 1.5 cm x 1.5cm strip. This equates to 196mm^2 measured out of the total of 225mm^2, i.e., 87.1%.

4.4.1.4 Time cost

The weighing method is the most variable in terms of time to complete the procedure, compounded by the fact that each tape needs to be weighed twice. In addition, as the mass of a tape changes with environmental conditions, 3-5 blank correction tapes must be weighed during both weighing sessions. For the 6 tapes, the average time taken to complete the 15 replicate *blank tape* and *tape with SC* weighings was 72±22 min. Both the UV pseudo-absorption and imaging methods are faster, with the 15 replicates performed in approximately 30 minutes for the pseudo-absorption assessment; and 15 minutes for the imaging method (data not shown).

Tape stripping typically required 20-25 strips per site and experiments usually consist of 2-4 test sites, along with 1 site to assess SC thickness. Obviously, the weighing method thus required a long and unpredictable length of time for weighing. The other two methods are quicker, and less likely to vary with environmental conditions. Additionally, the imaging method has the potential for automation using a slide feeder.

4.4.2 Correlation between SC amounts measured by each method

A series of tape strips were collected from intact untreated SC. All mass and greyscale values were collected within a short space of time, and so are analysed together in Figure 4-1 B. For tape set 1 (■), the UV pseudo-absorption scans were also performed at the same time. For tape sets 2 and 3 (● and ×), the UV pseudo-absorption measurements were taken some months after the mass/imaging measurements, and are thus presented separately in Figure 4-1 A and C.

Firstly, comparing the weighing method to the UV pseudo-absorption (Figure 4-1 A). A significant positive correlation is seen for all three tape sets, with higher masses of SC

associated with higher pseudo-absorption at 430nm. The strength of the non-parametric correlation is similar for all sets with Spearman correlation coefficients, r_s, of 0.53 – 0.57. The pseudo-absorption values are generally reproducible over the four rotations.

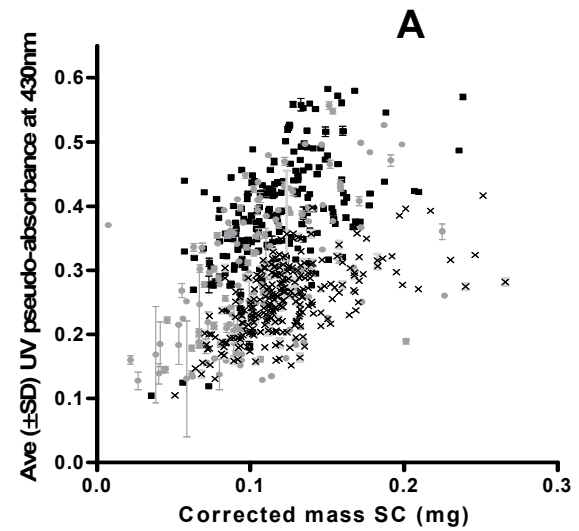

A. Weighing vs. mean (±SD) UV pseudo-absorption (n=4 rotations) measured at 430nm.

r_s values are 0.53, 0.53 and 0.57 for data sets 1 (■, n=202), 2 (●, n=152) and 3 (×, n=249) respectively.

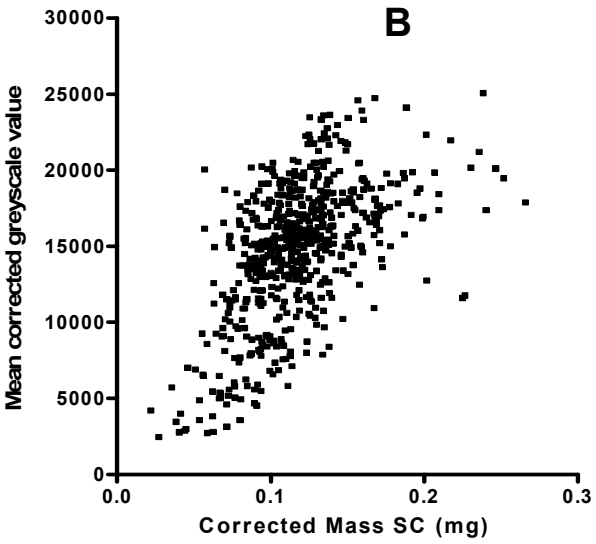

B. Weighing vs. imaging (n=601).
r_s value is 0.55.

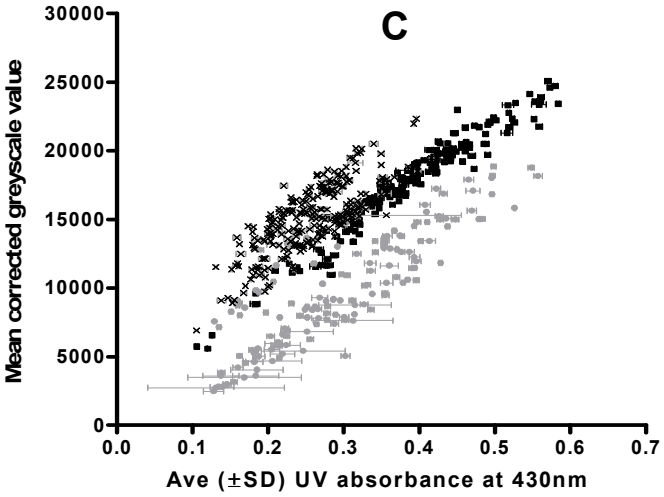

C. Imaging vs. mean (±SD) UV pseudo-absorption (n=4 rotations) measured at 430nm.

r_s values are 0.98, 0.85 and 0.75 for data sets 1 (■, n=202), 2 (●, n=149) and 3 (×, n=249) respectively.

Figure 4-1: Correlation of SC measurements by weighing, UV-pseudo-absorption and imaging methods. All correlations significant ($p<0.0001$) with a 2-tail Gaussian approximation and non-parametric Spearman correlation coefficients, r_s, presented.

It is interesting to note that our correlation coefficient is not as 'good' as that purported in the literature (linear regression (sic), r^2 of 0.93 ± 0.05 [142] or 0.92 ± 0.02 [102]) however, this can be explained as we did not eliminate any tapes from the correlation. We argue that the elimination of tapes on the grounds of "SC inhomogeneity" [102, 142] is not useful for the overall aim of using a technique to normalise drug penetration profiles for dermato-pharmacokinetic studies, since all tapes *must* be included for these profiles to provide meaningful pharmacokinetic measurements.

Figure 4-1 B similarly shows a significant positive correlation between the mass of SC on the tapes and the resultant mean greyscale value (Spearman correlation coefficient, r_s = 0.55). There are a large number of data points with a mass of SC between 0.08 – 0.13 mg. This suggests that the gravimetric approach is unable to distinguish between these masses, consistent with our findings in 4.4.1. We believe that the resultant poor correlation is mainly due to a lack of sensitivity and large inherent error of the weighing approach rather than the greyscale values. Nonetheless, this lack of correlation is problematic for converting the greyscale values into a workable quantity of SC for normalisation purposes.

Finally, comparing the mean greyscale with the pseudo-absorption, a better correlation is seen, with a Spearman coefficient of 0.75 – 0.98 depending on when the pseudo-absorption measurements were made relative to the imaging measurement. It is not appropriate to perform a linear regression, as neither variable is 'controlled'. However, it can be seen from Figure 4-1 C that the slope of the three groups is similar. This is perhaps not surprising considering the similarities seen when both measurements were correlated with the mass (Figure 4-1 A and B). The broad range of both the pseudo-absorption and mean greyscale measurements imply these methods offer a greater level of sensitivity compared to the gravimetric approach. It is thus easier to distinguish between the quantity of SC on the tapes using these methods. Of course, it is not known whether the quantities of SC are indeed as different as these methods suggest, however, considering the variability inherent with the gravimetric method, and the strength of the correlations ($p<0.0001$), these two methods would certainly be hard to dismiss outright.

Considering the range of values obtained by each method, the mass values also show a lack of sensitivity, with most values in the range of 0.08 – 0.13mg (factor = 0.62). Both the pseudo-absorption and imaging methods show a wider spread of values, between 0.1 – 0.6 (factor = 6) and 5000 – 25000 (factor = 5) respectively, which will increase their sensitivity for the very slight differences in SC amount on the tapes.

There are differences seen between the correlations depending on when the UV pseudo-absorption measurements were made relative to the other two measurements (Figure 4-1 A and B). In Figure 4-1 A, tapes which had their UV pseudo-absorption measured after a delay (sets 2 (●) and 3 (×) have lower UV pseudo-absorption values for given masses of SC than those measured immediately (tape set 1 (■). In Figure 4-1 C, tape sets 2 and 3 have a similar slope but different position to tape set 1. For given greyscale values, tape set 2 has lower UV pseudo-absorption values, but set 3 has higher ones. Possible reasons for this are unclear; possibly the tapes have changed with time or the lamp of the spectrophotometer has aged. It is merely important to note that pseudo-absorption measurements should be taken from fresh tapes.

Full raw data and calculations for the tape set from one site, with SC measured by the three methods (weighing, imaging, and UV pseudo-absorption) is shown in Appendix 3-D, as an example.

4.5 Conclusions

The weighing method of assessing SC amount per tape is clearly associated with numerous problems: namely low precision, extremely low signal:noise ratio (up to 1:2000), and a long, variable time needed to obtain measurements. These results call into question the usefulness of this method.

Two alternative methods have been considered concurrently, namely the UV-pseudoabsorption method already discussed in the literature, and a promising novel imaging method developed in the course of this work.

The pseudo-absorption method has high precision, is quick to perform and has an acceptable signal:noise ratio. However, the absorbance of the some tape strips is very similar to that of the blank tapes which brings into question the specificity of the method. Furthermore, the area of SC available to be measured is limited to only 1 cm^2. Finally, if the tapes are inhomogeneous, the method can be affected by light scattering artefacts [143].

The imaging method seems very promising: not only is it very precise, but the signal for the SC layer is high relative to the blank tape. In addition, the method is quick and simple to perform, and is able to measure any sample area up to 2.2 cm x 3.5 cm (1mm less than the internal measurements of the slide holder). Furthermore, permanent records of the SC measurements are obtained, which may be examined further using image analysis software.

The low precision, reproducibility and signal:noise ratio of the weighing measurements, coupled with poor correlations with the pseudoabsorption and imaging, demonstrates conclusively that the weighing method is not sufficiently sensitive nor robust to evaluate the amount of SC per tape strip.

From these results, the imaging method seems the most promising method to quantify the amount of SC per tape strip. It offers numerous practical benefits and high sensitivity. For further work, we consider whether the greyscale values can be used as a sensitive relative measure of the amount of SC per tape, as a direct substitute for SC thickness per tape in relevant dermato-pharmacokinetic equations.

4.6 Acknowledgements

We thank Sarah Cordery for technical assistance with the some of the UV pseudo-absorption measurements.

Chapter 5

Quantification of stratum corneum by imaging: application to dermato-pharmacokinetic studies.

5 Quantification of stratum corneum by imaging: application to dermato-pharmacokinetic studies

5.1 Abstract

An objective method to assess the rate and extent of drug permeation through the skin from topical formulations is required for bioequivalence purposes. Tape stripping the stratum corneum (SC) with adhesive tapes has emerged as a promising technique. When tapes are analysed individually, drug penetration profiles through the SC are plotted. To make comparisons between sites from different volunteers, the volunteer's total SC thickness is measured and used to normalise the drug penetration profiles. Crucial to creating such normalised profiles is that the amount of SC per tape is measured.

In this study, we compare two methods to quantify SC amount per tape, in terms of their potential to quantify total SC thickness, and to normalise drug penetration depths reached within the SC. First, the established method of weighing tapes before and after stripping to calculate the mass of SC per tape is examined, easily converted into a SC thickness. Second, a novel imaging method, whereby a high resolution image of each tape is taken under controlled conditions, is considered. Each pixel, of each image, has an associated greyscale value which may be measured and analysed. The mean greyscale value is multiplied by the scaled tape strip area to calculate the integrated pixel density, which is taken as a relative measure of SC per tape

Initially, two non-linear profiles were fitted to an appropriate non-linear model: (i) transepidermal water loss (TEWL) against cumulative thickness removed or (ii) TEWL against cumulative integrated pixel density. This allowed estimates of total SC thickness, H and G respectively, to be derived and they were well correlated. Furthermore, by repeatedly measuring adjacent sites, the intra-subject variability was found to be lower for the greyscale profiles than the thickness profiles.

Both non-linear plots were subsequently normalised using the relevant total SC thickness derived. This allowed the plots from the thickness and greyscale plots to be superimposed and directly compared. The normalised cumulative depth values from the thickness and greyscale profiles (for each successive tape) were found to be well correlated. Improved sensitivity and fewer outliers were highlighted for the absolute normalised greyscale values over the thickness values. Theoretically, there should be a correlation between the initial TEWL measured before stripping, with the estimates of two parameters from the normalised non-linear models. This was found to exist, and indeed, a slightly better correlation was found for parameters derived from the greyscale rather than the thickness profiles.

To conclude, the cumulative greyscale values may be used directly in place of the traditional cumulative thickness values to measure normalised depth reached within the SC, without any conversion factor.

5.2 Introduction

There is currently a need for an objective method to assess the rate and extent of drug permeation through the skin from topical formulations for bioequivalence purposes. Topical formulations deliver very low levels of drug to the systemic circulation, so drug levels should be sampled within the skin.

Since the stratum corneum (SC) is the principal barrier to drug absorption, it may be assumed that the (dermatopharmaco)-kinetics (DPK) of drug passage through this layer are related to topical bioavailability [84]. Tape stripping, where layers of SC are removed sequentially with adhesive tapes (after formulation application and removal), has shown potential for deriving comparative DPK parameters.

When each tape is individually analysed, penetration profiles across the SC may be plotted. The mass of drug per tape is found after drug extraction and analysis. However, since each tape removes a variable amount of SC, it is important to measure the amount of SC per tape in order to:

- Relate the mass of drug extracted to a 'volume' of SC per tape
- measure the depth reached within the SC by each successive tape strip rather than plotting tape strip number
- estimate a volunteer's total SC thickness. The depth reached within the SC is thus expressed relative to the volunteer's total SC thickness.

Thus, by measuring and using the amount of SC per tape, robust, reproducible normalised profiles of drug concentration against relative depth reached within the SC are produced, allowing profiles from different sites and volunteers to be easily compared [51, 84, 92, 94, 109-112, 120]. Analysis of these profiles, using an appropriate solution of Fick's second law of diffusion, permits parameters describing the partitioning and diffusivity of the drug (reflecting the rate and extent of penetration, respectively) to be estimated and used to compare different formulations.

Traditionally, weighing tapes before and after stripping has been used to estimate a mass of SC per tape, which can be converted to SC thickness per tape, since the area and population SC density (1g/cm^3, [99]) are known. The cumulative SC thickness removed by sequential tapes is thus plotted. At an adjacent, untreated site, stripping is performed with concomitant TEWL measurements, to derive an estimate for the total SC thickness [1, 100].

In Chapter 4, a novel imaging method to quantify SC amount per tape was shown to produce more precise and sensitive values than the weighing method, with a higher signal:noise ratio. For the imaging method, a high resolution image of each tape is taken under highly controlled lighting conditions. The pixels of the image each have an associated greyscale value which may be measured and analysed. The mean greyscale value across all pixels of the image is being taken as a relative measure of SC per tape.

Also, in Chapter 4, it was shown that there is no simple conversion factor between the mass of SC per tape and the mean greyscale value per tape. This is probably due to the lower precision and sensitivity of the weighing method.

In this study, the cumulative integrated pixel densities (=mean greyscale value $\times$ scaled strip area) were substituted directly in place of the cumulative thickness values in a non-linear model to estimate SC thickness [100]. From these non-linear plots, the SC thickness estimates were correlated and the intra-subject variability compared.

Furthermore, the cumulative thickness and cumulative greyscale values were normalised by dividing by the total SC thicknesses estimated from each model. This allowed the data and parameter estimates derived from each model to be directly compared.

5.3 Materials and Methods

5.3.1 Subjects

Healthy volunteers, with no history of dermatological disease, participated in the study. Ethical approval was granted by the Salisbury Local Research Ethics Committee, the Declaration of Helsinki protocols were followed, and written informed consent was obtained from all volunteers. Participants refrained from using any topical products on the test area on the day of the experiments.

A total of 25 sites from eight volunteers (2 male, 6 female, age range 23-37 years) were examined over a period of 14 months. Subjects were given code numbers (1–8). Repeated participation on different occasions was coded with a letter. Multiple sites examined on the same day were denoted with a roman numeral. For example "Subject 1 d (i)" denotes the results from the 1st stripping site on the 4th occasion that Subject 1 participated. Repeat participation using the same arm was delayed by at least 1 month, which is sufficient for barrier regeneration [117-119].

5.3.2 Tape stripping

2cm x 3cm tapes were cut from Scotch Book tape 845 (3M, St. Paul, MN) and stored overnight in covered trays. Tapes were manipulated using a small corner of each tape folded back on itself.

Two pre-tapes (larger than 2cm x 3cm) were applied, with pressure from a roller, to each study site, stripped and discarded. These pre-tapes remove exogenous substances and prepare the skin surface in a systematic way. A plastic template was applied to delimit a constant area (1.5cm x 1.5cm) within the study site. This template had an outline marked on its underside of 2cm x 3cm to ensure the tape was always placed in the same position.

Initial transepidermal water loss (TEWL) measurements were taken, until stable, with a closed-chamber evaporimeter (Biox Aquaflux AF102, Biox Systems Ltd., London, UK; probe applied for at least 60 s, TEWL was obtained once the mean of 10 successive measurements had a CV < 1%). A pre-weighed (see section 5.3.3.1) tape (2cm x 3cm) was positioned over the template. Adhesion was ensured with six rolls with a roller before swift removal. TEWL was re-measured. This sequence of tape strip then TEWL measurement continued until the TEWL was 4-5 times its original value.

5.3.3 Techniques to quantify amount of SC on tapes

The amount of SC per tape was examined by the weighing and imaging methods. All statistical tests, as detailed with the corresponding results, were performed using Prism® version 4 (GraphPad Software, CA, USA).

5.3.3.1 Weighing method

Tapes were stored for at least 12 hours before their first weighing. Static electricity was discharged from the tapes prior to weighing (R50 discharging bar and ES50 power supply from Eltex Elektrostatik GmbH, Weil am Rhein, Germany). The tapes were weighed, before and after stripping, using a microbalance with precision 0.1 µg (Sartorius SE-2F from Sartorius AG, Goettingen, Germany). The mass difference equals the mass of SC.

Five blank tapes were weighed at the same time as the tapes used for the tape-stripping

experiments, both before and after stripping, to correct the calculated mass of SC for any variations in weight due to environmental or other conditions.

5.3.3.2 Imaging method

The slide holding the tape + SC was photographed (14 bit) using a Coolscan V ED slide scanner (Nikon UK Limited, Kingston upon Thames, UK) at a resolution of 4000 pixels per inch (157.5 pixels/mm). Photographs fully illustrating this method are shown in General Appendix I. Lighting conditions and photographic settings were kept constant, using the settings detailed in General Appendix II. A crop of 2213 x 2203 pixels (approximately 1.4cm x 1.4cm) was centred over the image, using the preview scan, before the full scan was taken.

Cropped images (9822 KB each) were saved and analysed with ImageJ (Rasband, W.S., U. S. National Institutes of Health, Bethesda, Maryland, USA; freeware from http://rsb.info.nih.gov/ij/). A scale of 159.07 pixels/mm was applied to the full image width, to calculate a scaled area (195.1mm^2). During image analysis, each of the 4875239 pixels in the image is assigned a greyscale value (16 bit) in the range 0- 64608, where 0 and 64608 designate black and white respectively. The mean greyscale over all pixels was calculated and then subtracted from that obtained from blank tapes to yield mean greyscale values which increase with image darkness (and hence with the amount of SC on the tape). The results used for the blank scan correction are detailed in General Appendix III. The mean greyscale value was multiplied by the scaled area of each strip (measured as 195.1mm^2 for all tapes) to produce an integrated pixel density. Although all tapes had the same area in this case, the integrated pixel density will ease comparisons when strips of different areas are used.

The mean greyscale value or the integrated pixel density of a tape is used as relative measures of SC amount per tape.

5.3.4 Estimating SC total thickness with non-linear modelling

The mass of SC per tape is obtained from the weighing method. Knowing this mass, the strip area and the SC density (1g/cm^3, [99]), the thickness of SC removed per tape is calculated.

As shown in a previous publication (Chapter 2, and [100]), a plot of the increasing TEWL measurements as tape strips progressively remove an increasing thickness of SC, can be non-linearly modelled using Eq. 5-1, to derive an estimate of the total SC thickness, H.

$$TEWL = B_h + \frac{D \cdot K \cdot \Delta C}{H - h} \qquad \text{Eq. 5-1}$$

where: B is a baseline correction factor; D is the diffusion coefficient of water in the SC; K is the SC-viable tissue partition coefficient of water; and ΔC is the water concentration gradient across the SC. For a given volunteer on a given day, D, K and ΔC are assumed constant, and thus only the composite $D{\cdot}K{\cdot}\Delta C$ term is estimated by the model.

In this work, for each site, estimates of H were found using Eq. 5-1.

In addition, for all sites, the integrated pixel density of each tape, derived from the imaging method, was also used to quantify SC amount. The cumulative integrated pixel densities, *g*, were substituted in place of cumulative thickness values, *h*, in Eq. 5-1, to find a 'greyscale-based' estimate of SC thickness, G, using Eq. 5-2.

$$TEWL = B_g + \frac{(D \cdot K \cdot \Delta C)_g}{G - g} \qquad \text{Eq. 5-2}$$

For each site, the TEWL values measured are identical, but the cumulative integrated pixel densities (*g*) are several orders of magnitude larger than the corresponding thickness values (h). Thus, the estimates of the other parameters (D·K·ΔC and B) will also be numerically different when either Eq. 5-1 or Eq. 5-2 is used. Those estimated from the greyscale model (Eq. 5-2) have hence been attributed subscripts '*g*'.

Plots from each experimental site were evaluated separately using WinNonLin® software (Version 5.1, Pharsight Corporation, Mountain View, CA) using ASCII user-defined non-linear models written according to Eq. 5-1 and Eq. 5-2. In all cases, no data points were excluded; uniform weighting was applied; and no bounds were used.

Non-linear models rely upon good initial parameter estimates in order to converge. For data fitted to Eq. 5-1, the initial parameter estimates for modelling were: H = final h value + 1; D·K·ΔC = 30; B = initial TEWL value before stripping. For data fitted to Eq. 5-2, the initial parameter estimates for modelling were calculated from ratios of those used for the cumulative thickness measurements, namely: G = ((final h + 1) × final *g*)/final h; (D·K·ΔC)*g* = final *g* × 3; and B = initial TEWL value before stripping.

Iterations continued until the relative change in weighted sum of squares was <0.0001. The model derived parameter estimates were used as the new 'initial' values in the model, and the model rerun until there was no change in the parameter output. All parameter estimates presented are those from the final iteration of the model, with the smallest resultant residual sum-of-squares; however, usually no change was seen after the first run, suggesting that the modelling was stable.

The precision of the parameter estimates derived from both non-linear models (Eq. 5-1 and Eq. 5-2) is described by both the standard error of the regression (SER) and the coefficient of variation (CV (%)) as described in Chapter 2.

5.3.5 Comparison of normalised plots

To compare easily whether the plots of TEWL against either cumulative thickness or cumulative integrated pixel density, and the resultant fits to Eq. 5-1 or Eq. 5-2 respectively, are equivalent, the profiles were normalised.

To normalise the TEWL vs. cumulative thickness plots, all cumulative thickness values, *h*, were divided by the total thickness, H, generating *h*/H values. To normalise the TEWL vs. cumulative integrated pixel density plots, all integrated pixel densities, *g*, were divided by the total thickness, G, resulting in *g*/G values.

Two new directly comparable normalised plots of TEWL against relative depth reached within the SC, either *h*/H or *g*/G, are thus produced and can be superimposed for comparison.

In order to non-linearly model these normalised plots, if *h* is replaced with *h*/H in Eq. 5-1, and *g* is replaced with *g*/G in Eq. 5-2, the following models are deduced.

$$TEWL = B + \frac{(D \cdot K \cdot \Delta C)/H}{1 - h/H} \qquad \text{Eq. 5-3}$$

$$TEWL = B_g + \frac{(D \cdot K \cdot \Delta C)_g / G}{1 - g/G} \qquad \text{Eq. 5-4}$$

Of course, Eq. 5-3 and Eq. 5-4 are mathematically equivalent to Eq. 5-1 and Eq. 5-2, respectively.

5.3.5.1 Absolute normalised SC measured per tape

Correlating *h*/H with *g*/G values to compare the mass and imaging methods is possible. However, as these are cumulative values, the values of a single site are not independent, with higher values calculated using the values of lower tape numbers. To assess whether the mass and imaging methods produce comparable values for *each tape* individually, the absolute normalised thickness of tape *i* (ANT_i) and the absolute normalised integrated pixel density of tape *i* (ANG_i) were calculated with Eq. 5-5 and Eq. 5-6 respectively.

$$ANT_i = \left(\frac{h}{H}\right)_i - \left(\frac{h}{H}\right)_{i-1} \qquad \text{Eq. 5-5}$$

$$ANG_i = \left(\frac{g}{G}\right)_i - \left(\frac{g}{G}\right)_{i-1} \qquad \text{Eq. 5-6}$$

5.3.5.2 Comparison of D·K·ΔC/H, $(D \cdot K \cdot \Delta C)_g$/G, and $TEWL_0$

From the fits of the normalised plots to Eq. 5-3 and Eq. 5-4, the estimates of D·K·ΔC/H and $(D \cdot K \cdot \Delta C)_g$/G may be compared directly.

Furthermore, before any tape strips have been made, Eq. 5-1 and Eq. 5-2 will simplify to Eq. 5-7and Eq. 5-8 respectively.

$$TEWL_0 = B + \frac{D \cdot K \cdot \Delta C}{H} \qquad \text{Eq. 5-7}$$
$$\Leftrightarrow TEWL_0 - D \cdot K \cdot \Delta C / H = B$$

$$TEWL_0 = B_g + \frac{(D \cdot K \cdot \Delta C)_g}{G} \qquad \text{Eq. 5-8}$$
$$\Leftrightarrow TEWL_0 - (D \cdot K \cdot \Delta C)_g / G = B_g$$

Where $TEWL_0$ is the measured initial TEWL.

Estimates of B and B_g, as well as D·K·ΔC/H and $(D \cdot K \cdot \Delta C)_g$/G were derived from the fits to Eq. 5-3 and Eq. 5-4 respectively.

To verify the validity of the non-linear model, the correlation between the measured $TEWL_0$ and the estimated normalised B and D·K· ΔC factors was established.

5.4 Results and Discussion

5.4.1 Comparison of the total thickness estimates: H and G

For each tape stripping site, two estimates of total SC thickness, H and G, have been determined non-linearly from TEWL plotted against either the cumulative thickness of SC (measured by weighing method and fitted to Eq. 5-1) or the cumulative greyscale value (measured by the imaging method and fitted to Eq. 5-2) respectively. Plots of the raw data, and fits to the non-linear models, for Subject 2 is presented are Figure 5-1 A and B as an example.

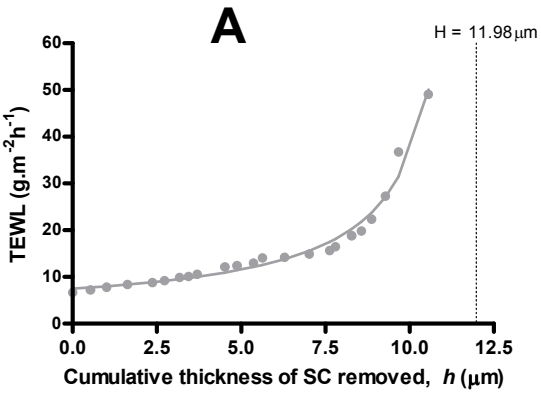

A. TEWL vs. cumulative thickness of SC removed (experimental data points (●) and resultant fit to Eq. 5-1 (▬)).
H estimate = 11.98μm.

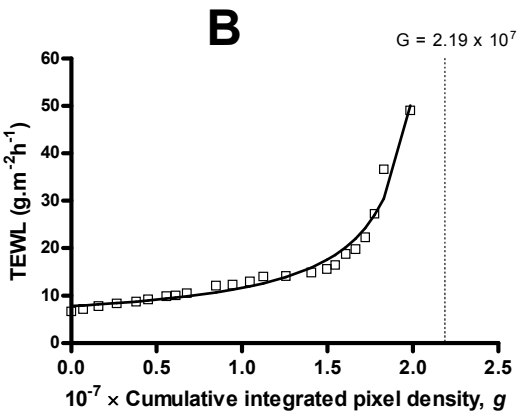

B. TEWL vs. cumulative integrated pixel density of SC removed (experimental data points (□) and resultant fit to Eq. 5-2).
G estimate = 2.19×10^7

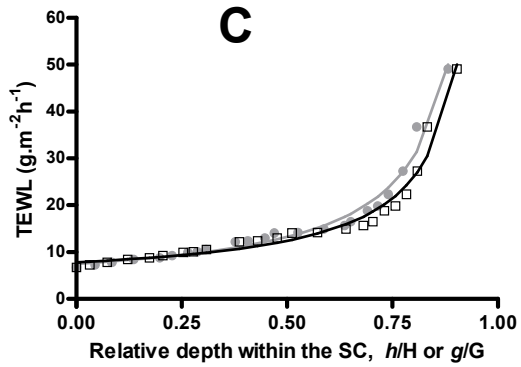

C. Normalised profiles superimposed for comparison: (i) TEWL vs. normalised cumulative thickness, *h*/H (●) and the resultant fit to Eq. 5-3 (▬); (ii) TEWL vs. normalised cumulative integrated pixel density, *g*/G (□) and the resultant fit to Eq. 5-4 (▬).

Figure 5-1: TEWL vs. cumulative thickness and cumulative integrated pixel density values for Subject 2

Table 5-1 details the non-linear modelling estimates from the two non-linear models for 25 independent experiments. The thicknesses measured with the gravimetric method vary from 8.9 – 22.6 µm, with a mean (±standard deviation) of 13.6 ± 4.0 µm. The mean thickness is in agreement with previous findings (Chapter 2 / [100]). The SC thicknesses obtained from the imaging method, G, are also shown in Table 5-1 but are not directly comparable with H values.

Subject[1]	Parameter estimates derived from cumulative thickness calculations (Eq. 5-1)						Parameter estimates derived from cumulative mean greyscale calculations (Eq. 5-2)					
	H (µm)	SER	CV (%)[2]	D·K·ΔC	SER	CV (%)	10^{-7} × G	10^{-7} ×SER	CV (%)[2]	10^{-7} × D·K·ΔC	10^{-7} × SER	CV (%)
1 a	11.7	0.17	1.5	45.1	5.9	13.1	2.51	0.03	1.1	7.3	0.8	11.5
1 b	8.9	0.13	1.5	88.7	12.7	14.4	2.33	0.03	1.1	24.4	2.6	10.5
1 c	14.1	0.08	0.6	91.0	4.9	5.4	3.14	0.01	0.4	17.5	0.7	4.1
1 d (i)	11.8	0.14	1.2	109.1	10.9	10.0	4.44	0.04	1.0	45.6	3.4	7.4
1 d (ii)	10.2	0.04	0.4	114.2	4.9	4.3	4.19	0.02	0.4	50.5	2.2	4.3
1 d (iii)	9.4	0.05	0.6	66.7	3.9	5.9	3.87	0.02	0.5	29.5	1.5	5.0
1 d (iv)	12.0	0.18	1.5	126.7	13.9	11.0	4.13	0.06	1.5	44.3	4.7	10.6
2	12.0	0.16	1.4	68.3	8.0	11.8	2.2	0.03	1.2	10.0	1.3	12.6
3	9.1	0.15	1.6	104.4	11.7	11.2	2.31	0.04	1.6	24.5	2.9	12.0
4 a	10.7	0.08	0.7	82.8	5.2	6.3	4.69	0.03	0.7	33.0	2.2	6.6
4 b	15.9	0.11	0.7	44.6	6.9	6.5	6.58	0.04	0.6	26.5	1.7	6.5
5	18.0	0.10	0.6	106.6	4.7	10.6	4.72	0.02	0.5	27.3	1.7	6.3
6 a	18.7	0.23	1.2	107.3	8.7	8.1	7.34	0.08	1.1	41.2	3.1	7.4
6 b (i)	22.6	0.68	3.0	160.3	26.1	16.3	7.36	0.21	2.9	49.4	7.8	15.9
6 b (ii)	18.2	0.49	2.7	122.0	16.4	13.5	6.36	0.14	2.2	34.0	4.3	12.7
6 b (iii)	16.9	0.28	1.6	86.4	10.5	12.2	6.21	0.10	1.6	30.0	3.7	12.2
7 (i)	9.9	0.02	0.3	47.6	1.7	3.5	3.22	0.01	0.3	16.3	0.7	4.5
7 (ii)	10.2	0.18	1.7	98.5	10.5	10.7	3.9	0.08	2.1	40.3	5.0	12.4
7 (iii)	10.5	0.22	2.1	96.9	15.1	15.6	3.94	0.09	2.3	38.2	6.2	16.1
7 (iv)	9.4	0.13	1.4	70.9	7.3	10.3	3.63	0.05	1.4	26.6	2.9	10.9
8 (i)	13.7	0.34	2.5	79.5	16.8	21.2	5.31	0.19	3.5	42.9	9.9	23.1
8 (ii)	14.1	0.18	1.3	132.3	13.8	10.4	5.13	0.05	0.9	47.6	3.5	7.2
8 (iii)	14.2	0.24	1.7	103.0	15.4	14.9	5.36	0.09	1.7	44.6	5.8	13.1
8 (iv)	18.9	0.21	1.1	111.4	14.4	12.9	5.36	0.06	1.1	31.2	4.0	13.0
8 (v)	19.7	0.24	1.2	150.3	17.6	11.7	6.35	0.07	1.2	50.1	5.4	10.8
Average	13.6	0.19	1.4	96.6	10.7	10.9	4.58	0.06	1.3	33.3	3.5	10.3
SD	4.0			30.0			1.54			12.5		
RSD (%)	29.0			31.1			33.7			37.5		

Table 5-1: Estimation of non-linear parameter estimates for the cumulative thickness and cumulative greyscale models for 25 experiments. Goodness-of-fit of data to non-linear model is shown as standard error of the regression (SER) and coefficient of variation (CV (%))

[1] Each volunteer given a code number (1-8); repeated participation given a letter (a-d); repeated participation on the same day (different sites, same arm) given a roman numeral (i-v).

[2] No significant difference in coefficient of variation (CV, %) of H and G estimates (non-parametric paired 2-tail T test with Wilcoxon signed rank test ($p>0.05$); pairing was significantly effective ($p<0.0001$)).

Figure 5-2 shows the significant correlation plot between the H and G estimates (with their SER) over the 25 sites ($p<0.0001$, 2-tailed Gaussian approximation, Spearman correlation coefficient, $r_s = 0.80$). This is much better than the correlation seen between individual SC mass and SC greyscale values on individual tapes ($r_s = 0.55$, Section 4.4.2), even with fewer replicates. A possible reason for this is the large error associated with the weighing method of assessing SC amount, as discussed in Chapter 4. Considering a single measurement of an individual tape, weighing errors can distort the correlation with the tape mean greyscale value considerably. On the other hand, the G and H measurements are global, incorporating the individual SC measurements of many tapes, so errors on a few tapes will not have such a great effect on the correlation.

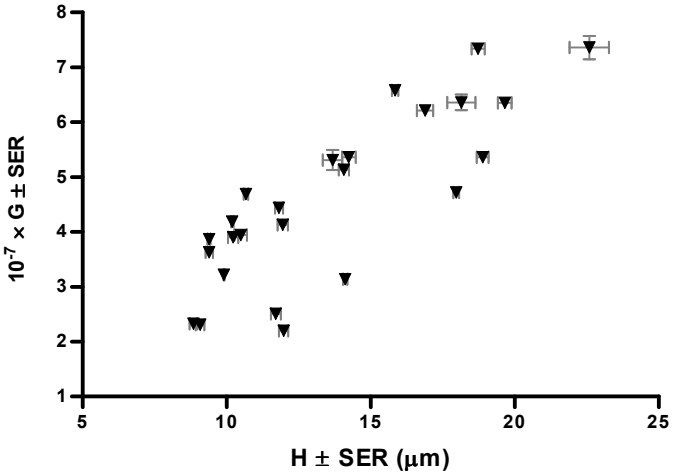

Figure 5-2: Correlation between the SC thickness estimates, H and G, with their respective standard error of the regression (SER), for 25 experimental sites. Correlation is significant ($p<0.0001$) with a 2-tailed Gaussian approximation, Spearman correlation coefficient, $r_s = 0.80$

5.4.1.1 Intra-subject variability of H and G

The SC thickness is measured at one site, in order to normalise the results from DPK experiments at adjacent sites. Therefore, it is assumed the thickness is constant, and the estimate of SC thickness should be similar across adjacent sites. For four volunteers, we estimated the SC thickness on 3-5 adjacent skin sites on the same arm on the same day, using the thickness (Eq. 5-1) and greyscale (Eq. 5-2) models, and the variability is presented in Table 5-2.

	Subject 1 (n = 4)		Subject 6 (n = 3)		Subject 7 (n = 4)		Subject 8 (n = 5)	
	H (μm)	10^{-7} x G	H (μm)	10^{-7} x G	H (μm)	10^{-7} x G	H (μm)	10^{-7} x G
Average	10.8	4.2	19.2	6.6	10.8	4.2	19.2	6.6
SD	1.3	0.2	3.0	0.6	1.3	0.2	3.0	0.6
RSD (%)	11.6	5.6	15.6	9.4	11.6	5.6	15.6	9.4

Table 5-2: Variability in H and G for 4 volunteers where multiple sites were examined on the same arm on the same day.

Comparing the relative standard deviation (RSD) values for the two models, in Subjects 1, 6 and 8, the estimate for G has a lower RSD than the corresponding H estimate. It is also interesting to note that the G estimates from the numerous sites always had a RSD <10%, whereas the H estimates for Subjects 1, 6 and 8 have RSD >10%. These data suggest that the G estimate of SC thickness (from Eq. 5-2) is less variable than the H estimate (from Eq. 5-1).

For tape stripping experiments, the SC thickness is assumed constant across adjacent sites examined. As the SC thickness is measured at one dedicated 'thickness' site, which should be representative of the surrounding sites, these data suggest that the greyscale measure of SC thickness, G, with lower inter-site variability on the same volunteer, is preferable for assessing SC thickness.

5.4.2 Comparison of normalised plots

In order to compare easily the plots produced by the thickness (Eq. 5-1) and greyscale (Eq. 5-2) models, the cumulative thickness values were all divided by H (to produce *h*/H values); and the cumulative integrated pixel densities, *g*, were all divided by G (to produce *g*/G values) as explained in section 5.3.5. TEWL vs. h/H and g/G are modelled with Eq. 5-3 and Eq. 5-4 respectively. The data and fits from both models may then be superimposed, as shown in Figure 5-1 C.

5.4.2.1 Comparison of *h*/H and *g*/G values

The absolute SC thickness, H or G, is not interesting for dermato-pharmacokinetic studies *per se*, but rather is useful as a tool to present the relative depth reached within the SC, namely *h*/H and *g*/G, for different volunteers on different days.

In Figure 5-3, the *h*/H and corresponding *g*/G values for 388 tapes shown. There is a significant ($p<0.0001$) positive correlation, with a Spearman correlation coefficient, r_s of 0.99. This implies that the *h*/H and *g*/G values are interchangeable and that the results of the imaging method could be used to describe the relative position reached within the SC for dermato-pharmacokinetic studies.

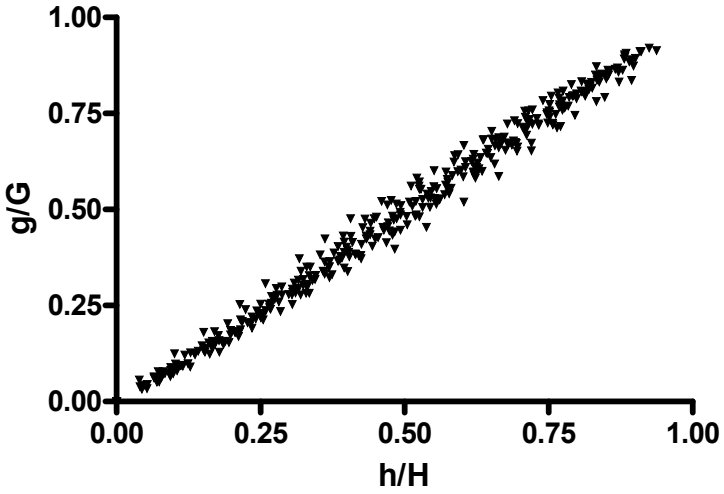

Figure 5-3: Correlation between the *h*/H and *g*/G values from 25 separate experiments (n = 388). The correlation (2 tail) is significant ($p<0.0001$), with a Spearman correlation coefficient, $r_s = 0.99$.

5.4.2.2 Comparison of absolute normalised SC measured per tape

The *h*/H and *g*/G values shown in Figure 5-3 are cumulative values, with each successive value between 0 and 1 including the values of earlier tape strips from that tape stripping site. Hence, the values are not independent. Thus; the absolute normalised thickness (ANT_i,) and absolute normalised integrated pixel density (ANG_i,) values of each tape, *i*, were calculated using Eq. 5-5 and Eq. 5-6 respectively. These, along with means and

standard deviations, are plotted in Figure 5-4.

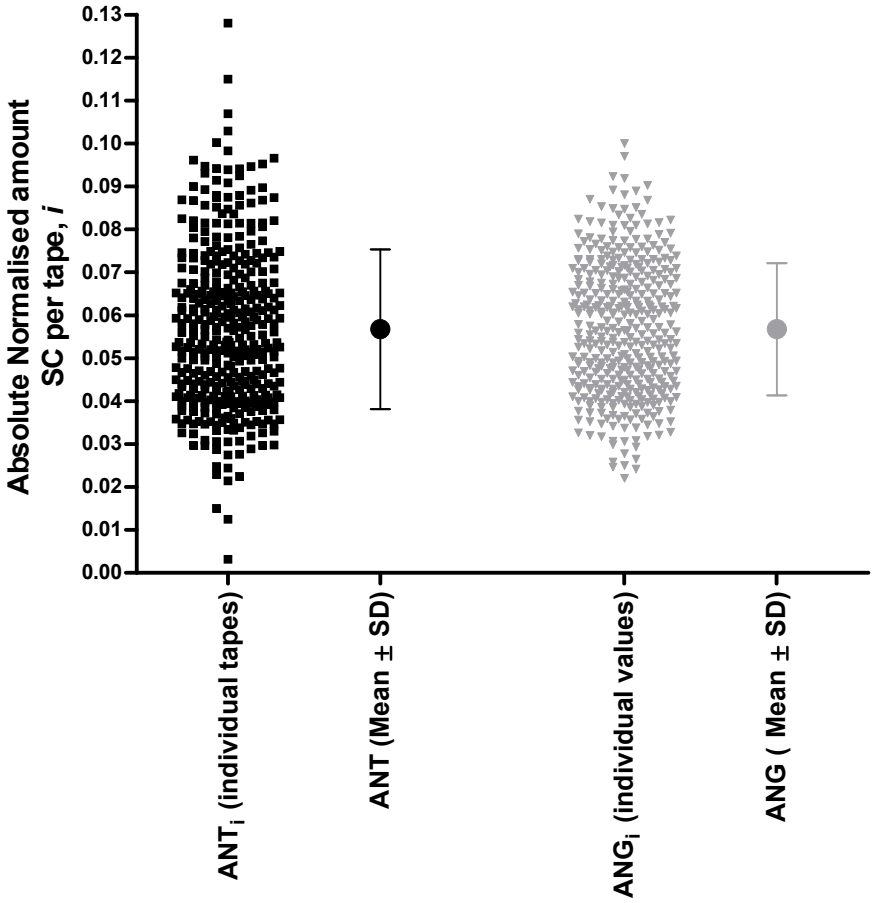

Figure 5-4: The absolute normalised thickness (ANT_i, ■, Eq. 5-5) and absolute normalised integrated pixel density (ANG_i, ▼, Eq. 5-6) values for each tape, *i* (n=388); no significant difference between the ANT and ANG values (paired 2-tail T test (p = 0.98; pairing was effective (p<0.0001)). Mean (●) and SD (I) values also presented for each method.

There is no statistical difference between the ANT_i and ANG_i values (paired 2-tail T-test, p = 0.98). However, the values derived from the weighing method (ANT_i) have more extreme values than those derived from the imaging method (ANG_i). Furthermore, the standard deviation of the ANG values (0.0154) is smaller than that of the ANT values (0.0186). This is consistent with the lower precision of the weighing method, as discussed in Chapter 4.

It is also noted that the majority of values derived from the weighing method (ANT_i) are clustered in the range 0.04 – 0.07, whereas the values derived from the imaging method are more widely and uniformly distributed (0.03 – 0.08). This suggests that the imaging method may have a higher sensitivity to distinguish between the subtly different amounts of SC on tape strips.

5.4.2.3 Links between D·K·ΔC/H, $(D{\cdot}K{\cdot}\Delta C)_g/G$, and $TEWL_0$

The initial TEWL measured before stripping ($TEWL_0$), and the normalised D·K·ΔC estimates, with measures of their precision (SER and CV), are presented in Table 5-3. The normalised values derived from the weighing method (D·K·ΔC/H) and the imaging method ($(D{\cdot}K{\cdot}\Delta C)_g/G$) are not significantly different (paired 2-tail T-test (p>0.05); pairing significantly effective (p<0.0001)). This, along with the lack of significant difference

between the *h*/H and *g*/G values (section 5.4.2.1 above) implies that the normalised curves produced by both methods overlap.
The average values over all 25 data sets are remarkably similar: 7.38±2.27 and 7.47±2.49 for D·K·ΔC/H and $(D{\cdot}K{\cdot}\Delta C)_g/G$ respectively. The goodness-of-fit of the parameters to the relevant normalised models is also similar (Table 5-3).

Subject[1]	Experimental $TEWL_0$		Normalised with H			Normalised with G		
	Average	SD	D·K·ΔC/H estimate	SER	CV (%)	D·K·ΔC/H estimate	SER	CV (%)
1 a	6.6	0.34	3.9	0.51	13.2	2.9	0.34	11.8
1 b	10.9	0.24	10.0	1.44	14.4	10.5	1.15	11.0
1 c	10.8	0.27	6.5	0.35	5.4	5.6	0.24	4.3
1 d (i)	10.5	0.35	9.3	0.92	10.0	10.3	0.8	7.8
1 d (ii)	13.1	0.46	11.2	0.48	4.3	12.1	0.55	4.6
1 d (iii)	11.7	0.59	7.1	0.42	5.9	7.6	0.4	5.2
1 d (iv)	10.3	0.2	10.5	1.17	11.1	10.7	1.18	11.0
2	6.7	0.15	5.7	0.68	11.8	4.5	0.59	12.9
3	15.4	0.19	11.6	1.31	11.3	10.7	1.34	12.5
4 a	8.7	0.07	7.7	0.49	6.3	7.0	0.48	6.8
4 b	8.9	0.57	5.9	0.38	6.4	5.8	0.38	6.5
5	10.4	0.41	2.8	0.3	10.6	4.1	0.27	6.7
6 a	7.0	0.48	5.7	0.46	8.1	5.6	0.44	7.8
6 b (i)	8.3	0.36	7.0	1.14	16.2	6.8	1.13	16.7
6 b (ii)	7.5	0.18	6.7	0.91	13.5	5.4	0.72	13.4
6 b (iii)	9.5	0.42	5.2	0.63	12.2	4.9	0.63	12.9
7 (i)	17.6	0.79	4.8	0.17	3.5	5.1	0.24	4.7
7 (ii)	18.2	0.54	9.8	1.04	10.7	10.4	1.36	13.1
7 (iii)	20.3	0.54	9.2	1.44	15.6	9.8	1.64	16.8
7 (iv)	15.3	0.73	7.6	0.78	10.3	7.4	0.85	11.4
8 (i)	9.3	0.4	5.9	1.26	21.2	8.2	1.98	24.2
8 (ii)	10.0	0.39	9.4	0.98	10.4	9.3	0.7	7.6
8 (iii)	9.8	0.03	7.2	1.08	14.9	8.3	1.14	13.7
8 (iv)	11.6	0.6	6.0	0.77	12.9	5.8	0.79	13.4
8 (v)	14.5	0.63	7.7	0.9	11.7	7.9	0.88	11.2
Average	11.32	0.40	7.38	0.80	10.87	7.47	0.81	10.72
SD	3.70		2.27			2.49		

Table 5-3: Estimate of normalised D·K·ΔC parameters from the two models, along with their respective SER and CV (%); and the experimental initial TEWL before stripping ($TEWL_0$).

The significant positive correlation seen between D·K·ΔC/H and $(D{\cdot}K{\cdot}\Delta C)_g/G$ is also highlighted in Figure 5-5 ($\alpha = 0.05$, Spearman correlation coefficient = 0.93). Eq. 5-7 and Eq. 5-8 predict that before any stripping has occurred, the original non-linear equations (Eq. 5-1 and Eq. 5-2 respectively) can be simplified. As such, for the cumulative thickness curves (with SC measured by weighing), there should be a correlation between B and $TEWL_0 - D{\cdot}K{\cdot}\Delta C/H$; and for the cumulative integrated pixel density curves, a correlation between B_g and $TEWL_0 - (D{\cdot}K{\cdot}\Delta C)_g/G$. These two correlations are shown in Figure 5-6 A and B, and are indeed very good, with Spearman correlation coefficients of 0.91 and 0.94 for the weighing and imaging methods respectively. This confirms that the original non-linear models fit the data well and indeed that the imaging method performs slightly better than the weighing method.

Full raw data and calculations for the tape set from Subject 1c, is shown in Appendix 5-A, as an example.

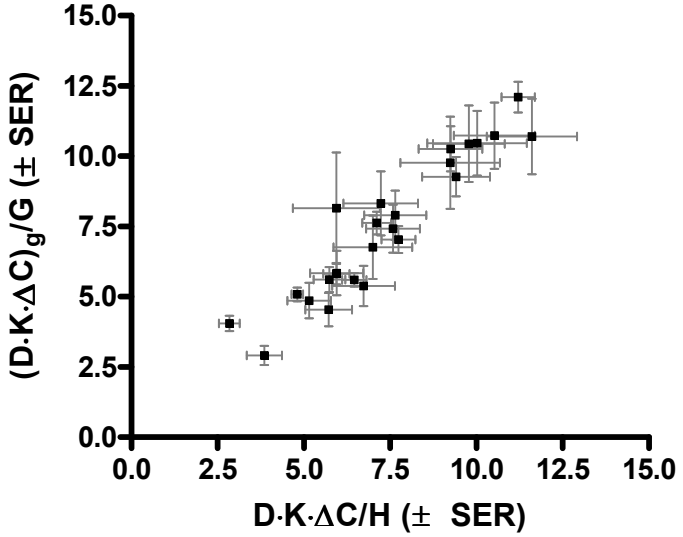

Figure 5-5: Comparison of the (normalised) D·K·ΔC/H and D·K·ΔC/G estimates (with their respective SER) for 25 different sites; significant correlation (α = 0.05) found with a 2-tail non-parametric correlation (p<0.0001, Spearman coefficient = 0.93).

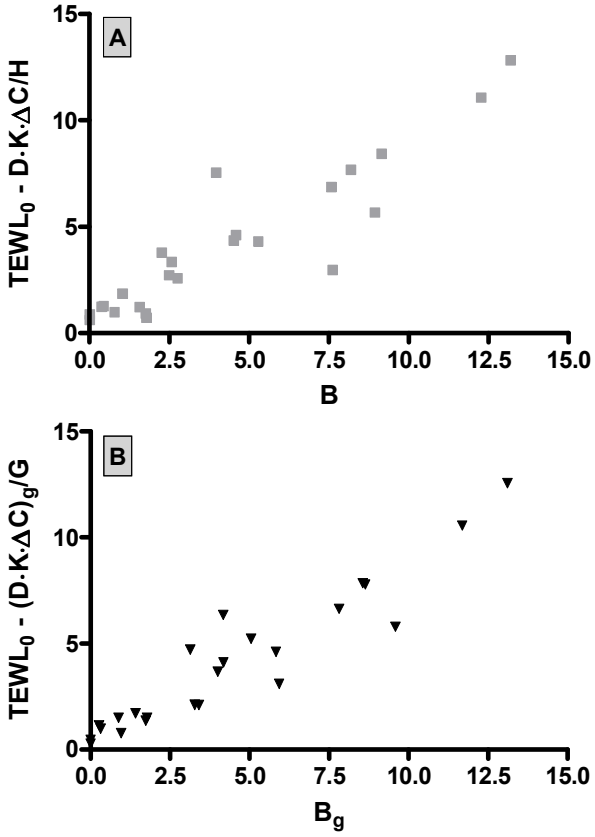

A. Positive significant correlation between ($TEWL_0$ - D·K·ΔC/H) and B for 25 sites (p<0.0001, Spearman correlation coefficient, r_s = 0.91).

B. Positive significant correlation between ($TEWL_0$ – $(D·K·\Delta C)_g/G$) and B_g for 25 sites (p<0.0001, Spearman correlation coefficient, r_s = 0.94).

Figure 5-6: Testing the correlation between $TEWL_0$ and normalised non-linear parameter estimates.

5.5 Conclusions

In this study, the SC on tapes from 25 untreated sites has been quantified by weighing *and* a novel imaging method. The use of the mass of SC per tape in dermato-pharmacokinetic studies is established [51, 84, 92, 94, 109-112, 120]. When stripping is performed on an adjacent site, coupled with TEWL measurements, the total SC thickness may be estimated from a non-linear model (Chapter 2 / [100]).

In this study, it was shown that the total SC thickness can be derived using cumulative greyscale values of successive tapes instead of cumulative thickness values in the non-linear model previously described (Chapter 2 / [100]) The SC total thicknesses derived from either model correlate well, but the intra-subject variability is lower for the greyscale model.

When the original plots are normalised using the SC thickness estimated from either model, such that the relative depth within the SC is plotted, the model outputs may be directly compared. Fortunately, the normalised profiles overlap and provide comparable non-linear parameter outputs: h/H correlated with g/G; and $D{\cdot}K{\cdot}\Delta C/H$ correlated with $(D{\cdot}K{\cdot}\Delta C)_g/G$. Dermato-pharmacokinetic studies plot drug concentration as a function of the relative depth across the SC. Since both relative measures, h/H and g/G investigated here are significantly correlated, they may be used interchangeably. There is therefore no need to perform any conversion of the imaging results to mass measurements.

The absolute normalised SC amount per tape was also calculated for both models. The values from the greyscale model had fewer outliers (indicating better precision), and showed a greater spread of values (indicating better sensitivity) than the weighing method. This is consistent with findings in Chapter 4.

Finally, before any stripping commences, the non-linear model simplifies to predict a relationship between the initial TEWL before stripping, the estimates of the baseline-correction factor, B, and the estimates of the normalised $D{\cdot}K{\cdot}\Delta C$ parameter. This is indeed the case, with a slightly better correlation seen between these parameters for the imaging rather than the weighing method.

The mean cumulative greyscale values, derived from the imaging method, may therefore be used instead of the cumulative thickness values derived from the weighing method to directly measure the relative depth reached within the SC with each tape. Indeed, the cumulative greyscale values are more precise and sensitive; the normalised cumulative greyscale plots have less intra-subject variability; and a better correlation is seen when verifying normalised $D{\cdot}K{\cdot}\Delta C$ and B estimates with the initial TEWL measured before stripping. Considering the other benefits that the imaging method provides in terms of speed and ease of analysis; precision; signal:noise ratio; reproducibility; large proportion of tape assayed; and a permanent record of the tape's image (see Chapter 4), this is extremely promising. These results indicate that the imaging method can, and perhaps should replace the weighing method for assessing SC on tape strips.

Chapter 6

Dermato-pharmacokinetics: methodological refinement of the tape stripping technique and future challenges

6 Dermato-pharmacokinetics: methodological refinement of the tape stripping technique and future challenges

6.1 Abstract

Tape stripping is a minimally invasive method to measure drug permeation through the stratum corneum (SC). Analysing the concentration of drug on each tape, as a function of the relative position within the SC, allows parameters characterising the penetration process to be derived after fitting the data to an appropriate solution of Fick's second law of diffusion.

Traditionally, drug penetration profiles measured the amount of SC per tape by weighing each tape before and after stripping. We have developed a novel imaging method which offers advantages in terms of sensitivity, reproducibility, precision, stability and speed over weighing. High resolution images, taken under controlled conditions, are analysed in terms of pixel greyscale values and distributions. The integrated pixel density (=mean greyscale value x strip area) of each tape is used as a measure of SC amount. In this article, we compare the drug penetration profiles from two acyclovir creams obtained using the mass of SC per tape, to those obtained by substituting the cumulative thickness measurements with cumulative integrated pixel densities. The drug penetration profiles are comparable.

Furthermore, the images taken of each tape may be used to assess SC inhomogeneity. The original FDA guidance on dermato-pharmacokinetics stipulated that the tape stripping method is not suitable for formulations which disrupt SC structure and cohesivity, as drug partitioning into, and diffusivity through, the barrier may be affected. Here, we examine a formulation which caused significant SC disruption, where resultant tape strips were inhomogeneous and sometimes contained large clumps of tissue. Three methods were used to further analyse the stored images, to assess SC inhomogeneity. This could be a useful, objective method with which to reject SC-disrupting formulations from further clinical applications.

6.2 Introduction

Dermato-pharmacokinetics is the study of the rate and extent of drug permeation through the SC. Tape stripping is a minimally invasive method to measure drug concentrations at different depths within the SC. In studies where data are gleaned from each tape individually, drug penetration profiles are produced, relating a concentration of drug measured per tape (in terms of mass of drug per volume of SC) to a particular depth reached within the SC (this depth is expressed relative to the total SC thickness, measured separately). These drug concentration penetration profiles can be fitted to an appropriate solution of Fick's second law, to derive the SC-vehicle partition coefficient and a measure of the drug's diffusivity in the SC. These parameters may be compared for different formulations. The amount of SC on each tape is required (i) to express the drug mass measured per tape as a concentration (in terms of a 'volume' of SC); (ii) to measure the depth reached within the SC; and (iii) to measure the total SC thickness at a separate site, in order to express the depth reached relative to the total SC thickness per volunteer.

Traditionally, the amount of SC per tape has been determined gravimetrically, whereby the tape is weighed before and after stripping and the mass of SC deduced. Knowing this

mass, the area of SC stripped and the density of SC (1g/cm^3, [99]), the thickness removed per tape, and hence the cumulative thickness removed by each successive tape, is calculated.

As an alternative method to assess the amount of SC per tape, a novel imaging technique has been investigated, whereby a high resolution image of each tape is taken under controlled lighting conditions. Each pixel of this image has an associated greyscale value, and the mean greyscale value across all pixels is used as a relative measure of SC amount per tape. We have already shown that the mean greyscale value of a tape is a more sensitive, precise, reproducible, rapid and stable method to assess the quantity of stratum corneum (SC) on tapes, as compared with weighing (Chapter 4). The integrated pixel densities are calculated simply by multiplying mean greyscale values by the strip area (in this study, 195.1mm^2 for all strips) We have also shown that the cumulative integrated pixel densities (g) derived from tapes on an untreated site, with concomitant transepidermal water loss (TEWL) measurements, can be used to derive a measure of total SC thickness (G) for a volunteer (Chapter 5) Furthermore, the total (greyscale) thickness, G, can be used to measure the relative depth reached within the SC, denoted g/G (Chapter 5).

Now we examine the usefulness of the greyscale measure of SC amount per tape to produce dermato-pharmacokinetic profiles for assessing and comparing topical formulations. Two types of drug penetration profiles are constructed for two acyclovir (ACV) creams: (i) 'mass' DPK profiles where the mass of SC is used to measure SC amount per tape; and (ii) 'imaging' DPK profiles where integrated pixel densities are used as a measure of SC amount per tape.

Furthermore, the images of tapes which stripped an inhomogeneous layer of SC were studied further. Three image analysis techniques have been investigated to quantify the extent of inhomogeneous SC removal by these tapes.

6.3 Materials and Methods

6.3.1 Subjects and formulations

Two female healthy volunteers (both 30 years old), with no history of dermatological disease, participated in this study. Ethical approval was granted by the Salisbury Local Research Ethics Committee, the Declaration of Helsinki protocols were followed, and written informed consent was obtained. Two 5% acyclovir cream formulations were compared: (i) Zovirax cream (GlaxoSmithKline plc, Brentford, UK), and (ii) a generic cream (Pliva Pharma, Ltd, Petersfield, UK). Each volunteer provided five study sites: 2 sites for each of the two formulations, and one site to calculate SC thickness.

6.3.2 Tape stripping

Prior to any tape stripping experiment, loose outer layers of the stratum disjunctum at the skin sites was removed with two light "pre-tapes" and discarded. This was done to prepare all skin sites in a systematic way. 400µl (HandyStep® volume dispenser, Brand GMBH & Co. KG, Wertheim Germany) of each formulation was spread over a demarcated area (2cm x 2cm, foam template, No.1772, 3M United Kingdom PLC, Bracknell, UK), covered with plastic and left in place for 30 minutes. This corresponds to an infinite dose, chosen such that (i) the reservoir of drug cannot be depleted during the course of the experiment, and (ii) and the dermato-pharmacokinetic models developed, based on Fick's second law, may be used. At the end of the application, the site was carefully cleaned with 3 wipes each of a dry tissue, and an alcohol wipe (Klercide, Shield Medicare Ltd,

Farnham, UK) and allowed to dry for 5 minutes. A plastic template delimiting an area of 1.5 cm x 1.5 cm was centred over the application area.

Initial transepidermal water loss (TEWL) measurements were taken at the site using a closed-chamber evaporimeter (Aquaflux AF102, Biox Systems Ltd, London, UK; measurement range 0-100 $g.m^2h^{-1}$; resolution ±0.05 $g.m^2h^{-1}$; the TEWL was taken when the mean of 10 successive measurements had a CV<1%) until stable. A pre-cut, pre-weighed (see below) piece (2cm x 3cm) of Scotch Book tape 845 (3M, St Paul, MN) was placed over the template and adhesion to the skin was ensured using a weighted roller. Further pre-weighed tape strips were taken at the site, with periodic TEWL measurements, until the TEWL reached ~4 times its original value.

For all sites, the amount of SC per tape was assessed by two methods, to construct the 'mass' and 'greyscale' DPK profiles respectively.

A. Mass of SC per tape

Tapes were cut and stored (covered) for 12 hours in ambient conditions. Each blank tape was discharged of static electricity (R50 discharging bar with ES50 power supply from Eltex Electrostatik GmbH, Weil am Rhein, Germany), weighed using a microbalance (SE-2F, precision 0.1µg; Sartorius AG, Goettingen, Germany) and then stored (maximum 24 hours) before being used for tape stripping. Following tape stripping, all tapes were again discharged of static electricity and reweighed. The mass difference between the two allowed the mass of SC on each tape to be calculated. To correct for any variations in environmental conditions, and the change in mass that may occur with time, 3-5 blank correction tapes were weighed at the same time as the tapes used for stripping. The change in mass of these blank tapes was used to correct the calculated mass of SC on each tape. Knowing the mass of SC on the tape, the area, and the density of SC ($1g/cm^3$) [99], the thickness of SC on each tape could be calculated, and hence the cumulative SC thickness removed derived.

B. Integrated pixel density of tape

The procedure followed the steps outlined above but, after the second weighing, the tapes were mounted onto slides before being photographed under controlled lighting conditions using a Coolscan V ED (Nikon UK Limited, Kingston upon Thames, UK) slide scanner. Photographs fully illustrating this method are shown in General Appendix I. Image resolution was 4000 pixels per inch. The scanner was set to positive scan in the greyscale colour space of 14 bit depth, with no transformations or camera adjustments. Full scanner settings are detailed in General Appendix II. Cropped images, 2213 x 2203 pixels (approximately 1.4cm x 1.4cm; 9822 KB each) were taken, then analysed with ImageJ (Rasband, W.S., U. S. National Institutes of Health, Bethesda, Maryland, USA; freeware from http://rsb.info.nih.gov/ij/). A scale of 159.07 pixels /mm was applied by measuring the full length of one side of the image. During image analysis, the 16 bit greyscale value of each of the 4875239 pixels in the image is found. This greyscale value is between 0 and 64608, designating black and white respectively. The mean corrected greyscale value across all pixels was 'corrected' by subtracting from the mean greyscale value for a blank tape (64355) (Full calculations shown in General Appendix III); such that large corrected mean greyscale values correspond to dark images, and more stratum corneum. The mean greyscale value of each tape was multiplied by the tape strip area ($195.1mm^2$ for all tapes in this study) to derive the integrated pixel density, which has been shown to be a useful measure of the amount of SC per tape (Chapter 5).

6.3.3 SC thickness determination

To determine the SC thickness of each volunteer, tape stripping was performed on an

adjacent, untreated site with TEWL measurements taken before and after each tape strip. The sequence was repeated until the TEWL value was 3-4 times its initial value (usually 60-80g.m^{-2}h^{-1}).

This allowed the SC thickness, H or G, to be estimated from the baseline-corrected non-linear model using either the SC thickness or integrated pixel densities respectively, as described previously (Chapter 5 [100]) using Eq. 6-1 and Eq. 6-2.

$$TEWL = B + \frac{K \cdot D \cdot \Delta C}{H - h} \qquad \text{Eq. 6-1}$$

$$TEWL = B_g + \frac{(K \cdot D \cdot \Delta C)_g}{G - g} \qquad \text{Eq. 6-2}$$

In Eq. 6-1, the thickness of the SC removed (h), is determined gravimetrically. The change in TEWL as a function of thickness of SC stripped is fitted to Eq. 6-1 to obtain values of the SC thickness (H), the product of the SC-viable epidermal partition coefficient of water (K), its diffusivity in the barrier (D), and the concentration gradient (ΔC) of water across the membrane, and the baseline correction factor (B).

In Eq. 6-2, the SC removed by each strip is assessed by the cumulative integrated pixel density (*g*), and the fitting yields the total SC thickness (*G*), and once again, values for D·K·ΔC and B. Values derived from this model are denoted with subscript '*g*'.

Non-linear fitting of Eq. 6-1 and Eq. 6-2 was performed in WinNonLin® (software version 5.1, Pharsight Corporation, Mountain View, CA) using an ASCII user-defined model.

The derived values of H or G are used to normalise the measurements of *h* or g, respectively so that all concentration profiles, from either volunteer, at any treatment site, to which either formulation has been applied, could be expressed on a relative scale of 0 to 1, where 0 corresponds to the SC surface, and 1 to the SC-stratum granulosum interface.

6.3.4 Acyclovir extraction and analysis

After imaging, tapes were cut from the slide holders, and extracted overnight in 1ml of distilled water, shaken at 210 shakes /minute. Samples were filtered (Chronus® 0.45µm nylon filters, SMI-LabHut Ltd, Maisemore, UK) before HPLC analysis (PG80 pump, ASI-100 autosampler, TCC-100 column oven, PDA-100 UV lamp from Dionex Corporation Sunnyvale, California, USA) using a 15cm Acclaim 120 column (C18, 5µm, 120Å) at 25°C and a mobile phase of 0.5% acetic acid, 5% methanol, and 94.5% water (pH 2.97) running at 1ml/min.

Standard solutions of acyclovir (Sequoia Research Products Ltd., Pangbourne, United Kingdom) were prepared in distilled water, over the concentration range 0.024 – 1.96 µg/ml.

6.3.5 Dermato-pharmacokinetic profiles

Two concentration profiles were constructed, one based on SC depth determined by mass, the other according to the integrated pixel density.

For the 'mass-derived' concentration profiles, the concentration of drug at a particular depth (C_x) can be expressed in terms of ACV mass per mass of SC on the tape; however,

when the SC is quantified by imaging, the ACV mass is divided by the corresponding mean greyscale value, expressed as C_g. To allow the two approaches to be directly compared, therefore, a normalisation procedure is used. The two sets of concentration data are divided, respectively, by the average concentration of drug in the SC as determined by mass (R_m) and the average concentration of drug is the SC as determined by imaging (R_g) from Eq. 6-3 and Eq. 6-4, respectively. Estimates for the average concentration of drug in the SC may also be estimated from the area under the concentration profile curves, as indicated in Eq. 6-3 and Eq. 6-4

$$Ave.\,concentration\,of\,ACV\,in\,SC\,(R_m) = \frac{Total\,mass\,ACV\,from\,all\,tapes\,(\mu g)}{Total\,mass\,SC\,from\,all\,tapes\,(mg)} \approx \int_0^1 C_x d\left(\frac{h}{H}\right) \qquad \text{Eq. 6-3}$$

$$\text{Ave. concentration of ACV in SC}\,(R_g) = \frac{\text{Total mass ACV from all tapes}\,(\mu g)}{\text{Total mean greyscale value from all tapes}} \approx \int_0^1 C_x d\left(\frac{g}{G}\right) \qquad \text{Eq. 6-4}$$

The normalised concentration of drug (C_x/R_m or C_g/R_g), as a function of time (t) and of position (h or g) in the SC of total thickness (H or G) may be expressed by the following two solutions of Fick's second law of diffusion:

$$\frac{C_x}{R_m} = \frac{K_m}{R_m} \cdot C_V \left[(1 - \frac{h}{H}) - \frac{2}{\pi} \sum_{n=1}^{10} \frac{1}{n} \sin(n\pi \cdot \frac{h}{H}) \exp(-\frac{D}{H^2} n^2 \pi^2 t) \right] \qquad \text{Eq. 6-5}$$

$$\frac{C_g}{R_g} = \frac{K_g}{R_g} \cdot C_V \left[(1 - \frac{g}{G}) - \frac{2}{\pi} \sum_{n=1}^{10} \frac{1}{n} \sin(n\pi \cdot \frac{g}{G}) \exp(-\frac{D}{H^2} n^2 \pi^2 t) \right] \qquad \text{Eq. 6-6}$$

where C_v is the drug concentration in the vehicle. Dermato-pharmacokinetic parameters may be estimated from this model; namely a normalised estimate of the drug's SC-vehicle partition coefficient (K_m/R_m or K_g/R_g for the mass and greyscale measurements respectively) and its characteristic diffusion parameter (D/H^2). Using Eq. 6-5 and Eq. 6-6 assumes the following boundary conditions: (i) that an infinite dose is applied; (ii) that the SC is initially drug-free; (iii) that the barrier is homogeneous in its barrier properties; and (iv) that the viable epidermis provides a perfect sink for permeating drug.

All statistical tests were performed, and graphs produced, with GraphPad Prism® (version 4.00 for Windows, GraphPad Software, San Diego, CA).

6.3.6 Assessing SC inhomogeneity

In an attempt to quantify potential inhomogeneity of tapes, three further image analysis techniques were proposed and tested on homogeneous and inhomogeneous tapes from Volunteer 1, Pliva Site 2.

6.3.6.1 Relative standard deviation of greyscale values

Each tape strip has ~4.9 x 10^6 pixels, each of a particular greyscale value. The original standard deviation determined from Image J refers to the original greyscale values where low greyscale values correspond to dark pixels. The corrected greyscale variance of each tape strip ($s^{B\text{-}X}$) was calculated using Eq. 6-7:

$$s^{B-X} = \frac{1}{n-1}\sum_{i}\left[\left(B_i - S_i\right) - \left(b - s\right)\right]^2 \qquad \text{Eq. 6-7}$$

where n is the number of pixels per image (4875239); B_i is the greyscale value of pixel, i, on the blank tape; S_i is the greyscale value of pixel, i, of the tape strip; and b and s are the mean greyscale values of the blank tape and the tape strip respectively. The standard deviation is the square root of the variance. As 98.8% of all pixels on the blank tape had a greyscale value of 64419 (where the palest possible greyscale value is 64608), this value was used as the greyscale value of all blank pixels (namely all B_i).

6.3.6.2 Use of 'particle analysis' software application

Inhomogeneous 'clumps' on tape strips from volunteer 1 site 2 were highlighted and measured by converting to 8-bit images (such that pixels have greyscale values between 0 (dark) and 256 (light)), and applying an 'auto' threshold using Image J. The threshold highlights dark areas. The lower threshold was 0, and the upper threshold varied from 145-161, depending on the mean greyscale of the particular image. From amongst those pixels highlighted by the threshold function, 'particle analysis' was performed by ImageJ (with no size or circularity restrictions, no shaped outlines drawn, and holes within clumps included) to find and measure inhomogeneous SC areas on the tape. Results from this analysis provide information about the clumps on the tape strip: total, and fraction of, image area affected; the average size; and a count of the pixels not contributing to clumps.

6.3.6.3 Sectional profile plots

Selected images from volunteer 1 site 2 were divided into five vertical sections. A plot of the greyscale values with distance across the tape was obtained for each of the five sections using the "plot profile" function in Image J. Inhomogeneous regions on the image are highlighted in these profiles by peaks or troughs.

6.4 Results and Discussion

6.4.1 Use of imaging to produce drug-permeation profiles

Drug penetration profiles resulting from tape stripping experiments can be modelled using an appropriate solution of Fick's second law to derive dermato-pharmacokinetic parameters. These can be used to characterise the rate and extent of drug permeation through the SC for different formulations, and hence compare different formulations of the same drug.

Traditionally, the drug permeation profiles are constructed using mass measurements per tape to calculate the cumulative depth reached within the SC. Measuring the mass of SC per tape is neither precise nor reproducible, and a novel imaging method has been examined extensively in this work. Firstly, the imaging method is easy to use, quick to perform, precise and reproducible. The greyscale values calculated for each tape using the imaging method may be used to calculate a relative measure of total SC thickess, G. This thickness, G, may be used to normalise drug-permeation profiles to ease comparisons between different volunteers.

In this work, two acyclovir creams were compared. All tapes from each application site were assessed for SC quantity by both the weighing and imaging methods. This generated two sets of drug-permeation profiles, allowing differences (i) between the weighing and imaging profiles, and (ii) between the two different acyclovir formulations, to be considered.

Unfortunately, one Pliva site (volunteer 1, site 2) produced such significant SC disruption that its DPK results could not be considered. However, images from this set of tapes were used for inhomogeneity assessment as described in section 6.4.2.

Figure 6-1 shows the non-normalised data for all Zovirax and Pliva sites. The data from the Zovirax sites are more reproducible than the Pliva sites. Overall, the profiles constructed using the mass of SC are of comparable shape to those constructed with the mean greyscale values (imaging method) of the tapes.

Clearly, the mass (A and B) and imaging (C and D) drug-permeation profiles in Figure 6-1 are not directly comparable due to scale. Therefore, the *y*-axes were normalised using the average concentration of ACV in the total SC removed (calculated using Eq. 6-3 and Eq. 6-4 for the weighing and imaging methods respectively).

The fully normalised DPK data, for both the mass and imaging SC quantification methods, are presented in Figure 6-3 (Zovirax sites) and Figure 6-4 (Pliva sites). It is apparent that the normalised profiles overlap well in all cases. This suggests that the measurements derived from the imaging method may be used directly in drug-permeation profiles, and do not require conversion to actual depths reached within the SC. Rather, the imaging method provides a perfectly usable relative measure of the amount of SC per tape.

By fitting these normalised concentration profiles to Eq. 6-5 and Eq. 6-6, the DPK parameters of ACV diffusivity in the SC (D/H^2), and the normalised partition coefficients, K_m/R_m and K_g/R_g, are found for the mass and imaging methods respectively (Table 6-1). Neither the normalised K values, nor the D/H^2 values, derived from the mass or imaging DPK plots, are significantly different from each other (2-tail paired non-parametric t-test, $p>0.05$). This reflects the similarity seen when the two different normalised drug-permeation profiles were superimposed (Figure 6-3 and Figure 6-4).

K_m and K_g estimates were derived from fitting the original, non-normalised concentration profiles to Eq. 6-5 and Eq. 6-6. The estimates found for the mass versus the imaging method are linearly related, with a regression coefficient, r^2 = 0.73 (Table 6-1). The average concentrations of drug in the SC, R_m (Eq. 6-3) and R_g (Eq. 6-4) are also presented in Table 6-1. There is a linear relationship between the two ratios, with a regression coefficient, r^2 of 0.92 (Figure 6-2). This relationship between R_m and R_g may be used to convert K_g/R_g values into a true vehicle-SC partition coefficient, K_m. This will allow future dermato-pharmacokinetic studies of formulations performed using the imaging method to be directly compared with previously studied formulations, in which SC per tape was evaluated by the weighing method.

The K_m values obtained from the Zovirax sites are largely reproducible, with K_m varying between 3.7 to 6.4, and K_g varying between 3.1 x 10^{-5} to 9.5 x10^{-5} over the four sites. The D/H^2 values are consistently between 0.02 and 0.04 h^{-1} for both SC quantification methods. The higher D/H^2 value for Volunteer 1 Zovirax site 1 (Table 6-1) is due to the peaks in ACV concentration approximately half way into the SC (*h*/H or *g*/G values ~0.6) (Figure 6-3A), which could be due to contamination.

The partition coefficients, K_m, obtained here for acyclovir (log P = -1.6, MW = 225 g.mol^{-1}), are within the same order of magnitude as those obtained previously for ibuprofen (log P = 3.97, MW = 206 g.mol^{-1}), betamethasone valerate (log P = 3.6, MW = 477 g.mol^{-1}) and terbinafine (log P = 5.9, MW = 328 g.mol^{-1}); they are all numerically close to 1. This is surprising considering the different physicochemical properties of these molecules. In other words, the drug concentration in the SC at the surface of the barrier approximately equals its concentration in the vehicle. One interpretation for this (apparent) coincidence is that residual formulation remains on the skin surface, or in the skin furrows, after formulation removal. An alternative hypothesis is that the drug, and key excipients in which the drug is soluble, enter the SC as a "unit", only separating from one another deeper within the SC layers.

From the above observations, it is clear that quantifying the amount of SC per tape using mass or greyscale measurements, provides comparable pharmacokinetic parameters for comparison. The greyscale method is thus useful for assessing and comparing formulations for bioequivalence studies, and given its advantages in terms of time, reproducibility, sensitivity and stability (see Chapter 4), it can offer a viable alternative to weighing tapes.

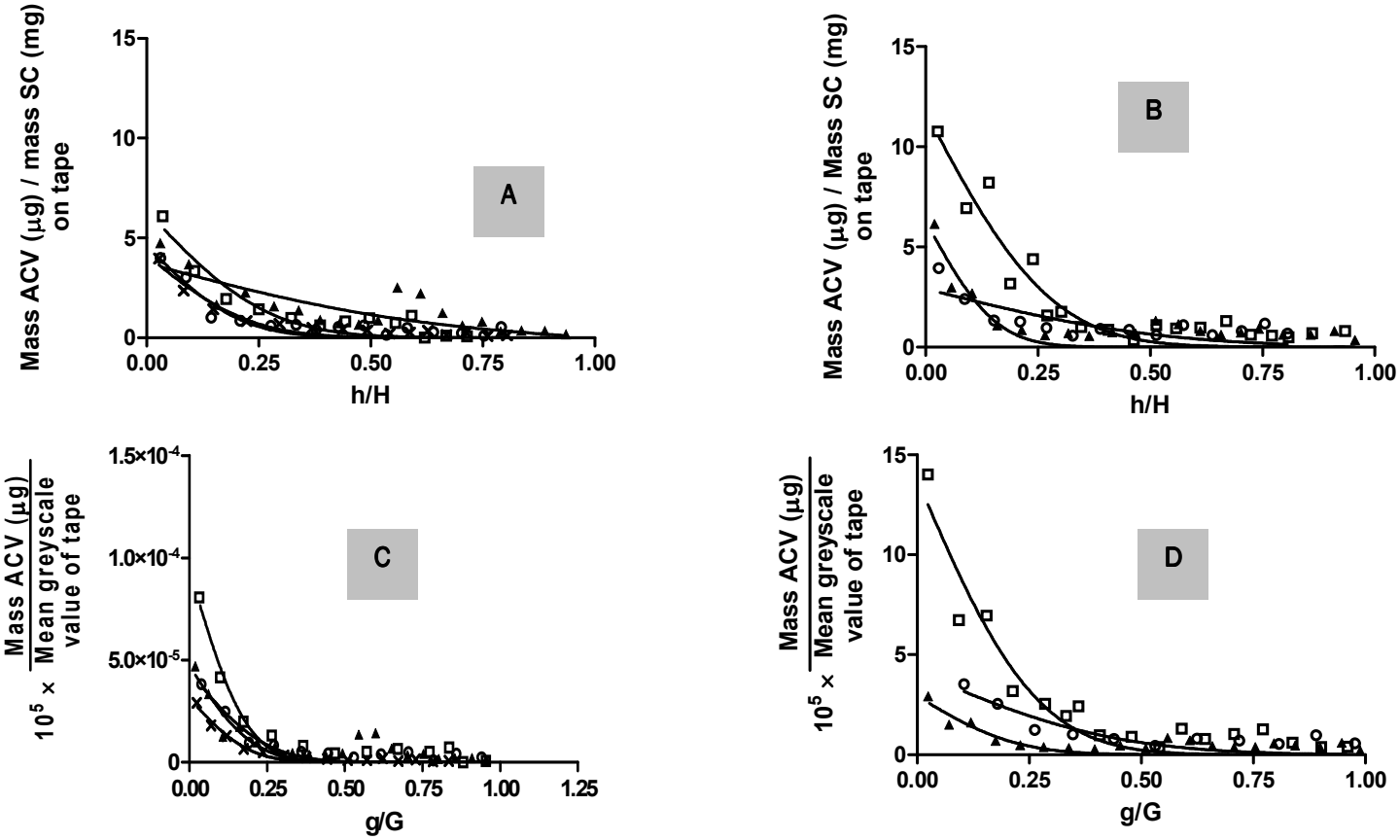

Figure 6-1: Data and resultant fits to Fick's second law (Eq. 6-7). For all graphs, ▲ data from Volunteer 1 Site 1; × data from Volunteer 1 Site 2; □ data from Volunteer 2 site 1; and ○ data from Volunteer 2 Site 2. **A**: plots generated for Zovirax sites using mass of SC on tapes. **B**: plots generated for Pliva sites using mass of SC on tapes. **C**: plots generated for Zovirax sites using mean greyscale values of tapes. **D**: plots generated for Pliva sites using mean greyscale values of tapes.

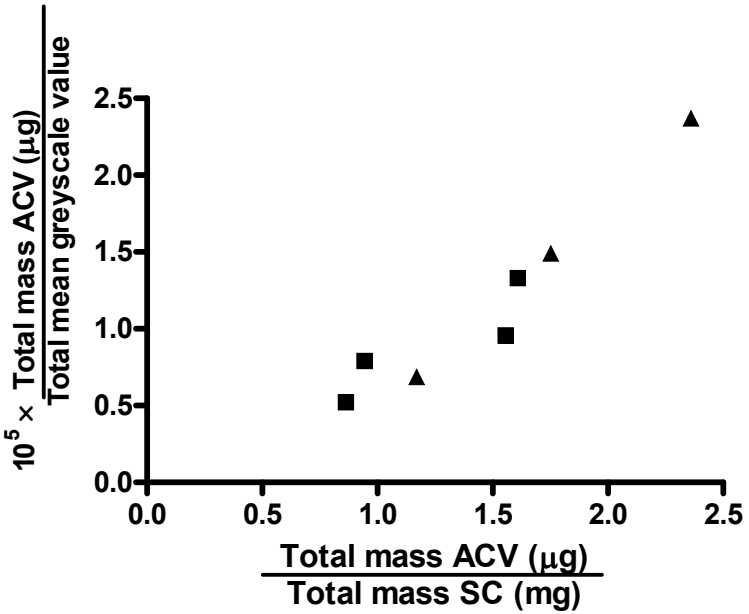

Figure 6-2: Comparison of the total mass of ACV relative to the total mass of SC (*x*-axis) or the total mean greyscale value (*y*-axis) from Zovirax (■) and Pliva (▲) sites. R^2 =0.92. NB. No data shown for Volunteer 1 Pliva site 2 as significant SC disruption (see section 6.4.2).

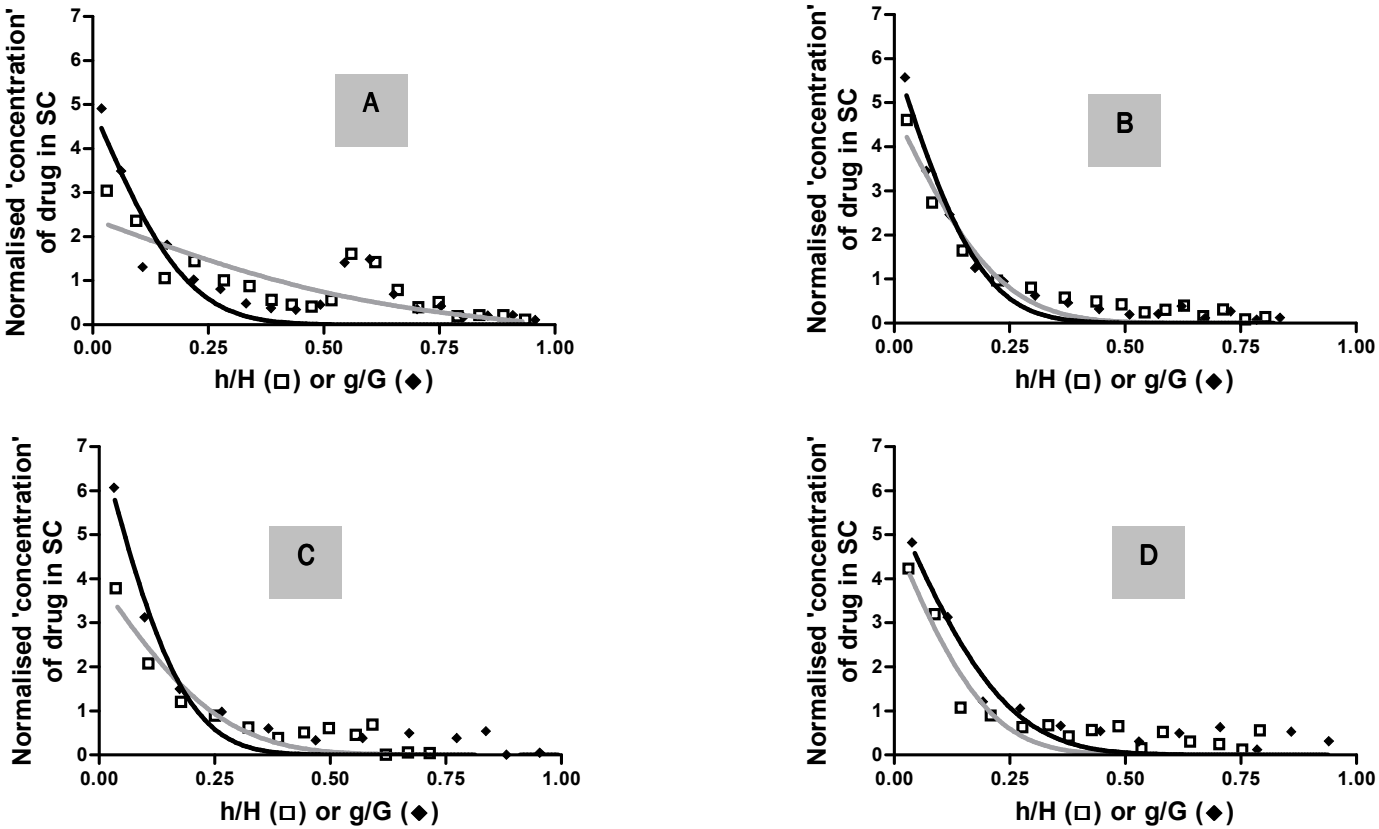

Figure 6-3: Direct comparison of the mass and imaging Zovirax DPK profiles, through normalisation of the *y*-axis concentrations. For tape data derived from SC *mass* (□), normalised concentration of ACV in SC is calculated as Eq. 6-3. For tape data derived from SC *mean greyscale* (◆), normalised concentration of ACV in SC is calculated as using the ratios calculated from Eq. 6-4. Fits to Eq. 6-5 (▬) and Eq. 6-6 (▬) also shown.

Graphs A and B: Volunteer 1, sites 1 and 2 respectively. Graphs C and D: Volunteer 2, sites 1 and 2 respectively.

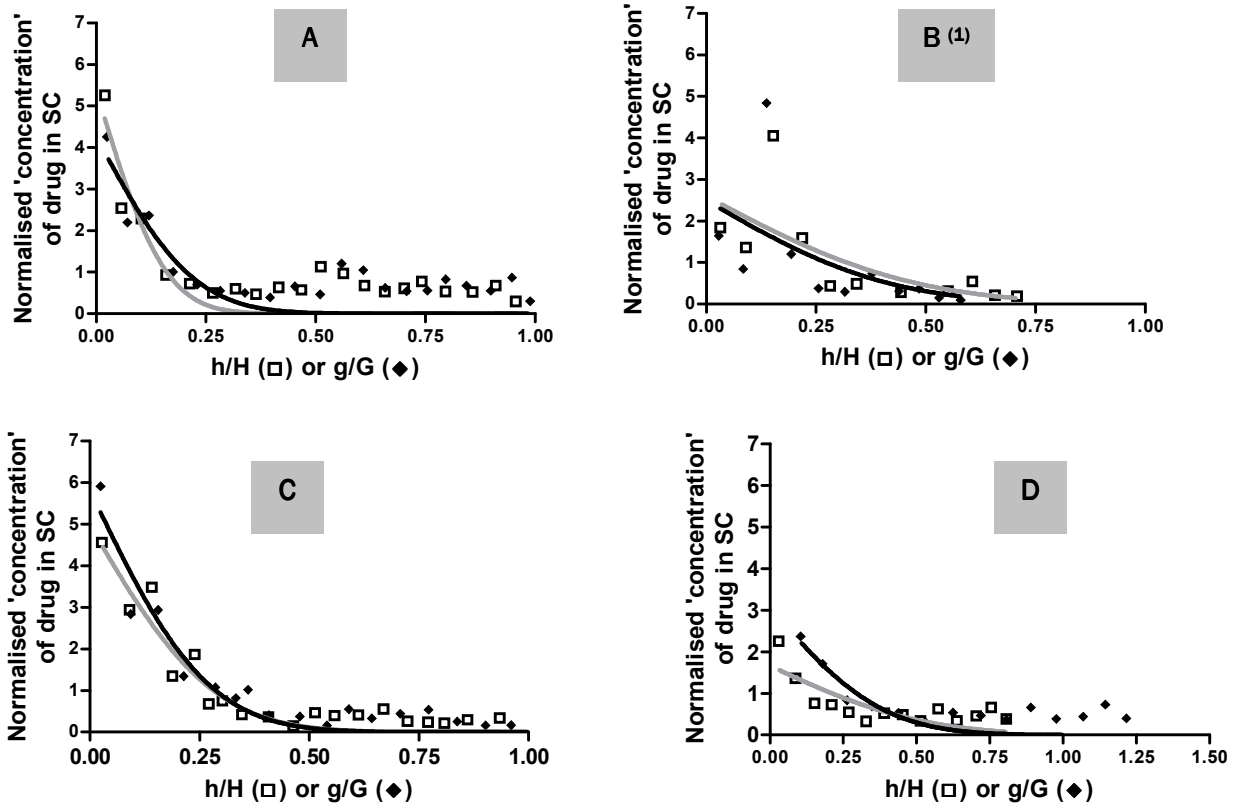

Figure 6-4: Direct comparison of the mass and imaging Pliva DPK profiles, through normalisation of the *y*-axis concentrations. For tape data derived from SC *mass* (□), normalised concentration of ACV in SC is calculated using the normalisation ratio, R_m (Eq. 6-3); For tape data derived from SC *mean greyscale* (◆), normalised concentration of ACV in SC is calculated from the normalisation ratio, R_g (Eq. 6-4). Fits to Eq. 6-5 (▁) and Eq. 6-6 (▁) also shown.

Graphs A: Volunteer 1, site 1. Graphs C and D: Volunteer 2, sites 1 and 2 respectively.
(1) Graph B is Volunteer 1 Site 2, shown for information only, as this site had SC disruption (see section 6.4.2 and Figure 6-5) and is not considered for DPK analysis.

Volunteer	Site No.	R_m (1)	$10^5 \times R_g$ (1)	Normalised data		$(D/H^2)_{mass}$	$(D/H^2)_{greyscale}$	K_m (2)	$10^5 \times K_g$ (2)
				K_m/R_m (3) (4)	K_g/R_g (3) (4)	(h^{-1}) (4)	(h^{-1}) (4)		
1	Zov. 1	1.6	1.0	2.4 ± 0.3	4.9 ± 0.7	0.24 ± 0.09	0.03 ± 0.01	3.7 ± 0.5	4.7 ± 0.6
	Zov. 2	0.9	0.5	4.8 ± 0.4	6.0 ± 0.3	0.03 ± 0.01	0.02 ± 0.00	4.1 ± 0.3	3.1 ± 0.2
2	Zov. 1	1.6	1.3	4.0 ± 0.4	7.1 ± 0.5	0.04 ± 0.01	0.02 ± 0.00	6.4 ± 0.7	9.5 ± 0.8
	Zov. 2	0.9	0.8	4.9 ± 0.5	5.6 ± 0.5	0.03 ± 0.01	0.04 ± 0.01	4.6 ± 0.5	4.4 ± 0.4
1	Pliva 1	1.2	0.7	5.4 ± 0.7	4.3 ± 0.7	0.01 ± 0.01	0.03 ± 0.01	6.3 ± 0.9	2.9 ± 0.5
2	Pliva 1	2.4	2.4	5.0 ± 0.4	5.8 ± 0.4	0.05 ± 0.01	0.04 ± 0.01	11.8 ± 0.9	13.8 ± 1.1
	Pliva 2	1.8	1.5	1.7 ± 0.3	2.8 ± 0.5	0.17 ± 0.07	0.12 ± 0.04	2.9 ± 0.5	4.2 ± 0.7

Table 6-1: Estimates (± standard error) of K and D/H^2 from Fick's second law (Eq. 6-5), with SC measured using mass and mean greyscale techniques.

(1) Normalisation ratios:

R_m = [Total mass ACV from all tapes] / [Total mass SC from all tapes]

R_g = [Total mass ACV from all tapes] / [Total mean greyscale value from all tapes]

(2) Linear regression of K estimate from mass (K_m) or greyscale (K_g) DPK plots results in a regression coefficient, $r^2 = 0.73$

(3) Normalised DPK plots fitted to Eq. 6-5 and Eq. 6-6 provide normalised partition coefficient estimates, K_m/R_m and K_g/R_g for the mass and greyscale measures of SC respectively. These have been verified to equal the original partition coefficient normalised by the respective ratio.

(4) No statistical difference between the normalised K values, nor the D/H^2, derived from the mass or greyscale methods [2-tail paired non-parametric t-test, $p>0.05$].

6.4.2 Using imaging to assess inhomogeneity

We have previous experience that a 1-hour application of the Pliva formulation results in tapes on which SC clumping is observed (Appendix 5-A). Similarly, some degree of inhomogeneous SC removal was seen for three out of the four generic application sites (Figure 6-5, Appendix 6-H and Appendix 6-I) in this study, with an application of only 30 minutes. For Volunteer 1, site 2, this is dramatically seen for tape 7 (Figure 6-5). Inhomogeneous layers were not seen for the Zovirax formulation (Appendices 6-F, 6-G, 6-J and 6-K). Formulations which affect SC cohesivity, such as the Pliva cream studied here, are clearly undesirable for most clinical applications. Drug-permeation profiles of these formulations are unsuitable for DPK analysis as the SC homogeneity is affected in an unpredictable way. Hence comparisons between the two formulations in terms of dermatopharmackinetics and bioequivalence, in section 6.4.1 above, are limited.

However, the imaging method enables us to identify formulations affecting SC cohesivity in this way. Furthermore, the images of each tape record these effects shortly after tape stripping, before extraction of the drug, a significant further advantage over weighing the tapes to assess SC content. In order to exclude formulations that exhibit this effect, quantification of the degree of the problem would be useful. Three methods, using the tape strip images, have been investigated. Since the generic site 2 of volunteer 1 exhibits this effect most dramatically, this set of images (Figure 6-5) is used to test the inhomogeneity quantification methods.

	Tape 01	Tape 02	Tape 03
	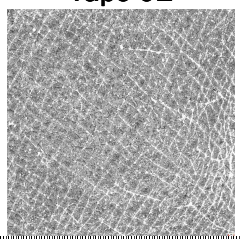	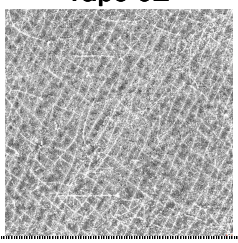	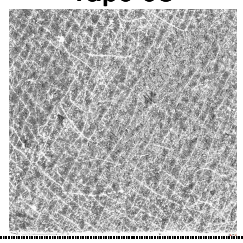
1	21731	20013	20173
2	12080	12048	13079
3	55.6	60.2	64.8
4	0.079	0.051	0.098
	Tape 04	**Tape 05**	**Tape 06**
	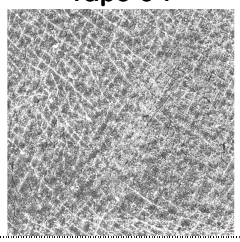	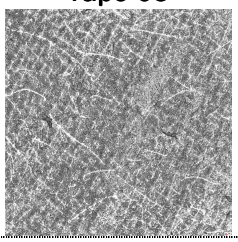	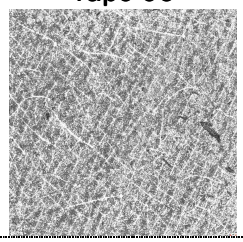
1	21679	25248	20154
2	13735	12830	14149
3	63.4	50.8	70.2
4	0.067	0.089	0.049
	Tape 07	**Tape 08**	**Tape 09**
	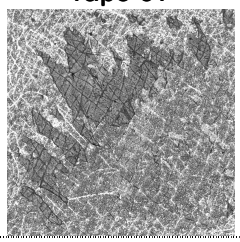	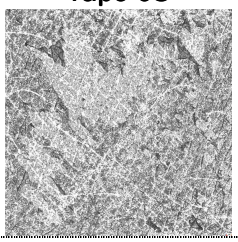	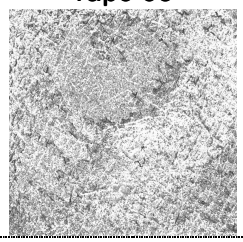
1	26627	19253	14876
2	13734	14366	13491
3	51.6	74.6	90.7
4	0.283	0.077	0.040
	Tape 10	**Tape 11**	
	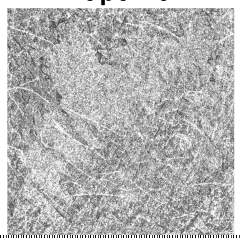	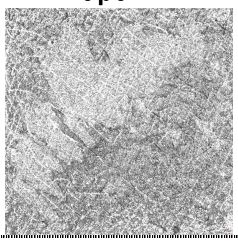	
1	19540	17824	
2	13455	13091	
3	68.9	73.4	
4	0.056	0.035	

Figure 6-5: Images and SC measurements for Volunteer 1, Pliva, Site 2.

1. Mean corrected greyscale value; *2.* Corrected standard deviation;

3. Relative standard deviation; *4.* Mass of SC (mg)

6.4.2.1 Relative standard deviation of pixel greyscale values

It was hypothesised that inhomogeneous tapes may have a larger standard deviation (SD) of greyscale values than homogeneous tapes. Considering the tapes from Volunteer 1 Pliva Site 2 (Figure 6-5), pair-wise comparisons of: Tape 07 (clumps, SD = 13733.8) with Tape 04 (homogeneous, SD = 13734.8); and Tape 11 (pale hole corresponding to missing SC layers, SD = 13091) with Tape 03 (homogeneous, SD = 13078.6) show that the SD measurement is not able to distinguish inhomogeneous tapes specifically. The SD is a global measure of the pixel greyscale distribution, and as all tapes will have some white pixels, darker images tend to have the higher standard deviations, although there is no simple relationship.

6.4.2.2 Use of 'particle analysis' software application

By applying a threshold to highlight the darkest pixels of an image, it is possible to analyse and highlight these areas, using ImageJ's 'particle analysis' function. Images with highlighted clumps of SC are shown for selected tapes in panels A of Figure 6-6, Figure 6-7, Figure 6-8 and Figure 6-9.

This function works particularly well for tapes which have removed inhomogeneous layers of SC, such as tape 07 (Figure 6-7 A and B). The darker inhomogeneous layer highlighted corresponds to 84.9% of the total area. It is clear that the 'particle analysis' function does not distinguish between the darkest fractions (sections to the left of the left-lower-to-right-upper diagonal) and the slightly darker areas to the right of this same diagonal. Examining next Tape 08, the paler section is clearly highlighted by the procedure, and directly corresponds to the area where several layers of SC were removed by Tape 07 (Figure 6-6 A and B). Tape 07 obviously removed many layers of SC as this pale area is still visible on the final tape (Tape 11) (Figure 6-9 A and B).

It should be noted that the 'particle analysis' function of the software is designed to pick out distinct particles on, for example, plates of bacterial colonies. Homogeneous images thus provide a considerable challenge as it is looking for differences that are not there. The software thus finds patches which are relatively darker than the adjacent pixels, as seen for Tape 01 in Figure 6-6 A/B. For this homogeneous strip, a large artefactual particulate area is highlighted and measured. It is clearly not appropriate to perform this procedure on all tapes therefore; they must first be assessed visually for true areas of inhomogeneity. However, tapes with true areas affected by SC clumping can be assessed.

6.4.2.3 Sectional profile plots

Each image may be divided into segments, which are analysed for variability in greyscale values across the full width of the image. These are presented in Figure 6-6, Figure 6-7, Figure 6-8 and Figure 6-9, panels C. Note that these are the original greyscale values, thus low greyscale values correspond to dark pixels.

Considering firstly Tape 01 (Figure 6-6 C), the greyscale plot rarely fluctuates by more than 5000 units. The greyscale value is generally between 40000 and 45000, corresponding to approximately 10% variability. This narrow fluctuation range indicates its homogeneity.

The profile plots for Tape 07 (Figure 6-7 C) reflect well the inhomogeneity seen. Going from left to right along the profiles, troughs are seen when lumpy areas are seen on the tape. The variability of the greyscale value varies between 30000 and 50000, representing a variability of 20-40% over the 5 sections.

Since Tape 07 removed a many layers of SC together in an inhomogeneous lump, tapes 08 and 11 have a pale patch corresponding to this area (Figure 6-8 B and Figure 6-9 B). On the profile plots (Figure 6-8 C and Figure 6-9 C), peaks correspond to these pale areas. The variability of the greyscale value is again high: with greyscale values from 35000 to 55000, representing 27-36% of the highest greyscale value.

The profile plots shown are useful for quantifying the degree of inhomogeneity. The variability in the greyscale values across the plot increase markedly from ~10% for homogeneous strips to 20-40% for strips with lumps. This could be used to eliminate SC-disrupting formulations from further clinical development studies.

Full raw data and calculations for the tape set from Volunteer 1 Zovirax Site 1 are shown as an example in Appendices 6-A and 6-B. In Appendix 6-A, the calculations to derive H and G at an untreated site are given; in Appendix 6-B the data used to derive the drug concentration as a function of normalised depth within the SC profiles is provided.

Thus, the stored images may be assessed for inhomogeneity by studying greyscale variability across sections of each tape (using sectional profile plots). These assessments could form the basis of an objective method to determine a formulation's suitability for tape stripping studies. Although we consider here the 'drug-in-SC profiling' method for interpreting DPK data, the determination of a formulation's suitability for tape stripping assessment would also be relevant to the 'two-time' metric described in Chapter 1.

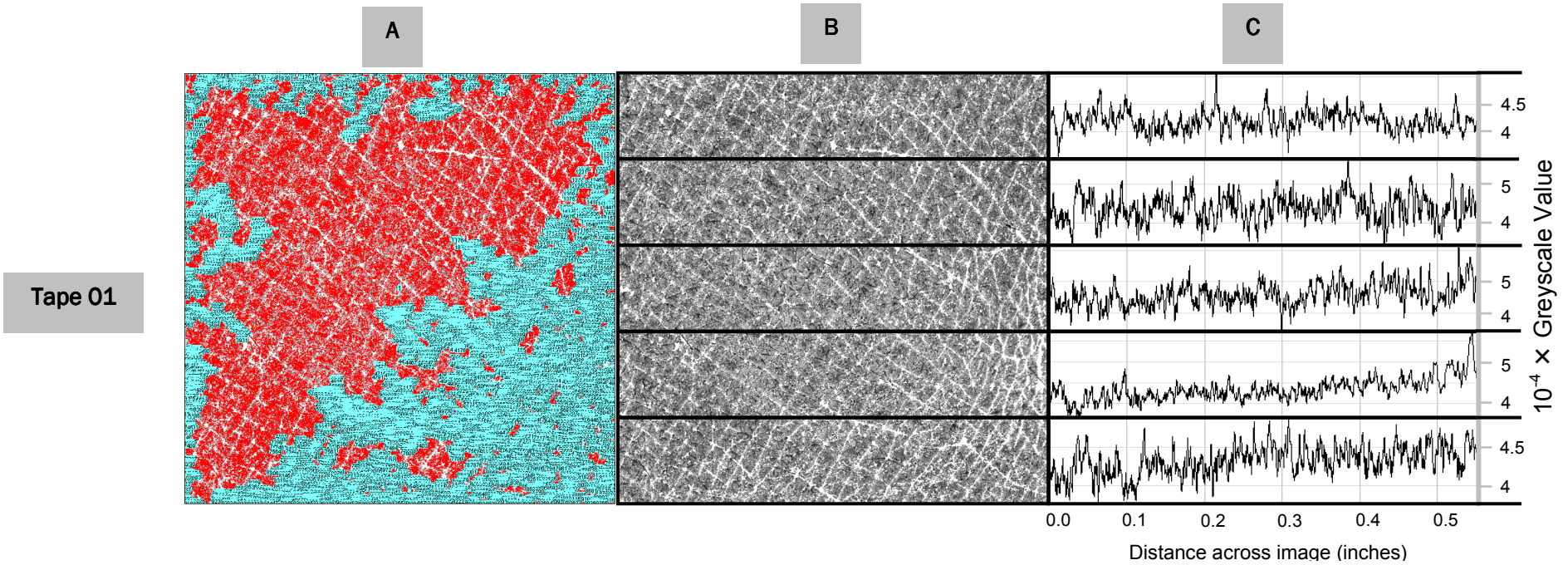

Figure 6-6: Image of Tape 01 from Volunteer 1 Pliva site 2 (B) along with the particle analysis plot and the fraction of area highlighted by this analysis (A); and the profile plots for the 5 segments (C). The segments in Panel C show the original greyscale values, such that high greyscale values correspond to pale pixels and vice versa.

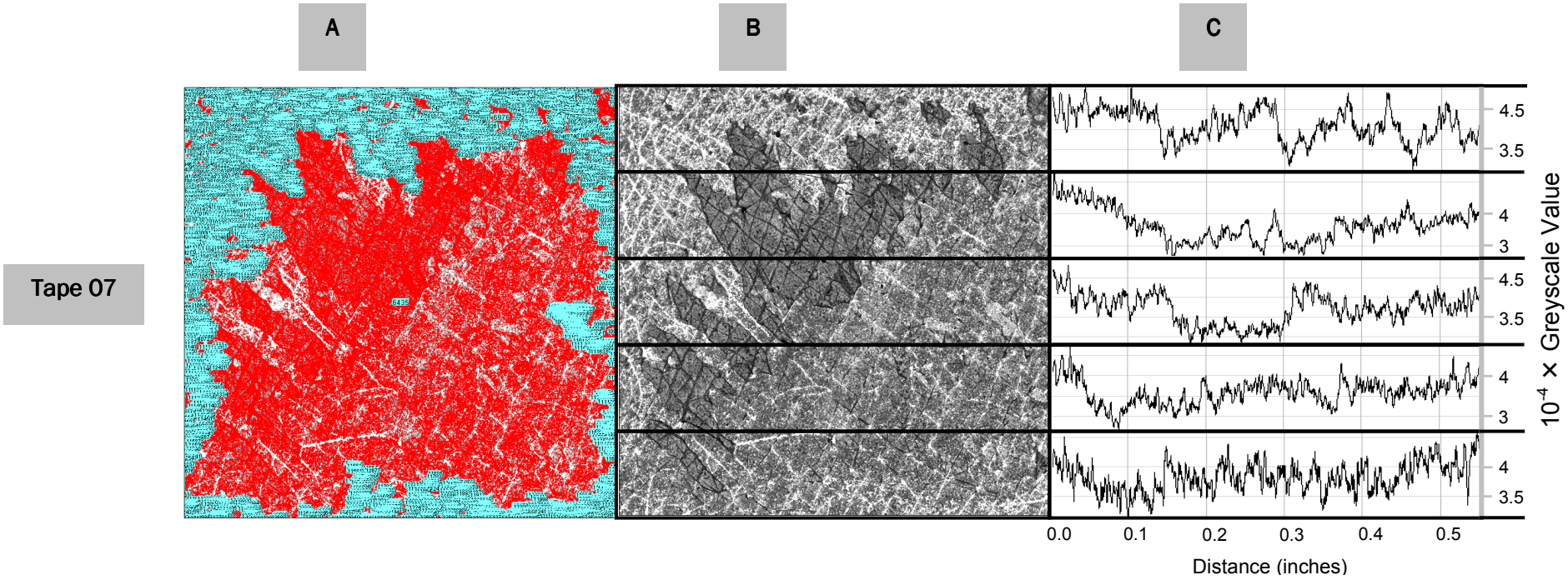

Figure 6-7: Images of Tape 07 from Volunteer 1 Pliva site 2 (B) along with the particle analysis plot and the fraction of area highlighted by this analysis (A); and the profile plots for the 5 segments (C). The segments in Panel C show the original greyscale values, such that high greyscale values correspond to pale pixels and vice versa.

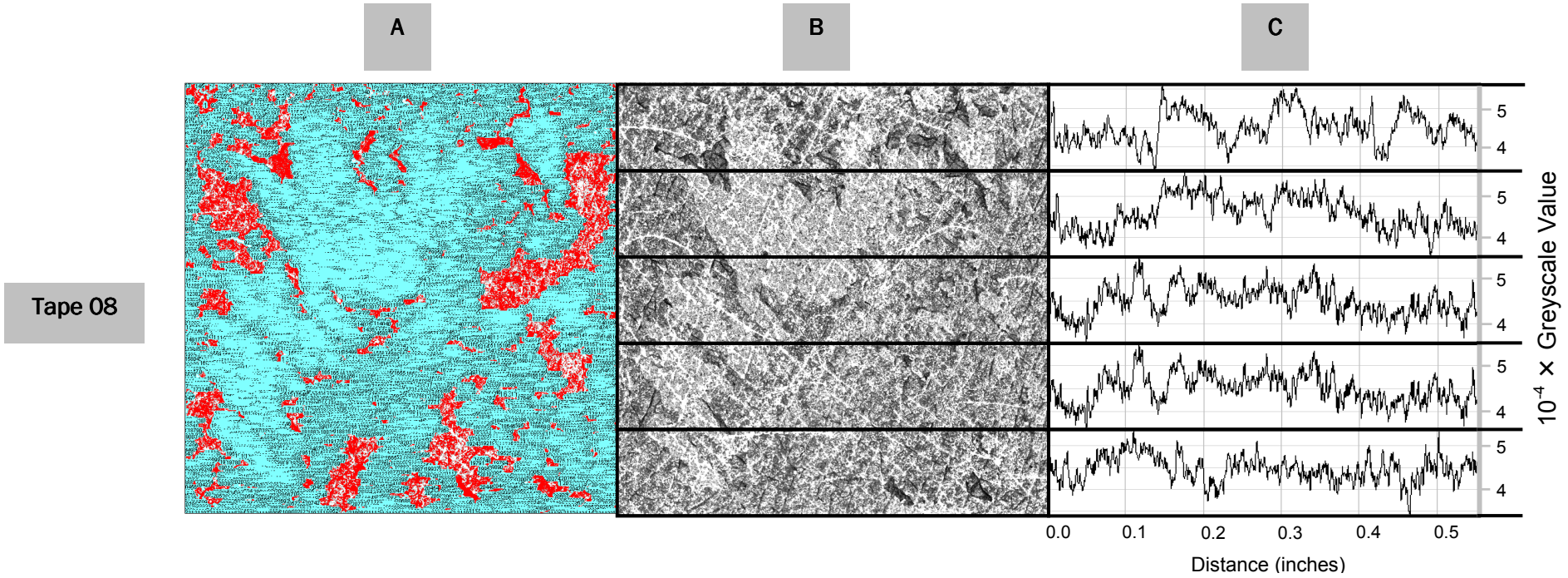

Figure 6-8: Images of Tape 08 from Volunteer 1 Pliva site 2 (B) along with the particle analysis plot and the fraction of area highlighted by this analysis (A); and the profile plots for the 5 segments (C). The segments in Panel C show the original greyscale values, such that high greyscale values correspond to pale pixels and vice versa.

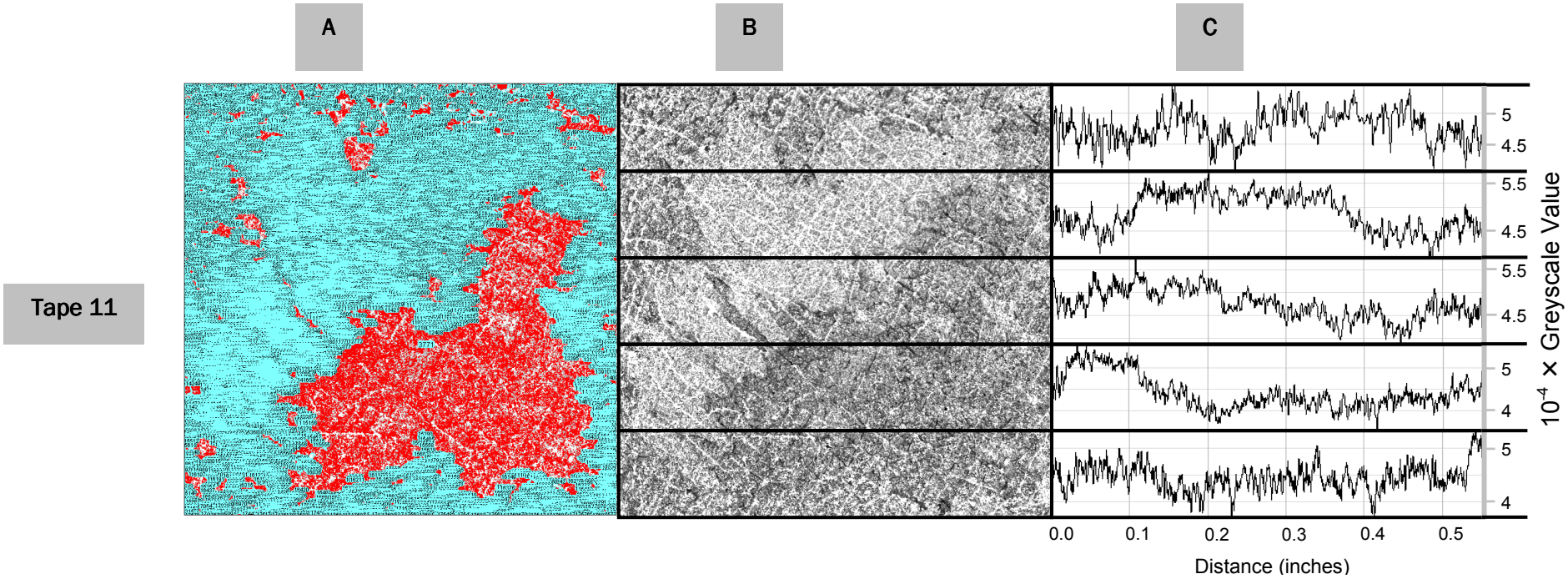

Figure 6-9: Images of Tape 11 from Volunteer 1 Pliva site 2 (B) along with the particle analysis plot and the fraction of area highlighted by this analysis (A); and the profile plots for the 5 segments (C). The segments in Panel C show the original greyscale values, such that high greyscale values correspond to pale pixels and vice versa.

6.5 Conclusions

We have discussed the use of a novel imaging method to quantify the amount of SC per tape strip, and the application to dermato-pharmacokinetic studies. This novel imaging method has previously been shown to be more sensitive, precise, reproducible, stable and rapid than weighing.

Two commercial acyclovir creams were studied, with the amount of SC per tape measured using the weighing and novel imaging methods. When the drug-permeation curves thus produced were normalised, the results from the weighing and imaging methods were comparable. Dermato-pharmacokinetic parameters were estimated from the appropriate solutions to Fick's second law, and no significant difference was found between the parameters obtained from either method. The diffusivity estimates are the same for both methods, and the partition coefficient from the drug-permeation profiles from the imaging method may easily be compared with those derived from mass measurements. This allows the results of future studies, performed using the imaging method, to be compared with previous work.

We have shown that the mean greyscale values derived from the imaging method may be used to substitute mass measurements for all aspects of the tape stripping dermato-pharmacokinetic analysis.

The partition coefficients, K_m, obtained here for acyclovir, are within the same order of magnitude (numerically close to 1) as other drugs studied previously, despite remarkably different physicochemical properties. In other words, the drug concentration in the SC at the surface of the barrier approximately equals its concentration in the vehicle. One interpretation for this (apparent) coincidence is that residual formulation remains on the skin surface, or in the skin furrows, after formulation removal. An alternative hypothesis is that the drug, and key excipients in which the drug is soluble, enter the SC as a "unit", only separating from one another deeper within the SC layers. Some evidence that this may be the case has already been presented; it has been shown that the proportion of a cosolvent, such as propylene glycol, in formulations of equal thermodynamic activity, can affect partitioning in a manner not easily related to drug concentration [111]. Further, propylene glycol has been shown to permeate more rapidly through the SC than ibuprofen, helping to maintain a saturated drug concentration in the SC after formulation removal, and hence affecting the kinetics of clearance from the SC [113]. Therefore, bioequivalence assessments between formulations must consider differences between their excipients. This presents analytical challenges for future work as excipient proportions are generally not released for commercial reasons.

Of the two acyclovir creams considered in this study, it is apparent that the generic Pliva formulation disrupts SC structure and cohesivity. This formulation is thus unsuitable for clinical use, as barrier function may be compromised and drug permeation will be altered.

The stored images of each tape strip may be assessed for inhomogeneity by studying greyscale variability across sections of each tape (using sectional profile plots). Furthermore, the area of the tape affected by SC clumping may be measured. These assessments could form the basis of a rapid, objective method to determine a formulation's suitability for clinical evaluation. Although we consider here the 'drug-in-SC profiling' method for interpreting DPK data, the determination of a formulation's suitability for tape stripping assessment would also be relevant to the 'two-time' metric described in Chapter 1.

The imaging method is thus recommended to replace the traditionally used weighing method to determine the amount of SC on each tape strip. It is simple, rapid, sensitive, and reproducible. The greyscale values obtained are sensitive relative measures of the amount of SC per tape and may be used directly in dermato-pharmacokinetic studies to obtain useful parameters to describe the rate and extent of permeation. Drug-permeation profiles and dermato-pharmacokinetic parameters may be used to assess and compare formulations. In addition, the permanent records of each tape may be analysed further to rapidly assess any clinically undesirable disruption to SC cohesivity.

Thesis Conclusions

The assessment of most topical formulations currently relies on expensive, subjective clinical trials. While new chemical entities must, of course, be assessed in this way, the development of generic formulations would benefit from objective, validated measurements of drug permeation, to assess bioequivalence.

Tape stripping has been established as a promising method to assess the rate and extent of drug permeation through the SC. Since its inception, tape stripping progressed rapidly, resulting in the formalisation of the technique into FDA draft guidance in 1998 [86]. However, contradictory results from two different laboratories prompted the withdrawal of the guidance in 2002. Since then, methodological problems with the initial guidance have been identified and rectified. Furthermore, the metric originally described, whereby total drug amount after four uptake and four clearance times is measured, akin to the assessment of oral formulations, has been criticised as unnecessarily onerous in terms of time, skin sites and analysis.

Two alternative metrics have been proposed. First, the total drug amount permeated after one uptake and one elimination time are compared (the 'two-time' metric). This metric seems very promising, and is particularly good where low levels of drug are found per tape, as tapes are combined for drug extraction. Additionally, it is quick to execute. The second metric is that considered in this thesis, whereby the concentration of drug as a function of depth reached within the SC is measured, and the resultant profiles fitted to an appropriate solution of Fick's second law. Dermato-pharmacokinetic parameters are thus derived, to assess the rate and extent of drug permeation. Although more time consuming than the 'two-time' metric, drug penetration profiles can offer reasons to explain differences between formulations, and propose mechanisms for the influence of excipients on drug permeation [111, 113]

To produce drug penetration profiles across the SC, data from each tape is required. To ease the comparison between different volunteers, it is important to normalise the depth reached within the SC relative to the total SC thickness, measured separately. The drug penetration profiles thus cover a range from 0 (at the skin surface) to 1 (at the SC-stratum granulosum interface). In this thesis, a novel non-linear model has been developed to measure the total SC thickness more accurately; objectively taking into the account any stratum corneum disjunctum layers as applicable.

In order to calculate the SC thickness as above, determine the depth reached within the SC, and express masses of drug as a concentration relative to the 'volume' of SC per tape, the amount of SC per tape must be measured. Traditionally, weighing tapes before and after stripping has been used to estimate SC mass; protein extraction [103-108], UV- and IR-pseudoabsorption [102, 103], and have all been explored and have been further evaluated here.

With regards protein extraction and analysis, the use of concentrated NaOH is not recommended, as it degrades SC keratins, and fails to extract all protein from the SC. A thiol/urea mixture described herein is suitable for protein extraction from keratin, and analysis may be performed with the universally compatible EZQ protein assay. The analysis is insufficiently sensitive however to distinguish between the very small masses of SC on 1.5 x 1.5 cm tape strips. Larger tape strips or combining tape strips could be considered for future use of this protein assay.

Problems were noticed early on with the weighing method to assess SC amount per tape: variability with environmental conditions; low mass of SC relative to the mass of the tape; and tediousness, compounded by the fact that each tape had to be weighed twice.

Therefore, alternative methods were investigated. The UV-pseudoabsorption method has been already reported in the literature, but as large numbers of inhomogeneous tapes were discarded in these studies, due to light scattering, further evaluation was undertaken. The imaging method was developed after initially taking photographs of the tapes to illustrate clumping. Subsequently, analytical photography was investigated as a means to quantify the amount of SC per tape.

Comparing the method features, the UV-pseudoabsorption and imaging methods have much better precision and signal:noise ratios than the weighing method, as well as being significantly quicker and less laborious. The imaging method, however, offers a some advantages over the UV pseudoabsorption method, in terms of signal:noise ratio, sensitivity range, proportion of strip analysed, and time costs. Moreover, it is not only able to measure the SC on inhomogeneous tapes, it can also assess the degree of inhomogeneity in order to exclude formulations from further study.

To use the mean greyscale value, or integrated pixel density of a tape instead of the mass of SC, it was firstly attempted to correlate the two measurements for a collection of 600 tapes to derive a conversion factor. This correlation, although significant, was not good enough to derive such a conversion factor. Looking at the data from these tapes, the weighing method appears less sensitive than the imaging method: global SC mass range was 0.05 to 0.15mg, whereas global greyscale values were between 5000 and 25000. This is no doubt a contributing factor to the poor correlation. Given the problems inherent with the weighing method, the value of such a correlation is questionable. It is a *relative* measure of SC amount per tape which is required to normalise drug permeation profiles, and this is most certainly provided by the precise and sensitive mean greyscale value or integrated pixel density.

Thus, for 25 sites, the thickness was assessed using the previously developed non-linear model, but where the amount of SC per tape was measured by both the weighing and imaging methods. The cumulative integrated pixel densities replaced the cumulative thickness in the model. The measures of SC thickness by both methods were well-correlated and when used to normalise the respective TEWL vs. cumulative depth profiles, the profiles overlapped. In addition, intra-subject variability was lower for the imaging method; the absolute greyscale values had fewer extreme values and better sensitivity than the corresponding absolute thickness values; and a better correlation was seen when normalised parameter estimates from the greyscale profiles were related to the initial TEWL, than when the parameters derived from the thickness profiles were used.

Substituting the mass measurements for each tape with the corresponding integrated pixel density in dermato-pharmacokinetic comparisons of two acyclovir creams produced comparable drug permeation profiles. These were analysed using the appropriate solution to Fick's second law and usable dermato-pharmacokinetic parameters were produced to compare formulations.

Furthermore, the images produced may be examined to glean other interesting information. One acyclovir cream disrupted the SC structure and some SC was removed in clearly visible clumps. The area affected by these clumps can be highlighted and measured using greyscale threshold functions. The images may also be divided into sections to consider the variation in greyscale values across the image. Peaks and troughs can then be used to measure the inhomogeneous regions.

When strips are always photographed in the same orientation, as was done in all these experiments, it is possible to stack all images from a particular site and construct a 3-dimensional image of the SC removed, as shown:

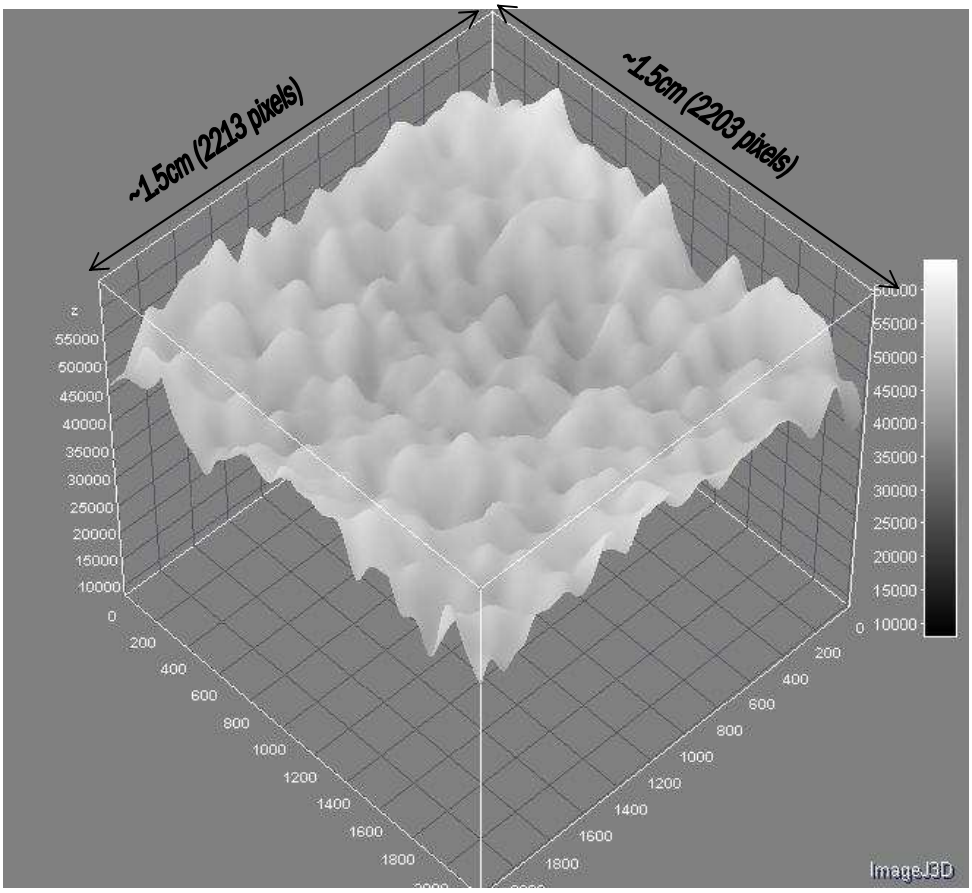

It is thus possible to visualise furrows in the skin, which may have importance for drug permeation. If the z-axis co-ordinate of these images was correlated with the resultant SC thickness estimated from the non-linear model, it may be possible to assign a scale to the thickness seen in the 3-dimensional images. It may then be possible estimate the depth reached by furrows in the SC.

It is also possible, when full rather than cropped scans are taken, to accurately measure the area of a strip using the threshold function again. Taking both scans would not be unnecessarily arduous, and would allow a more accurate integrated pixel density to be measured if that was required for other applications.

Thus far, dermato-pharmacokinetic studies using the 'drug in SC permeation profiles' have been conducted for terbinafine, ibuprofen, betamethasone valerate and acyclovir. The estimated partition coefficients, K_m, for these physicochemically different drugs, formulated in different vehicles, have been estimated to be numerically close to 1. This implies that the drug concentration in the SC at the surface of the barrier is approximately equal to the concentration of drug in the vehicle. One possible explanation for this apparent coincidence is that residual formulation remains on the SC surface after the end of the application period. That is, the cleaning procedure to remove the formulation after the application period is inadequate. Comparisons have been made between cleaning the skin surface with dry tissues versus an alcohol wipe, after application of a gelled microemulsion formulation of betamethasone valerate [94]. Cleaning with an alcohol wipe reduced both the SC-vehicle partition coefficient, K_m, and the deduced saturation levels of BMV in the SC, by approximately 50%. The total amount of drug in the SC, measured by the AUC, was also reduced. However, no effect was seen on the diffusivity of betamethasone valerate in the SC, suggesting that the brief exposure to alcohol during the cleaning procedure did not cause penetration enhancement. As these experiments

have only been performed with betamethasone valerate, and with two simple gelled formulations, further work is needed to establish the effects of the cleaning procedure on formulations more similar to those used commercially.

Traditional topical formulations warrant evaluation of a suitable cleaning procedure. To attempt to measure a drug's SC-vehicle partition coefficient, uninfluenced by residual formulation, simple patch formulations of drugs may be applied and the dermato-pharmacokinetics of drug permeation studied by tape stripping. Patch removal will remove all applied drug cleanly, with no formulation remaining on the surface or in putative skin furrows.

To this end, preliminary *in vitro* and *in vivo* work has been performed with various patch formulations of betamethasone valerate, as presented in Appendix A – preliminary further work. Unfortunately, strong patch adhesion *in vitro*, and in limited (placebo) *in vivo* experiments, resulted in a significant fraction of the SC being removed by the patch, and subsequent tape strips of the deeper SC contained unquantifiable levels of drug. These studies need to be repeated using less aggressive patches. Incidentally, during this work, it was found that images of the patches, post removal from the skin, allowed them to be rapidly screened for excessive adhesivity.

An alternative hypothesis to explain the apparent similarity between the SC-vehicle partition coefficients measured for terbinafine, ibuprofen, betamethasone valerate and acyclovir, is that the drug and key excipients, in which the drug is most soluble, enter the SC as a unit, and only separate from one another deeper within the barrier [111, 113]. This hypothesis could be tested further by concurrently measuring drug and key excipient concentrations on each tape strip, or remaining on the skin after each tape has been removed.

Further work is also required to test drugs with different physicochemical properties and to examine multiple, clinically relevant, formulations of the same drug.

Sufficient evidence has been presented in this work to replace the practice of weighing tapes before and after stripping to assess SC mass, with the imaging method, which provides a precise and sensitive relative measure of the amount of SC per tape. The majority of the strip is analysed, and the method boasts a high signal: noise ratio.

The use of such an imaging method will simplify and quicken tape stripping experiments considerably, while still enabling drug concentration as a function of SC depth profiles to be produced, and usable dermato-pharmacokinetic parameters to be derived to compare formulations.

Appendix A – Preliminary Further Work

Deducing the stratum corneum – vehicle partition coefficient from dermato-pharmacokinetic studies

Abstract

Tape stripping stratum corneum (SC) following application of a formulation allows drug concentration as a function of depth within the SC to be determined. Fitting these data to an appropriate solution of Fick's second law of diffusion allows the drug's diffusivity across the SC and its SC-vehicle partition coefficient to be assessed, and these derived dermato-pharmacokinetic (DPK) parameters can then be used to compare different formulations. It has been noted that the derived partition coefficients for three drugs of distinct physicochemical properties, derived from quite different vehicles, are all rather similar and numerically close to 1. This could be due to the influence of residual formulation, incompletely removed by the cleaning procedures used, on the skin surface, or that drug plus key excipients (in which the active is quite soluble) are taken up into the SC together and then only separate when they have travelled further into the barrier.

In this preliminary study, betamethasone valerate was formulated into simple adhesive patches, the removal of which should unambiguously avoid any potential artefacts. However, patch adhesion in vitro; and in limited (placebo) in vivo experiments, was substantial such that (i) a significant fraction of SC was removed with the patch, and (ii) the level of drug in the remaining SC was too low to quantify. While the investigation needs to be repeated, therefore, using less aggressive patches, it was noted that the high resolution imaging procedure used was able to simply and rapidly assess the extent to which the adhesive removed the SC.

Introduction

Tape stripping involves removing sequential layers of the stratum corneum (SC). It can be performed with minimum discomfort and relative ease *in vivo,* usually on the volar forearm of healthy volunteers.

If a formulation is applied to the skin prior to tape stripping, drug may be extracted from the tapes to quantify the mass of drug which has permeated into the SC. Since the SC is the principal barrier to drug absorption, the pharmacokinetics of drug passage through this layer have been related to topical bioavailability [84]. Topical formulations may be compared and bioequivalence assessed, therefore, from the derived data.

The original United States Food and Drug Administration (FDA) guidance [86], on the determination of dermato-pharmacokinetic from tape stripping experiments (since withdrawn) is unnecessarily arduous (see Chapter 1). An alternative approach is to determine the profile of drug concentration (C_x) as a function of depth within the SC (h) after an application time (t). Data are fitted to the appropriate solution of Fick's second law of diffusion (Eq. A-1) to derive the drug's SC-vehicle partition coefficient (K_m) and its diffusivity in the SC (D); of total thickness H:

$$C_x = K_m C_v \left[(1 - \frac{h}{H}) - \frac{2}{\Pi} \sum_{n=1}^{10} \frac{1}{n} sin(n\Pi \cdot \frac{h}{H}) exp(-\frac{D}{H^2} n^2 \Pi^2 t) \right] \qquad \text{Eq. A-1}$$

where C_v is the drug concentration in the vehicle. At the skin surface, h/H = 0, and the concentration of drug (C_x) equals $K_m C_v$.

The literature reveals that the derived values of K_m from this analysis for terbinafine [84, 92], ibuprofen [51, 109, 110] and betamethasone valerate [77, 112], three drugs of different physicochemical properties, delivered from a number of quite different formulations, are (almost without exception), numerically very close to a value of 1. In other words, the drug concentration in the SC at the surface of the barrier approximately equals its concentration in the vehicle. One interpretation of this (apparent) coincidence is that residual formulation at the end of the application period has not been effectively removed by the cleaning procedure employed. An alternative hypothesis is that the drug and key excipients, in which the drug is most soluble, enter the SC as a "unit", and only separate from one another deeper within the barrier [113].

To explore this question further, betamethasone was formulated into some simple adhesive patches. It was anticipated that the systems would ensure that no residual vehicle would be left on the skin upon their removal and permit, as a result, an unambiguous estimation of K_m. Experiments have been performed *in vitro* on porcine skin and, in a more limited fashion, using a placebo patch, *in vivo* in a human volunteer. The amount of SC removed with each tape has been assessed gravimetrically and also by high resolution imaging. The imaging technique was used in addition to quantify the amount of the barrier removed by the patch itself.

Materials and Methods

Patches

Simple patches, were prepared by LTS Lohmann Therapie Systeme (Andernach, Germany) (Table A-1). *In vitro* studies were performed with either silicone or polyacrylate adhesive patches containing betamethasone valerate (BMV). The limited *in vivo* studies were carried out with a placebo polyacrylate patch.

	Silicone[1]	Polyacrylate[2]	Polyacrylate[2] (placebo)
Adhesive (%)	98	95	100
BMV concentration (%)	2	5	0
Area (cm^2)	4.9	4.9	4.8
Shape	Circle	Circle	Square
Application time (hrs)	2	6	2
Experiment	*In vitro*	*In vitro*	*In vivo*

Table A-1: Patch characteristics. [1] Bio-PSA 4301, [2] Durotak 387-2287.

Skin penetration experiments

Prior to any procedure (*in vitro* or *in* vivo) loose outer layers of stratum disjunctum at the skin sites to be examined were removed with two light "pre-tapes" and discarded.

In the *in vitro* experiments, abdominal porcine skin was used. Tissue was obtained immediately post-slaughter of the animal, washed under cold, running water, dried and then dermatomed to approximately 750µm (Zimmer™ Electric Dermatome, Dover, OH). The skin was cut into pieces which were individually wrapped in parafilm before storing at -20°C until use. Before use, the skin was thoroughly defrosted and hairs were carefully trimmed before patch application.

Patches were applied for 2 or 6 hours as indicated in Table A-1. After patch removal, a 1.5 cm x 1.5 cm square plastic template was centred over the application area. A pre-

weighed (Sartorius Microbalance SE-2F, precision 0.1µg; Sartorius AG, Goettingen, Germany) piece of Scotch Book tape 845 (3M, St Paul, MN) was placed over the template and adhesion to the skin was systematically assured by running a clean cotton bud over the tape. All tapes were reweighed post-stripping. To correct for any variation in environmental conditions, and for changes in the mass of a tape that may occur with time, 3-5 blank correction tapes were weighed at the same time as the experimental tape strips. The change in mass of these blank tapes was used to correct the calculated mass of SC on each tape.

Subsequently, all tapes were mounted onto slides and photographed under controlled lighting conditions using a Coolscan V ED slide scanner (Nikon UK Limited, Kingston upon Thames, UK). Image resolution was 4000 pixels per inch (157.5 pixels/mm). Photographs fully illustrating this method are shown in General Appendix I. The scanner was set to positive scan in the greyscale colour space of 14 bit depth, with no transformations or camera adjustments. Further information on the detailed settings is presented in General Appendix II. Cropped images, 2213 x 2203 pixels (approximately 1.4cm x 1.4cm; 9822 KB each) were recorded and then analysed with ImageJ (Rasband, W.S., ImageJ, U. S. National Institutes of Health, Bethesda, Maryland, USA; freeware from http://rsb.info.nih.gov/ij/). A scale of 159.07 pixels/mm was applied by measuring the full length of one side of the image. During image analysis, each of the 4875239 pixels in the image was assigned a greyscale value (16 bit) between 0 and 64608, representing black and white, respectively. The mean corrected greyscale value across all pixels was 'corrected' by subtraction from the mean greyscale value for a blank tape (64355); in this way, large values corresponded to dark images, and more SC. The mean greyscale values were multiplied by the total strip area (195.1mm^2 for all tapes in this study, measured from the scaled images) to produce an integrated pixel density of each tape. The cumulative integrated pixel density has been shown to be relative measure of amount of SC per tape (Chapters 5 and Chapter 6).

Next, the tapes extracted overnight in 1ml of 60:40 acetonitrile:water, with vigorous shaking. Samples were then filtered (Chronus 0.45µm filters) before analysis for betamethasone valerate before HPLC analysis (PG80 pump, ASI-100 autosampler, TCC-100 column oven, PDA-100 UV lamp from Dionex Corporation Sunnyvale, California, USA) using a 25cm column (HiQSil C18) at 25°C and 65:35 acetonitrile:water mobile phase running at 1ml/min. No interfering peaks were seen from the patch nor tape. Standards of betamethasone 17-valerate (Sigma-Aldrich Company Ltd, Gillingham, UK) were prepared in 60:40 acetonitrile:water over the range: 0.02-0.96 µg/ml.

For the *in vivo* study, 3 placebo patches were applied to the volar forearm of one healthy female volunteer (26 years old, no history of dermatological disease) for 2 hours. Ethical approval was granted by the Salisbury Local Research Ethics Committee; the Declaration of Helsinki protocols were followed, and written informed consent was obtained. Tape stripping (with mass and greyscale measurements made for each tape) was performed as above, but with transepidermal water loss measurements made before and after each strip using a closed-chamber evaporimeter (Biox Aquaflux AF102, Biox Systems Ltd, London, UK; measurement range 0-100 g.m^{2}h^{-1}; resolution ±0.05 g.m^{2}h^{-1}; the TEWL was obtained as mean of 10 successive measurements having a CV<1%). This was to determine the thickness of the SC remaining after patch removal, and that of an untreated adjacent site, as described below.

Determination of SC thickness

In vivo, at the sites where a placebo patch had been applied, and at an adjacent untreated skin site, TEWL was measured before and after each strip. The sequence was repeated until the TEWL value was 3-4 times the initial value (usually 60-80g.m^{-2}h^{-1}). This allowed the SC thickness, H or G, to be estimated from the baseline-corrected non-linear

model, using both the mass and imaging measurements respectively, as described previously (Chapter 2 and Chapter 5) using Eq. A-2 and Eq. A-3:

$$TEWL = B + \frac{D \cdot K \cdot \Delta C}{H - h} \qquad \text{Eq. A-2}$$

$$TEWL = B_g + \frac{(D \cdot K \cdot \Delta C)_g}{G - g} \qquad \text{Eq. A-3}$$

In Eq. A-2, the thickness of the SC removed (*h*), is determined gravimetrically. The change in TEWL as a function of thickness of SC stripped is fitted to Eq. A-2 to obtain values of the SC thickness (H), the product of the SC-viable epidermal partition coefficient of water (K), its diffusivity in the barrier (D), and the concentration gradient of water (ΔC) across the membrane, and the baseline correction factor, B.

In Eq. A-3, the SC removed by each strip is assessed by the cumulative greyscale value (g), and the fitting yields the total SC greyscale value (G), and, once again, values for D·K·ΔC and B. Values derived from this model are denoted with subscript '*g*'.

Fitting was performed with WinNonLin® (software version 5.1, Pharsight Corporation, Mountain View, CA) using an ASCII user-defined model. All statistical tests and graphs utilised GraphPad Prism® (version 4.00 for Windows, GraphPad Software, San Diego, CA).

Results and Discussion

Silicone patches containing 2% BMV, applied for 2 hours, did not deliver a quantifiable amount of BMV into porcine SC, as assessed by tape stripping (n=4). It was thought that this could have been due to the very hydrophobic nature of the adhesive, for which BMV would have considerable affinity. The experiment was then repeated (n=4) with the less hydrophobic polyacrylate patch applied for 6 hours. However, once again, levels of drug on the tape strips were lower than the limit of quantification and were often less than the level of detection.

A possible explanation for these results is that the patches themselves removed a significant fraction of the SC upon their removal at the end of the application period. As a consequence, the BMV, which had been released from the patch, would have been removed with the SC adhered to the patch. To determine whether the adhesive patches did, in fact, strip off an appreciable amount of SC, a limited number of *in vivo* measurements of SC thickness remaining after (placebo) polyacrylate patch removal were compared to the corresponding values at an adjacent, untreated site. *In vivo* experiments were preferred because (a) they are more relevant, and (b) they are simpler to perform and generally more reproducible.

The results of these experiments are shown in Figure A-1 and Figure A-2 which show the evaluation of apparent SC thickness by the gravimetric and imaging methods (TEWL data fitted to Eq. A-2 and Eq. A-3 above), respectively. Irrespective of the measurement method, the conclusion is unambiguous: the adhesive patches stripped off ~45-60% of the SC when removed at the end of the 2hr application period. The measured TEWL at skin sites immediately post-patch removal is approximately double that of untreated, unstripped skin. Even allowing for any occlusive effects of the patch application, it is clear that this elevation in TEWL confirms a substantial disruption of the barrier function.

Using the imaging method, it was possible to derive a mean greyscale value for each of the three placebo patches, after removal from the skin, by photographing them in the scanner. These values were corrected using the mean greyscale value of an unused patch. Figure A-3 (a) shows tape 1 from the untreated skin site. It is darker than the corresponding first tapes from the skin sites 1-3 to which the patches have been applied (Figure A-3 (c)), implying a greater quantity of SC removed. Indeed, normally, more SC is removed from the upper layers of SC. The darkness of the patches post-application, on the other hand, is striking in comparison (Figure A-3 (d)). As the unused patch is very pale (Eq A-3 (b)), the intensity and mean greyscale values shown by the patches post-application confirms the removal of a significant amount of SC. This suggests a simple means for rapidly evaluating other, less adhesive, patches when this work is continued. The aggressive nature of the patch can be further appreciated from the full scan shown in Figure A-3 (e), which shows that layers of SC at the edges of the application area were also removed.

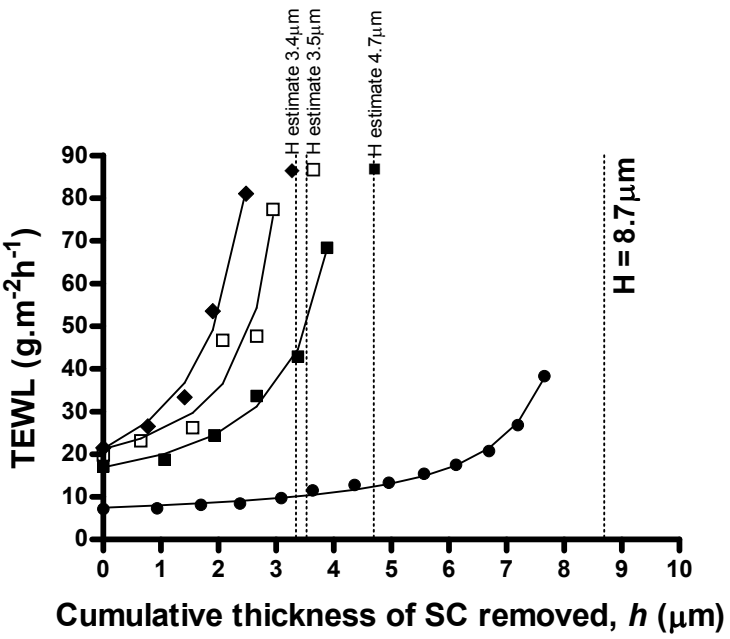

Figure A-1: TEWL versus cumulative thickness of SC removed at an untreated skin site (●) and at sites 1 (■), 2 (□) and 3 (◆) to which placebo adhesive patches have been applied. The calculated SC thicknesses (H) deduced from fitting Eq. A-2 to the profiles (–) are indicated.

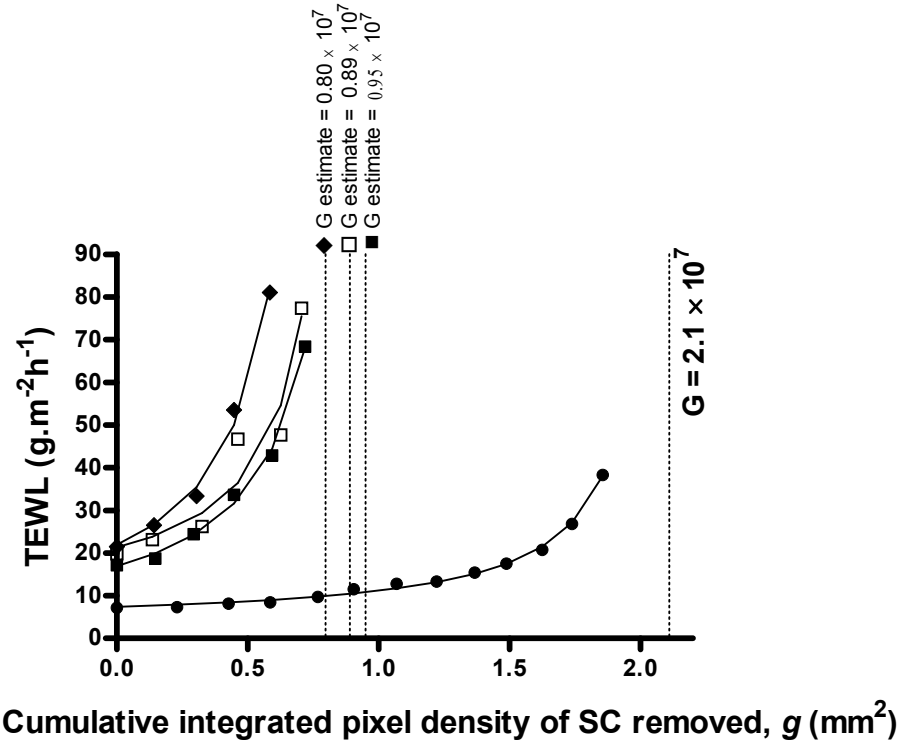

Figure A-2: TEWL versus cumulative integrated pixel density of SC removed at an untreated skin site (●) and at sites 1 (■), 2 (□) and 3 (◆) to which placebo adhesive patches have been applied. The calculated SC thicknesses (G) deduced from fitting Eq. A-3 to the profiles (–) are indicated.

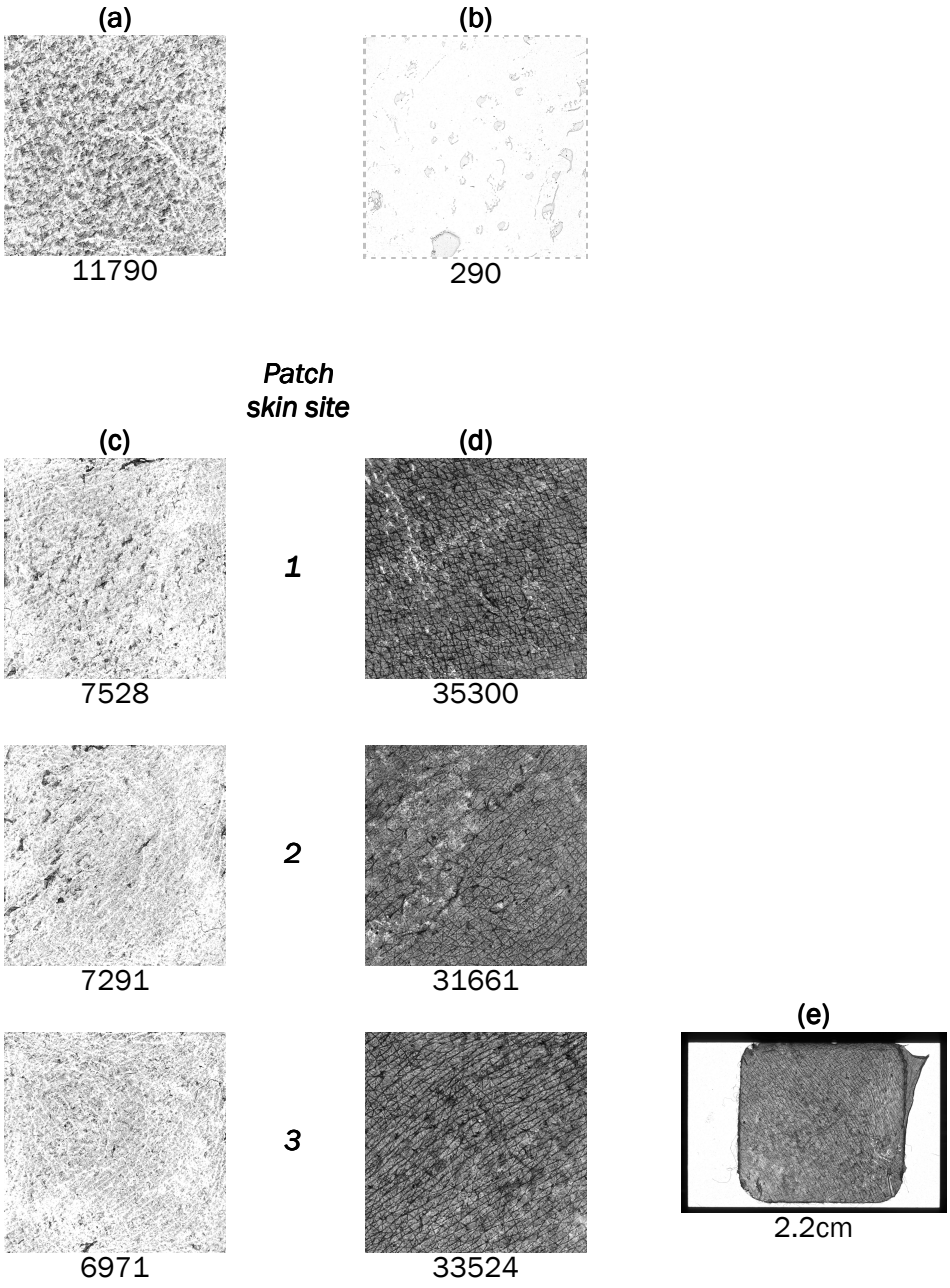

Figure A-3: Images from the *in vivo* experiments, with their corresponding corrected mean greyscale values underneath.

(a) Tape 1 from untreated skin.

(b) Adhesive surface of patch before application to skin

(c) Tape 1 from skin after patch removal from skin sites 1-3.

(d) Adhesive surface of patch post-removal from skin sites 1-3.

(e) Complete scan of patch 3 showing SC removal at edges of application area.

Conclusions

While the initial objective of this study was not successful, the experiments have revealed a potentially valuable approach with which to rapidly screen patch formulations for their *in vivo* adhesivity. To pursue the goal of unambiguously determining an SC-formulation partition coefficient, the experimental protocol should be repeated with patches formulated with a less aggressive adhesive.

General Appendix I

Illustrated instructions for the novel imaging method

1) Mount tape strip on slide

- SC strip centred in middle of slide

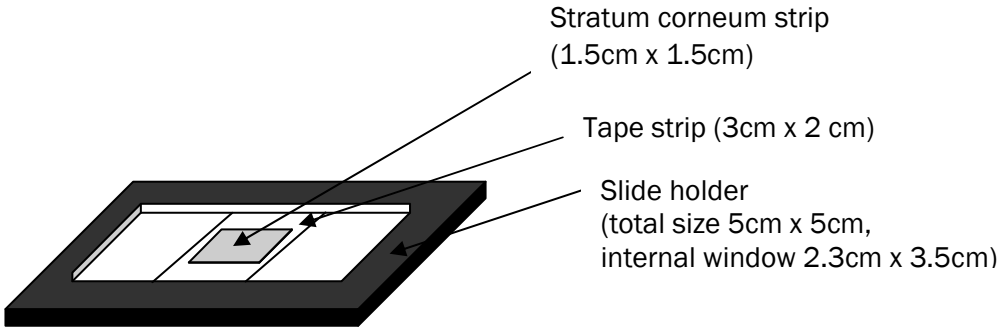

2) Insert slide into Nikon Scan V.

Slide feeder available to enable automation of slide scanning

3) Perform scan

a) Settings set in Nikon Scan 4.0.2 software, as described in General Appendix III.

b) Preview scan performed (~10 seconds)

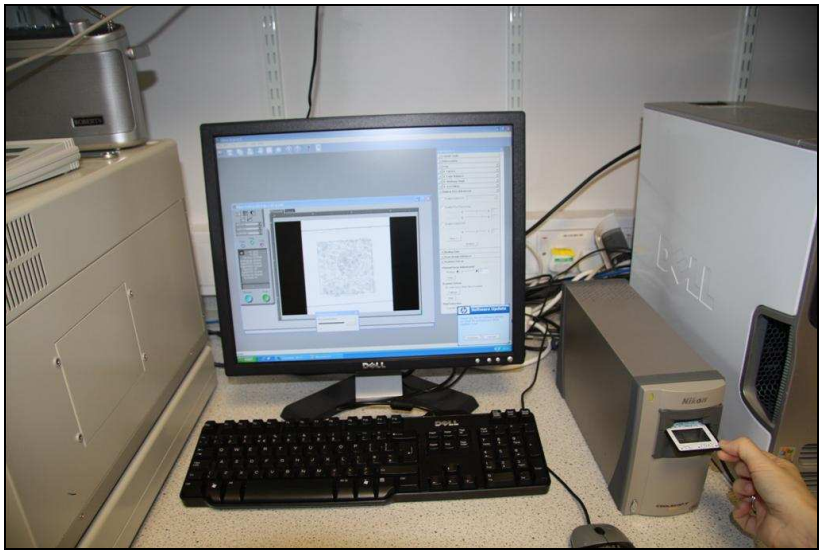

c) Crop centred over preview image (2213 pixels x 2203 pixels, approximately 14 mm x 14mm).

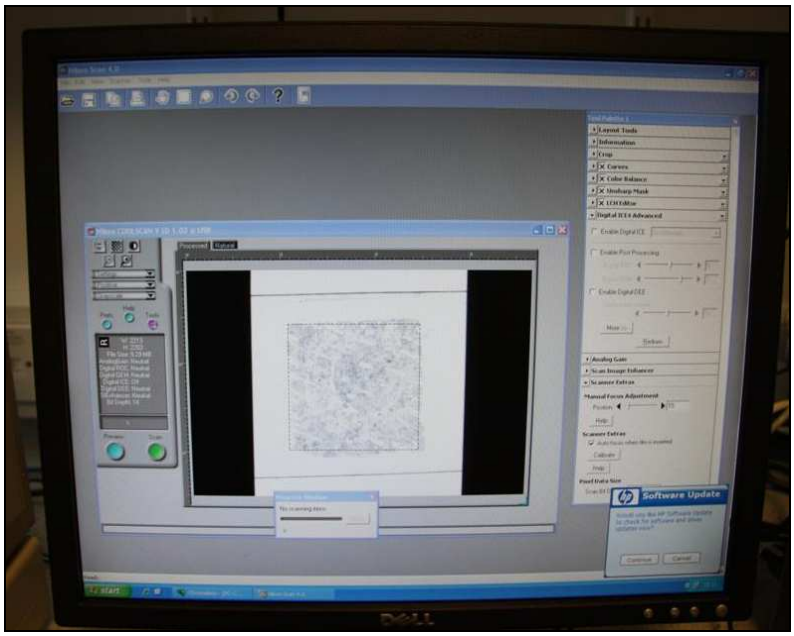

d) Full scan performed (~30 seconds)

- Schematic of the internal workings of the Nikon Coolscan V

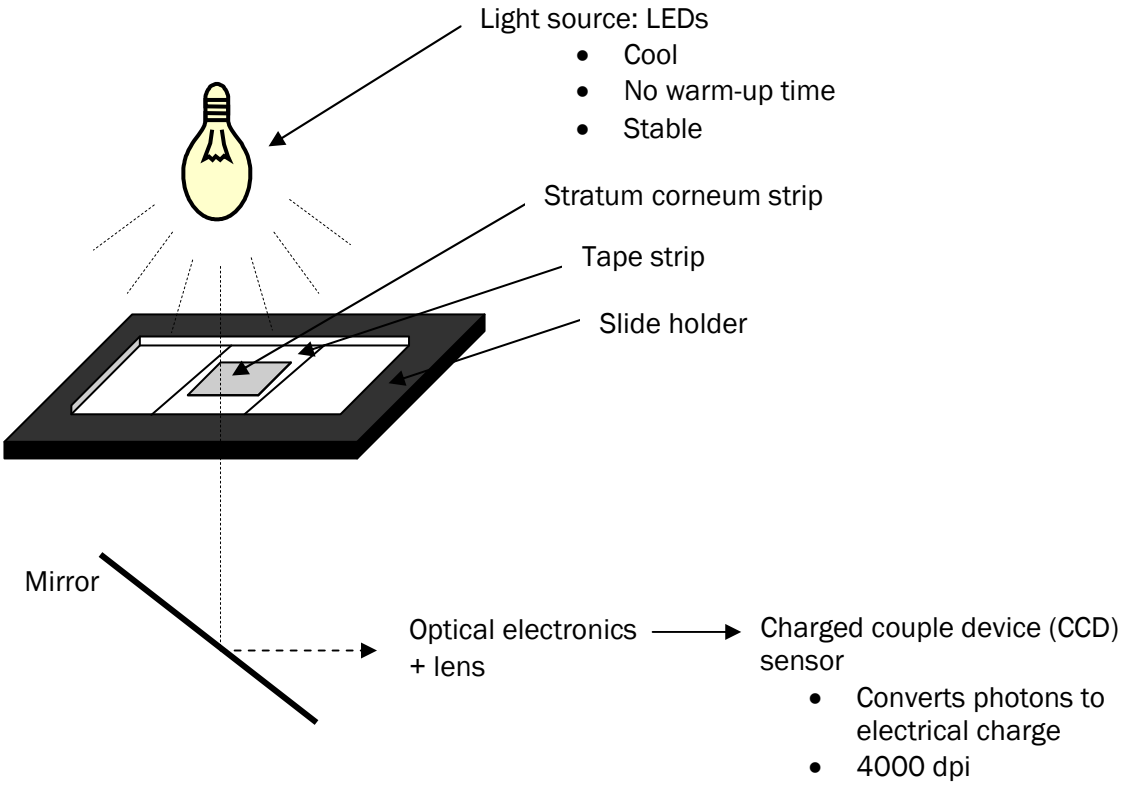

4) Analyse image using Image J

a) Import image sequence (File → Import → Image sequence). This opens all tape strip images from one or more experiments.

b) Set scale (select full width of scan with 'line' tool, then Analyse → Set scale, and note known width of scan). Scale set to 158.09 pixels/mm

c) Analyse images (Analyse → Measure (or: ctrl + M))

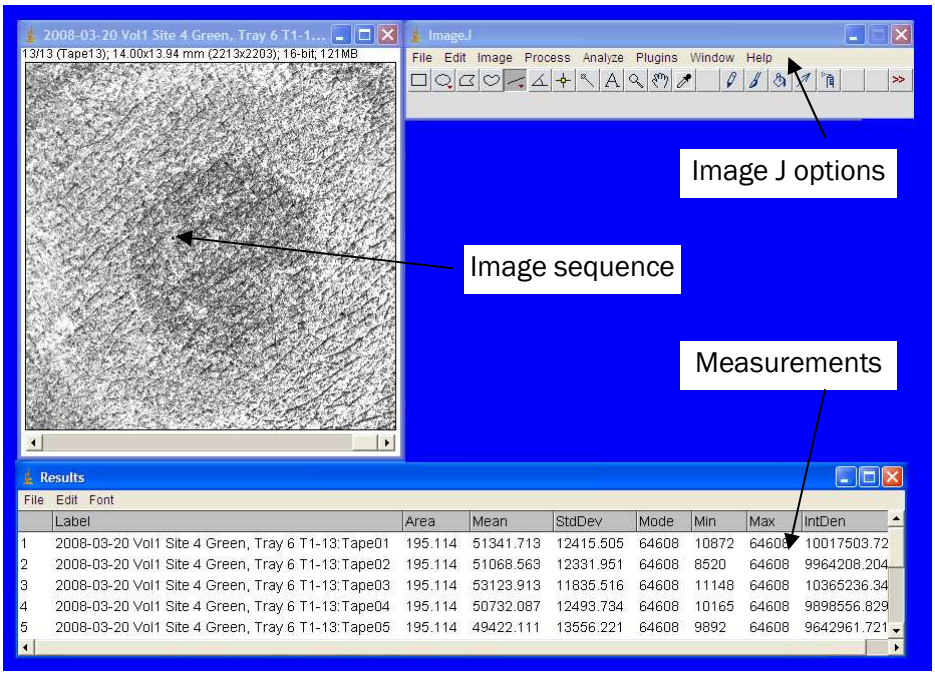

d) Save results as Excel spreadsheet

General Appendix II

Settings for capturing images using Nikon Scan 4.0.2

Tool Palette Settings

- Crop: *2213 x 2203 pixels*
- Curves: *Off*
- Colour Balance: *Off*
- Un-sharp Mark: *Off*
- LCH Editor: *Off*
- Analogue gain: *Off*
- Scan Image Enhancer: *Off*
- Scanner Extras: *Off*

Scanner

- Film Type: *Positive*
- Scan Colour Space*: Greyscale*
- Bit Depth: *14*
- Transformations: *None*
- Settings: *see under preferences below.*

Preferences (subsequently saved under method file name)

- Gamma: *Off*
- Colour Management: *Use Nikon colour management system*
    - Monitor: *Use factory default*
    - RGB Colour Space: s*RGB*
    - CMYK: *use factory default CMYK profile*
- Single Scan: *All Unselected*
- Batch Scan:
    - *Prompt for information before scan*
    - *Create scan log*
    - *Save to disk*
    - *Stop on errors*
    - *All others unselected*
- File Saving*: Default file format – TIFF*
- Automatic Actions: *All unselected*
- Advanced Colour:
    - *RGB*
    - *White point target: Master 255, Red 255, Green, 255, Blue 255*
    - *Grey point target: Red 128, Green 128, Blue 128*
    - *Black target point: Master 0, Red 0, Green 0, Blue 0*
- Greyscale:
    - *White point target: Greyscale 255*
    - *Blank point target: Greyscale 0*
- Auto-contrast calculations (% excluded):
    - *Black: 0.5*
    - *White: 0.5*
    - *Sample point size: 1x1*
- Preview settings: *all unselected except "cache preview image for single image adapter"*
- Grid settings:
    - *Colour: Black*
    - *Display grid lines every: 10 inches*
    - *Display 4 subdivisions per line*
    - *Unselected: show grid for new windows*

General Appendix III

Mean greyscale values for blank tapes for correction of all mean greyscale values

Six blank tapes were photographed (14 bit) using a Coolscan V ED slide scanner (Nikon UK Limited, Kingston upon Thames, UK) at a resolution of 4000 pixels per inch (157.5 pixels/mm) with a crop of 2213 x 2203 pixels. Photographs fully illustrating this method are presented in General Appendix I. All settings were exactly the same as for tapes with SC from all experiments. Full scanner settings are detailed in General Appendix II.

Cropped images (9822 KB each) were saved and analysed with ImageJ (Rasband, W.S., U. S. National Institutes of Health, Bethesda, Maryland, USA; freeware from http://rsb.info.nih.gov/ij/). A scale of 159.07 pixels/mm was applied to the full image width. During image analysis, each of the 4875239 pixels in the image is assigned a greyscale value (16 bit) in the range 0 - 64608, where 0 and 64608 designate black and white respectively.

The results are shown in the table below. The blank tapes, with a total of 6 × 4875239 pixels, were very homogeneous with 98.5 ± 0.6% of all pixels having the highest (i.e. palest) greyscale value, namely 64424 ± 7. The overall average greyscale value over 6 × 4875239 pixels, was 64355 ± 29. All mean greyscale values reported for *tapes with SC* have been corrected by subtracting from 64355.

	Greyscale value [1]	No. of pixels	% of pixels at palest greyscale	Average
Tape 01	<64267 64438	42966 4832273	99.1	64402
Tape 02	<64240 64424	57080 4818159	98.8	64365
Tape 03	<64238 64423	93652 4781587	98.1	64355
Tape 04	<64240 64424	116421 4758818	97.6	64315
Tape 05	<64231 64419	60406 4814833	98.8	64355
Tape 06	<64230 64419	74535 4800704	98.5	64335
Average	64424 [2]		98.5	64355
SD	7 [2]		0.6	29.4

[1] These are original greyscale values such that high values correspond to pale pixels.
[2] Mean and SD of the greyscale values of the palest pixels across all tapes.

Appendix 2-A

Raw data obtained from Subject 7

Tape No.	Mass tape strip (mg)	Mass tape strip + SC (mg)	Mass SC (mg)	Corr. mass SC (mg)	Thickness of SC (µm)	Cum. SC thickness removed (µm)	Half way Cum. thickness h (µm)	TEWL ($g.m^{-2}h^{-1}$)	For LM: 1/TEWL ($m^2h.g^{-1}$)	Prediction: S-NL ($g.m^{-2}h^{-1}$)	Prediction: BC-NL ($g.m^{-2}h^{-1}$)
1	50.1394	50.2577	0.1183	0.1014	0.68	0.68	0.34	15.41	0.065	14.17	14.35
2	50.6286	50.7342	0.1056	0.0887	0.59	1.27	0.97	15.98	0.063	14.98	15.14
3	49.8001	49.9034	0.1033	0.0864	0.58	1.84	1.55	16.28	0.061	15.85	15.99
4	49.9540	50.0587	0.1047	0.0878	0.59	2.43	2.14	15.61	0.064	16.85	16.96
5	49.6118	49.7325	0.1207	0.1038	0.69	3.12	2.77	18.33	0.055	18.15	18.23
6	50.1635	50.2725	0.1090	0.0921	0.61	3.73	3.43	19.86	0.050	19.77	19.82
7	49.6808	49.7778	0.0970	0.0801	0.53	4.27	4.00	19.70	0.051	21.52	21.53
8	49.4506	49.544	0.0934	0.0765	0.51	4.78	4.52	22.64	0.044	23.47	23.44
9	49.7122	49.8307	0.1185	0.1016	0.68	5.45	5.12	25.71	0.039	26.26	26.19
10	50.6022	50.7276	0.1254	0.1085	0.72	6.18	5.82	28.76	0.035	30.76	30.62
11	50.1265	50.2226	0.0961	0.0792	0.53	6.71	6.44	36.53	0.027	36.60	36.39
12	49.5563	49.6404	0.0841	0.0672	0.45	7.15	6.93	44.18	0.023	43.21	42.97
13	51.3989	51.4996	0.1007	0.0838	0.56	7.71	7.43	56.13	0.018	53.51	53.28
14	49.9554	50.0644	0.1090	0.0921	0.61	8.33	8.02	74.01	0.014	75.11	75.19
Correction tapes							**H (µm)**	**estimate**	10.59	9.65	9.38
1	50.1585	50.1757	0.0172					SER	0.41	0.08	0.11
2	49.7582	49.7686	0.0104					CV (%)	3.83	0.78	1.21
3	50.6124	50.6278	0.0154				**D·K·ΔC**	**estimate**	147.32	120.50	97.55
4	49.6526	49.6811	0.0285					SER	8.42	4.04	8.75
5	49.6156	49.6287	0.0131					CV (%)	5.71	3.35	8.97
							B	**estimate**			3.38
								SER			1.29
								CV (%)			38.19
							WRSS			34.77	22.84
							DF			13.00	12.00
							AIC			18.61	14.31

Abbreviations:

Corr: corrected
Cum. cumulative

Appendix 3-A

Statistical tests to compare linear regression outputs

A pair of data sets is fitted to a linear regression. The null hypothesis (H_0) is that the slope of line 1 = slope of line 2. This is tested by firstly calculating the following for each of the two data sets:

Equation set A: Calculating data set-specific parameters

$\sum x^2$
$\sum y^2$
$\sum xy$

$$b = \frac{\sum xy}{\sum x^2}$$

$$\textit{Residual sum of squares (RSS)} = \sum y^2 - \frac{(\sum xy)^2}{\sum x^2}$$

Residual degrees of freedom (RDF) = number of data points – 2

The parameters calculated above for the two data sets are used as follows:

Equation set B: Comparing the 2 data sets

$$(s^2_{y.x})_p = \frac{RSS_{DataSet\,1} + RSS_{DataSet\,2}}{RDF_{DataSet\,1} + RDF_{DataSet\,2}}$$

$$s_{b1-b2} = \sqrt{\frac{(s^2_{y.x})_p}{\sum x^2{}_{(DataSet\,1)}} + \frac{(s^2_{y.x})_p}{\sum x^2{}_{(DataSet\,2)}}}$$

$$t = \frac{b_{DataSet\,1} - b_{DataSet\,2}}{S_{b1-b2}}$$

$$v = RDF_{DataSet\,1} + RDF_{DataSet\,2}$$

We reject H_0 if $|t| \geq t_{\alpha(2),v}$ where $t_{\alpha(2),v}$ may be found in *t* tables.

As the slopes were found to be different, comparisons of intercepts was not necessary, but if required, the methods are given in Section 17.2 [141].

Appendix 3-B

Protein assay comparison table

	Reference [1]	Name of test	λ (nm)	Protein range (mg/ml)	Time stable (min)	Incompatibilities							
						PMSF (mM)	Tris (mM)	Sodium azide (%)	Urea (M)	NaCl (M)	2-ME (mM)	NaOH (mM)	HCl (mM)
A	P / 23225 [138]	BCA	560	5-25 mg [2]		1	250	0.20	3	1	1	100	100
B	S / TP0200 [144]	Biuret (Onishi/Barr)	550-750	150-1000	30		IC		IC				
C	P / 23200 [138]	Bradford = Bio-Rad = Coomassie	465-595	100-1400	60	1	2000	0.50	3	5	1000	100	100
D	P / 23236 [138]	Lowry = bio-rad DC	750	200-1500	60		100	0.05	4		TIC	500	500
G	P / 23235 [138]	Micro-BCA	562nm	2-40	10	1	50	0.20	3	1	1	50	10
H	P / 23240 [138]	Modified Lowry	750nm	1-1500	10	1	10	0.20	3	1	1	100	1000
I	I / N6666 [145]	Nanoorange	Fluo. 470/570	0.01-10	360	IC	IC	10mM	1	0.02	100	10	10
J	I / C6667 [146]	CBQCA	Fluo. 465/550	0.01-150	300		IC				0.1 [4]		
K	I / R33200 [147]	EZQ	Fluo. 485/590	20-5000	>240 [3]	All ok							
L	I / Q33210 [148]	Quant-IT	Fluo. 470/570	0.25-5	180					0.02	1		

Table for Appendix 3-B: Protein assay methods (suitable for 96-well high throughput assay) considered for assaying protein extracted from tape strips. Invitrogen EZQ method chosen as: washing stages result in universal compatibility; relatively high sensitivity.

Fluo. : fluorescence. IC: Incompatible, but concentration unspecified. TIC: totally incompatible. 2-ME: 2-mercaptoethanol (a reducing agent). PMSF: phenylmethanesulphonylfluoride Tris: tris(hydroxymethyl)aminomethane

Notes: [1] Reference given as: company (P: Pierce Biotechnology; S: Sigma-Aldrich, I: Invitrogen) / product number, with corresponding technical reference.
[2] Limit of total protein per sample
[3] As checked by author during research
[4] Limit is 0.1mM but may be able to block interference with N-ethylmaleimide

Appendix 3-C

Summary of extraction solutions used to extract Keratin from skin

Ref.	Protein assay used [1]	pH	PMSF (mM)	Tris (mM)	Urea (M)	2-ME (mM)	NaOH (M)	HCl (M) [2]	Others	Comments
[134, 135]		9	2	50	9	50				
[149]							0.2		0.1N or 1N acetic acid used to neutralise -> causes precipitation	degrease with di-ethyl ether first. Fractions named after pH at which they precipitate
[103]	G						1	1		
[104, 105]	D						1	1		750nm
[106]	D, modified Bradford						1	1		
[107, 108]	C						1	1		595nm
[140]	skinMAP								0.2%SDS, 30min, 0.5%propylene glycol, PBS, temp 4-10oC	Used SkinMAP and Luminex

Table for Appendix 3-C: Summary of extraction solutions used to extract keratin from the skin.
2-ME: 2-mercaptoethanol (a reducing agent). PMSF: phenylmethanesulphonylfluoride Tris: tris(hydroxymethyl)aminomethane

Notes: [1] for code see Appendix 3-B.
[2] Equal volume of HCl added to NaOH extraction solution to neutralise before analysis (1M NaOH not compatible with tests)

Appendix 3-D

Full raw data and calculations, from 4 different SC quantification methods, for one skin site.

This example data is provided, for reference, for Chapters 3 and 4.

Tape No.	1. Weighing method				2. Imaging method				
	Mass blank tape (mg)	Mass tape +SC (mg)	Mass SC (mg)	Corrected mass SC (mg)	Area (mm^2)	Mean greyscale value	Corrected mean greyscale value (1)	Corrected standard deviation (2)	Integrated pixel density (3)
1	50.3071	50.4371	0.1300	0.1410	195.1	44636	19719	8423	3847140
2	51.9762	52.0280	0.0518	0.0628	195.1	51763	12591	10501	2456540
3	50.9307	51.0233	0.0926	0.1036	195.1	47450	16904	10903	3297997
4	51.2327	51.3040	0.0713	0.0823	195.1	48845	15510	11710	3026023
5	50.5219	50.6281	0.1062	0.1172	195.1	45607	18748	13482	3657668
6	51.9184	52.0378	0.1194	0.1304	195.1	44798	19557	13071	3815520
7	51.5153	51.6669	0.1516	0.1626	195.1	45231	19123	11463	3730968
8	51.8138	51.9621	0.1483	0.1593	195.1	40427	23928	11660	4668278
9	51.1054	51.2086	0.1032	0.1142	195.1	47822	16532	14190	3225488
10	49.6921	49.7850	0.0929	0.1039	195.1	47396	16959	11897	3308720
11	50.6760	50.7796	0.1036	0.1146	195.1	45670	18685	10981	3645361
12	52.4643	52.5597	0.0954	0.1064	195.1	44968	19386	13355	3782278
13	50.7187	50.8268	0.1081	0.1191	195.1	46045	18310	12156	3572274
14	51.8426	51.9085	0.0659	0.0769	195.1	52680	11674	13810	2277630
15	48.9446	49.0594	0.1148	0.1258	195.1	44112	20243	13784	3949413
16	50.6424	50.7072	0.0648	0.0758	195.1	52226	12128	14032	2366262
17	50.3263	50.4643	0.1380	0.1490	195.1	43056	21299	13267	4155439
18	51.4064	51.5068	0.1004	0.1114	195.1	47222	17132	14794	3342532

Corrected tapes			
1	50.1658	50.1539	-0.0119
2	48.6800	48.6672	-0.0128
3	50.3839	50.3744	-0.0095
4	51.2590	51.2491	-0.0099
5	49.6129	49.6019	-0.0110
		Average	-0.011
		SD	0.00137

Notes:

(1) Mean greyscale value of blank tape = 64355

(2) Corrected SD calculated from Eq. 6-7

(3) Integrated pixel density = Mean corrected greyscale x strip area

3-D Continued.

Tape No.	3. Protein method							
	Corrected mean fluo. Replicate 1	Protein conc (µg/ml)	Corrected mean fluo. Replicate 2	Protein conc (µg/ml)	Corrected mean fluo. Replicate 2	Protein conc (µg/ml)	Mean protein conc (µg/ml)	SD protein conc (µg/ml)
1	1721.3	55.4	1768.9	56.3	1909.9	58.8	56.8	1.7
2	1383.3	49.4	1191.6	46.0	1605.3	53.3	49.6	3.7
3	2110.3	62.3	2155.9	63.2	2024.6	60.8	62.1	1.2
4	1088.7	23.3	1139.1	24.7	1560.1	36.6	28.2	7.3
5	1113.7	24.0	1017.4	21.3	1154.1	25.1	23.5	2.0
6	1173.4	25.7	1568.7	36.8	1888.7	45.8	36.1	10.1
7	1604.4	37.8	1513.4	35.3	853.7	16.7	29.9	11.5
8	1535.7	35.9	1334.7	30.2	1998.1	48.9	38.3	9.6
9	1178.7	25.8	1785.7	42.9	1435.4	33.1	33.9	8.6
10	377.1	ND	468.4	ND	857.7	16.8	ND	
11	709.7	ND	633.4	10.5	1062.1	22.6	ND	
12	1298.1	29.2	1371.1	31.2	1349.7	30.6	30.4	1.1
13	1449.1	33.4	1092.4	23.4	910.7	18.3	25.0	7.7
14	573.1	ND	703.4	ND	1094.7	23.5	ND	
15	1956.1	47.7	1825.4	44.0	2129.4	52.6	48.1	4.3
16	100.4	ND	467.4	ND	875.7	ND	ND	
17	3376.4	87.7	2470.1	62.2	2608.7	66.1	72.0	13.7
18	1040.4	21.9	1491.1	34.6	842.7	16.4	24.3	9.3

2 EZQ plates used to analyse tapes

Tape 1-3 (plate A)

Blank tape extracted. Fluorescence = 10140

Calibration curve: y =56.1x - 1387.9, R^2 = 0.99

Tapes 4-18 (plate B)

Blank tape extracted. Fluorescence = 11164

Calibration curve: y =35.55x - 260.35, R^2 = 0.98

Abbreviations: fluo: fluorescence conc: concentration ND: not detectable

3-D Continued.

Tape No.	4. UV pseudoabsorption method			
	Average abs. (430nm)	SD abs. (430nm)	Mean abs. (278nm)	SD abs. (278nm.)
1	0.4902	0.0031	0.5692	0.0072
2	0.2700	0.0010	0.2999	0.0028
3	0.3754	0.0034	0.4311	0.0070
4	0.3231	0.0028	0.3694	0.0026
5	0.3865	0.0016	0.4422	0.0048
6	0.4192	0.0023	0.4741	0.0040
7	0.4141	0.0015	0.4649	0.0011
8	0.5610	0.0043	0.6336	0.0062
9	0.3446	0.0084	0.3970	0.0117
10	0.3643	0.0035	0.4068	0.0032
11	0.4160	0.0019	0.4624	0.0030
12	0.4205	0.0019	0.4616	0.0042
13	0.3910	0.0009	0.4307	0.0029
14	0.2809	0.0050	0.3215	0.0107
15	0.4664	0.0029	0.5294	0.0051
16	0.2775	0.0053	0.3140	0.0071
17	0.5160	0.0076	0.5975	0.0134
18	0.3571	0.0019	0.3902	0.0026

Abbreviation Abs: absorbance

Appendix 5-A

Full raw data and calculations, for gravimetric and imaging methods, for site 1c.

Tape No.	Gravimetric method				
	Mass blank tape (mg)	Mass tape +SC (mg)	Mass SC (mg)	Corrected mass SC (mg)	Thickness of SC (µm)
1	48.4974	48.5745	0.0771	0.0842	0.56
2	49.6639	49.7861	0.1222	0.1293	0.86
3	50.3989	50.4985	0.0996	0.1067	0.71
4	48.0222	48.1480	0.1258	0.1329	0.89
5	49.1347	49.2219	0.0872	0.0943	0.63
6	50.0676	50.1861	0.1185	0.1256	0.84
7	48.7472	48.8335	0.0863	0.0934	0.62
8	49.1190	49.2063	0.0873	0.0944	0.63
9	48.0312	48.1378	0.1066	0.1137	0.76
10	48.9488	49.0714	0.1226	0.1297	0.86
11	48.8877	49.0532	0.1655	0.1726	1.15
12	50.5865	50.8058	0.2193	0.2264	1.51
13	50.3418	50.4579	0.1161	0.1232	0.82
14	50.2114	50.3392	0.1278	0.1349	0.90
15	49.9968	50.0976	0.1008	0.1079	0.72
Correction tapes					
1	49.0345	49.0282	-0.0063		
2	50.7700	50.7598	-0.0102		
3	49.3648	49.3574	-0.0074		
4	48.7818	48.7782	-0.0036		
5	50.5135	50.5057	-0.0078		
		Average	**-0.0071**		
		SD	0.0024		

5-A Continued.

Tape No.	Gravimetric method (continued)				
	Cum. SC thickness removed, h (µm)	Measured TEWL ($g.m^{-2}h^{-1}$) (1)	Predicted TEWL (from BCNL) ($g.m^{-2}h^{-1}$)	*h*/H	ANT_i
1	0.56	11.6	11.3	0.04	0.04
2	1.42	11.7	11.7	0.10	0.06
3	2.13	12.2	12.1	0.15	0.05
4	3.02	12.6	12.7	0.21	0.06
5	3.65	12.7	13.2	0.26	0.04
6	4.49	13.6	14.0	0.32	0.06
7	5.11	15.1	14.6	0.36	0.04
8	5.74	14.9	15.4	0.41	0.04
9	6.49	16.7	16.5	0.46	0.05
10	7.36	18.1	18.0	0.52	0.06
11	8.51	22.3	20.8	0.60	0.08
12	10.02	25.8	26.8	0.71	0.11
13	10.84	31.5	32.3	0.77	0.06
14	11.74	43.6	42.8	0.83	0.06
15	12.46	59.3	59.4	0.88	0.05
H (µm) estimate		14.12	**H/H (µm) estimate**		1.00
SER		0.08	SER		0.01
CV (%)		0.60	CV (%)		0.60
D·K·ΔC estimate		91.03	**D·K·ΔC/H estimate**		6.46
SER		4.87	SER		0.35
CV (%)		5.35	CV (%)		5.35
B estimate		4.54	**B estimate**		4.51
SER		0.51	SER		0.51
CV (%)		11.30	CV (%)		11.38

Abbreviation Cum: cumulative

Notes:
(1) Initial TEWL before stripping = 10.8 $g.m^{-2}h^{-1}$

5-A Continued.

Tape No.	Imaging method						
	Mean greyscale value	**Mean corr. Greyscale value (1)**	**10^{-6} x Integrated pixel density (mm^2) (2)**	**10^{-6} x Cum. integrated pixel density, g (mm^2)**	**Pred. TEWL (from BCNL) ($g.m^{-2}h^{-1}$)**	**g/G**	**ANG_i**
1	55290	9064	1.77	1.77	11.0	0.06	0.06
2	53377	10978	2.14	3.91	11.5	0.12	0.07
3	55444	8911	1.74	5.65	11.9	0.18	0.06
4	52710	11644	2.27	7.92	12.6	0.25	0.07
5	55621	8733	1.70	9.63	13.1	0.31	0.05
6	53904	10450	2.04	11.66	14.0	0.37	0.07
7	56091	8264	1.61	13.28	14.8	0.42	0.05
8	55793	8562	1.67	14.95	15.7	0.48	0.05
9	57216	7138	1.39	16.34	16.7	0.52	0.04
10	54509	9846	1.92	18.26	18.4	0.58	0.06
11	50716	13639	2.66	20.92	21.8	0.67	0.08
12	52569	11786	2.30	23.22	26.6	0.74	0.07
13	56341	8014	1.56	24.79	31.7	0.79	0.05
14	54665	9689	1.89	26.68	42.4	0.85	0.06
15	56772	7582	1.48	28.16	59.7	0.90	0.05

10^{-6} x G estimate (mm^2)	31.36	**G/G estimate**	1.00
10^{-6} x SER	0.13	SER	0.00
CV (%)	0.41	CV (%)	0.43
10^{-6} x $(D{\cdot}K{\cdot}\Delta C)_g$ estimate	174.68	**$D{\cdot}K{\cdot}\Delta C/G$ estimate**	5.60
10^{-6} x SER	7.20	SER	0.24
CV (%)	4.12	CV (%)	4.28
B_g estimate	5	**B_g estimate**	5.05
SER	0	SER	0.40
CV (%)	7.51	CV (%)	7.90

Abbreviations:

Corr: corrected
Cum: cumulative
Pred: predicted

Notes:

(1) Mean corrected greyscale value of blank tape = 64355

(2) Integrated pixel density = area of strip x Mean corrected greyscale value. Area of all strips = 195.1mm^2

Appendix 6-A

Calculation of SC thickness, H and G: Full raw data and calculations for Volunteer 1.

Tape No.	Gravimetric method								
	Mass blank tape (mg)	Mass tape +SC (mg)	Mass SC (mg)	Corr. mass SC (mg)	Thickness of SC (µm)	Cum. SC thickness removed, (µm)	Half way cum. thickness, h (µm)	Pred. TEWL (BCNL) ($g.m^{-2}h^{-1}$)	Measured TEWL ($g.m^{-2}h^{-1}$) (1)
1	53.9051	54.0944	0.1893	0.1837	0.8	0.8	0.4	13.0	12.4
2	50.2336	50.4174	0.1838	0.1782	0.8	1.6	1.2	13.6	13.8
3	50.8033	50.9486	0.1453	0.1397	0.6	2.2	1.9	14.2	13.8
4	54.3478	54.4768	0.1290	0.1234	0.5	2.8	2.5	14.8	15.0
5	51.4377	51.5983	0.1606	0.1550	0.7	3.5	3.1	15.6	15.5
6	51.5380	51.6628	0.1248	0.1192	0.5	4.0	3.7	16.3	17.1
7	52.2722	52.4271	0.1549	0.1493	0.7	4.7	4.3	17.5	18.8
8	54.8702	54.9969	0.1267	0.1211	0.5	5.2	4.9	18.6	19.1
9	49.4688	49.5988	0.1300	0.1244	0.6	5.8	5.5	20.0	19.6
10	49.3366	49.4512	0.1146	0.1090	0.5	6.2	6.0	21.6	20.5
11	50.7056	50.8491	0.1435	0.1379	0.6	6.8	6.5	24.1	25.3
12	52.0782	52.2049	0.1267	0.1211	0.5	7.4	7.1	27.2	26.3
13	50.9585	51.0660	0.1075	0.1019	0.5	7.8	7.6	30.7	30.0
14	50.0080	50.1310	0.1230	0.1174	0.5	8.4	8.1	36.6	36.2
15	49.8609	50.0010	0.1401	0.1345	0.6	9.0	8.7	48.2	49.4
16	50.3391	50.4548	0.1157	0.1101	0.5	9.4	9.2	67.4	67.1
Correction tapes									
1	51.4273	51.4366	0.0093			**H (µm) estimate**		10.5	
2	50.5463	50.5463	0.0000			SER		0.06	
3	51.5717	51.5813	0.0096			CV (%)		0.52	
4	52.8375	52.8358	-0.0017			**D·K·ΔC estimate**		65.6	
5	52.1444	52.1551	0.0107			SER		3.48	
						CV (%)		5.31	
		Average	**0.0056**			**B estimate**		6.3	
		SD	0.0059			SER		0.57	

Abbreviations:

Corr: corrected
Cum: cumulative
Pred: predicted

Notes:

(1) Initial TEWL (before stripping) = 12.5 $g.m^{-2}h^{-1}$

Continued.

Tape No.	Imaging method					
	Mean greyscale value	**Mean corr. Greyscale value (1)**	**10^{-5} x Integrated pixel density (mm^2) (2)**	**10^{-6} x Cum. Integrated pixel density, g (mm^2)**	**Pred. TEWL (BCNL) ($g.m^{-2}h^{-1}$)**	**Measured TEWL ($g.m^{-2}h^{-1}$) (3)**
1	42297	22058	4.30	4.30	13.2	12.4
2	40999	23355	4.56	8.86	13.7	13.8
3	44127	20228	3.95	12.81	14.2	13.8
4	43462	20892	4.08	16.88	14.7	15.0
5	40789	23566	4.60	21.48	15.5	15.5
6	42384	21971	4.29	25.77	16.3	17.1
7	41185	23170	4.52	30.29	17.3	18.8
8	42890	21465	4.19	34.48	18.5	19.1
9	43199	21155	4.13	38.61	19.9	19.6
10	44921	19434	3.79	42.40	21.5	20.5
11	42226	22128	4.32	46.71	24.0	25.3
12	43752	20602	4.02	50.73	27.1	26.3
13	45518	18836	3.68	54.41	31.0	30.0
14	44736	19619	3.83	58.24	37.2	36.2
15	44607	19747	3.85	62.09	47.7	49.4
16	45582	18772	3.66	65.75	67.4	67.1
			10^{-6} × G estimate (mm^2)			73.42
			10^{-6} × SER			0.46
			CV (%)			0.63
			10^{-6} × $(D \cdot K \cdot \Delta C)_g$ estimate			467.20
			10^{-6} × SER			29.07
			CV (%)			6.22
			B_g estimate			6.47
			SER			0.67
			CV (%)			10.31

Notes:

(1) Mean corrected greyscale value of blank tape = 64355

(2) Integrated pixel density = area of strip x Mean corrected greyscale value.
Area of all strips = 195.1mm^2

(3) Initial TEWL (before stripping) = 12.5 $g.m^{-2}h^{-1}$

Appendix 6-B

Deriving data for normalised drug concentration as a function of SC depth profiles: full raw data and calculations for Volunteer 1, Zovirax site 1.

Tape No.	Depth reached within the SC – Gravimetric method							
	Mass blank tape (mg)	Mass tape +SC (mg)	Mass SC (mg)	Corr. mass SC (mg)	Thickness of SC (µm)	Cum. SC thickness removed, h (µm)	*h*/H[(1)]	Half way *h*/H
1	52.5413	52.6842	0.1429	0.1443	0.64	0.64	0.06	0.03
2	52.0141	52.17	0.1559	0.1573	0.70	1.34	0.13	0.09
3	52.1938	52.3265	0.1327	0.1341	0.60	1.94	0.18	0.16
4	51.4062	51.5756	0.1694	0.1708	0.76	2.70	0.26	0.22
5	53.4335	53.5644	0.1309	0.1323	0.59	3.28	0.31	0.28
6	50.8222	50.9478	0.1256	0.1270	0.56	3.85	0.37	0.34
7	51.5398	51.6388	0.099	0.1004	0.45	4.30	0.41	0.39
8	52.1515	52.2575	0.106	0.1074	0.48	4.77	0.45	0.43
9	51.6394	51.7334	0.094	0.0954	0.42	5.20	0.49	0.47
10	52.6538	52.7579	0.1041	0.1055	0.47	5.67	0.54	0.52
11	49.6137	49.7135	0.0998	0.1012	0.45	6.12	0.58	0.56
12	52.9664	53.1071	0.1407	0.1421	0.63	6.75	0.64	0.61
13	50.4293	50.5173	0.088	0.0894	0.40	7.15	0.68	0.66
14	51.1609	51.2806	0.1197	0.1211	0.54	7.68	0.73	0.70
15	51.7623	51.847	0.0847	0.0861	0.38	8.07	0.77	0.75
16	50.1586	50.2668	0.1082	0.1096	0.49	8.55	0.81	0.79
17	50.2949	50.4057	0.1108	0.1122	0.50	9.05	0.86	0.84
18	50.1672	50.3007	0.1335	0.1349	0.60	9.65	0.92	0.89
19	50.7595	50.8464	0.0869	0.0883	0.39	10.05	0.95	0.94
			Total (mg) =	**2.26**				
Correction tapes								
1	50.5838	50.5863	0.0025					
2	53.4481	53.4549	0.0068					
3	50.2542	50.2476	-0.0066					
4	49.8504	49.8452	-0.0052					
5	52.0591	52.0544	-0.0047					
		Average	**-0.0014**					
		SD	0.0058					

Notes:
(1) H = 10.5 µm (see Appendix 6-A)

Continued.

Tape No.	Depth reached within the SC – Imaging method					
	Mean greyscale value	Mean corr. greyscale value (1)	10^{-6} ×Integrated pixel density (mm^2) (2)	10^{-6} ×cum. Integrated pixel density (mm^2)	g/G (3)	Half way g/G
1	49805	14550	2.84	2.84	0.04	0.02
2	47081	17273	3.37	6.21	0.08	0.06
3	46739	17615	3.44	9.65	0.13	0.11
4	42248	22106	4.31	13.96	0.19	0.16
5	43129	21226	4.14	18.10	0.25	0.22
6	41970	22385	4.37	22.47	0.31	0.28
7	45045	19309	3.77	26.24	0.36	0.33
8	42872	21483	4.19	30.43	0.41	0.39
9	45496	18858	3.68	34.11	0.46	0.44
10	43339	21015	4.10	38.21	0.52	0.49
11	45542	18812	3.67	41.88	0.57	0.55
12	42256	22099	4.31	46.19	0.63	0.60
13	47749	16606	3.24	49.43	0.67	0.65
14	42593	21762	4.25	53.68	0.73	0.70
15	47405	16950	3.31	56.98	0.78	0.75
16	44617	19737	3.85	60.83	0.83	0.80
17	44795	19560	3.82	64.65	0.88	0.85
18	42868	21487	4.19	68.84	0.94	0.91
19	49616	14738	2.88	71.72	0.98	0.96
	Total =	**367574**				

Abbreviations

Corr: corrected
Cum: cumulative

Notes:

(1) Mean corrected greyscale value of blank tape = 64355

(2) Integrated pixel density = area of strip x Mean corrected greyscale value.
Area of all strips = 195.1mm^2

(3) G = 73.42 x 10^6 (see Appendix 6-A)

Continued.

Tape No.	ACV concentration					
			Gravimetric method		Imaging method	
	Peak area (mAU)	Mass ACV per tape (µg) [1]	C_x (µg/mg) [2]	C_x/R_m [3]	$10^6 \times C_g$ (µg) [4]	C_g/R_g [5]
1	2.05	0.68	4.73	3.04	46.94	4.91
2	1.73	0.58	3.67	2.36	33.42	3.49
3	0.66	0.22	1.64	1.06	12.51	1.31
4	1.15	0.38	2.25	1.45	17.39	1.82
5	0.62	0.21	1.57	1.01	9.78	1.02
6	0.52	0.17	1.36	0.88	7.74	0.81
7	0.27	0.09	0.88	0.57	4.58	0.48
8	0.23	0.08	0.72	0.46	3.58	0.37
9	0.18	0.06	0.64	0.41	3.25	0.34
10	0.27	0.09	0.86	0.56	4.34	0.45
11	0.76	0.25	2.51	1.61	13.50	1.41
12	0.94	0.31	2.21	1.42	14.20	1.48
13	0.33	0.11	1.23	0.79	6.63	0.69
14	0.22	0.07	0.61	0.39	3.39	0.35
15	0.21	0.07	0.80	0.51	4.06	0.42
16	0.10	0.03	0.30	0.19	1.67	0.17
17	0.12	0.04	0.34	0.22	1.96	0.21
18	0.14	0.05	0.34	0.22	2.11	0.22
19	0.05	0.02	0.17	0.11	1.04	0.11
	Total (µg) =	**3.52**				

Calibration curve: $y = 3.01x - 0.0162$, $R^2 = 1.0$ (see Appendix 6-C)

Notes:

(1) As tapes extracted in 1ml water, this is equal to the concentration of ACV measured by HPLC.

(2) Cx: concentration of drug at position *x* within the SC (as measured by cumulative thickness measurements).

(3) See Eq. 6-5 for definition.
$R_m = 1.56$ µg/mg.

(4) Cg: concentration of drug at position *x* within the SC (as measured by cumulative integrated pixel densities).

(5) See Eq. 6-6 for definition.
$R_g = 9.57 \times 10^{-6}$ µg.

Appendix 6-C

Calibration curve for acyclovir assayed by HPLC.

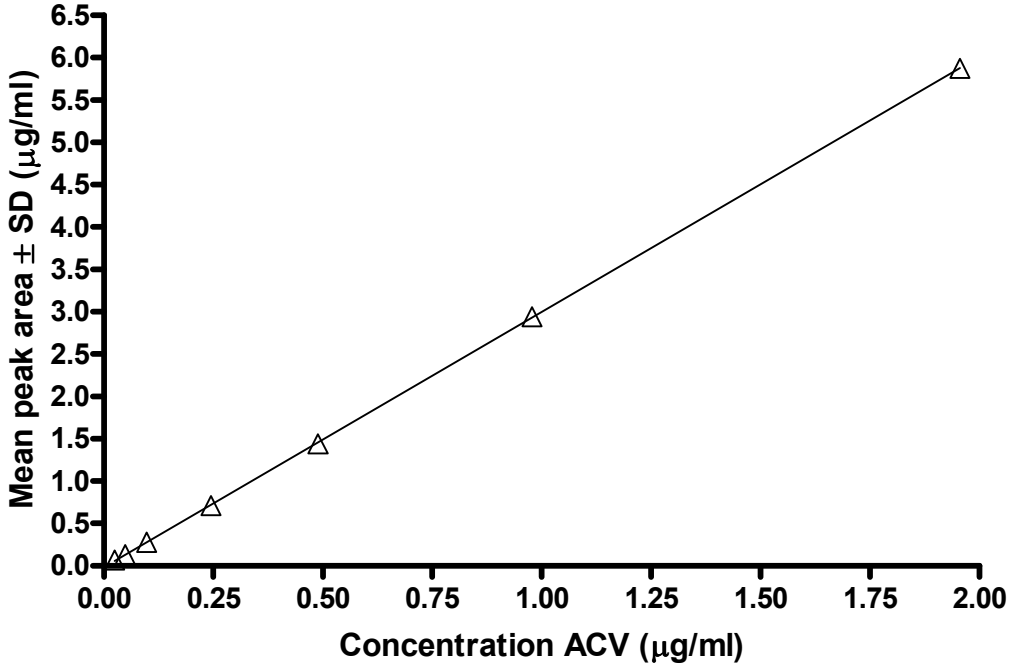

Notes:
RSD varies from 0.03 – 14 %
y= 3.012 *x* -0.016
R^2 = 0.999

Appendix 6-D

Images from 1 site after 1 hour Pliva 5% Acyclovir cream application.

Tape 01	Tape 02	Tape 03	Tape 04
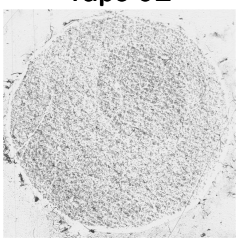	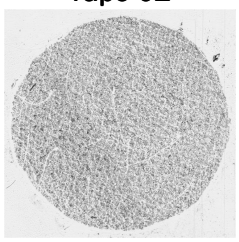	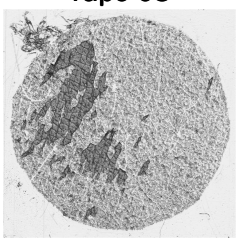	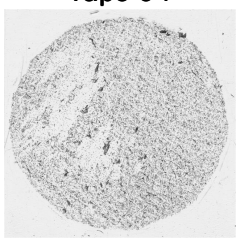
Tape 05	**Tape 06**	**Tape 07**	**Tape 09**
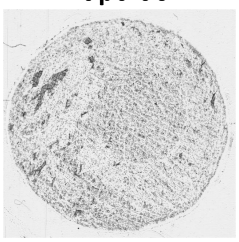	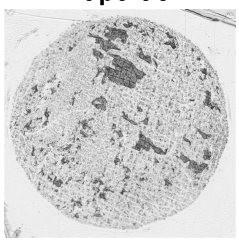	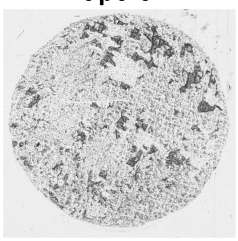	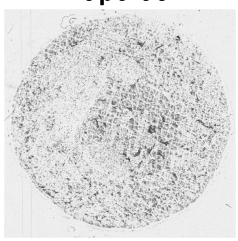
Tape 10	**Tape 11**	**Tape 12**	
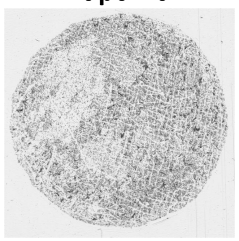	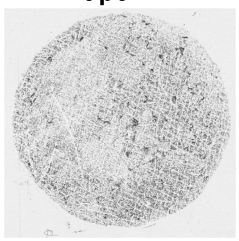	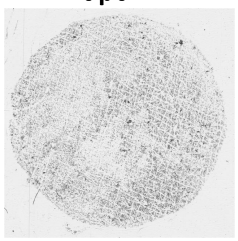	

Appendix 6-E

Images and stratum corneum measurements for Volunteer 1, Pliva, Site1

	Tape 01	Tape 02	Tape 03	Tape 04
	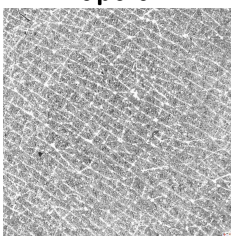	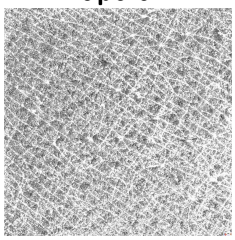	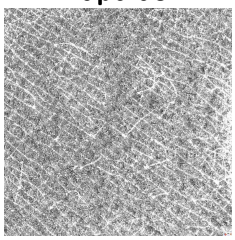	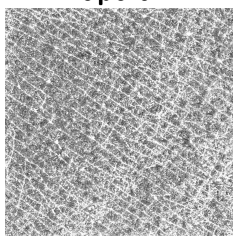
1	18665	16374	20597	20735
2	11636	13317	12543	13364
3	62.3	81.3	60.9	64.5
4	0.089	0.083	0.125	0.132
	Tape 05	**Tape 06**	**Tape 07**	**Tape 08**
	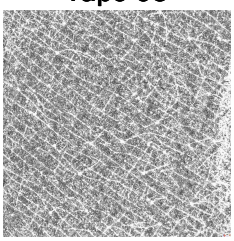	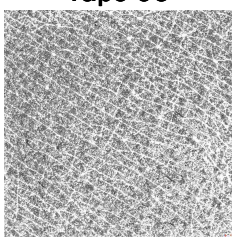	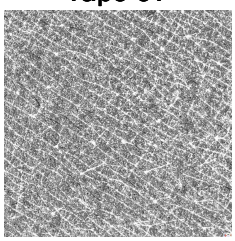	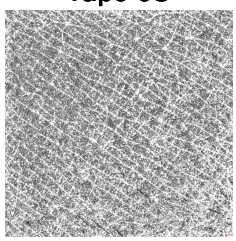
1	20604	18728	23300	20098
2	14025	14610	14294	14606
3	68.1	78.0	61.3	72.7
4	0.117	0.123	0.115	0.097
	Tape 09	**Tape 10**	**Tape 11**	**Tape 12**
	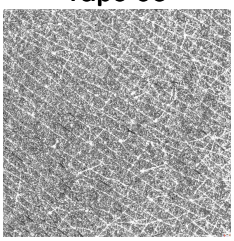	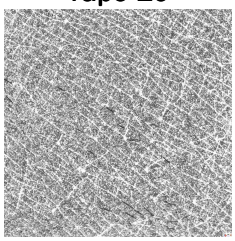	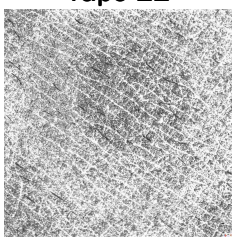	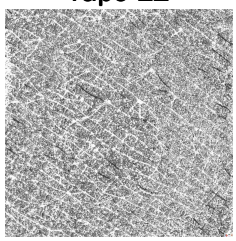
1	22857	20107	16846	20151
2	14078	13903	13704	14552
3	61.6	69.1	81.3	72.2
4	0.140	0.096	0.106	0.127

	Tape 13	Tape 14	Tape 15	Tape 16
	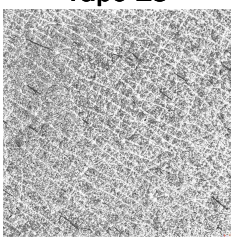	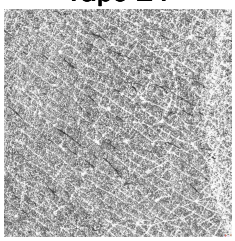	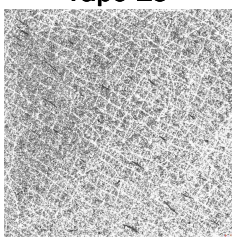	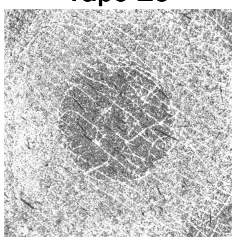
1	17357	19582	15886	15628
2	14532	14405	14728	13881
3	83.7	73.6	92.7	88.8
4	0.094	0.117	0.085	0.098
	Tape 17	**Tape 18**	**Tape 19**	**Tape 20**
	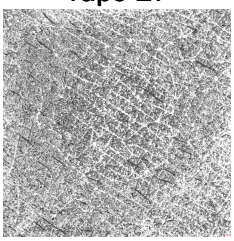	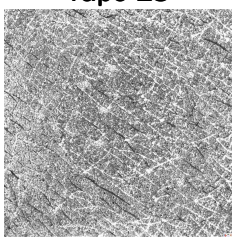	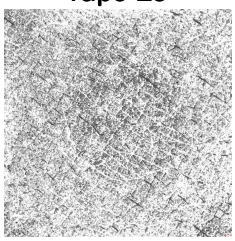	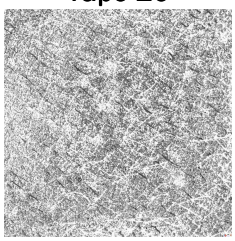
1	19808	22207	13802	17306
2	14368	14166	13833	14343
3	72.5	63.8	100.2	82.9
4	0.148	0.138	0.104	0.102

1. Mean corrected greyscale value;
2. Corrected standard deviation;
3. Relative standard deviation;
4. Mass of SC (mg)

Appendix 6-F

Images and SC measurements for Volunteer 1, Zovirax, Site1

	Tape 01	Tape 02	Tape 03	Tape 04
	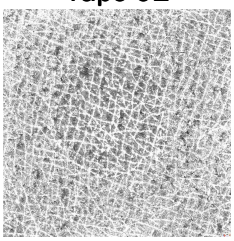	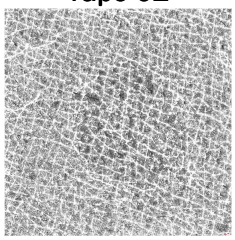	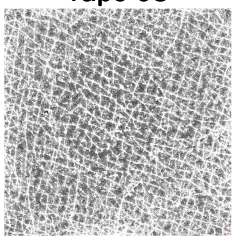	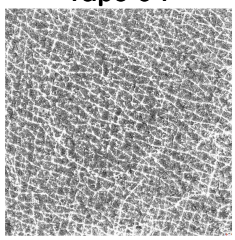
1	14550	17273	17616	22107
2	12816	13000	13913	14290
3	88.1	75.3	79.0	64.6
4	0.144	0.157	0.134	0.171
	Tape 05	**Tape 06**	**Tape 07**	**Tape 08**
	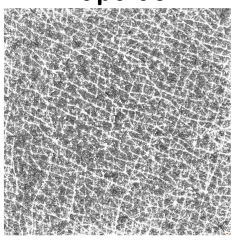	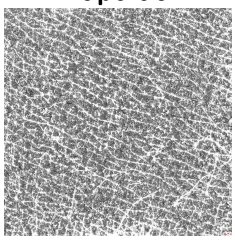	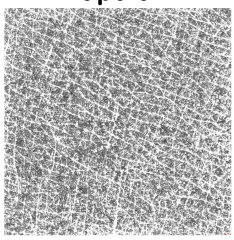	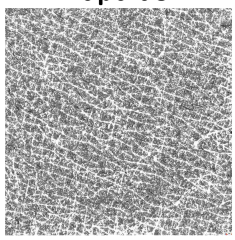
1	21226	22385	19309	21483
2	14802	14821	15111	15145
3	69.7	66.2	78.3	70.5
4	0.132	0.127	0.100	0.107
	Tape 09	**Tape 10**	**Tape 11**	**Tape 12**
	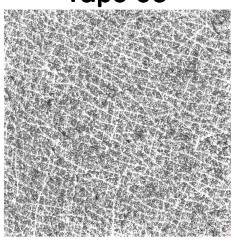	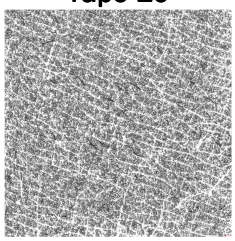	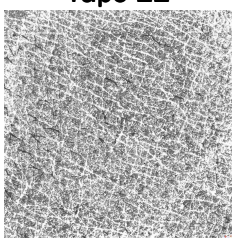	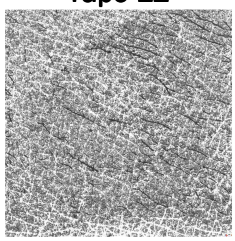
1	18858	21015	22099	16606
2	15203	15220	15465	14561
3	80.6	72.4	70.0	87.7
4	0.095	0.106	0.101	0.142

	Tape 13	Tape 14	Tape 15	Tape 16
	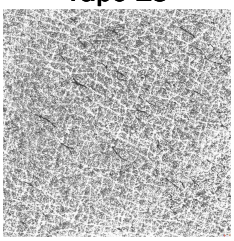	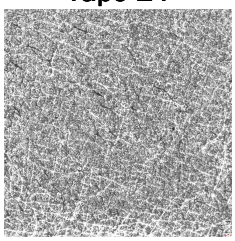	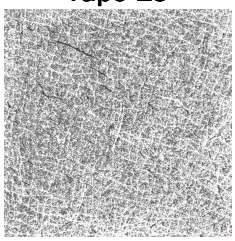	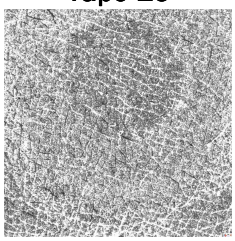
1	21762	16950	19738	19738
2	14343	14504	14813	14813
3	65.9	85.6	75.0	75.0
4	0.089	0.121	0.086	0.110

	Tape 17	Tape 18	Tape 19
	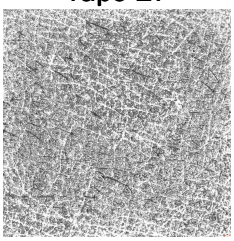	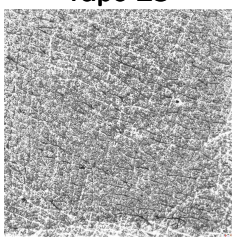	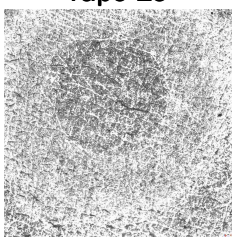
1	19560	21487	14738
2	14258	13985	13727
3	72.9	65.1	93.1
4	0.112	0.135	0.088

1. Mean corrected greyscale value;
2. Corrected standard deviation;
3. Relative standard deviation;
4. Mass of SC (mg)

Appendix 6-G

Images and SC measurements for Volunteer 1, Zovirax, Site2

	Tape 01	Tape 02	Tape 03	Tape 04
	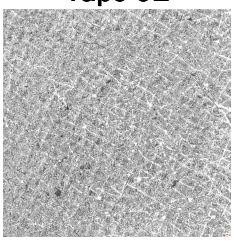	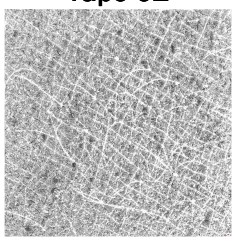	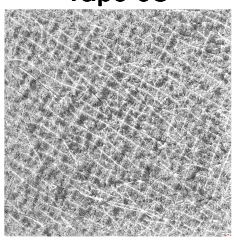	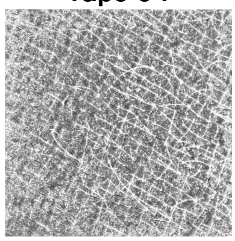
1	17892	16895	20405	21541
2	11842	11889	13159	13539
3	66.2	70.4	64.5	62.9
4	0.131	0.129	0.183	0.169
	Tape 05	**Tape 06**	**Tape 07**	**Tape 08**
	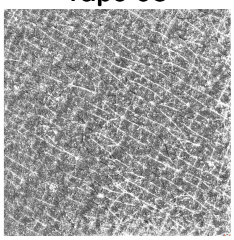	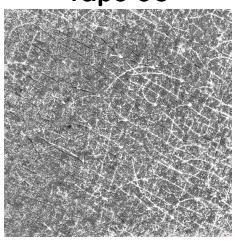	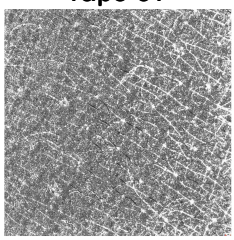	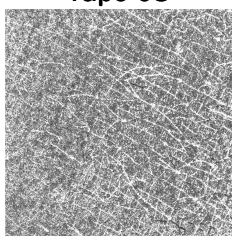
1	24969	26269	27113	23492
2	13579	13767	13498	14599
3	54.4	52.4	49.8	62.1
4	0.177	0.171	0.152	0.107
	Tape 09	**Tape 10**	**Tape 11**	**Tape 12**
	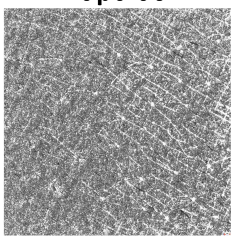	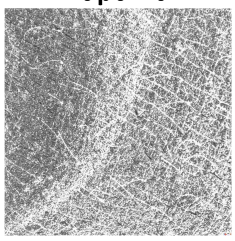	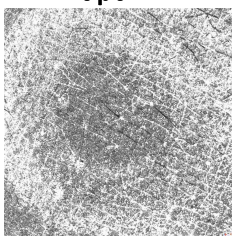	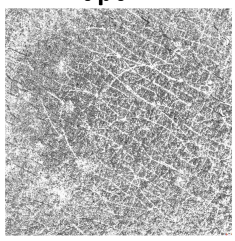
1	26373	20357	18053	19714
2	14323	15044	14742	14215
3	54.3	73.9	81.7	72.1
4	0.129	0.086	0.106	0.089

	Tape 13	Tape 14	Tape 15
	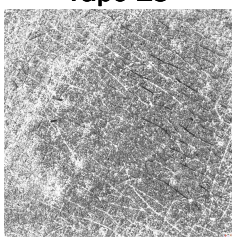	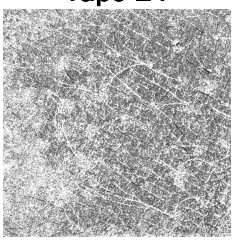	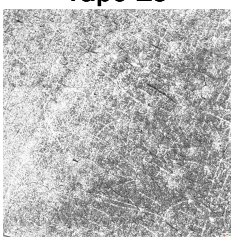
1	22066	20169	17931
2	14675	14510	14871
3	66.5	71.9	82.9
4	0.117	0.110	0.100

1. Mean corrected greyscale value;
2. Corrected standard deviation;
3. Relative standard deviation;
4. Mass of SC (mg)

Appendix 6-H

Images and SC measurements for Volunteer 2, Pliva, Site1

	Tape 01	Tape 02	Tape 03	Tape 04
	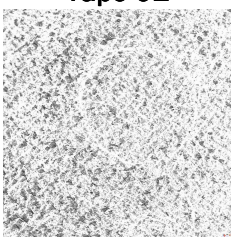	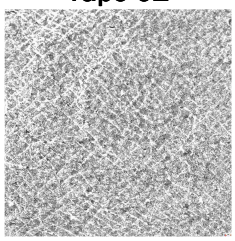	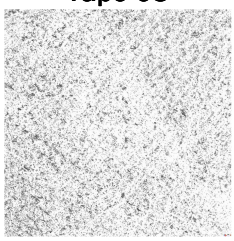	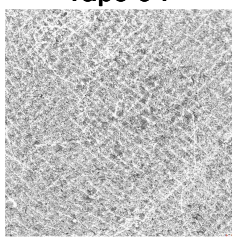
1	9040	16567	6797	14944
2	12382	12582	10648	11818
3	137.0	75.9	156.7	79.1
4	0.118	0.161	0.058	0.150
	Tape 05	**Tape 06**	**Tape 07**	**Tape 08**
	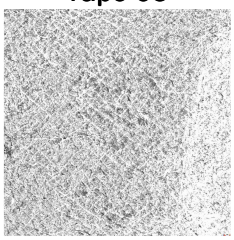	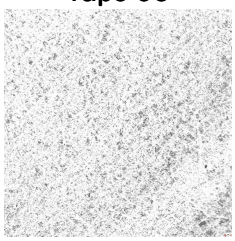	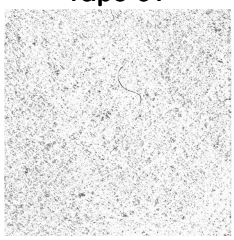	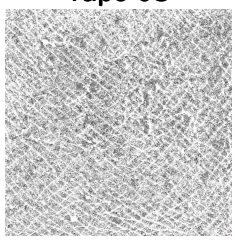
1	11826	5704	4669	13123
2	12190	8933	8837	12573
3	103.1	156.6	189.3	95.8
4	0.069	0.070	0.064	0.129
	Tape 09	**Tape 10**	**Tape 11**	**Tape 12**
	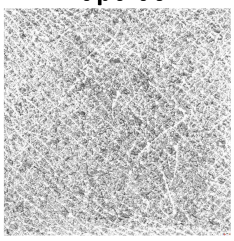	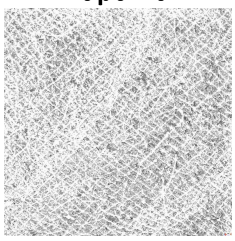	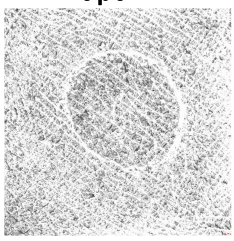	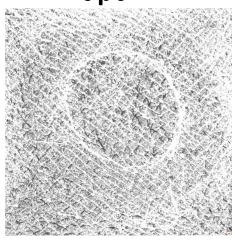
1	13172	9811	8873	10515
2	12569	11426	11591	12209
3	95.4	116.5	130.6	116.1
4	0.137	0.109	0.106	0.088

	Tape 13	Tape 14	Tape 15	Tape 16
	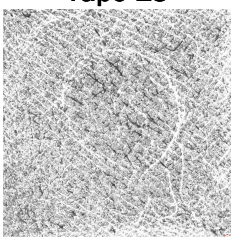	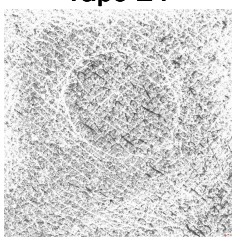	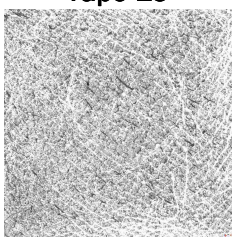	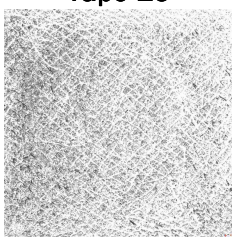
1	13721	10462	13950	10016
2	12793	12227	13035	12294
3	93.2	116.9	93.4	122.7
4	0.148	0.103	0.136	0.067

	Tape 17	Tape 18	Tape 19
	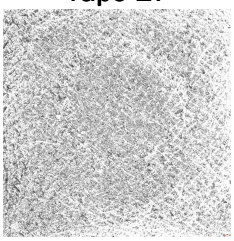	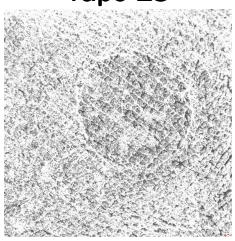	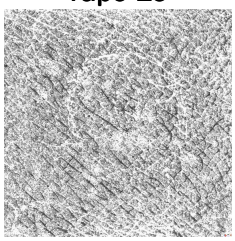
1	11763	10545	16561
2	11945	12351	13869
3	101.5	117.1	83.7
4	0.094	0.137	0.186

1. Mean corrected greyscale value;
2. Corrected standard deviation;
3. Relative standard deviation;
4. Mass of SC (mg)

Appendix 6-I

Images and SC measurements for Volunteer 2, Pliva, Site 2

	Tape 01	Tape 02	Tape 03	Tape 04
	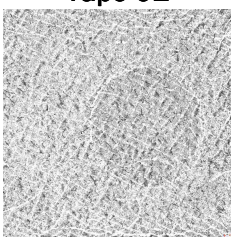	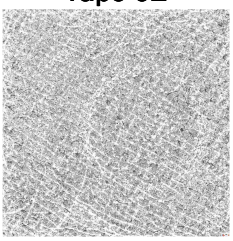	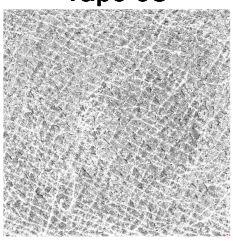	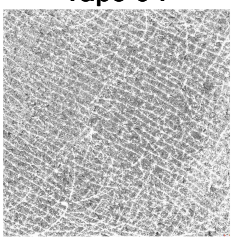
1	12543	13877	14207	16685
2	11841	11284	11409	12332
3	94.4	81.3	80.3	73.9
4	0.016	0.124	0.151	0.156
	Tape 05	**Tape 06**	**Tape 07**	**Tape 08**
	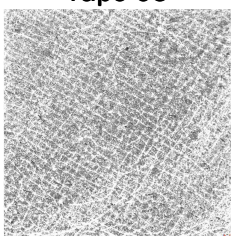	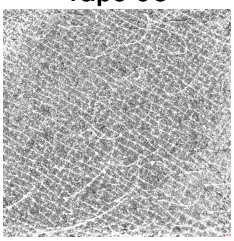	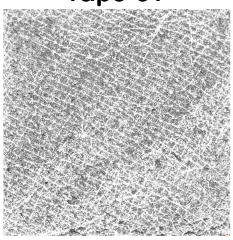	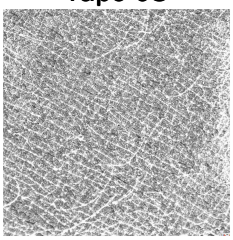
1	15085	18970	15468	19332
2	12199	12850	12816	12449
3	80.9	67.7	82.9	64.4
4	0.121	0.158	0.122	0.170
	Tape 09	**Tape 10**	**Tape 11**	**Tape 12**
	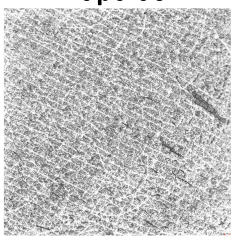	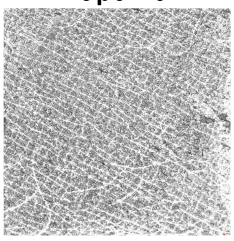	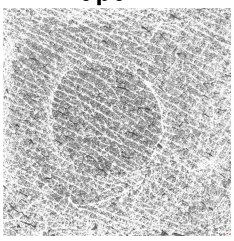	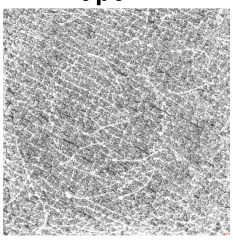
1	16008	16779	14160	18238
2	12981	12835	12868	13086
3	81.1	76.5	90.9	71.7
4	0.132	0.156	0.127	0.178

	Tape 13	Tape 14	Tape 15
	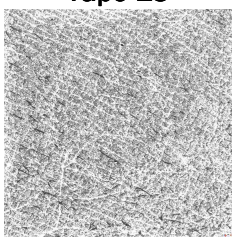	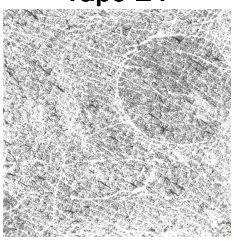	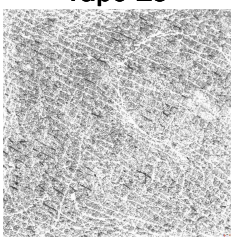
1	15837	12614	14000
2	13558	12422	12788
3	85.6	98.5	91.3
4	0.131	0.118	0.125

1. Mean corrected greyscale value;
2. Corrected standard deviation;
3. Relative standard deviation;
4. Mass of SC (mg)

Appendix 6-J

Images and SC measurements for Volunteer 2, Zovirax, Site1

	Tape 01	Tape 02	Tape 03	Tape 04
	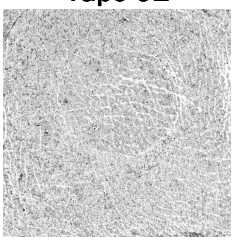	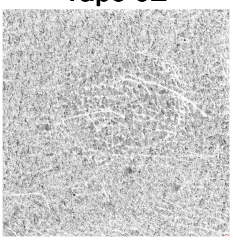	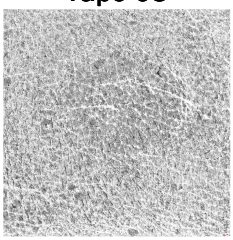	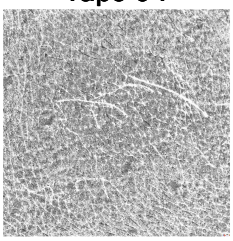
1	12109	12644	15381	18591
2	9807	10669	10828	11659
3	81.0	84.4	70.4	62.7
4	0.161	0.157	0.158	0.169
	Tape 05	**Tape 06**	**Tape 07**	**Tape 08**
	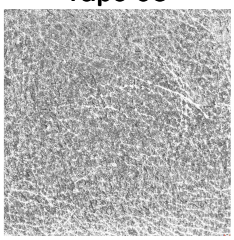	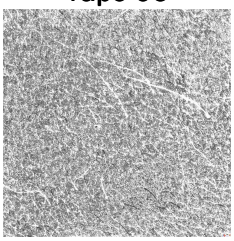	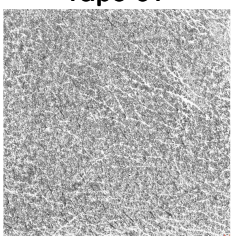	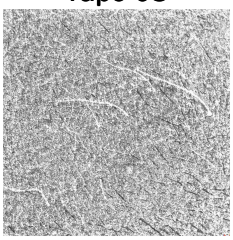
1	19180	18950	19011	18500
2	12107	12922	12933	12915
3	63.1	68.2	68.0	69.8
4	0.154	0.134	0.117	0.124
	Tape 09	**Tape 10**	**Tape 11**	**Tape 12**
	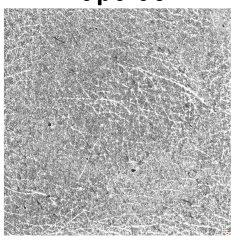	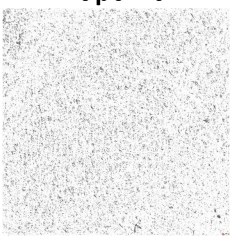	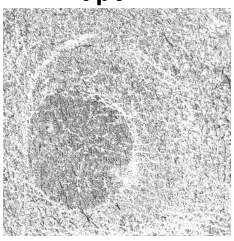	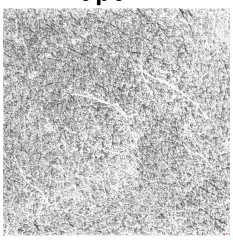
1	19795	3795	12744	14273
2	12139	7721	11960	12603
3	61.3	203.5	93.8	88.3
4	0.136	0.025	0.107	0.108

Tape 13	
	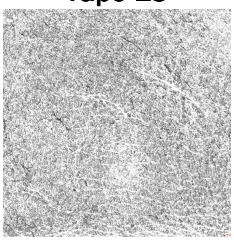
1	14037
2	12186
3	86.8
4	0.099

1. Mean corrected greyscale value;
2. Corrected standard deviation;
3. Relative standard deviation;
4. Mass of SC (mg)

Appendix 6-K

Images and SC measurements for Volunteer 2, Zovirax, Site2

	Tape 01	Tape 02	Tape 03	Tape 04
	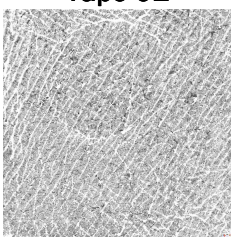	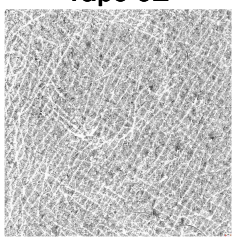	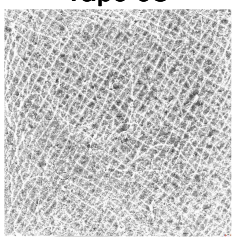	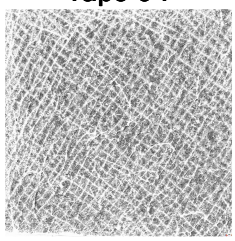
1	14349	14506	13860	16199
2	11560	12042	12399	13019
3	80.6	83.0	89.5	80.4
4	0.137	0.119	0.131	0.159
	Tape 05	**Tape 06**	**Tape 07**	**Tape 08**
	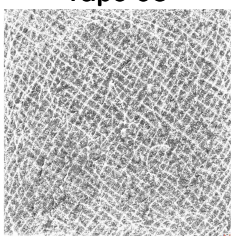	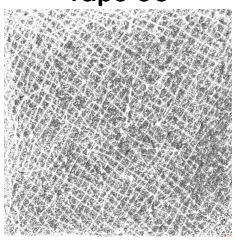	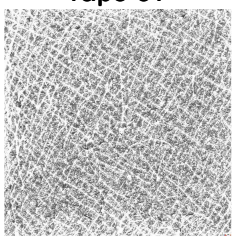	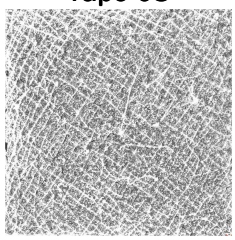
1	16521	15696	15332	17160
2	13808	14235	14159	14100
3	83.6	90.7	92.4	82.2
4	0.145	0.105	0.095	0.127
	Tape 09	**Tape 10**	**Tape 11**	**Tape 12**
	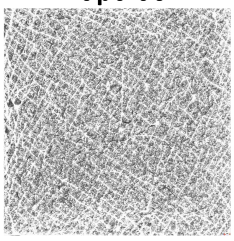	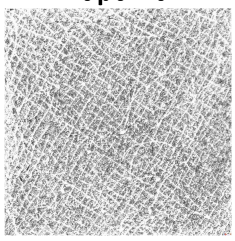	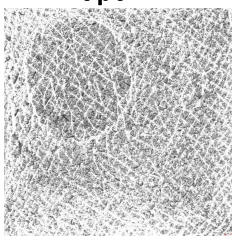	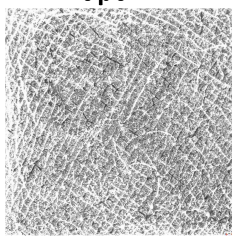
1	15802	14074	13508	16786
2	14153	13458	13280	13908
3	89.6	95.6	98.3	82.9
4	0.128	0.096	0.114	0.145

	Tape 13	Tape 14	Tape 15
	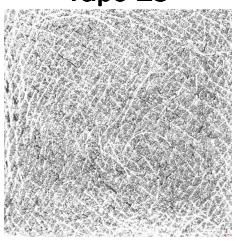	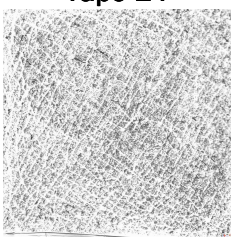	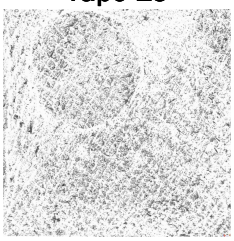
1	13821	10615	7276
2	12889	11820	10718
3	93.3	111.3	147.3
4	0.137	0.087	0.081

1. Mean corrected greyscale value;
2. Corrected standard deviation;
3. Relative standard deviation;
4. Mass of SC (mg)

References

1. Y.N. Kalia, F. Pirot, and R.H. Guy. Homogeneous transport in a heterogeneous membrane: water diffusion across human stratum corneum in vivo. Biophys J. 71:2692-2700 (1996).
2. N. Sekkat, Y.N. Kalia, and R.H. Guy. Porcine ear skin as a model for the assessment of transdermal drug delivery to premature neonates. Pharm Res. 21:1390-1397 (2004).
3. J. Hadgraftand R.H. Guy. Feasibility assessment in topical and transdermal delivery: Mathematical models and in vitro studies. In R.H. Guyand J. Hadgraft (eds.), Drugs and the pharmaceutical sciences 123 -Transdermal drug delivery, M. Dekker, New York, 2003, pp. viii, 383 p.
4. J. Crank. Chapter 4: Diffusion in plane sheet. The mathematics of diffusion, Clarendon Press, Oxford, 1975, pp. viii, 414p.
5. G.L. Flynn. Physicochemical determinants of skin absorption. In T.R. Gerrityand C.J. Henry (eds.), Principles of route-to-route extrapolation for risk assessment Elsevier, New York, 1990, p. 322p.
6. B.E. Vecchiaand A.L. Bunge. Evaluating the transdermal permeability of chemicals. In R.H. Guyand J. Hadgraft (eds.), Drugs and the pharmaceutical sciences 123 - Transdermal drug delivery, M. Dekker, New York, 2003, pp. viii, 383 p.
7. F.M. Williams. Evaluations and predictions of dermal absorption of toxic chemicals (EDETOX) - Final Report, European Commission, 2004.
8. J. Kruse, D. Golden, S. Wilkinson, F. Williams, S. Kezic, and J. Corish. Analysis, interpretation, and extrapolation of dermal permeation data using diffusion-based mathematical models. J Pharm Sci. 96:682-703 (2007).
9. R.O. Pottsand R.H. Guy. Predicting skin permeability. Pharm Res. 9:663-669 (1992).
10. R.L. Cleekand A.L. Bunge. A New Method for Estimating Dermal Absorption from Chemical-Exposure .1. General-Approach. Pharm Res. 10:497-506 (1993).
11. D. Fitzpatrick, J. Corish, and B. Hayes. Modelling skin permeability in risk assessment - the future. Chemosphere. 55:1309-1314 (2004).
12. G.P. Lian, L.J. Chen, and L.J. Han. An evaluation of mathematical models for predicting skin permeability. J Pharm Sci. 97:584-598 (2008).
13. B.E. Vecchiaand A.L. Bunge. Skin absorption databases and predictive equations. In R.H. Guyand J. Hadgraft (eds.), Drugs and the pharmaceutical sciences 123 - Transdermal drug delivery, M. Dekker, New York, 2003, pp. viii, 383 p.
14. J. Hadgraftand C. Valenta. pH, pK(a) and dermal delivery. Int J Pharm. 200:243-247 (2000).
15. W.J. Pughand J. Hadgraft. Ab-Initio Prediction of Human Skin Permeability Coefficients. Int J Pharm. 103:163-178 (1994).
16. M.S. Roberts, W.J. Pugh, J. Hadgraft, and A.C. Watkinson. Epidermal permeability penetrant structure relationships .1. An analysis of methods of predicting penetration of monofunctional solutes from aqueous solutions. Int J Pharm. 126:219-233 (1995).
17. M.S. Roberts, W.J. Pugh, and J. Hadgraft. Epidermal permeability: Penetrant structure relationships .2. The effect of H-bonding groups in penetrants on their diffusion through the stratum corneum. Int J Pharm. 132:23-32 (1996).
18. W.J. Pugh, M.S. Roberts, and J. Hadgraft. Epidermal permeability - Penetrant structure relationships .3. The effect of hydrogen bonding interactions and molecular size on diffusion across the stratum corneum. Int J Pharm. 138:149-165 (1996).

19. W.J. Pugh, I.T. Degim, and J. Hadgraft. Epidermal permeability-penetrant structure relationships: 4, QSAR of permeant diffusion across human stratum corneum in terms of molecular weight, H-bonding and electronic charge. Int J Pharm. 197:203-211 (2000).
20. M. Turowskiand R. Kaliszan. Keratin immobilized on silica as a new stationary phase for chromatographic modelling of skin permeation. J Pharm Biomed Anal. 15:1325-1333 (1997).
21. A. Nasal, M. Sznitowska, A. Bucinski, and R. Kaliszan. Hydrophobicity parameter from high-performance liquid chromatography on an immobilized artificial membrane column and its relationship to bioactivity. J Chromatogr A. 692:83-89 (1995).
22. J.J. Martínez-Pla, Y. Martín-Biosca, S. Sagrado, R.M. Villanueva-Camañas, and M.J. Medina-Hernández. Biopartitioning micellar chromatography to predict skin permeability. Biomed Chromatogr. 17:530-537 (2003).
23. J.J. Martínez-Pla, Y. Martín-Biosca, S. Sagrado, R.M. Villanueva-Camañas, and M.J. Medina-Hernández. Evaluation of the pH effect of formulations on the skin permeability of drugs by biopartitioning micellar chromatography. J Chromatogr A. 1047:255-262 (2004).
24. I.T. Degim. New tools and approaches for predicting skin permeability. Drug Discov Today. 11:517-523 (2006).
25. T. Degim, J. Hadgraft, S. Ilbasmis, and Y. Ozkan. Prediction of skin penetration using artificial neural network (ANN) modeling. J Pharm Sci. 92:656-664 (2003).
26. L.J. Chen, G.P. Lian, and L.J. Han. Prediction of human skin permeability using artificial neural network (ANN) modeling. Acta Pharmacologica Sinica. 28:591-600 (2007).
27. C.W. Lim, S. Fujiwara, F. Yamashita, and M. Hashida. Prediction of human skin permeability using a combination of molecular orbital calculations and artificial neural network. Biol Pharm Bull. 25:361-366 (2002).
28. A.K. Pannier, R.M. Brand, and D.D. Jones. Fuzzy modeling of skin permeability coefficients. Pharm Res. 20:143-148 (2003).
29. R.O. Pottsand R.H. Guy. A predictive algorithm for skin permeability: the effects of molecular size and hydrogen bond activity. Pharm Res. 12:1628-1633 (1995).
30. M.H. Abraham, F. Martins, and R.C. Mitchell. Algorithms for skin permeability using hydrogen bond descriptors: the problem of steroids. J Pharm Pharmacol. 49:858-865 (1997).
31. A.L. Bungeand R.L. Cleek. A New Method for Estimating Dermal Absorption from Chemical-Exposure .2. Effect of Molecular-Weight and Octanol Water Partitioning. Pharm Res. 12:88-95 (1995).
32. A.L. Bunge, R.L. Cleek, and B.E. Vecchia. A New Method for Estimating Dermal Absorption from Chemical-Exposure .3. Compared with Steady-State Methods for Prediction and Data-Analysis. Pharm Res. 12:972-982 (1995).
33. S. Mitragotri. A theoretical analysis of permeation of small hydrophobic solutes across the stratum corneum based on scaled particle theory. J Pharm Sci. 91:744-752 (2002).
34. M.E. Johnson, D. Blankschtein, and R. Langer. Evaluation of solute permeation through the stratum corneum: Lateral bilayer diffusion as the primary transport mechanism. J Pharm Sci. 86:1162-1172 (1997).
35. S. Mitragotri, M.E. Johnson, D. Blankschtein, and R. Langer. An analysis of the size selectivity of solute partitioning, diffusion, and permeation across lipid bilayers. Biophys J. 77:1268-1283 (1999).
36. S. Mitragotri. Modeling skin permeability to hydrophilic and hydrophobic solutes based on four permeation pathways. J Controlled Release. 86:69-92 (2003).
37. EC. Council Directive 76/768/EEC, of 27 Jul 1976, on the approximation of the laws of the Member States relating to cosmetic products (as amended), 1976.
38. EC. Council Directive 2004/23/EC, of the 31 Mar 2004, on setting standards of quality and safety for the donation, procurement, testing, processing,

preservation, storage and distribution of human tissues and cells, 2004.
39. N.A. Monteiro-Riviere, A.O. Inman, T.H. Snider, J.A. Blank, and D.W. Hobson. Comparison of an in vitro skin model to normal human skin for dermatological research. Microsc Res Tech. 37:172-179 (1997).
40. F. Netzlaff, M. Kaca, U. Bock, E. Haltner-Ukomadu, P. Meiers, C.-M. Lehr, and U.F. Schaefer. Permeability of the reconstructed human epidermis model Episkin® in comparison to various human skin preparations. Eur J Pharm Biopharm. 66:127-134 (2007).
41. F. Netzlaff, C.M. Lehr, P.W. Wertz, and U.F. Schaefer. The human epidermis models EpiSkin®, SkinEthic® and EpiDerm®: An evaluation of morphology and their suitability for testing phototoxicity, irritancy, corrosivity, and substance transport. Eur J Pharm Biopharm. 60:167-178 (2005).
42. T. Welss, D.A. Basketter, and K.R. Schröder. In vitro skin irritation: facts and future. State of the art review of mechanisms and models. Toxicol In Vitro. 18:231-243 (2004).
43. B. Godinand E. Touitou. Transdermal skin delivery: Predictions for humans from in vivo, ex vivo and animal models. Adv Drug Deliv Rev. 59:1152-1161 (2007).
44. F.P. Schmook, J.G. Meingassner, and A. Billich. Comparison of human skin or epidermis models with human and animal skin in in-vitro percutaneous absorption. Int J Pharm. 215:51-56 (2001).
45. S. Lombardi Borgia, P. Schlupp, W. Mehnert, and M. Schäfer-Korting. In vitro skin absorption and drug release - A comparison of six commercial prednicarbate preparations for topical use. Eur J Pharm Biopharm. 68:380-389 (2008).
46. S.D. Roy, J. Fujiki, and J.S. Fleitman. Permeabilities of Alkyl P-Aminobenzoates through Living Skin Equivalent and Cadaver Skin. J Pharm Sci. 82:1266-1268 (1993).
47. B. van Ravenzwaayand E. Leibold. A comparison between in vitro rat and human and in vivo rat skin absorption studies. Hum Exp Toxicol. 23:421-430 (2004).
48. M.E. Robertsand K.R. Mueller. Comparisons of Invitro Nitroglycerin (Tng) Flux across Yucatan Pig, Hairless Mouse, and Human Skins. Pharm Res. 7:673-676 (1990).
49. U. Jacobi, M. Kaiser, R. Toll, S. Mangelsdorf, H. Audring, N. Otberg, W. Sterry, and J. Lademann. Porcine ear skin: an in vitro model for human skin. Skin Res Technol. 13:19-24 (2007).
50. S. Singh, K. Zhao, and J. Singh. In vitro permeability and binding of hydrocarbons in pig ear and human abdominal skin. Drug Chem Toxicol. 25:83 - 92 (2002).
51. C. Herkenne, A. Naik, Y.N. Kalia, J. Hadgraft, and R.H. Guy. Pig ear skin ex vivo as a model for in vivo dermatopharmacokinetic studies in man. Pharm Res. 23:1850-1856 (2006).
52. EMEA. Modified Release Oral and Transdermal Dosage Forms. Section II: Pharmacokinetic and Clinical Evaluation. In C.f.P.M. Products (ed.), 1999.
53. V.P. Shah. Transdermal drug delivery system regulatory issues. In R.H. Guyand J. Hadgraft (eds.), Drugs and the pharmaceutical sciences 123 -Transdermal drug delivery, M. Dekker, New York, 2003, pp. viii, 383 p.
54. A. de la Pena, P. Liu, and H. Derendorf. Microdialysis in peripheral tissues. Adv Drug Del Rev. 45:189-216 (2000).
55. E.C.M. de Lange, A.G. de Boer, and D.D. Breimer. Methodological issues in microdialysis sampling for pharmacokinetic studies. Adv Drug Del Rev. 45:125-148 (2000).
56. I. Tegeder, U. Muth-Selbach, J. Lotsch, G. Rusing, R. Oelkers, K. Brune, S. Meller, G.R. Kelm, F. Sorgel, and G. Geisslinger. Application of microdialysis for the determination of muscle and subcutaneous tissue concentrations after oral and topical ibuprofen administration. Clin Pharmacol Ther. 65:357-368 (1999).
57. M. Kreilgaard, M.J.B. Kemme, J. Burggraaf, R.C. Schoemaker, and A.F. Cohen. Influence of a microemulsion vehicle on cutaneous bioequivalence of a lipophilic model drug assessed by microdialysis and pharmacodynamics. Pharm Res.

18:593-599 (2001).
58. E. Benfeldt, J. Serup, and T. Menne. Effect of barrier perturbation on cutaneous salicylic acid penetration in human skin: in vivo pharmacokinetics using microdialysis and non-invasive quantification of barrier function. Br J Dermatol. 140:739-748 (1999).
59. I. Tegeder, L. Brautigam, M. Podda, S. Meier, R. Kaufmann, G. Geisslinger, and M. Grundmann-Kollmann. Time course of 8-methoxypsoralen concentrations in skin and plasma after topical (bath and cream) and oral administration of 8-methoxypsoralen. Clin Pharmacol Ther. 71:153-161 (2002).
60. M. Kreilgaard. Assessment of cutaneous drug delivery using microdialysis. Adv Drug Deliv Rev. 54:S99-S121 (2002).
61. S. Schmidt, R. Banks, V. Kumar, K.H. Rand, and H. Derendorf. Clinical microdialysis in skin and soft tissues: An update. J Clin Pharmacol. 48:351-364 (2008).
62. M.I. Davies, J.D. Cooper, S.S. Desmond, C.E. Lunte, and S.M. Lunte. Analytical considerations for microdialysis sampling. Adv Drug Deliv Rev. 45:169-188 (2000).
63. E. Benfeldtand L. Groth. Feasibility of measuring lipophilic or protein-bound drugs in the dermis by in vivo microdialysis after topical or systemic drug administration. Acta Derm Venereol. 78:274-278 (1998).
64. L. Stahle. On mathematical models of microdialysis: geometry, steady-state models, recovery and probe radius. Adv Drug Del Rev. 45:149-167 (2000).
65. FDA. Guidance for Industry - Topical Dermatologic Corticosteroids: in vivo bioequivalence. In F.a.D.A. U.S. Department of Health and Human Services, Centre for Drug Evaluation and Research (CDER) (ed.), 1995.
66. H.Y. Gaoand A.L.W. Po. Topical Formulations of Fluocinolone Acetonide - Are Creams, Gels and Ointments Bioequivalent and Does Dilution Affect Activity. Eur J Clin Pharmacol. 46:71-75 (1994).
67. S.Y. Chanand A.L.W. Po. Quantitative Skin Blanching Assay of Corticosteroid Creams Using Tristimulus Color Analysis. J Pharm Pharmacol. 44:371-378 (1992).
68. E.W. Smith, J.M. Haigh, and R.B. Walker. Analysis of chromameter results obtained from corticosteroid-induced skin blanching. I: Manipulation of data. Pharm Res. 15:280-285 (1998).
69. J.M. Haighand I. Kanfer. Assessment of topical corticosteroid preparations: the human skin blanching assay. Int J Pharm. 19:245-262 (1984).
70. L.K. Pershing, B.S. Silver, G.G. Krueger, V.P. Shah, and J.P. Skelley. Feasibility of Measuring the Bioavailability of Topical Betamethasone Dipropionate in Commercial Formulations Using Drug Content in Skin and a Skin Blanching Bioassay. Pharm Res. 9:45-51 (1992).
71. L.K. Pershing, S. Bakhtian, C.E. Poncelet, J.L. Corlett, and V.P. Shah. Comparison of skin stripping, in vitro release, and skin blanching response methods to measure dose response and similarity of triamcinolone acetonide cream strengths from two manufactured sources. J Pharm Sci. 91:1312-1323 (2002).
72. R. Woodfordand B.W. Barry. Bioavailability and Activity of Betamethasone 17-Benzoate in Gel and Cream Formulations - Comparison with Proprietary Topical Corticosteroid Preparations in Vasoconstrictor Assay. Current Therapeutic Research-Clinical and Experimental. 16:338-345 (1974).
73. L.K. Pershing, L.D. Lambert, V.P. Shah, and S.Y. Lam. Variability and Correlation of Chromameter and Tape-Stripping Methods with the Visual Skin Blanching Assay in the Quantitative Assessment of Topical 0.05-Percent Betamethasone Dipropionate Bioavailability in Humans. Int J Pharm. 86:201-210 (1992).
74. J.R. Gibson, J.M. Kirsch, C.R. Darley, S.G. Harvey, C.A. Burke, and M.E. Hanson. An Assessment of the Relationship between Vasoconstrictor Assay Findings, Clinical Efficacy and Skin Thinning Effects of a Variety of Undiluted and Diluted Corticosteroid Preparations. Br J Dermatol. 111:204-212 (1984).
75. E.W. Smith, J.M. Haigh, and C. Surber. Quantification of corticosteroid-induced

skin vasoconstriction: visual ranking, chromameter measurement or digital imaging analysis. Dermatology. 205:3-10 (2002).
76. S. Wiedersberg, C.S. Leopold, and R.H. Guy. Bioavailability and bioequivalence of topical glucocorticoids. Eur J Pharm Biopharm. 68:453-466 (2008).
77. S. Wiedersberg, C.S. Leopold, and R.H. Guy. Topical application of betamethasone 17-valerate formulations: tape stripping versus pharmacodynamic response. In PhD thesis: Dermatopharmacokinetics and Pharmacodynamics of topical glucorcoritcoids. To be published. , *Department of Pharmacy and Pharmacology*, University of Bath, Bath, 2006.
78. B. Müller, M. Kasper, C. Surber, and G. Imanidis. Permeation, metabolism and site of action concentration of nicotinic acid derivatives in human skin: Correlation with topical pharmacological effect. Eur J Pharm Sci. 20:181-195 (2003).
79. M.C. Poelman, B. Piot, F. Guyon, M. Deroni, and J.L. Leveque. Assessment of Topical Non-Steroidal Anti-Inflammatory Drugs. J Pharm Pharmacol. 41:720-722 (1989).
80. R. Parker, P. Lehman, and T. Franz. Human *In vivo* bioequivalence assay for topical retinoic acid formulations (PIII-10. Only abstracts of papers from the "95th annual meeting of the American Society for Clinical Pharmacology and Therapeutics" published). Clin Pharmacol Ther. 55:184 (1994).
81. T. Franzand P. Lehman. Bioequivalence methodology for tretinoin products (PDD 7222. Only conference abstract published). Pharm Res. 12:S-248 (1995).
82. T. Franz, P. Lehman, N. Agrawal, and S. Franz. Tretinoin Bioavailability / Bioequivalence: use of transepidermal water loss (TEWL) technique (PDD 7302. Only conference abstract published). Pharm Res. 13:S-308 (1996).
83. J.W. Fluhr, M.P. Vienne, C. Lauze, P. Dupuy, W. Gehring, and M. Gloor. Tolerance profile of retinol, retinaldehyde and retinoic acid under maximized and long-term clinical conditions. Dermatology. 199:57-60 (1999).
84. I. Alberti, Y.N. Kalia, A. Naik, and R.H. Guy. Assessment and prediction of the cutaneous bioavailability of topical terbinafine, in vivo, in man. Pharm Res. 18:1472-1475 (2001).
85. A. Rougier, D. Dupuis, C. Lotte, R. Roguet, and H. Schaefer. In vivo correlation between stratum corneum reservoir function and percutaneous absorption. J Invest Dermatol. 81:275-278 (1983).
86. FDA. Guidance for Industry: Topical Dermatological Drug Product NDAs and ANDAs — In Vivo Bioavailability, Bioequivalence, In Vitro Release, and Associated Studies (Draft guidance). In F.a.D.A. U.S. Department of Health and Human Services, Centre for Drug Evaluation and Research (CDER) (ed.), 1998.
87. D.o.H.a.H.S. US FDA. Draft Guidance for Industry on Topical Dermatological Drug Product NDAs and ANDAs—In Vivo Bioavailability, Bioequivalence, In Vitro Release and Associated Studies; Withdrawal. [Docket Number 98D-0388]. Fed Regist. 67:35122 (2002).
88. T. Franz. Study No.1, Avita Gel 0.025% vs Retin-A Gel 0.025%, Advisory Committee for Pharmaceutical Sciences Meeting, Centre for Drug Evaluation and Research (CDER), Food and Drug Administration (FDA), Rockville, MD, November 29, 2001. (2001).
89. L.K. Pershing, J.L. Nelson, J.L. Corlett, S.P. Shrivastava, D.B. Hare, and V.P. Shah. Assessment of dermatopharmacokinetic approach in the bioequivalence determination of topical tretinoin gel products. J Am Acad Dermatol. 48:740-751 (2003).
90. L. Pershing. Bioequivalence Assessment of three 0.025% tretinoin gel products: Dermatopharmacokinetic vs. Clinical Trials Methods, Advisory Committee for Pharmaceutical Sciences Meeting, Centre for Drug Evaluation and Research (CDER), Food and Drug Administration (FDA), Rockville, MD. November 29, 2001. (2001).
91. L.K. Pershing, J.L. Corlett, and J.L. Nelson. Comparison of dermatopharmacokinetic vs. clinicial efficacy methods for bioequivalence

assessment of miconazole nitrate vaginal cream, 2% in humans. Pharm Res. 19:270-277 (2002).
92. I. Alberti, Y.N. Kalia, A. Naik, J.D. Bonny, and R.H. Guy. In vivo assessment of enhanced topical delivery of terbinafine to human stratum corneum. J Control Release. 71:319-327 (2001).
93. A.L. Bunge, B. N'Dri-Stempfer, W. Navidi, and R.H. Guy. Therapeutic equivalence of topical products: Revised final report. Submitted to Department of Health and Human Services, Food and Drug Administration, Colorado School of Mines,, Golden, Colorado, 2008.
94. S. Wiedersberg, C.S. Leopold, and R.H. Guy. Dermatopharmacokinetics of betamethasone 17-valerate: Influence of formulation viscosity and skin surface cleaning procedure. Eur J Pharm Biopharm. 71:362-366 (2009).
95. W. Navidi, A. Hutchinson, B. N'Dri-Stempfer, and A. Bunge. Determining bioequivalence of topical dermatological drug products by tape-stripping. Journal of Pharmacokinetics and Pharmacodynamics. 35:337-348 (2008).
96. B. N'Dri-Stempfer, W.C. Navidi, R.H. Guy, and A.L. Bunge. Optimizing metrics for the assessment of bioequivalence between topical drug products. Pharm Res. 25:1621-1630 (2008).
97. L.K. Pershing. Dermatopharmacokinetic bioequivalence study on three tretinoin, 0.025%, products. Final Report to the Food and Drug Administration (FDA). In S.L.C. University of Utah (ed.), 2000.
98. B. N'Dri-Stempfer, W. Navidi, R. Guy, and A. Bunge. Improved bioequivalence assessment of topical dermatological drug products using dermatopharmacokinetics, In preparation.
99. R.L. Andersonand J.M. Cassidy. Variations in physical dimensions and chemical composition of human stratum corneum. J Investig Dermatol. 61:30-32 (1973).
100. L.M. Russell, S. Wiedersberg, and M.B. Delgado-Charro. The determination of stratum corneum thickness - An alternative approach. Eur J Pharm Biopharm. 69:861-870 (2008).
101. Y.N. Kalia, I. Alberti, N. Sekkat, C. Curdy, A. Naik, and R.H. Guy. Normalization of stratum corneum barrier function and transepidermal water loss in vivo. Pharm Res. 17:1148-1150 (2000).
102. H.J. Weigmann, U. Lindemann, C. Antoniou, G.N. Tsikrikas, A.I. Stratigos, A. Katsambas, W. Sterry, and J. Lademann. UV/VIS absorbance allows rapid, accurate, and reproducible mass determination of corneocytes removed by tape stripping. Skin Pharmacol Appl Skin Physiol. 16:217-227 (2003).
103. R. Voegeli, J. Heiland, S. Doppler, A.V. Rawlings, and T. Schreier. Efficient and simple quantification of stratum corneum proteins on tape strippings by infrared densitometry. Skin Res Technol. 13:242-251 (2007).
104. F. Dreher, A. Arens, J.J. Hostynek, S. Mudumba, J. Ademola, and H.I. Maibach. Colorimetric method for quantifying human Stratum corneum removed by adhesive-tape stripping. Acta Derm Venereol. 78:186-189 (1998).
105. F. Dreher, B.S. Modjtahedi, S.P. Modjtahedi, and H.I. Maibach. Quantification of stratum corneum removal by adhesive tape stripping by total protein assay in 96-well microplates. Skin Res Technol. 11:97-101 (2005).
106. Y.C. Chaoand L.A. Nylander-French. Determination of keratin protein in a tape-stripped skin sample from jet fuel exposed skin. Ann Occup Hyg. 48:65-73 (2004).
107. A. Bornkessel, M. Flach, M. Arens-Corell, P. Elsner, and J.W. Fluhr. Functional assessment of a washing emulsion for sensitive skin: mild impairment of stratum corneum hydration, pH, barrier function, lipid content, integrity and cohesion in a controlled washing test. Skin Res Technol. 11:53-60 (2005).
108. J.W. Fluhr, J. Kao, M. Jain, S.K. Ahn, K.R. Feingold, and P.M. Elias. Generation of free fatty acids from phospholipids regulates stratum corneum acidification and integrity. J Invest Dermatol. 117:44-51 (2001).
109. C. Herkenne, A. Naik, Y.N. Kalia, J. Hadgraft, and R.H. Guy.

Dermatopharmacokinetic prediction of topical drug bioavailability in vivo. J Invest Dermatol. 127:887-894 (2007).
110. C. Herkenne, A. Naik, Y.N. Kalia, J. Hadgraft, and R.H. Guy. Ibuprofen transport into and through skin from topical formulations: in vitro-in vivo comparison. J Invest Dermatol. 127:135-142 (2007).
111. C. Herkenne, A. Naik, Y.N. Kalia, J. Hadgraft, and R.H. Guy. Effect of propylene glycol on ibuprofen absorption into human skin in vivo. J Pharm Sci. 97:185-197 (2008).
112. S. Wiedersberg, A. Naik, C.S. Leopold, and R.H. Guy. Pharmacodynamics and dermatopharmacokinetics of betamethasone 17-valerate: assessment of topical bioavailability. Br J Dermatol. 160:676-686 (2009).
113. S. Nicoli, A.L. Bunge, M.B. Delgado-Charro, and R.H. Guy. Dermatopharmacokinetics: factors influencing drug clearance from the stratum corneum. Pharm Res. 26:865-871 (2009).
114. M.B. Reddy, A.L. Stinchcomb, R.H. Guy, and A.L. Bunge. Determining dermal absorption parameters in vivo from tape strip data. Pharm Res. 19:292-298 (2002).
115. V.P. Shah, G.L. Flynn, A. Yacobi, H.I. Maibach, C. Bon, N.M. Fleischer, T.J. Franz, S.A. Kaplan, J. Kawamoto, L.J. Lesko, J.P. Marty, L.K. Pershing, H. Schaefer, J.A. Sequeira, S.P. Shrivastava, J. Wilkin, and R.L. Williams. Bioequivalence of topical dermatological dosage forms--methods of evaluation of bioequivalence. Pharm Res. 15:167-171 (1998).
116. K.A. Holbrookand G.F. Odland. Regional differences in the thickness (cell layers) of the human stratum corneum: an ultrastructural analysis. J Invest Dermatol. 62:415-422 (1974).
117. M. Denda, L.C. Wood, S. Emami, C. Calhoun, B.E. Brown, P.M. Elias, and K.R. Feingold. The epidermal hyperplasia associated with repeated barrier disruption by acetone treatment or tape stripping cannot be attributed to increased water loss. Arch Dermatol Res. 288:230-238 (1996).
118. G. Erikssonand L.O. Lamke. Regeneration of human epidermal surface and water barrier function after stripping. A combined study with electron microscopy and measurement of evaporative loss. Acta Derm Venereol. 51:169-178 (1971).
119. T. Frodinand M. Skogh. Measurement of transepidermal water loss using an evaporimeter to follow the restitution of the barrier layer of human epidermis after stripping the stratum corneum. Acta Derm Venereol. 64:537-540 (1984).
120. I. Alberti, Y.N. Kalia, A. Naik, J. Bonny, and R.H. Guy. Effect of ethanol and isopropyl myristate on the availability of topical terbinafine in human stratum corneum, in vivo. Int J Pharm. 219:11-19 (2001).
121. F. Pirot, Yogeshvar N. Kalia, Audra L. Stinchcomb, G. Keating, A. Bunge, and Richard H. Guy. Characterization of the permeability barrier of human skin in vivo, *Proc Natl Acad Sci USA*, Vol. 94, 1997, pp. 1562-1567.
122. F. Pirot, E. Berardesca, Y.N. Kalia, M. Singh, H.I. Maibach, and R.H. Guy. Stratum corneum thickness and apparent water diffusivity: facile and noninvasive quantitation in vivo. Pharm Res. 15:492-494 (1998).
123. E.H. Choi, M.-Q. Man, F. Wang, X. Zhang, B.E. Brown, K.R. Feingold, and P.M. Elias. Is Endogenous Glycerol a Determinant of Stratum Corneum Hydration in Humans? J Investig Dermatol. 125:288-293 (2005).
124. P. Corcuff, F. Fiat, and A.M. Minondo. Ultrastructure of the human stratum corneum. Skin Pharmacol Appl Skin Physiol. 14 Suppl 1:4-9 (2001).
125. M. Haftek, M. Simon, and G. Serre. Corneodesmosomes: pivotal actors in the stratum corneum cohesion and desquamation. In P.M. Eliasand K.R. Feingold (eds.), Skin barrier, Taylor & Francis, New York, N.Y. ; London, 2006, pp. 171-190.
126. R.I. Spearman. Some light microscopical observations on the stratum corneum of the guinea-pig, man and common seal. Br J Dermatol. 83:582-590 (1970).
127. J. Gabrielssonand D. Weiner. Modeling strategies. In J. Gabrielssonand D. Weiner (eds.), Pharmacokinetic / Pharmacodynamic data analysis : concepts and

applications, Apotekarsocieteten, Stockholm, 2006, pp. 389-463.
128. H. Motulskyand A. Christopoulos. Comparing models using Akaike's Information Criterion (AIC). In H. Motulskyand A. Christopoulos (eds.), Fitting models to biological data using linear and nonlinear regression: a practical guide to curve fitting, Oxford University Press, Oxford, 2004.
129. H. Motulskyand A. Christopoulos. Comparing models using the extra sum-of-squares F test. In H. Motulskyand A. Christopoulos (eds.), Fitting models to biological data using linear and nonlinear regression: a practical guide to curve fitting, Oxford University Press, Oxford, 2004.
130. J.H. Zar. Appendix B: Statistical Tables and Graphs. In J.H. Zar (ed.), Biostatistical analysis, Prentice-Hall, Englewood Cliffs, N.J., 1984.
131. J.S. Lo, H.A. Oriba, H.I. Maibach, and P.L. Bailin. Transepidermal potassium ion, chloride ion, and water flux across delipidized and cellophane tape-stripped skin. Dermatologica. 180:66-68 (1990).
132. M. Haftek, M. Simon, and G. Serre. Corneodesmosomes: pivotal actors in the Stratum Corneum Cohesion and Desquamation. In P.M. Eliasand K.R. Feingold (eds.), Skin barrier, Taylor & Francis, New York, N.Y. ; London, 2006.
133. A.G. Matoltsyand C.A. Balsamo. A study of the components of the cornified epithelium of human skin. J Biophys Biochem Cytol. 1:339-360 (1955).
134. T. Kitaharaand H. Ogawa. The extraction and characterization of human nail keratin. J Dermatol Sci. 2:402-406 (1991).
135. T. Kitaharaand H. Ogawa. Variation of differentiation in nail and bovine hoof cells. J Invest Dermatol. 102:725-729 (1994).
136. O.H. Lowry, N.J. Rosebrough, A.L. Farr, and R.J. Randall. Protein measurement with the Folin phenol reagent. J Biol Chem. 193:265-275 (1951).
137. Sigma-Aldrich. Technical Bulletin for Product B6916 (2004). Accessed Nov 2008 from http://www.sigmaaldrich.com/sigma/bulletin/b6916bul.pdf.
138. PierceBiotechnology. Protein Assay Technical Handbook (2005). Accessed Nov 2008 from http://www.piercenet.com/files/1601325ProteinAssay.pdf.
139. PierceBiotechnology. Modified Lowry Protein Assay kit (Instructions) (2005). Accessed Nov 2008 from http://www.piercenet.com/files/0389dh4.pdf.
140. S.W. Hendrix, K.H. Miller, T.E. Youket, R. Adam, R.J. O'Connor, J.G. Morel, and B.E. Tepper. Optimization of the skin multiple analyte profile bioanalytical method for determination of skin biomarkers from D-Squame tape samples. Skin Res Technol. 13:330-342 (2007).
141. J.H. Zar. Chapter 17, section 17.1. Biostatistical analysis, Prentice Hall ; London : Prentice-Hall International, Upper Saddle River, N.J., 1996, p. 1 v. (various pagings).
142. H.J. Weigmann, J. Lademann, H. Meffert, H. Schaefer, and W. Sterry. Determination of the horny layer profile by tape stripping in combination with optical spectroscopy in the visible range as a prerequisite to quantify percutaneous absorption. Skin Pharmacol Appl Skin Physiol. 12:34-45 (1999).
143. E. Marttin, M.T.A. NeelissenSubnel, F.H.N. DeHaan, and H.E. Bodde. A critical comparison of methods to quantify stratum corneum removed by tape stripping. Skin Pharmacol. 9:69-77 (1996).
144. Sigma-Aldrich. Micro Lowry, Onishi & Barr Modification - Technical Bulletin (2004). Accessed Nov 2008 from http://www.sigmaaldrich.com/sigma/bulletin/tp0200bul.pdf.
145. Invitrogen-MolecularProbes. NanoOrange® Protein Quantitation Kit (N6666) (2008). Accessed Nov 2008 from http://probes.invitrogen.com/media/pis/mp06666.pdf.
146. Invitrogen-MolecularProbes. CBQCA Protein Quantitation Kit (C-6667) (2001). Accessed Nov 2008 from http://probes.invitrogen.com/media/pis/mp06667.pdf.
147. Invitrogen-MolecularProbes. EZQ ® Protein Quantitation Kit (R33200) (2005). Accessed Nov 2008 from http://probes.invitrogen.com/media/pis/mp33200.pdf.
148. Invitrogen-MolecularProbes. Quant-iT ™ Protein Assay Kit (Q33210) (2007).

Accessed Nov 2008 from http://probes.invitrogen.com/media/pis/mp33210.pdf.
149. F.W. Bauer. Studies on isolated keratin fractions from mammalian epidermis. I. Physicochemical properties of the fractions. Dermatologica. 144:217-228 (1972).